Voltage and pH monitoring of Electrochemical Cells

James Mooney

A thesis submitted for a degree of Doctor of Philosophy to the Institute of Energy and Environment, Department of Electrical and Electronic Engineering
University of Strathclyde

September 2009

Declaration

The copyrights of this thesis belongs to the author under the terms of the United Kingdom Copyright Acts as qualified by the University of Strathclyde Regulation 3.49. Due acknowledgement must always be made of the use of any material contained in, or derived from, this thesis.

ABSTRACT

This thesis investigates ways of monitoring electrochemical cells with a view to predicting cell polarity reversal and thereby pre-empting potentially catastrophic failure in batteries and fuel cells. Novel contributions are claimed on the basis of the development of a low cost cell voltage monitor for fuel cell stacks, and also the discovery of disturbance in the measured value of pH during the over-discharge of lead acid batteries.

List of Figures

List of Tables

ACKNOWLEDGEMENT

I would like to express my gratitude to Professor Jim McDonald for the opportunity to develop this research within the Department of Electronic and Electrical Engineering. I would also like to thank my supervisor Dr Andrew Cruden for his guidance and supervision, and my colleagues at the University of the West of Scotland for their support.

This thesis would not have been possible without the patience, encouragement and understanding of my family: Kathleen, Claire and Paul.

CHAPTER 1 INTRODUCTION

The widespread adoption of electrochemical systems such as batteries and fuel cells as a means of providing both motive and static power will require diagnostic systems capable of supporting these systems during their service life. A means of condition monitoring and ultimately end-of-life prediction is desirable for the continuing successful penetration of these systems into the transport and static power markets.
Since the 1920's the use of electrochemical systems as a power source for vehicles has been predominately for auxiliary systems as opposed to being used as the main source of traction power. Internal combustion systems have been the primary energy convertor used in transport and power generation over the last century. Recent developments in the energy and environmental sectors have given a fresh impetus in the search for alternative energy sources, for example in the automotive sector recent interest has focused on energy from electrochemical cells as a possible replacement for the internal combustion engine.

This thesis concentrates on techniques for predicting degradation and failure of electrochemical cells based on the measurement of certain key parameters. The research is based on a battery/fuel cell hybrid power system for an electrically powered vehicle, and both the battery and fuel cell are studied in this thesis.

1.1 Motivation and justification of research

The work undertaken in this thesis is based on a requirement for creating monitoring systems for use on a hybrid battery/fuel cell electric vehicle shown in figures 1.1 and 1.2; the main energy source for the vehicle are lead acid batteries which supply the electric motor which powers the car, with the fuel cell functioning as a range extender by charging the batteries as the vehicle is in use.

Figure 1.1: Electric Vehicle

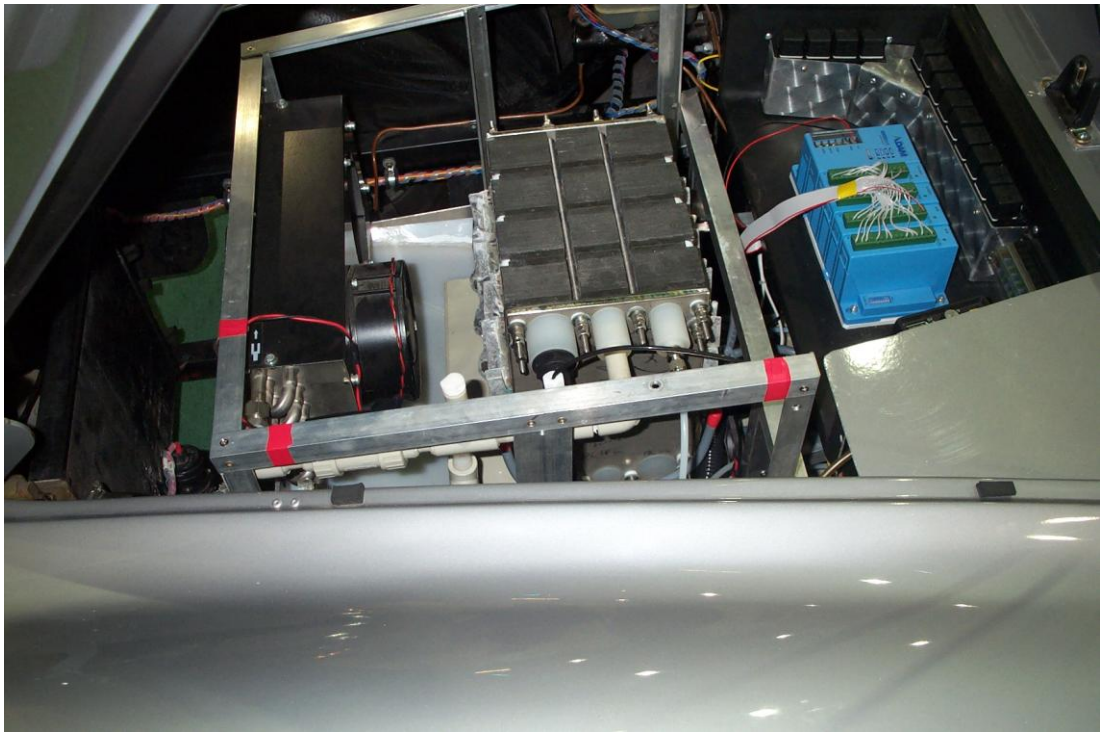

Figure 1.2: Electric Vehicle showing fuel cell system.

The original aim of this research was to develop a system which gave an early warning of an individual cell failure caused by voltage reversal within a fuel cell stack, such as the one in use in the electric vehicle. Individual cell failure is a common cause of failure in both fuel cell stacks and batteries.

Therefore the scope of the research was broadened to include batteries, the other element of the electric vehicle power system, also with a view to developing early warning of an individual cell failure caused by voltage reversal within the battery cells. The work undertaken in this thesis has produced two principle outcomes:

- A cell voltage monitoring unit for fuel cell stacks.
- A pH dip phenomenon, which could be used as early warning of cell reversal in a lead acid battery.

1.2 Fuel Cell Stack Voltage Monitoring

Cell failure is a problem common to both batteries and fuel cells and in both cases can lead to catastrophic failure. Individual cell voltage measurements are crucial to protect a fuel cell stack and ensure maximum lifetime [1]. With this in mind, it was decided that individual cell monitoring would be implemented on the fuel cell stack within the hybrid power system.

The author has developed a working cell voltage-monitoring system which has been the subject of a poster presentation and a journal paper (still under review), the cell voltage monitor has been successfully to monitor a fuel cell stack during a research programme. This cell voltage monitor offers a low cost, scalable monitoring solution and has been designed to protect the fuel cell in the event of a relay malfunction.

The focus of the work then turned to the battery element of the hybrid power system.

1.3 Battery Monitoring

Batteries have now been in commercial use for over 100 years, and yet aspects of battery behaviour remain unexplained.

“The industrial production began over 100 years ago and it demonstrates the difficulty implemented in electrochemical elements that even today sometimes the behaviour of a battery can’t be foreseen or explained totally” [2].

Despite the widespread use of batteries for a wide range of applications, the operational profiles of batteries in service can still not be completed defined. An accurate "battery fuel gauge" is the 'Holy Grail', so to speak of battery research, and many so called battery management systems using techniques based on measurement of parameters such as voltage, current and temperature have been developed with the aim of trying to quantify the remaining available energy within a battery.
The battery pack for the electric vehicle mentioned above comprised 6 Hawker Genesis 12 volt 70 amp hour lead acid automotive batteries connected in series to provide the 72 volts dc required for the electric drive motors.

There are concerns regarding these types of battery installations, in particular battery failures caused by cell voltage reversal as reported by Perone, "a concern regarding the occurrences, in long strings of lead acid cells, of cell reversals (the phenomenon associated with the continued forcing of a large discharge current through a completely discharged cell within a string of cells which have not yet reached an overall capacity or cut-off voltage)" [3].

1.4 Objectives of the PhD project and Thesis Contributions to the Field

The main objective of this PhD was to investigate new and improved means of monitoring of electrochemical cells in order to detect impending cell failure, in order to prevent catastrophic failure of cell within a larger number of cells in series, such as found in battery and fuel cell electric vehicle power systems.
The contribution of this thesis to the field of monitoring of electrochemical cells, arising from the work undertaken in the PhD programme is:

- The identification of a change in pH of the battery electrolyte referred to as a "pH dip".
- The provision of an explanation of the "pH dip".
- The novel use of pH measurement of the sulphuric acid electrolyte in a Lead-Acid battery as a means of predicting cell failure.
- A low cost scalable cell voltage monitoring system
- A cell voltage monitor which provides isolated cell voltage measurement.

1.5 Project Timeline

The PhD work described in this thesis started in October 2000, with the author originally embarking on an M.Phil. programme beginning in October 2000 on a part-time basis. The author was then and remains a member of the academic staff of the University of the West of Scotland (formerly Bell College of Technology). The initial aim of this work was to develop a monitoring system for an alkaline fuel cell stack, which included individual cell monitoring. The fuel cell system was being developed as part of a fuel cell/battery hybrid power system for an electric vehicle. This work was chosen because of the potential for catastrophic failure of a hydrogen fuel cell stack resulting from the polarity reversal of one of the cells within the stack. Therefore it is highly desirable to be able to measure the individual cell voltages of each cell within the stack.

The M.Phil objective was achieved in September 2002 with the successful testing of an alkaline fuel cell system under load with individual cell voltage monitoring of each cell on the fuel cell stack. The author was then given the opportunity to convert to a part-time PhD programme, where the initial phase of this work continued the theme started in the M.Phil programme; investigating ways of monitoring individual cells within a fuel cell stack. The outcome of this work was the development of a second cell voltage monitoring system, which addressed some of the limitations of the first system, in particular increasing the scanning frequency of the cell voltage monitor.

In January 2005 the work programme entered a new phase when it was decided to broaden the scope of the work to investigate cell failure in batteries, in particular lead-acid batteries, as this would include both types of electrochemical cell used in the fuel cell/battery hybrid power system.

It was decided to investigate using measurement of the pH of the battery electrolyte as a means of monitoring State of Charge (SoC) and State of Health (SoH) of lead acid batteries, using pH measurement as means of predicting and avoiding cell failure.

The outline of this Thesis is as follows:

Chapter 2

This chapter gives on overview of lead-acid batteries and fuel cells, with sections on types in use, operation and failure mechanisms.

Chapter 3

Reviews electrochemical devices such as fuel cells and batteries which are both types of electrochemical device. This chapter provides information necessary to underpin the study of these devices.

Chapter 4

Provides a review of the theory applicable to batteries and fuel cells, this theory is then applied in Chapter six to develop a theoretical battery model.

Chapter 5

This chapter describes the Zetek alkaline fuel cell system used in the experimental work of this thesis and details the development of monitoring for the fuel cell system, and in particular individual cell voltage monitoring for the fuel cell stack.

Chapter 6

This chapter describes the salient features of lead-acid batteries in terms of construction and operation. It then goes on to develop a theoretical model of a lead-acid battery based on the theory outlined in chapter 4.

Chapter 7

This chapter discusses the parameters associated with determining the battery condition and gives examples of test equipment that are currently available.

Chapter 8

This chapter outlines the procedures used in the tests carried out on lead-acid batteries and describes the test equipment which was used.

Chapter 9

This chapter presents an analysis of the results of the tests detailed in chapter eight and compares the test results with the theoretical model developed in chapter six. It then discusses differences between test results and the results predicted by the theoretical model and offers explanations of these differences.

Chapter 10

This chapter discusses the pH disturbance identified from the test results of chapter 9 and offers explanations for the pH disturbance in both new and aged batteries.

Chapter 11

Chapter eleven draws conclusions from the work carried out in the thesis and states the two out comes which are the development of a simple low cost cell voltage monitor for fuel cell stacks, and the identification of a previously unreported phenomenon, that is a disturbance in the measured value of pH during over-discharge of a lead-acid battery.

Chapter 12

Chapter twelve offers some suggestions for further research based upon the outcomes of this thesis, and also possible commercialisation with the pH sensing system embedded in batteries.

1.6 Associated Publications

The following list of publications was generated as a result of this PhD research, and is presented in support of the claims to the contribution in the field of monitoring of electrochemical cells.

Journal Papers (Submitted).

Mooney, J., Cruden, A., Cell voltage Monitoring System for an alkaline fuel cell, submitted to IEEE Instrumentation and Measurement.

Conference Papers (Published)

Mooney, J., Cruden, A., A fuel gauge for a battery, Bell college research conference, 2007.

Mooney, J., Cruden, A., Cell voltage monitoring of an alkaline fuel cell, Labview Conference, Dublin, September 2007.

Mooney, J., Cruden, A., Cell voltage monitoring of an alkaline fuel cell, Bell research conference, 2006.

Author J.Mooney.

Poster presentation (Published)

Mooney, J., Cruden, A., Cell voltage Monitoring System for an alkaline fuel cell. Fuel cell and Hydrogen Conference, Birmingham 28th March 2004.

CHAPTER 2 ELECTROCHEMICAL SYSTEMS

The electrochemical devices, which form the subject of this thesis, are commonly known by the terms:

1. Batteries
2. Fuel Cells

They have a number of similarities, namely:

- Originated from scientific work in the 19th century
- Directly convert chemical energy into electrical energy.
- They are modular and scalable.
- For most practical applications they require monitoring systems in order to operate reliably and efficiently.

However, batteries and fuel cells are quite different in terms of their operation; a battery is essentially an energy storage device, whereas a fuel cell is an energy converter. That is a battery has a finite energy capacity within its physical case, whereas, a fuel cell can be considered as a 'continuously operating battery' for as long as fuel is supplied to it.

2.1 Batteries

Batteries fulfil two main functions. First and foremost they act as portable sources of electrical power. The second function is based on the ability of certain electrochemical systems to store electrical energy supplied by an external source [4].
A battery is an electrochemical power source, which converts energy stored in the chemical bonds of a material into electrical energy by means of oxidation/reduction (redox) reactions.
Redox reactions are electro-chemical reactions in which an electron is either required or produced. For primary (disposable or non-rechargeable) batteries, this is a one-way process, where the chemical energy is converted into electrical energy. This means that a primary battery cannot be recharged, and an example of a primary battery is a battery used in a torch, or a remote control unit, as shown in Figure 2.1

Figure 2.1: Primary batteries [5].

However, for a secondary (i.e. a rechargeable) battery, the conversion process between electrical and chemical energy is reversible, that is the chemical energy is converted to electrical energy, and subsequently electrical energy can be re-converted to chemical energy, allowing the battery to be recharged. In secondary cells the chemical reaction is reversible, allowing a discharge phase when chemical reaction leads to the generation of electrical power, and a charging phase when the processes are reversed.

The basic electrochemical unit is called a cell, it generates voltage and current from a chemical reaction and this process may be reversible. More commonly the word battery is used for one or more cells connected in series/parallel. Secondary batteries can be charged and discharged many times before irreversible processes render them too inefficient for further use [4]. The most widely used secondary cell is the Lead-acid cell.

Common applications of secondary batteries are the lead-acid batteries used in vehicles, such as the one in Figure 2.2, and lithium-ion batteries used in high power consumer electronic equipment such as laptop computers, camcorders, mobile phones and digital cameras.

Figure 2.2: Lead-acid secondary battery [6].

2.2 Battery Operation

The basis of battery operation is the exchange of electrons, during simultaneous oxidation and reduction reactions, combined under the term redox. The conversion of chemical to electrical energy occurs through electrochemical redox or charge transfer reactions.

A battery comprises one or more cells, each cell has two electrodes, and the cell can be constructed as shown in figures 2.3 and 2.4. The components of a battery consist of an electrode and electrolyte for both the reduction and oxidation reaction, a means to transfer electrons between the reduction and oxidation reaction (usually this is accomplished by a wire connected to each electrode) and a means to exchange charged ions between the two reactions.

These reactions involve the exchange of electrons between the active materials in the two electrodes through an electrical circuit external to the battery. These reactions take place at the electrode/electrolyte interfaces. When current flows through a battery, an oxidation (loss of electrons) reaction takes place at the anode, and a reduction (gain of electrons) reaction at the cathode. The oxidation reaction yields electrons to the external circuit, while the reduction reaction accepts these electrons from the external circuit. The electrolyte serves as an intermediate between the electrodes. It offers a medium for the transfer of ions, hence current flow is supported by ions inside the electrolyte and externally the current flows through the charger or load [7].

The key aspect of a battery, which differentiates it from other redox reactions such as corrosion reactions e.g. rusting, is that the two reactions are physically separated, which allows the insertion of a load between the two reactions. The electrochemical potential between the two sides of the cell is the voltage, and the flow of electrons from the oxidation to the reduction reaction provides the current.

The main components of the battery are shown in figures 2.3 and 2.4 [8]. The positive and negative electrodes (often referred to as plates), the electrolyte, provision for electron transport between the positive and negative electrodes, and provision for ion transport between the negative and positive electrodes are all clearly identified. The ion transport is either a salt bridge, if the electrolyte for the

positive and negative electrodes is different or a single chemical bath if the electrolyte is common to both electrodes.

If the electrolyte is common to both electrodes, then a porous plate is often inserted between the positive and negative electrodes to keep them from physically touching and short-circuiting the battery. This plate is referred to as a separator.

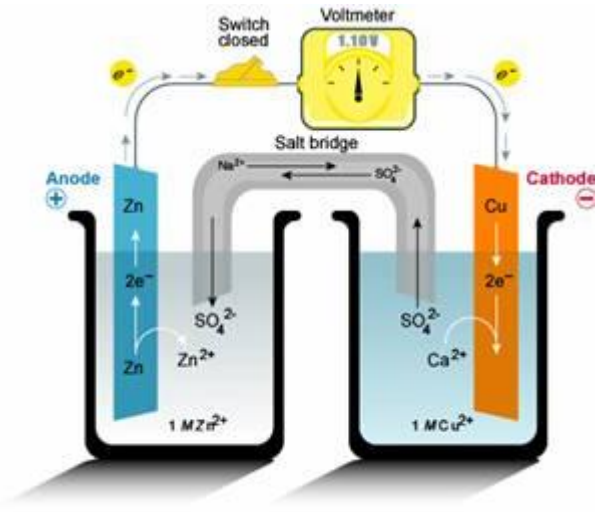

Figure 2.3 Battery cell in which the oxidation and reduction electrolyte reactions are different [8].

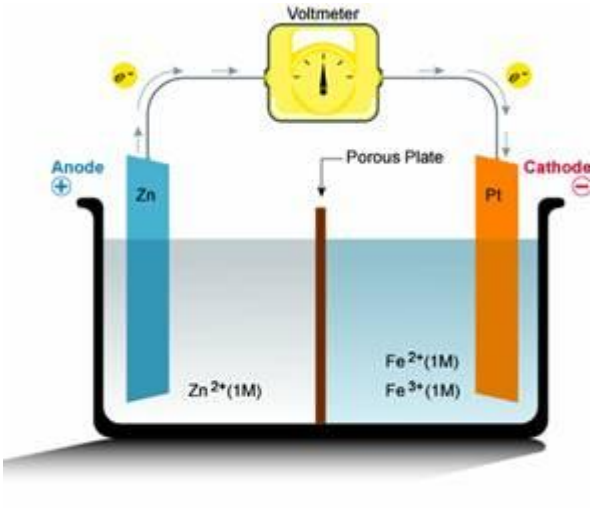

Figure 2.4 Battery cell in which electrolyte reactions is the same for both reactions [8].

The components, which differentiate one battery type from another, are the electrode materials and electrolyte used for both the oxidation and reduction reactions. The electrode/electrolyte interface is the physical location where the redox reaction takes place.

In all battery systems, including lead-acid and alkaline batteries, the electrode is a component in the reaction, being oxidised or reduced in the chemical reactions, while in other electrochemical systems, for example fuel cells, the electrode itself is inert and is only the site for the electron transfer from one reactant to another.

For a discharging battery, the electrode at which the oxidation reaction occurs is called the anode and it has a negative polarity, and the electrode at which the reduction reaction occurs is the cathode and has a positive polarity. However, during recharging of the battery the sites of the oxidation and reduction reactions switch, but by convention the terms anode and cathode refer to the reactions when discharging

The electrode alone is not sufficient for a redox reaction to take place, since a redox reaction involves the interaction of more than a single component. The other chemical components of the reaction are contained in the electrolyte. It is important that the chemical species in the electrolyte are mobile and that they can move to the site on the electrode where the chemical reaction takes place, and that the ions can move between electrodes.

The electrolyte contains reactant species necessary to complete the oxidation and reduction reactions. For example, in Lead-Acid batteries, the sulphate ion from the sulphuric acid electrolyte is essential in the formation of lead sulphate during the discharge process.

2.2.1 Battery Current

The current from the battery arises from the transfer of electrons between electrodes: during discharging oxidation reaction at the negative electrode generates electrons and the reduction reaction at the positive electrode uses these electrons. Therefore during discharge the external load circuit has electron flow from negative to positive electrode, whereas internal to the battery the electron flow, facilitated by electrolyte ions, is from positive to negative electrode.

The redox reactions, from a given battery chemistry, define many fundamental parameters about the battery system, including:

- Maximum battery cell voltage.
- Specific power or energy.
- Temperature dependency

Other key battery properties, including battery capacity, charging and discharging performance are influenced by the physical configuration of the battery, for example the amount of material in the battery and the geometry of the electrodes [9].

2.3 Battery Types

The range of portable, static and transport applications for batteries has given rise to a variety of battery types; table 2.1 lists some of these batteries along with their key performance data.

Battery Type	Electrolyte	Open-Circuit Voltage per cell (V)	On-load Voltage per cell (V)	Energy Density (Wh/kg)	Operating Temperature (^{o}C)
Sealed lead-acid	Sulphuric Acid	2.12	1.50-2.00	18-34	-40 to 60
Unsealed lead-acid	Sulphuric Acid	2.10	1.50-2.00	15-26	-50 to 60
Lithium-ion	Composite (solid) Lithium compounds	3.0	2.7-3.0	130-255	-55 to 150
Sealed nickel-cadmium	Potassium Hydroxide	1.35	1.00-1.25	18-44	-40 to 60
Vented nickel-cadmium	Potassium Hydroxide	1.35	1.1-1.25	26-80	-40 to 90

Table 2.1 Battery data [10].

2.4 Lead Acid Batteries

By far the largest sector of the battery industry worldwide is based upon the 'lead-acid' aqueous cell whose dominance is due to a combination of low cost, versatility and the excellent reversibility of the electrochemical system, in spite of having the lowest energy density of the battery types listed in table 2.1.

Lead acid batteries are the battery of choice for the automotive industry, and is likely to remain so for the foreseeable future, furthermore the lead acid battery is widely used in stationary applications also it is the battery type used in the electric vehicle

mentioned in chapter 1. Therefore the decision was taken to focus the battery section of this thesis only on lead acid batteries.

2.5 Applications of Lead-Acid Batteries

Lead-acid cells are used extensively and can be classified by application as follows:

- Standby (stationary) batteries
- Motor vehicle starting, lighting and ignition (SLI)
- Traction (propulsion) batteries

Batteries, with the exception of specialist applications, fall into two main categories as far as their design is concerned:

1. Starting batteries
2. Deep Cycle batteries

2.5.1 Starting Batteries

The main application for starting batteries is the automotive sector for so-called starting, lighting and ignition (SLI).

Traditionally, a motor vehicle starting, lighting and ignition (SLI) battery is the source of electrical energy for the engine starter motor, for the ignition system (spark ignition engines) and lighting when the vehicle engine is not operating.

A vehicle electrical system typically consists of an alternator, battery, a voltage regulator and the various loads supplied by the alternator/battery. The battery provides smoothing and storage of the output of the alternator, and meets the demand from the starter motor.

Additional loads are now imposed on the stationary vehicle due to security devices such as alarms, In Car Entertainment (ICE) systems, central door locking systems and keyless entry systems which “listen” for a signal from the remote key fob. The result is that a modern vehicle battery can be discharged to below 70% of its normal state of charge following a few days inactivity due to the combined load of the systems outlined above.

SLI batteries are not designed for deep cycling, that is being discharged below 80% state of charge on a regular basis, apart from the demand for engine starting, the SLI battery is normally recharged from the vehicle electrical system following a starting discharge, and once the battery is recharged it then goes onto a so-called float or trickle charge at a regulated voltage set by the voltage regulator on the vehicle electrical system , this maintains the battery at a predetermined voltage by charging at a rate equal to the self discharge rate of the battery thereby ensuring that the battery is maintained at full capacity . Essentially the battery provides storage or capacity in the vehicle electrical system, and meets any instantaneous power demands.

Almost 250 million batteries for starting, lighting and ignition in internal combustion engine vehicles are manufactured annually, using over one-third of the total world output of lead. Such batteries are required to 'turn' engines with high compression, often at low temperatures when the viscosity of the oil is high, resulting in currents of up to 500 amps being required for "cold starting". In addition, the battery must supply power for ignition, lighting, ventilation rear window heaters etc. Most modern car electric circuits employ a nominal 12 Volt system implying the batteries have six lead-acid cells in series, with capacities typically in the order of 40-90 Ampere-hours. Significant improvements in materials and design have resulted in energy densities of SLI batteries of approximately 45 Watt-hours/kg (75 Watt-hours/$dm^{3)}$, while retaining durability and service life. The development of new lead alloys, and innovations in battery design has led to the emergence of the maintenance–free (MF) SLI battery that requires no (or minimal) addition of water during its lifetime, excellent charge retention during storage and no significant terminal corrosion. Due to their large scale manufacture, SLI batteries are relatively inexpensive and are therefore often used quite successfully for other applications, e.g. in emergency lighting units and to provide traction power applications [4].

Lead-acid batteries comprise of a number of cells in order to obtain the required output voltage, the most common arrangement being a nominal 12-volt output containing 6 cells, the arrangement used for Starting Lighting and Ignition (SLI)

duties in passenger and light commercial vehicle. Lead-acid batteries have been progressively refined, and modern batteries are now more durable, and have greater power to weight ratios and lighter cases than their earlier counterparts. They have good power output, are relatively low cost, and are easy to manufacture however, they have do have low specific energy and poor cold temperature performance [11].

2.5.2 Deep cycle batteries

Deep-cycle cells are required for applications where the batteries are regularly discharged, such as photovoltaic systems, electric vehicles (fork-lift trucks, electric vehicles and other) and uninterruptible power supplies (UPS). These batteries have thicker plates that can deliver less peak current, but can withstand frequent discharging [12]. Deep cycle batteries are used for stationary power and traction power, which have different duty cycles to automotive SLI batteries. Traction batteries are subjected to prolonged periods of significant loading, followed by a prolonged recharging period, stationary batteries can also be subjected prolonged discharge and charge cycles.

2.5.3 Stationary batteries

Large battery installations that are called upon only occasionally to supply power, usually in emergency or auxiliary power supply circumstances, are referred to as stationary or standby batteries. Such installations having total capacities in hundreds of ampere-hours are in used particularly in the IT industry, but also maintaining fire, security and communication systems, supplying power to vital production processes or even to supply the power necessary to affect a controlled safe shutdown of a process.

Classic cases of the use of standby power are in an operating theatre and an airport where in the event of a mains failure, power is required for lighting, communications and the operation of vital equipment. Power stations, telephone exchanges, lighthouses and computer installations are other examples of the applications of stationary or standby batteries [13].

The choice of a standby system is between batteries, usually a lead-acid or nickel-cadmium, and generators, or a combination of the two. For many applications, the

battery's ability to provide the power required instantly makes it more suitable. Indeed, even in large installations for which a generator is essential, batteries are often used both to start the generator and provide power for the initial period until the generator is run up to speed.

Batteries are often integral elements of stand-alone renewable power systems to help buffer the stochastic renewable energy supply to a regular demand profile, small scale systems comprising of wind turbines and photovoltaic panels have been used to charge batteries in remote locations, for example on navigation buoys, since the 1960s.

Large-scale battery systems have also been tested in so-called load levelling schemes, which meet demand in the electricity grid, and provide energy storage during periods of low demand. In 1988 Southern California Edison installed a load levelling battery rated at 40 MWh; this lead-acid series-parallel array operates at 2000 volts and can supply the grid with 5000 Amps for up to 4 hours, achieving an output power of 10 MW [4].

Figure 2.5: Lead Acid Plantè Cells for deep discharge stationary applications [14].

2.5.4 Plantè Cells

Figure 2.5 shows Plantè cells, named after Gaston Plantè, who developed the first lead-acid cell. Used in standby power applications, these are deep discharge single cell lead-acid cells which can be routinely discharged from the fully charged voltage of 2.04 to 1.70 volts. This type of cell, along with SLI batteries were used in the experimental work of this thesis.

2.5.5 Traction (propulsion) batteries

The lead-acid battery can also be used as an electric vehicle traction battery where the batteries are either the primary power source as in the case of a Battery Electric Vehicle (BEV), or combined with another power source such as an internal combustion engine or a fuel cell, in the case of a hybrid electric vehicle.

The advantages of the use of electric batteries for vehicle traction are numerous: in addition to improvements to the environment effected by the silent, pollution-free operation of electric vehicles, conservation of oil supplies and a more efficient performance of the mains electricity generating system, brought about by the load levelling due to over-night charging of electric vehicle batteries, would result.

Traction batteries, like batteries used for stationary power applications are deep-cycle types, typically having a prolonged discharge periods during use, followed by long (usually overnight) charging periods.

Electric vehicles have a long history, stretching back to the 1830's, however there is currently no major production line for commercially competitive electric passenger or freight vehicles. The reason for the lack of success of electric road vehicles up to the present lies in the battery specification required in order to deliver a performance, and cost approaching those of internal combustion powered vehicles. The speed, acceleration and range of most present-day electric-vehicles are limited by the low energy and power densities of their traction batteries [4]. However, developments such as the Tesla sports car, this is an all electric sport car produced by the Tesla Motor Company, offers both very good performance and range unlike most of the electric vehicles in production, however it is very expensive with a retail price of 101,000 US dollars [15].

As far as specialised and off-road vehicles are concerned however, electric traction using rechargeable batteries forms a significant sector of this market. The materials handling industry makes extensive use of battery-powered vehicles, ranging from forklift and turret trucks to various tractors. The noise-free, easy starting and simple operation of these vehicles using electronic controls, together with the absence of exhaust fumes, makes them ideal for use in enclosed areas such as warehouses and factories. A wide variety of tractors is needed for baggage, supplies and personnel ('people movers') in airports, hospitals and large industrial complexes. Electric golf buggies and electric wheel chairs are a common sight worldwide. The UK has one of the world's largest fleets of registered electric vehicles. The reason for this is the existence of some 25000 'milk floats', or bottled milk delivery trucks [4].

2.6 The market for Lead-Acid Batteries

In terms of sales, the lead-acid battery occupies over 50% of the entire primary and secondary battery market, with an estimated value of £100 billion per annum before retail mark-up. A total of about three hundred million lead-acid cells are made every year, mainly for vehicle starting, lighting and ignition (SLI), and industrial use including traction and standby power. These range in size from 2 Wh (Watt-hour) cells to 100 Wh SLI systems, and to 40 MWh load-levelling modules such as the one installed in California in 1988 [18].

The wide use of the lead-acid battery in many designs, sizes and system voltages is accounted for by the low price and the ease of manufacture on a local geographical basis of this battery system. The lead-acid battery is almost always the least expensive storage battery for any application, while still providing good performance and life characteristics [16].

It is customary to divide the industrial battery market into two segments: stationary power and motive power. The stationary segment currently accounts for 59% of the total market, leaving 41% for motive power. Forklift trucks account for 95% of the motive power market [17].

Lead Acid batteries are the most common devices to store and deliver electricity in the range 5V to 24V DC [18]. Low price, high availability and ease of manufacture account for the widespread use of the lead acid battery in many designs, sizes, and system voltages.

By far the largest sector of the battery industry is based on the lead-acid aqueous cell whose dominance is due to a combination of low cost, versatility and the excellent reversibility of the electrochemical system. Lead-acid cells have extensive use both as portable power sources for vehicle services and traction, and in stationary applications ranging from small emergency supplies to load levelling systems.

2.6.1 Battery Recycling.

Batteries contain a range of recyclable materials and can therefore be used a source of raw materials.

The collection, processing and reuse (recycling) of used motor vehicle batteries form an important business activity. The regulation of these activities in favour of environmental protection is done via various national directives.

Lead can rightly be termed the classic recycling material. The first facilities for the recovery of lead from used batteries were developed about 100 years ago. In the beginning this was due exclusively to economic considerations, as lead has always been a valuable raw material. With the dramatic growth of automobile traffic, ecological and environmental aspects became increasingly important.

Currently recycling of spent lead-acid batteries is near to 100% as a result of contracts between user and supplier, recycling is not limited to the lead content of the battery. Plastic materials and metal parts can be recycled as well.

For Nickel-Cadmium and Lithium batteries recycling is still in the early stages, in particular cadmium being a dangerous heavy metal requires special recovery processes. [19].

2.7 Battery Ageing and Failure Modes

During the lifetime of a battery, its performance or 'health' tends to deteriorate gradually due to irreversible physical and chemical changes that take place with usage and with age until eventually the battery is no longer usable. Ageing of the battery is a complex process that involves many parameters of the battery (e.g. impedance, conductance, capacity) of which capacity is the most important [20]. However, prior to the battery becoming unserviceable due to loss of capacity as a result of ageing, premature failure can occur due to a number of factors.

The delivery and storage of electrical energy in lead-acid batteries depends upon the cell design, the materials used in construction, and the complex interplay between the multitudinous parameters involved in plate preparation, the chemical composition/structure of the active materials, and the duty/conditions of battery operation. It is not surprising therefore that the factors responsible for the degradation of battery performance, and eventual failure, are many and varied.

A distinction has to be made between catastrophic failure as characterised by a sudden inability of the battery to function, and progressive failure, as demonstrated by some more subtle deviation from optimum performance [21].

There are a number of conditions, which lead to battery failure, some of which are [22]:

- Sulphation
- Loss of Active material
- Loss of electrolyte
- Loss of Water
- Short Circuiting
- Electrolyte stratification
- Cell reversal.

2.7.1 Sulphation

Lead sulphate is a by-product of battery operation (charge and discharge) and if not removed, it will slowly and continuously reduce battery capacity, increase electrical resistance, reduce the operating voltage, and ultimately cause the battery to fail. The problem of sulphation affects all types of lead acid batteries. Sulphate build-up occurs in the form of lead sulphate crystals on the battery plates during the normal charge/discharge cycles. Lead-acid batteries generate electricity through using a sulphate forming chemical reaction. When the battery discharges, lead and lead dioxide, which are the active materials on the battery's plates, react with the sulphuric acid in the electrolyte to generate electrical current. A finely divided, amorphous form of lead sulphate is produced. If the battery is quickly recharged, most of the lead sulphate is changed back to the lead/lead dioxide of the fully charged battery.

However some of the lead sulphate will remain on the battery plates which over time builds up as a hard crystalline structure, with repeated use, the ability of a battery to reach a full charge gradually diminishes. This process is known as sulphation. The rate at which sulphation occurs depends on factors such as:

- The length of time that the battery remains discharged after use
- The depth of discharge
- The temperature of the battery during operation

During this process, some of the sulphate crystals enlarge to the point where they can't accept energy so they stay on the plate in a very stable crystalline form of lead sulphate. Over time these sulphate crystals can build-up, reducing the area of active material (lead/lead dioxide) on the plates, until the battery becomes incapable of powering its external load and is unserviceable. This process of sulphation is the most common cause of lead acid battery problems and failures. Sulphation can be minimised by keeping the battery fully charged in order to reduce the build-up of lead sulphate, and by not exposing the battery to high ambient temperatures.

2.7.2 Electrolyte Stratification

As the battery is discharged the acid is converted to water and as sulphuric acid has a higher density than water, therefore as the battery discharges the electrolyte becomes less dense. As long as the acid and water components behave as an evenly mixed homogeneous solution, the battery behaves as expected, but if the acid and water separate into layers due to the differing densities of the acid and water, battery performance can be adversely affected. This is known as stratification.

Stratification tends to occur if the charging voltage is too low, and the battery is not fully charged when it is put under load and discharged. This situation can occur where battery chargers and vehicle alternators are faulty. Also if a battery is left unused for extended periods, the more dense acid will gravitate to the lower region of the battery.

Stratification can be eliminated by charging the battery at a higher than normal voltage which will induce “gassing” at the battery electrodes, and the bubbles agitate the electrolyte solution, thus mixing the acid and water. This is sometimes referred to as an “equalisation charge”. This process must be carefully controlled to prevent excessive heating which can damage the battery in the form of warping of the battery plates, which can also result in short circuit of one or more of the cells.

SLI batteries do not tend to suffer as much from stratification as stationary batteries due to vibration arising from the motion of the vehicle, engine vibration and occasional jarring and tilting due to road surfaces and inclination. However,

excessive vibration can be harmful, dislodging material from the battery plates and increasing the rate of sludge formation in the battery.

2.7.3 Loss of Active (Plate) Material

The rectangular grid style design of the lead-acid battery is prone to deterioration due to the cyclic nature of battery operation. As the battery discharges and recharges there is heat cycling with expansion and contraction of the grids, also the formation of the lead sulphate deposits on the electrodes (plates) during discharge, and the subsequent deconstruction of the lead sulphate during recharging. This constant cycling results in fragments of material breaking away from the supporting grid. As the quantity of plate material diminishes, so does the battery's output, when the effective plate area is substantially diminished the battery's capacity falls as the reduced area of active material is not capable of sustaining a useful output.

A further problem associated with this loss of paste material is that it can become lodged between the positive and negative plates sandwiched into the battery structure, creating a short circuit leading to rapid discharge of the cell, rendering the battery unserviceable.

2.7.4 Loss of Electrolyte

Loss of electrolyte can occur by damage to the casing of the battery or spillage from the battery, primarily due to inappropriate use or neglect of the battery. Lead acid batteries which have so called "immobilised" electrolytes such as Gel or AGM batteries can tolerate harsher environments than the flooded or wet cell batteries, for example in motor-sport applications or in aviation where there may be substantial degrees of inclination from the vertical, and, in the case of military or sport aviation complete inversion.

2.7.5 Loss of Water (Dry-out)

This is associated with the recharging of the batteries where gassing can occurs, that is evolution of hydrogen and oxygen as a result of electrolysis of the water component of the electrolyte. Essentially the battery, which is a galvanic cell,

becomes an electrolytic cell when evolution of hydrogen and oxygen takes place as a result of the charging process.

Electrolytic cells are electrochemical cells, designed for the purpose of electrolysing solutions and separating them into their component parts by passing an electrical current, supplied from an external source through the electrolyte solution. The most well known application of electrolysis is the electrolysis of water; however, electrolysis is widely used in industrial processes for example the manufacture of aluminium [23].

The water in the battery electrolyte breaks down into its two components that is hydrogen (H_2) and Oxygen (O_2).

$$2H_2O(l) \rightarrow 2H_2(g) + O_2(g) \qquad 2.1$$

"Gassing" occurs to different degrees in batteries, this is determined by the nature of the electrode materials, and what is termed the hydrogen overvoltage. The lead-antimony alloy used recently in SLI batteries is more prone to gassing than the lead-calcium alloy used in modern units. This loss of water, also known as "dry out" due to the gassing or more correctly electrolysis of the water should be minimised to prevent damage to the cells in the battery [24].

During the recharging of the lead-acid battery the charging voltage has to be regulated to prevent the cells in the battery attaining a voltage where gassing can take place. It is difficult however, to eliminate gassing particularly in non-sealed or open vented batteries, and it is therefore necessary to periodically replenish the electrolyte level with distilled water, often known as "topping up".

Valve Regulated Lead Acid (VRLA) batteries are used mainly in SLI applications where there are known as maintenance-free batteries They use recombination technology whereby all of the Oxygen gas evolved at the positive electrode is reduced at the negative electrode, and vice versa for the hydrogen, this virtually eliminates loss of liquid to the external environment and therefore water loss is eliminated which negates the requirement for refilling or "topping up".

2.7.6 Short Circuiting

Short-circuiting can be either external or internal. External short circuits can destroy a battery, if the energy stored in a battery is discharged in a very short period a

considerable amount of heat is generated. A fully charged 12 volt 75 Amp-hour lead-acid automotive battery contains 3,240,000 joules of energy, and a short circuit across the battery terminals could cause rapid build up in the pressure in the battery casing resulting in rupture of the battery casing, and even fire to break out due the heat generated by the high short circuit current. Batteries are tested to ensure that short duration short circuits do not cause catastrophic failure of the battery, however, even if the battery itself survives wiring or components in the external circuit may overheat and fail with potentially serious results.

Internal short circuits can be caused by the deterioration of the battery internal cells. As the battery ages the paste, which is embedded in the grids of the electrodes, can break away from the grid and may bridge the gap between the positive and negative plates resulting in an internal short circuit. Lead sulphate formed during discharge exacerbates this condition, often leading to the formation of sludge which lies at the bottom of the battery. As the sludge level rises the possibility of the lower edges of the plates being short circuited becomes greater.

This internal short circuit will quickly discharge the cell rendering the battery unserviceable.

Short circuits can also be caused by subjecting the battery to excessive heating, for example due to charging at too high a voltage, causing the plate to warp or buckle, which may then result in contact between positive and negative plates, short circuiting the cell of the battery.

2.7.7 Cell Reversal

Cell reversal is the phenomenon associated with the continued forcing of a large discharge current through a completely discharged cell within a string of cells that have not yet reached an overall capacity limit or cut-off voltage. This is reported by S.Perone [25] in a study arising from the concerns regarding the occurrences, in long strings of lead acid cells, of cell reversals.

Cell reversal is a process confined primarily to high-voltage, multi-cell battery stacks, either primary or secondary battery stacks. Although it may occur in low-voltage, series-connected stacks, it is less likely in such batteries because of the

voltage cut-off requirements. When one cell becomes exhausted the voltage falls below useful service levels and the batteries are disconnected from their loads [26].
There are a number of dangers inherent in over-charging or over-discharging lead acid battery cells, as is relatively well known. What are less well known are the problems that can result from the charging or discharging of long series connected strings of lead acid cells. Without adequate controls a few cells of a long string of series connected cells could be permanently damaged during normal operations; moreover, it is possible that facility damage could result. The dangers of over--discharge include permanent capacity loss and ultimately cell reversal [27].

Manufacturing processes cannot ensure that each cell has identical capacity; therefore even in a new battery some cells may be have less capacity and therefore are effectively 'weaker' than other cells in the battery.

A common cause of failure in SLI batteries is failure of a single cell leaving the battery unserviceable. However a 'weak' cell in a long string of series connected batteries could be driven into reversal without making the entire battery pack unserviceable; consequently the reversed cell will absorb power from the battery pack which in turn results in heat generation and potentially serious failure.
Cell reversal in batteries has implications in terms of safety, as series arrangements of batteries are used in many applications. Typically series connected batteries are found in electric vehicles, solar power installations, emergency power supply and uninterruptible power supplies (UPS). Occurrences of cell reversals in these installations could be catastrophic.

This thesis is based on work carried out for an electric hybrid vehicle which uses both batteries and fuel cells in its power supply. Both batteries and fuel cells give DC electrical output and are modular and scalable and therefore there are similarities in terms of monitoring requirements, which is the subject of this thesis. However, unlike lead acid batteries, fuel cells are currently not in widespread use, although this

may change in the not to distant future as the demand for more efficient and environmentally friendly power sources gathers momentum.
Cell reversal can also occur during the operation of fuel cells when configured in multiple cell arrangements, that is a fuel cell stack, and a cell reversal and as in the case of batteries can result in the catastrophic failure of a fuel cell stack.

2.8 Fuel Cells

Fuel cells continuously produce a work output (electrical work) as long as they are supplied with fuel, typically hydrogen gas and oxygen (supplied from the air).
In fuel cells the cathodic and anodic reagents usually gases are stored externally and can be supplied to the electrochemical fuel cell on a continuous basis.
Fuel cells are direct electrochemical energy conversion devices and share some common characteristics with batteries; in fact fuel cells combine many of the advantages of engines and batteries. However, they also currently have some serious disadvantages in particular cost per kW and fuel storage.

Unlike combustion heat engines, electrochemical energy generators allow the direct conversion of chemical to electrical energy, and are likely to have a significant role to play in any future energy scenario not entirely dependent on fossil fuels.

Fuel cells and batteries, are both electrochemical devices, the difference being that a fuel cell requires a continuous supply of fuel, whereas a battery operates without any ‘fuel input’, however the battery requires to be charged once depleted, and the constant cycle of charging and discharging degrades the battery until eventually the battery is degraded and is unable to sustain its load.

In order to gain an understanding of the principles of electrochemical generators and the maximum electrical potential that can be generated in a reaction it is necessary to understand the interrelationship between the energy transformations and the chemical reactions inherent to the functioning of these devices.

Fuel cells are electrochemical devices that convert the chemical energy of the reactants directly into electrical energy and heat, without combustion as an intermediate step. There are similarities between fuel cells and batteries, i.e. both systems have two electrodes separated by an electrolyte and electrical energy is generated by the cell reaction. Unlike batteries, in a fuel cell the reactants are supplied from an external source, and the fuel cell will continue to operate as long as it is supplied with fuel and oxygen. In addition battery performance deteriorates when the charge level drops, whereas a fuel cell continues to operate at a constant load so long as fuel is supplied [28].

Sir William Grove invented the first working fuel cell in 1838. Fuel cells were further developed by a number of researchers, including Francis Bacon, a chemical engineer at Cambridge University, who in the1950s demonstrated the first practical fuel cell system to the Royal Navy, for applications in submarines.

Bacon started his important work on alkaline fuel cells in the 1930s, which lead to the development of a 5kW unit and the 15kW tractor of Allis Chalmers Manufacturing. Finally Pratt and Whitney licensed the Bacon patents and built the power units for NASAs Apollo capsules. The fuel cells were ideal in this regard because they have rising efficiency with decreasing load (unlike heat engines), hydrogen and oxygen gases were already on board the ship for propulsion and life support and the by-product water could be used for drinking and humidifying the atmosphere of the capsule. Although interests in fuel cells decreased strongly after the Apollo programme was abandoned, NASA continued to improve their alkaline system for their space shuttle (Orbiter). Today, their system is considered fully developed, which can be seen by the fact that there is no back-up electric power installed on the space craft. The cost is still quite high, but this is compensated by a high lifetime of 5000 h and more. This might not look much, but it equals more than 20 space flights [29]. This led to extensive research into fuel cell technology for use in outer space vehicles, initially for the Apollo programme, and as currently used in the space shuttle. Some types of fuel cells are shown in table 2.2.

The most common classification is by the type of electrode used in the fuel cell [30]. A fuel cell consists of an anode supplied by a gaseous fuel (hydrogen) and a cathode supplied by an oxidant (usually air or oxygen), separated by either an acidic or alkaline electrolyte. In an acid fuel cell (with acidic electrolyte), the hydrogen fuel at the anode dissociates into hydrogen cations and electrons. The hydrogen ions travel through the electrolyte to the cathode because of the electric field, while the electrons flow around the external load circuit to the cathode. At the cathode, the oxygen accepts the electrons to form oxide ions, and then it reacts with the hydrogen ions to form water. In an alkaline cell, the reaction path is the reverse, and the fuel/oxidant reactions occur at the anode.

A fuel cell is not a battery; it produces electricity, but is not an energy storage device as in the case of a battery. Unlike heat engines, fuel cell efficiency is not limited by Carnot cycle efficiency, with efficiency of energy conversion of 50% compared to 18% for an internal combustion engine [31].

Electrochemical fuel cells offer a number of benefits that make them appealing for transportation and also static power applications. Individual fuel cells are combined to form stacks to provide useful power outputs, and are regarded as potential alternatives to heat engines, for mobile and static power systems. The efficiency of fuel cells for generating electricity is 40%–60% and can reach 85%–90% in a CHP (combined heat and power) mode, i.e. if the heat generated from the fuel cell is also used [32]. Fuel cells emit low or zero emissions, and low noise levels [33]. The fuel cell, then, promises to be efficient, quiet, reliable, maintenance free and clean in operation; it compares favourably in these respects with mechanical means of electricity [34].

Fuel Cell Classification			
Type	Electrolyte	Operating Temperature (^{o}C)	Principle applications
Alkaline fuel cell	Potassium hydroxide	50 - 200	Transport, space exploration.
Solid oxide fuel cell	Zirconium oxide	750 - 1000	Power generation and heat
Proton Exchange Membrane fuel cell	Poly-perfluoro sulfonic acid	25 - 100	Transport
Molten carbonate fuel cell	Lithium and potassium carbonates	600 - 700	Power generation and heat
Direct methanol fuel cell	Poly-perfluoro sulfonic acid	70 - 100	Transport
Phosphoric acid fuel cell	Phosphoric acid	180 -200	Power generation.

Table 2.2: Fuel Cell by Type [35].

2.8.1 Fuel Cell Operation

The electrolysis of water, whereby water is broken down into its constituent parts is a reversible process, that is, it is possible to recombine hydrogen and oxygen at two electrodes to form water. Taking the example of the Alkaline Fuel Cell Hydrogen gas is supplied to one of the electrodes, where it reacts in the presence of a catalyst and the electrolyte to form hydrogen ions (H^{+}). Oxygen, supplied to the other electrode, reacts with water from the electrolyte to form hydroxyl ions, (OH^{-}). The H^{+} and OH^{-} combine in the electrolyte to form water. At the hydrogen electrode, electrons are released, and the electrode becomes negatively charged. Electrons are absorbed from the oxygen electrode, making it positively charged. Figure 2.6 shows the basic configuration of a fuel cell [36].

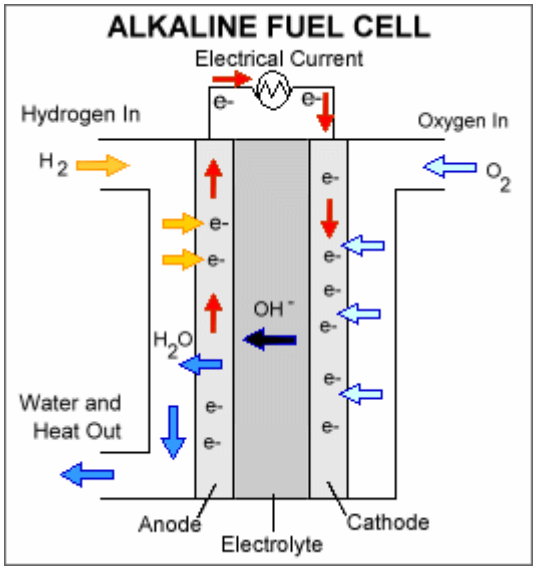

Figure 2.6: Basic configuration of a fuel cell [37].

The ideal performance of a fuel cell is defined by its Nernst potential, E, or the ideal cell voltage. The ideal standard potential (E_o) for a fuel cell in which H_2 and O_2 react is 1.229 volts with liquid water product, or 1.18 volts with gaseous water product.

To achieve a high power density (W/kg) the fuel cell stack should be operated at current densities above 300 m/cm^2 [38]. However, the current cannot be increased at will, as the power output will reach a maximum due to falling voltage as shown in figure 2.7.

The characteristic shown in figure 2.7 is common to all fuel cells types, it just happens to be a Proton Exchange Membrane (PEM) fuel cell characteristic that is shown in this figure.

After this maximum the power output will decrease with increasing current density. The maximum power density of a fuel cell stack is highly dependant on the operating parameters.

With increasing current density the following aspects have to be considered [39].

- The fuel cell efficiency decreases along with decreasing fuel cell voltage.
- The amount of heat, which has to be removed from the system, increases proportionally.
- The supply of the reactant gases is proportional to the current.
- The uniformity in cell voltages decreases.

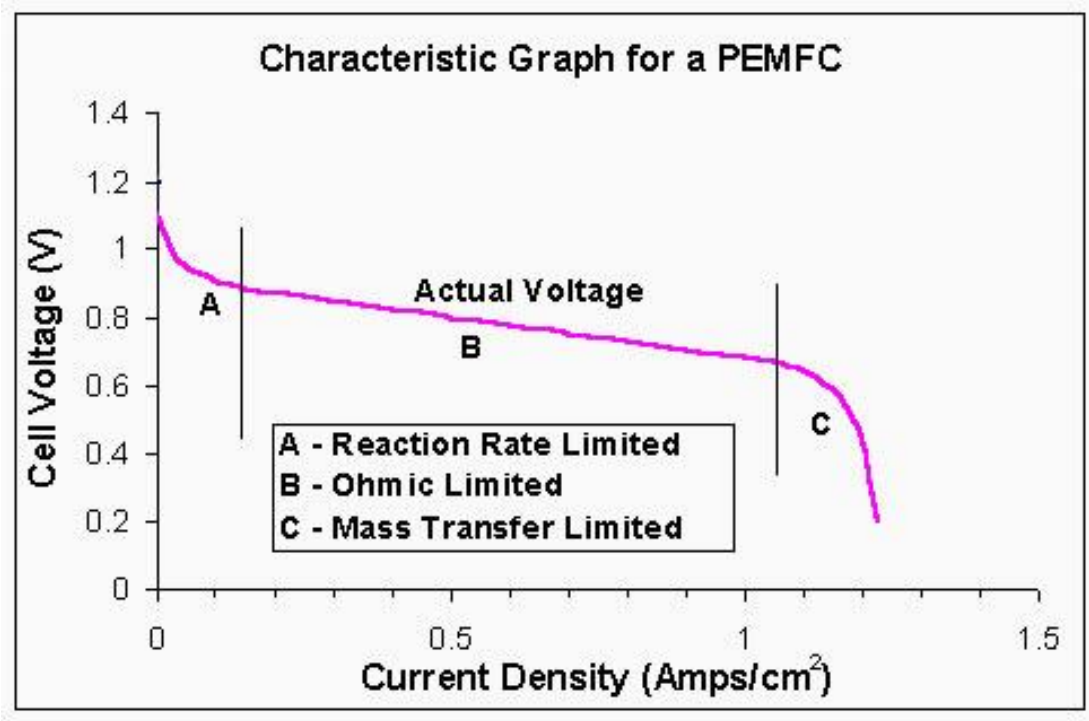

Figure 2.7: Fuel Cell Voltage Current Characteristic [40].

2.8.2 Fuel Cell Construction

Fuel cells are similar to batteries in their construction in that they usually comprise a number of individual cells connected together to form what is referred to as a fuel cell stack.

The cells are connected in series/parallel configuration to give the desired operating voltage and current.

2.8.3 Alkaline Fuel Cells

The fuel cell used in this research was an alkaline fuel cell type. An alkaline fuel cell converts the chemical energy of compressed hydrogen and oxygen into electricity and heat. It uses a solution of potassium hydroxide (KOH) as the electrolyte; in the cells hydroxyl ions OH^- migrate from the cathode to the anode. At the anode, hydrogen gas reacts with the OH^- ions to produce water and release electrons. Electrons generated at the anode supply electrical power to an external circuit then return to the cathode, where the electrons react with oxygen and water to produce

more hydroxyl ions, which then diffuse into the electrolyte. The overall reaction for the alkaline, and indeed, all fuel cell types is:

$$2H_2 + O_2 \Leftrightarrow 2H_2O \qquad 2.2$$

For an alkaline fuel cell this can be broken down into the two half cell reactions, at the anode and cathode respectively as shown in table 2.3.

Fuel Cell	**Anode Reaction**	**Cathode Reaction**
Alkaline	$H_2 + 2(OH)^- \rightarrow 2H_2O + 2e^-$	$½\ O_2 + H_2O + 2e^- \rightarrow 2(OH^-)$

Table 2.3: Alkaline Fuel Cell reactions

The cell layout of an alkaline fuel cell is shown in figure 2.8.

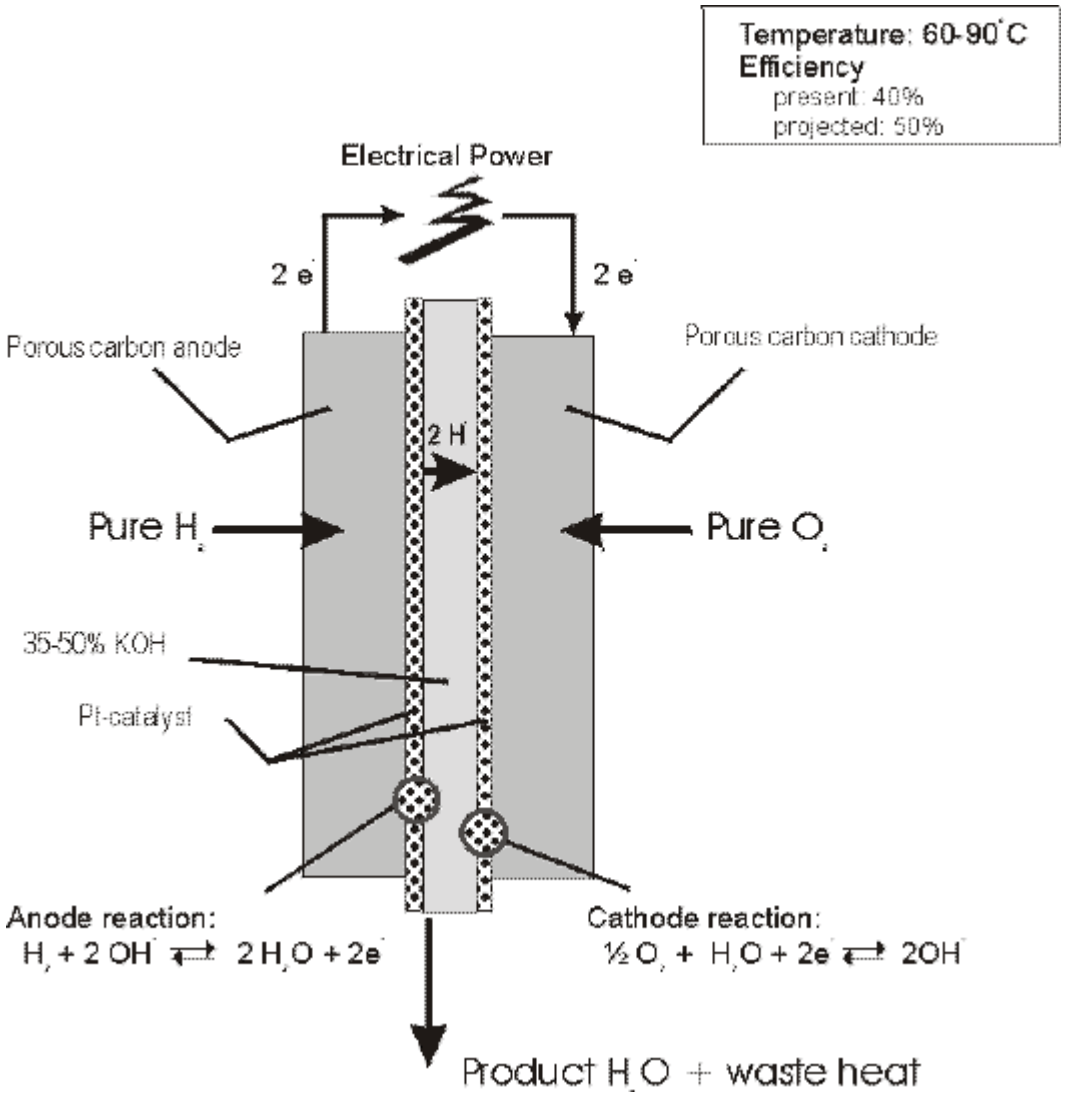

Figure 2.8: Operation of an alkaline fuel cell [41].

The alkaline fuel cell is a relatively simple device, and was the first type of fuel cell to be developed. An alkaline electrolyte such as potassium hydroxide is used with an activated nickel or other precious metal electrode. The electrolyte has excellent electrochemical properties but reacts with carbon oxides, which reduces performance; the cell is usually limited to operation with pure hydrogen and air, with the CO_2 removed by employing a soda lime scrubber.

Early systems operated at about 200^{o}C and 20 to 40 bars pressure. During the 1980s low-temperature operation (60 to 80^{o}C) was greatly improved, enabling rapid start-up, which is valuable feature for transport applications.

A major disadvantage is that alkaline cells need very pure hydrogen. The presence of impurities such as carbon dioxide (CO_2) in the oxygen/air supply can result in chemical reactions, which lead to the formation of a solid carbonate that disrupts the chemical reactions inside the cell. Since most methods of generating hydrogen from feedstock fuels produce some carbon dioxide, this requirement for pure hydrogen has slowed work on alkaline fuel cells in recent years.

2.9 Fuel Cell Ageing and Failure Modes

Fuel cells in common with other engineering systems, inevitably suffer problems related to ageing and can experience premature failure before the expected end of life period. There are particular weaknesses associated with fuel cell stack construction that can lead to failure.

The durability of low temperature fuel cells (AFC and PEMFC) is a critical issue to overcome. The targets for fuel cell durability required for mobile and stationary fuel cells have been determined by the U.S. Department of Energy to be 50000 and 40000 working hours, respectively. Issues to be overcome include electrolyte leaking and Carbon Dioxide poisoning [42].

2.9.1 AFC Failure Modes

Interest in the alkaline fuel cell, which has been in the shadow of the PEMFC for many years, rose again recently, as the development of low cost PEMFCs took more efforts than expected. Especially for medium-size systems (0.5-50 kW), the simplicity of AFCs with liquid electrolytes (like heat and water management) and their capability of being started up fast and being shut down for long periods, caused some companies and institutions to concentrate on this system. The main task was to increase the long-time stability of the AFC electrodes, which usually showed lifetimes of only a few thousand hours.

The decrease in performance during operation is mainly caused by wetting of the electrodes. The electrolyte slowly fills up the pores and this increases the diffusion path for the reaction gases to the reaction sites: a drop in cell voltage occurs. By improving the electrode structure, especially the hydrophobic agents, this effect can be diminished [43].

Improvements in materials and manufacturing processes offer the prospect of improved reliability in AFCs, some of the improvements which could be implemented are shown in table 2.4 [44].

Component	Existing material	Limitations to existing material	Proposed change
End plates	Plexiglass	Temperature/strength	Polyphenylene Oxide (PPO) or Polyphenylene Sulphide PPS
Frame	Epoxy	Temperature	PPO or PPS
Separator	PVC	Low flow temperature	Teflon
Current collector	Ni mesh	Bonding to carbon	Perforated Ni Foil
Gas diffusion layer	Carbon, PTFE	Not applicable	Not applicable
Active layer	Carbon, PTFE, catalysts	Not applicable	Not applicable
Anode catalyst	Micron-size PdCuMn	Expensive, large catalyst size	Nano-size Rancy Ni powder
Cathode catalyst	Micron-size Ag, AgMn, PdCuMn	Poor chemistry, large catalyst size	Nano-size Ag powder
Connectors	Small diameter	High resistance	Use busbars to increase cross-sectional area
Electrode design	Flat surface, no flow channels	Non-uniform electrolyte distribution	Add electrolyte flow channels
System design	Use of ‘glue’ and gasket to seal the electrodes together	Electrolyte leakage	Injection moulding

Table 2.4: Possible replacement for existing materials in an AFC

A fault commonly found in fuel cells in failure of gasket seals which separate the gas flow paths in the fuel cell. Husar et al reported on such a failure in a 7 cell PEMFC [45].

The Alkaline fuel cell (AFC) used in this thesis suffered from a similar failure, however, repairs were carried out, the gaskets replaced and as a result the performance of the stack was restored to normal operating conditions.

2.9.2 PEMFC Failure Modes

Failure modes for PEM fuel cells are not well documented and degradation causes and mechanisms are not fully understood. There are some factors known to affect the life of PEM fuel cells.

1. The mass transport properties degrade as a result of the accumulation of excess water in the gas diffusion pores.
2. Impurity ions affect the membrane proton conductivity and oxygen reduction kinetics.
3. It is possible that one or more membrane-electrode assemblies (MEAs) in a stack, or even a complete stack in a multi-stack system, will show a reverse in polarity during fuel cell operation [46].
4. PEMFC suffer from problems associated with the mechanical endurance of the proton exchange membranes and membranes electrode assemblies (MEA) as reported by Huang et al [47].

2.9.3 Cell Reversal in Fuel Cells

As discussed above, a reversal of polarity is a failure mechanism which is applicable to fuel cells. As soon as one cell cannot support the current drained from the stack the cell voltage will be reversed. The other cells still in normal operation, force a current through the damaged cell, but the normal reactions (O_2 reduction and H_2 oxidation) do not proceed but O_2 and/or H_2 evolution starts. The typically carbon based-electrodes cannot support gas evolution very long and mechanical damage

results. To prevent cell reversal, a careful control of all cells during production and also operation is necessary [48].

Various circumstances can result in a fuel cell being driven into reversal by other cells in the series stack. Irreversible damage may be caused to the MEA by such cell reversal incidents. The most damaging source of cell reversal is reactant starvation, an inadequate supply of fuel, to the membranes electrode assemblies (MEA) at the anode. Fuel and oxidant starvation can occur during a sudden change in reactant demand such as start-up and load change [49].

By monitoring individual cell voltages it is possible to take action to prevent cell reversal occurring. The design and implementation of a cell voltage monitor for an alkaline fuel cell stack is described in Chapter 5 of this thesis. There are two methods of measuring cell voltages shown in table 2.5

Principle	Direct voltage measurement	Cumulated voltage measurement
Advantage	Direct measurement, low resolution is possible	Low complexity
Disadvantage	Voltage difference measurement with higher complexity	Result only after calculation, larger resolution is necessary

Table 2.5: Possible methods of resolution for single cell voltage measurements [50].

In terms of the options for cell voltage monitoring table 2.6 summarises three possible solutions.

Possible Solutions	Switching by relays	Switching by semiconductors	Direct measurement by AD-convertors
Advantage	Ease of galvanic separation, simple construction	Unlimited switching cycles, simple construction.	Each value in digital form.
Disadvantage	Limited switching cycle	Galvanic separation is necessary	Requires a large expensive circuit board space

Table 2.6: Advantages and disadvantages of the possible voltage acquisition systems [51].

Examples of each type in table 2.6 are given in table 2.7. Switching by semiconductors is the subject a paper entitled "Measuring individual cell voltages by Webb and Moeller-Holst [1] the other two methods are embodied in the author's CVM1 and CVM2 designs are discussed in more detail in Chapter 5.

Switching by relays	Switching by semiconductors	Direct measurement by AD-convertors
Cell voltage monitor 1 (CVM1) by Author	Measuring individual cell voltage in fuel cell stacks [1].	Cell voltage monitor 2 by Author
	Multi-channel voltage control for fuel cells [51]	

Table 2.7: Examples of cell voltage acquisition systems.

Comparison of the cell voltage acquisition systems is the subject of a journal article by Mulder [51], where lab based systems similar to the examples in table 2.7 are compared with commercial systems. The commercial system used in this paper was a 'Cellsense' [52] cell voltage monitoring system, which uses one analogue to digital convertor per 4 cells. This has the advantage that

- It makes the monitor modular, i.e. as many convertors as desired can be added, so that it is easily adaptable to the stack size;
- It resists a high common mode voltage, accordingly it can be used in large stacks or multi stack configurations;

Cell voltage monitoring in the lab based systems such as CVM1 and CVM2 and the system developed by Webb [1] have slower scan rates than systems such as CellSense, due to their use of low cost multiplexers. However, the greater scan rate of the CellSense system is at the expense of a significantly greater cost compared to the low cost systems such as CVM1. This is discussed further in Chapter 5.

2.10 Chapter Conclusions

This chapter has provided information on both batteries and fuel cells in terms of the types available, applications and failure modes.

Cell reversal was identified as being one of the failure mechanisms which affects both batteries and fuel cells, and the requirement for individual cell voltage monitoring for a fuel cell stack was discussed.

CHAPTER 3 ELECTROCHEMICAL POWER SOURCES.

In order to convert energy into useful work more efficiently than the combustion heat engine, a different approach to energy conversion is required. Electrochemical power sources have an advantage over combustion heat engines, as they convert chemical energy directly to electrical energy, without the intermediate process of converting chemical energy into heat required by combustion heat engines.

There are two significant types of electrochemical power sources, which produce electricity by reactions within electrochemical cells.

1. Fuel cells
2. Batteries

Fuel cells and batteries, are both electrochemical devices, the difference being that a fuel cell requires a continuous supply of fuel, whereas a battery without any continuous fuel input, however the battery requires to be charged once depleted, and the constant cycle of charging and discharging degrades the battery until eventually the battery is degraded and is unable to sustain its load.

The term battery is used widely used to describe single or multiple cells arranged to give a range of voltage outputs. The cells used are collectively called galvanic cells; galvanic cells can be of two main types:

1. Primary cells
2. Secondary cells

Primary cells can only convert chemical energy into electrical energy, whereas secondary cells can convert chemical energy into electrical energy, and convert electrical energy into chemical energy.

3.1 Galvanic Cells

Galvanic cells (also referred to as Voltaic cells) are cells in which spontaneous reactions produce electrical energy. When a metal is placed in a liquid there is in general a potential difference established between the metal and the solution due to the metal yielding ions to the solution, or the solution yielding ions to the metal. In

the former case, the metal will become negatively charged with respect to the solution, in the latter case, the metal will become positively charged with respect to the solution.

3.1.1 Parameters that Influence the Cell reaction

There are two groups of parameters that have to be considered:

1. Thermodynamic or equilibrium parameters describe the system in equilibrium, when all reactions are balanced. In the electrochemical cell this applies when no current exists. This means that these parameters represent maximum values that only be reached under equilibrium conditions.
2. Kinetic parameters appear when the reaction occurs. These parameters are connected to current flow and they always aggravate the values given by the thermodynamic data. Kinetic parameters include mass transport by migration and diffusion, which is required to bring the reacting substances to the surface of the electrode. Furthermore, the voltage drop, caused by current flow in electron or ion conductors, is included in kinetic parameters. Kinetics parameters are influenced by design parameters of the cell, such as thickness and spacing of the electrodes [53].

During the operation of a galvanic cell a chemical reaction occurs at each electrode, and it is the energy of these reactions that provides the electrical energy of the cell.
When two electrodes of dissimilar metals are immersed in a conducting electrolyte and a wire connects the two electrodes, and then a current will flow.
At the surface of separation between electrode and the electrolyte solution there will be a potential difference called the electrode potential. The electromotive force (e.m.f.) of the cell is equal to the algebraic sum of the two electrode potentials [54].

Thermodynamic analysis of galvanic cells requires that the cell behaviour is reversible. A reversible cell must satisfy certain conditions:

1. When the cell is connected to an external source of e.m.f., and adjusted to balance that em.f. so that no current flows, there should be no chemical or other change in the cell.
2. If the external e.m.f. is decreased by an infinitesimally small amount, current will flow from the cell, and a chemical or other change, proportional to the electrical energy change of the cell will occur.
3. If the external e.m.f. is increased by the same amount, the change should be reversed.

Therefore galvanic cells can only be considered to be reversible when the currents passing are infinitesimally small, so that the system is always virtually in equilibrium. If large currents flow concentration gradients arise in the cell as diffusion is relatively slow; under these conditions the cell cannot be regarded as being in a state of equilibrium, therefore this will apply to most practical battery applications as the currents will be greater than the infinitesimal values required for reversible conditions.

3.1.2 Operation of Galvanic Cells

A galvanic cell is made by bringing together certain chemicals; whose reactions maintain the electric current taken from the cell by an external load.

The essential components of a galvanic cell are a positive and negative electrode, an electrolyte, a separator and a housing (or container). The positive and negative electrodes have to be as close as possible to each other in order to minimise the internal resistance of the cell. Typically this internal resistance is of the order of milliohms (mΩ), so that the voltage drop across the cell is not too great when drawing heavy currents. The internal resistance of the cell has two components:

1. The resistances of the electrode/electrolyte interface.
2. The resistance of the electrolyte.

In practice the relationship between the available voltage or Open Circuit Voltage (OCV) and the on-load or Terminal Voltage is given by equation 3.1

OCV = Terminal Voltage (V) + [Current (I) x Internal Resistance (R)] 3.1

Even with the best ion-conducting electrolytes, a low internal resistance is possible only when the separation between the electrodes is restricted to about 1 mm. The separator is a thin, usually porous, insulating material whose role is to prevent the two electrodes from touching each other and thereby, short circuiting the cell. Without the separator short-circuiting would either occur on cell assembly, or during extended operation. The pores of the separator are filled with electrolyte and the ionic current is conveyed through their pores. When there is excess of liquid electrolyte, the term 'wet' or 'flooded' cell is used, but if the electrolyte is immobilised within the separator the term starved electrolyte cell is sometimes used.
Separators in modern automotive batteries are made from pvc (polyvinyl chloride), which has good porosity and strength in the acidic environment of the battery cell. The essential features of a separator are:

1. High porosity; this ensures low resistance to passage of current between the plates and free diffusion of the acid.
2. Good insulation, to prevent metallic conduction between plates of opposite polarity.
3. It must be inert to the action of the sulphuric acid and electrochemical oxidation.
4. Absence of harmful impurities.

3.2 Standard Electrode Potential

The basis for an electrochemical cell such as the galvanic cell is always a redox (reduction-oxidation) reaction, which can be broken down into two half-reactions:
Oxidation at the anode (positive terminal) that is the loss of electrons.
Reduction the cathode (negative electrode) that is gain of electrons.
Electricity is generated due to the electrical potential difference between two electrodes. This potential difference is created as a result of the difference between the individual potentials of the two metal electrodes with respect to the electrolyte. Although the overall potential of a cell can be measured, there is no simple way to

accurately measure the individual electrode/electrolyte potentials in isolation. The electrode potential also varies with temperature, concentration and pressure. The standard electrode potential (E^o) is the measure of individual potential of Any electrode at standard ambient conditions (298K, solutes at 1M and gases at 1 bar) As the oxidation potential of a half-reaction is the negative of the reduction potential in a redox reaction, it is sufficient to calculate either one of the potentials. Therefore, standard electrode potential is commonly written as standard reduction potential.

3.2.1 Standard Electrode.

By convention, the potential of the hydrogen electrode under standard conditions, which are:

- an electrolyte of sulphuric acid, 0.5 molar concentration
- a pressure of 101.3 kPa
- a temperature of 25^{o}C

is set at zero volts. All electrode potentials are referred to this so-called Standard Hydrogen Electrode (SHE).

When the electrode under measurement is also in a standard state the Standard Electrode Potential (E^0) is obtained. The signs of electrode potentials are derived on the basis of reduction processes. Therefore the positive electrode of a cell, which undergoes a reduction reaction during discharge, for example the lead-acid cell discharge, has a positive potential; whereas the negative electrode, which experiences an oxidation reaction, has a negative potential.

The difference between the potentials of the positive and negative electrodes gives the reversible voltage or open circuit voltage of the cell; that is the voltage across the terminals when there is no net current flow. Under standard conditions this is the cell voltage (V^0). Therefore for the lead-acid battery:

$$V^0 = 1.690 – (-0.358) = 2.048 \text{ Volts.}$$

3.2.2 Electrode Reactions

The chemical reactions, which generate electricity, take place at the two electrodes. Each of the electrodes undergoing a so-called half-cell reaction:

Typical half-cell reactions are given in table 3.1 [55]:

Electrode Reaction	Standard electrode potential E^o (Volts)
$PbSO_4(s) + 2e = Pb(s) + SO_4^-(aq)$	-0.36
$H^+(aq) + e = (/2)H_2(g)$	0
$AgBr(s) + e = Ag(s) + Br^-(aq)$	0.07
$Sn^{4+}(aq) + 2e = Sn^{2+}(aq)$	0.15
$AgCl(s) + e = Ag(s) + Cl^-(aq)$	0.22
$(/2)I_2(s) + e = I^-(aq)$	0.54
$Fe^{3+}(aq) + e = Fe^{2+}(aq)$	0.77
$1/2Br_2(l) + e = Br^-(aq)$	1.08
$1/2O_2(g) + 2H^+(aq) + 2e = H_2O$	1.23
$CrO_7^{2-}(aq) + 14H^+(aq) + 6e = 2Cr^{3+}(aq) + 7H_2O$	1.33
$1/2Cl_2(g) + e = Cl^-(aq)$	1.36
$MnO_4^-(aq) + 8H^+(aq) + 5e = Mn^{2+}(aq) + 4H_2O$	1.51
$PbO_2(s) + SO_4^{2-}(aq) + 4H^+(aq) = PbSO_4(s) + 2H_2O$	1.69

Table 3.1: Standard electrodes potentials

Electrode reactions are oxidation-reduction processes of a somewhat unique nature which obey the relationship:

$$\text{Oxidised state} + ne \Leftrightarrow \text{Reduced state}$$

$$\text{oxidant} + ne \Leftrightarrow \text{reductant}$$

Where ne represents a transfer of n electrons.

The difference between chemical and electrochemical reactions lies in the different sources of electrons. A chemical oxidation-reduction system is made up of two individual systems, e.g.

$$Ox_1 + ne \Leftrightarrow Red_1$$

$$Red_2 - ne \Leftrightarrow Ox_2$$

Overall

$$Ox_1 + Red_2 \Leftrightarrow Red_1 + Ox_2$$

It is not possible to isolate the two contributing processes, since one can only observe changes in one system by coupling it with the second.

When two electrochemical redox (reduction-oxidation) systems are coupled together, one electrode providing and the other taking up electrons, the net effect will be similar to chemical systems in that there will be overall chemical reactions.

An electrode is made up of the chemicals, which undergo reaction; known as the active material (or active mass), and this is attached to a metal component, the current-collector (or grid). The driving force for the external current derived from a cell is the difference in the electrode potentials of the two half-cell reactions. An electrolytic cell, which produces current, is a galvanic cell. During discharge of the cell, the grid of the negative electrode gathers the electrons liberated by the chemical reaction. These electrons pass through the external load, thereby doing useful work, and are accepted by the grid of the positive electrode for participation in the complementary cell reaction. Thus we may represent the cell chemistry as follows:

At the negative electrode:

$$M \rightarrow M^{n+} + ne^{-}$$

At the positive electrode:

$$nX + ne^{-} \rightarrow nX^{-}$$

Where: M is a metal ; X is an oxidising agent, such as a metal oxide, e- is an electron.

3.3 Reversible cells

During discharge of a cell as shown in figure 3.1(a), negative ions (anions) move towards the positive electrode, and positive ions (cations) move towards the negaitive electrode. The flows of these ions are reversed during charging, and the cell becomes an electrolysis cell as in figure 3.1(b), where electrical energy is supplied from an external source. Two cells are shown connected in figure 3.1(c). If the upper

cell is of higher voltage than the lower cell, then it is undergoing discharge and is charging the lower cell.

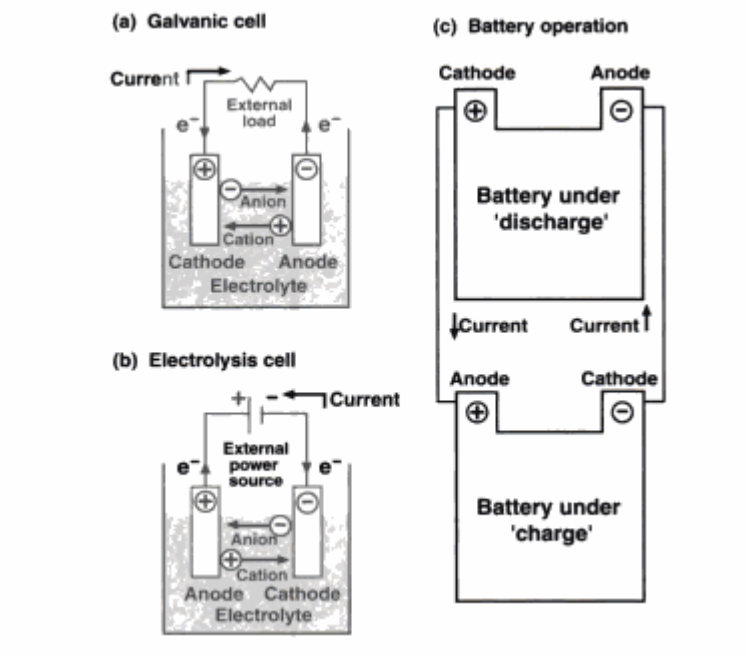

Figure 3.1 Schematic Representation of operation of electrochemical cells and batteries [56].

During discharge, the reaction at the negative electrode (anode) is an oxidation (or anodic) reaction, with liberation of electrons, and that at the positive electrode (cathode) is a reduction (or cathodic) reaction, with uptake of electrons. As batteries are generally considered to operate in the discharge mode, the negative electrode is often known as the anode and the positive electrode as the cathode, note for figure 3.1 the electrode names are reversed for the electrolysis cell is reversed. During the charging process, the anode becomes the cathode and the cathode becomes the anode. Nevertheless, the negative electrode remains a negative electrode, and the positive electrode a positive electrode. Therefore to avoid confusion the use of the terms positive electrode and negative electrode are often used in preference to anode and cathode.

Once depleted, the cell can be restored by reversing the flow of current through the cell in order to "recharge" the cell with energy. Cells, which can be recharged by the action of reverse current, are called accumulators because they "accumulate" chemical energy. Accumulators are more commonly known as storage batteries, where the term battery is used to denote that there are a number of single cells connected together. The term secondary battery is also used, this term dates from the early days of electrolysis, and the term primary battery is used for disposable batteries that cannot be electrically recharged.

3.3.1 Mass Transfer and Electron Exchange Processes

In considering electron-exchange reactions at electrodes we are concerned essentially with the layer of solution very close to the electrode surface. It must be borne in mind, however, that an oxidant or reductant in solution has to have some means of reaching the electrode vicinity. There are a number of ways in which this can occur and these are included under the general heading of mass transfer processes. These are:

1. Migration - the movement of cations and anions through a solution under the influence of an applied potential between electrodes placed in that solution.
2. Diffusion – an electrode reaction depletes the concentration of oxidant or reductant at an electrode surface and produces a concentration gradient there. This gives rise to the movement of species from higher to the area of lower concentration. Unlike migration, which only occurs for charged particles, diffusion occurs for both charged and uncharged species [57].

Typical metals, which form the negative active mass, are zinc, cadmium, lead and lithium. The positive active mass is likely to be an oxide of manganese, nickel or lead. Where the electronic conductivity of the positive active mass is inadequate to convey the electrons to the actual reaction sites in the active mass, it is conventional to mix the active material with a conducting substance, such as carbon black or graphite, and so provide an improved pathway for the electrons.

3.4 The Lead-Acid battery

This thesis concentrates on the lead-acid battery type, which has lead dioxide as the positive active mass, lead as the negative active material and sulphuric acid as the electrolyte. The half-cell reactions are as follows:

At the positive electrode:

$$PbO_2 + HSO_4^- + 3H^+ + 2e^- \underset{\text{Charge} \leftarrow}{\overset{\text{Discharge} \rightarrow}{\leftrightarrow}} PbSO_4 + 2H_2O \quad E^0 = +1.690\,V \qquad 3.2$$

At the negative electrode

$$Pb + HSO_4^- \underset{\text{Charge} \leftarrow}{\overset{\text{Discharge} \rightarrow}{\leftrightarrow}} PbSO_4 + H^+ + 2e^- \quad E^0 = -0.358\,V \qquad 3.3$$

Where E^0 is the standard electrode potential for each half-cell reaction.

The overall cell reaction is:

$$Pb + PbO_2 + 2H_2SO_4 \underset{\text{Charge} \leftarrow}{\overset{\text{Discharge} \rightarrow}{\leftrightarrow}} 2PbSO_4 + 2H_2O \quad V^0 = +2.048\,V \quad 3.4$$

Where V^0 is the standard cell voltage. It should be noted that the lead-acid battery is unusual among batteries in that the electrolyte takes part in the half-cell reactions. Generally, this is not the case electrolyte serves only to conduct the ions from one electrode to the other.

The voltage of a cell is the difference in the potentials of the two component electrodes. The absolute potential of any given electrode cannot be determined since all practical methods of measurement of electrode potential depend on completing the electrical circuit with a second electrode and this too will exert a potential. It is possible, however, to obtain a relative value by coupling the electrode to a second arbitrarily chosen, reference system.

3.5 Battery Construction

A battery consists of a number of series connected electrolytic cells, the individual cell stores energy in chemical form in its active materials and can convert this to electrical energy on demand, typically by means of an electrochemical

reduction/oxidation (redox) reaction. The cells are grouped together in a casing to form a battery as shown in figure 2.2.

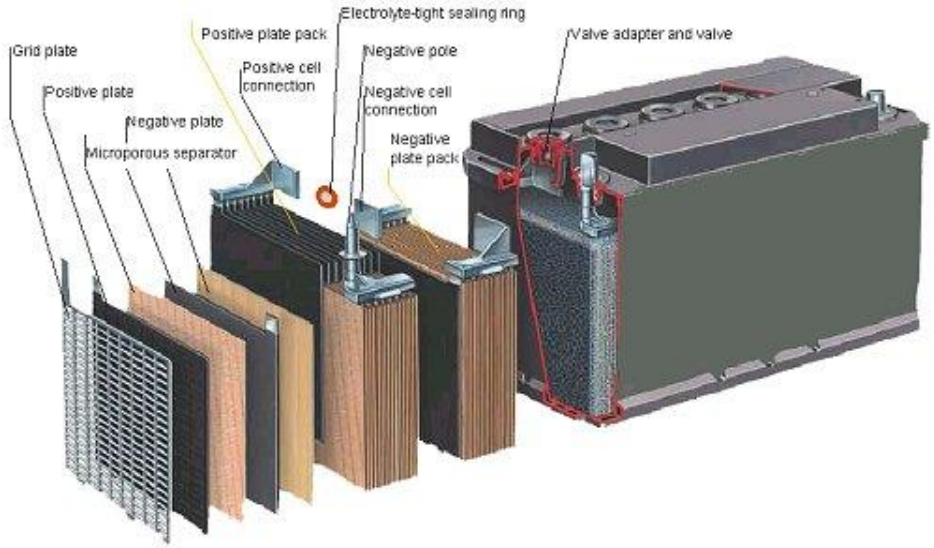

Figure 3.2 Battery construction [58].

Each cell has four components:

1. **The anode** or negative electrode (the oxidising or fuel electrode) gives up electrons to the external circuit and is oxidised during the electrochemical (discharge) reaction. It is generally a metal or an alloy but hydrogen is also used. The anodic process is the oxidation of the metal to form metal ions. Examples of anodes are lead and cadmium.
2. **The cathode** or positive electrode (the reducing electrode), which accepts electrons from the external circuit and is reduced during the electrochemical (discharge) reaction. It is usually a metallic oxide or a sulfide but oxygen is also used. The cathodic process is the reduction of the oxide to leave the metal. Examples of cathode are lead oxide and nickel oxyhydroxide.
3. **The electrolyte** (the ionic conductor); which provides the medium for transfer of charge, in the form of ions inside the cell between the anode and cathode. The electrolyte is typically a solvent containing dissolved chemicals providing ionic conductivity. It should be a non-conductor of electrons to avoid self-discharge of the cell. Electrolytes can be liquid solid, gel, paste or resin [59].

4. **The separator**, which electrically isolates the positive and negative electrodes [60].

There are essentially two types of cell that can be used for the storage and supply of electricity: primary cells and secondary cells. In primary cells a chemical reaction takes place in one direction only, and leads to the generation of electricity.
Primary cells are most commonly used in torches, and portable electrical and/or electronic devices. At the end of the life of the cell it is discarded.
In secondary cells the chemical reaction is reversible, allowing a discharge phase when chemical reaction leads to the generation of electrical power, and a charging phase when the processes are reversed. Secondary cells can be charged and discharged many times before irreversible processes render them too inefficient for further use. The most widely used secondary cell is the Lead-acid cell.
Commercial batteries have now been manufactured for well over a century, with energy storage ranging from miniature batteries with an energy storage capacity of less than 0.1 Wh to load levelling applications with capacities greater than 10 MWh, shown previously in chapter 1. Recent advances in electrochemistry and materials science have opened the way for new battery types with improved electrical performance.

3.6 Fuel Cells

Sir W.R.Grove first demonstrated his "gas battery" or "Fuel Cell" in 1839. Following Bacon's pioneering work on alkaline fuel cells in the 1950s; fuel cells were successfully developed for the American manned space programme. This success, together with a policy to commercialise space technology, led to substantial development programmes in America and Japan in the 1970s and 1980s and more recently in Europe.

Fuel cells produce a work output (electrical work) as long as they are supplied with fuel in common with combustion engines.
In fuel cells the cathodic and anodic reagents – usually gases – are stored externally and can be supplied to the electrochemical fuel cell on a continuous basis.

An example of a fuel cell is the Alkaline Fuel Cell (AFC) such as the type used in the work associated with this thesis.

Alkaline fuel cells use an electrolyte that is an aqueous (water-based) solution of potassium hydroxide (KOH) retained in a porous stabilized matrix. The concentration of KOH can be varied with the fuel cell operating temperature, which ranges from 65°C to 220°C. The charge carrier for an AFC is the hydroxyl ion (OH-) that migrates from the cathode to the anode where they react with hydrogen to produce water and electrons. Water formed at the anode migrates back to the cathode to regenerate hydroxyl ions. Therefore, the chemical reactions at the anode and cathode in an AFC are shown below. The following set of reactions in the fuel cell produces electricity and by-product heat.

$$\text{Positive Electrode reaction:} \quad 2H_2 + 4OH^- \Rightarrow 4H_2O + 4e^-$$

$$\text{Negative Electrode reaction:} \quad O_2 + 2H_2O + 4e \Rightarrow 4OH^-$$

$$\text{Overall Electrode reaction:} \quad 2H_2 + O_2 \Rightarrow 2H_2O$$

Fuel cells are electrochemical energy conversion devices and share some common characteristics with batteries; in fact fuel cells combine many of the advantages of engines and batteries. However, they also have some serious disadvantages in particular cost per kW and fuel storage.

Unlike combustion heat engines, electrochemical energy generators allow the direct conversion of chemical to electrical energy, and are likely to have a significant role to play in any future energy scenario not entirely dependant on fossil fuels.

In order to gain an understanding of the principles of electrochemical generators and the maximum electrical potential that can be generated in a reaction it is necessary to understand the interrelationship between the energy transformations and the chemical reactions inherent to the functioning of these devices. This requires an understanding of the science of Thermodynamics. Thermodynamics is the study of energy transformations, and determines the theoretical limits on the maximum electrical potential that can be generated in a reaction.

3.7 Chapter Conclusions

This chapter has reviewed theory, elements and function of electrochemical cells, with particular reference, toward the end of the chapter, to Lead Acid batteries and Alkaline Fuel Cells which form the subject of the experimental work of this thesis.

CHAPTER 4 THEORY RELATING TO ELECTROCHEMICAL CELLS

This thesis is focused on the study of electrochemical devices; the thermodynamic theory relating to these devices is common with heat engines, therefore it is worth considering heat engines before studying electrochemical devices.

4.1 Heat Engines

Heat engines come in various forms, the reciprocating internal combustion engine being the most widely used example of a heat engine. Heat engines differ considerably one from another, but they can all be represented by figure 4.1.

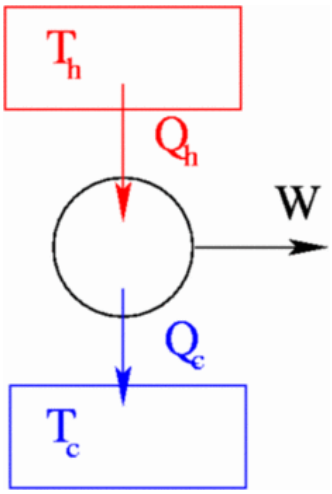

Figure 4.1 Heat engine model

Referring to Figure 4.1 the heat engine operating cycle is as follows:

1. The heat engine receives heat from a high temperature source.
2. Part of the heat is converted to work.
3. Waste heat is rejected to a low temperature sink.

Where:

T_h is the temperature of the high temperature source measured in degrees Kelvin

T_c is the temperature of the low temperature sink measured in degrees Kelvin

Q_h is the heat transfer from the high temperature source measured in Joules

Q_c is the heat transfer to the low temperature sink measured in Joules

W is the net work output measured in Joules

$W = Q_h - Q_c$ 4.1

The operating cycle can be "open" as in the case of the widely used reciprocating internal combustion engine and open cycle gas turbine, or "closed" as in the case of the condensing steam power cycle and the closed cycle gas turbine as used for large scale electrical power generation.

The efficiency ή of a heat engine cycle is given by:

$$\eta = \frac{W}{Q_h} \qquad 4.2$$

That is the net work output divided by the heat supplied. The maximum efficiency of a heat engine is limited by the governing equation under which all "heat engines" operate, that is the Carnot Cycle. This cycle imposes an upper limit on the theoretical thermal efficiency of a heat engine, which in turn translates to an even lower operating efficiency when parasitic losses are taken into account.

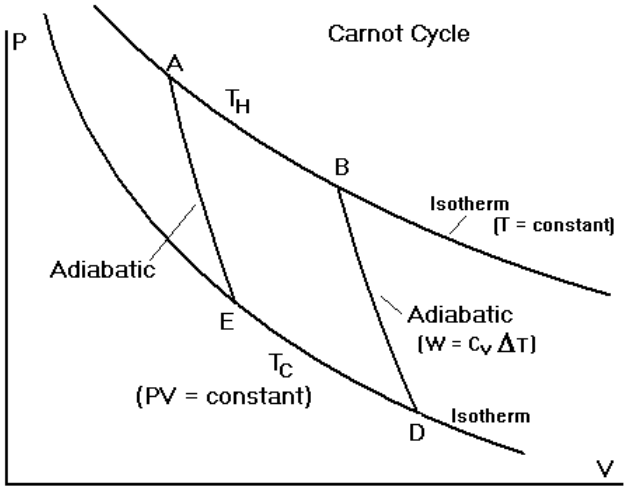

Figure 4.2: The Carnot Cycle on a pressure-volume property diagram [61].

Figure 4.2 shows the Carnot cycle on a pressure-volume property diagram, it can be seen that the heat transfer processes AB and DE take place at constant temperature; this is illustrated more clearly when the cycle is drawn on a temperature-entropy diagram figure 4.3, here the heat transfer to the system process 2, and heat rejection from the system process 4 are horizontal lines indicating that these processes take place at a constant temperature.

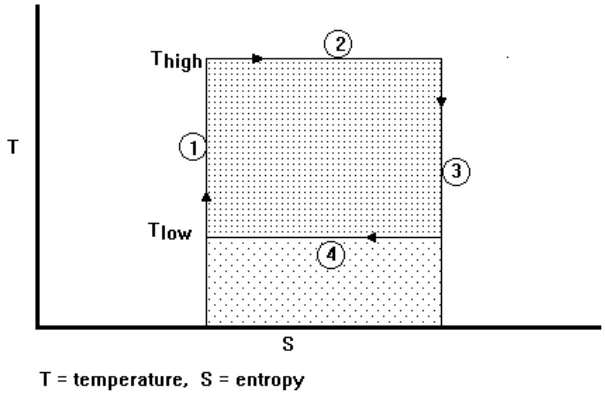

Figure 4.3 The Carnot Cycle on a temperature-entropy property diagram [62].

In the case of a Carnot cycle the efficiency can be expressed in terms of temperature alone as shown in equation 4.3.

Therefore the Carnot cycle efficiency can be expressed as a relationship purely dependent on the upper and lower cycle temperatures.

$$\eta_{Carnot} = 1 - \frac{T_{Low}}{T_{High}} \qquad 4.3$$

Taking a modern reciprocating internal combustion engine as an example, the maximum cycle temperature of about 1000^{o}C corresponding to T_{high}, taking an ambient temperature of 15 ^{o}C from equation 4.2 the Carnot efficiency is:

$$\eta_{Carnot} = 1 - \frac{15 + 273}{1000 + 273} = 0.7738 = 77.38\%.$$

Note that this is the maximum ideal efficiency, and does not take account of parasitic losses in the engine and drive train.

In order to convert energy into useful work more efficiently than the combustion heat engine, a different approach to energy conversion is required. Electrochemical power sources have an advantage over combustion heat engines, as they convert chemical energy directly to electrical energy, without the intermediate process of converting chemical energy into heat required by combustion heat engines.

4.2 Electrochemical Power Sources.

In order to convert energy into useful work more efficiently than the combustion heat engine, a different approach to energy conversion is required. Electrochemical power sources have an advantage over combustion heat engines, as they convert chemical energy directly to electrical energy, without the intermediate process of converting chemical energy into heat required by combustion heat engines.

4.2.1 Internal Energy

Electrochemical generators convert chemical energy into electrical energy, the total intrinsic energy of any substance is known as the internal energy (U), internal energy being the energy associated with the energy at a microscopic level relating to random molecular movements and interactions. Internal energy is a function of absolute temperature, measured in degrees Kelvin (K) and the atomic structure of the substance.

Only a proportion of the internal energy of a fuel can be converted into electrical energy, the limits of how much can be transformed is governed by the laws of thermodynamics.

4.2.2 Work and Heat

In contrast to internal energy, work and heat are not properties of matter, or of any particular system (e.g. substance or body). They represent energy in transit, in other words, energy that is transferred between substances or bodies.

In the case of work, this transfer of energy is accomplished by the application of a force over a distance. Heat, on the other hand is transferred between substances whenever they have different thermal energies, as manifested by differences in their temperature.

Due to the implications of the second law of thermodynamics, work is sometimes called the most 'noble' form of energy. Energy in the form of work can be converted into another form of energy at 100% theoretical efficiency, for example work can be entirely dissipated in the form of heat, for example friction resulting from relative motion between two surfaces in contact. In contrast, heat is the most 'ignoble' form of energy, any form of energy can be 100% dissipated to the environments as heat, but this heat can never be 100% converted back to work. This contrast between heat and work illustrates one of the central differences between electrochemical generators and heat engines.

A combustion engine burns fuel to produce heat and then converts some of this heat into work. As it first converts energy into heat, the combustion engine destroys some of the work potential of the fuel. This destruction of work potential is a "thermal bottleneck" which does not affect electrochemical energy converters [63].

4.2.3 Laws of Thermodynamics

The first and second laws of thermodynamics govern all energy conversions. The first law of thermodynamics, also known as the law of conservation of energy, states that energy can neither be created nor destroyed

Treating the electrochemical devices as closed systems, that is, ignoring the macroscopic effects of kinetic energy and gravitational potential energy associated with open systems, there are two ways that energy can be transferred between a closed system and its surroundings, that is, via heat (Q) and work (W), both of these quantities being measured in Joules (J).

The first law can then be expressed in the form in equation 4.4:

$$dU = dQ - dW \qquad 4.4$$

I.e. change in the internal energy of the closed system is a result of the difference in the reversible heat transfer to the system and the reversible work done by the system, the prefix reversible is used to indicate an ideal system base on ideal or reversible processes, the concept of reversibility being an outcome of the second law of thermodynamics.

The convention used is heat transfer to the system is taken as being positive, and work done by the system also as being positive.

The second law of thermodynamics introduces the concept of entropy (symbol S), which is a measure of the disorder or the unavailability of energy; the units of entropy are J/kg K. The entropy of a process can either increase or decrease, however the net change in entropy of a cyclic process will be zero for a cycle of ideal processes, or greater than zero for cycles involving non-ideal or real processes.

Therefore the second law of thermodynamics for a cycle of processes such as those making up a heat engine cycle can be summarised by equation 4.5

$$S \geq 0 \quad 4.5$$

That is that the change in entropy over the cycle is equal to or greater than zero, an ideal cycle such as the Carnot cycle has zero entropy change over the cycle, a non-ideal or real cycle will always have a net gain in entropy.

4.2.4 Thermodynamic Potentials

The first and second laws of thermodynamics can be used to determine an equation for internal energy based on entropy (S) and volume (V), equation 4.6 becomes:

$$dU = TdS - PdV \qquad 4.6$$

Where T is the absolute temperature measured in degrees Kelvin (K)

And P is the absolute pressure measured in N/m^2

Where TdS represents the reversible heat transfer and PdV the mechanical work done, electrical work will be considered in due course. Equation 4.6 therefore implies that internal energy is a function of entropy and volume.

Thermodynamic potentials are parameters of a thermodynamic system and have the dimensions of energy (J); they are called potentials because they quantify the potential energy in a system. Internal energy is a thermodynamic potential based on two independent variables entropy (S) and volume (V).

Entropy (S) characterises the energy loss or gain connected with the chemical or electrochemical process. The product $T\Delta S$ represents the heat exchange with the

surroundings when the process occurs reversibly. This is synonymous with minimal heat loss or gain of the system, which is only true when no current flows through an electrochemical cell.

However entropy and volume are not easily measured in experiments, whereas temperature and pressure can be measured directly. Therefore a new thermodynamic potential equivalent to internal energy based on temperature T and pressure P is derived.

$$\left(\frac{dU}{dS}\right)_V = T \qquad 4.7$$

$$\left(\frac{dU}{dV}\right)_S = -p \qquad 4.8$$

$$G = U - \left(\frac{dU}{dS}\right)_V S - \left(\frac{dU}{dV}\right)_S \left(\frac{dU}{dV}\right)_S \qquad 4.9$$

Substituting 4.7 and 4.8 in 4.9 gives

$$G = U - TS + pV \qquad 4.10$$

This thermodynamic potential is called the Gibbs free energy and it can be shown that:

$$G = -SdT + VdP \qquad 4.11$$

That is the Gibbs free energy is a function of temperature and pressure, Gibbs free energy, also referred to as the free enthalpy of reaction, is the maximum amount of non-expansion work which can be extracted from a closed system; this maximum work can be attained only in a completely reversible process.

Furthermore it represents the (maximum) amount of chemical energy that can be converted into electrical energy and vice versa.

Similarly a third potential can be developed that depends and pressure and entropy, that is Enthalpy H (S, p).

$$H = U - \left(\frac{dU}{dV}\right)_S V \qquad 4.12$$

As $\left(\frac{dU}{dV}\right)_S$ = -p, this gives

$$H = U + pV \qquad 4.13$$

Differentiating 4.13 gives

$$dH = dU + pdV + Vdp \qquad 4.14$$

From 4.6

$$dU = TdS - PdV$$

Therefore

$$dH = TdS + Vdp \qquad 4.15$$

Therefore the third potential, enthalpy is a function of entropy and pressure. Enthalpy of reaction ΔH, describes the amount of energy released or absorbed. It is derived from the energy content of the chemical compounds H [64].

Thermodynamic quantities like ΔH and ΔG depend on the concentration of the reacting components.

The fourth thermodynamic potential is a function of temperature T, and volume V and completes the relationships, this fourth potential is called the Helmholtz free energy F (T, V) this is the amount of useful work that can be extracted from a closed system at constant temperature.

$$F = U - TS \qquad 4.16$$

It can be shown that

$$dF = -SdT - pdV \qquad 4.17$$

Therefore to summarise the four thermodynamic potentials are included in a pneumonic diagram shown in figure 4.4 as first proposed by Schroder [65].

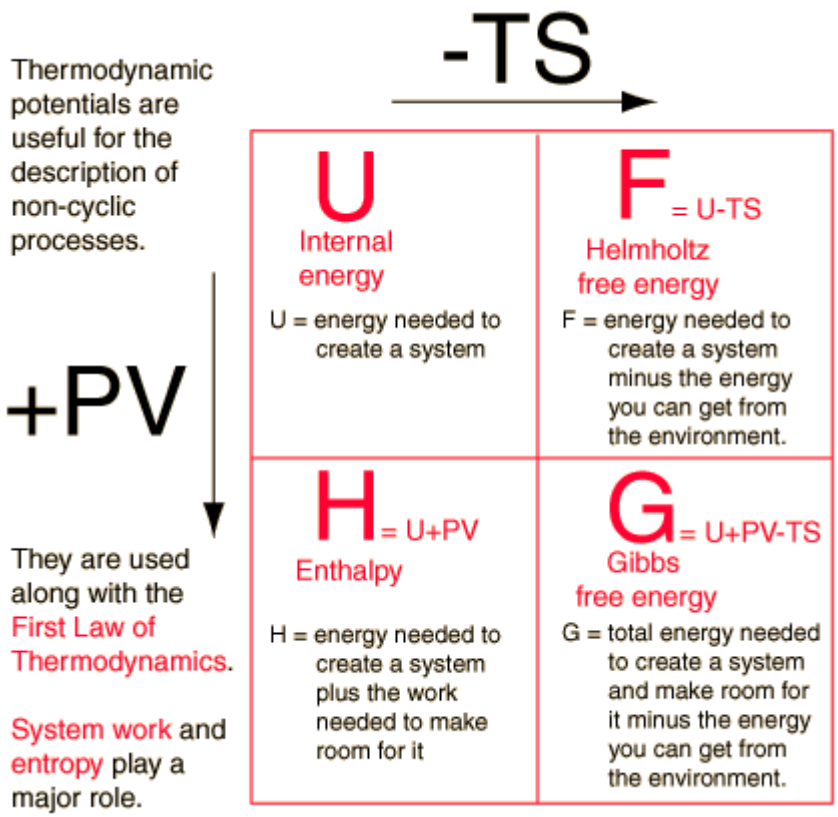

Figure 4.4 Four thermodynamic potentials.

Note: The sign of these thermodynamic parameters is positive when the system gains energy and negative when the system loses energy. Consequently, in discharge, the sign of ΔG is negative, because the (electrochemical storage) system delivers energy. When the battery is recharge, ΔG is positive [66].

4.2.5 Gibbs Free Energy

The Gibbs free energy, originally called available energy, was developed in the 1870s by the American mathematical physicist Willard Gibbs. In 1873, in a footnote, Gibbs defined what he called the "available energy" of a body as:

"The greatest amount of mechanical work which can be obtained from a given quantity of a certain substance in a given initial state, without increasing its total volume or allowing heat to pass to or from external bodies, except such as at the close of the processes are left in their initial condition" [67].

Gibbs free energy is the energy available to do useful work, sometimes referred to as work potential, and the symbol G is used in honour of Gibbs who developed the concept, and the equations, which describe it.

$G = H - TS$ 4.18

A change in the Gibbs free energy at constant temperature T is given by the equation

$\Delta G = \Delta H - T\Delta S$ 4.19

A reaction common to fuel cells using hydrogen and air is:

$$H_2 + \frac{1}{2}O_2 \Leftrightarrow H_2O$$

Molar quantities are often used to calculate energy transfer due to a chemical reaction.

For every mole of H_2 gas consumed the Gibbs free energy change G is -237 kJ/mol H_2 at room temperature and pressure.

Note that the term used for the calculation of energy changes in electrochemical cells is ΔG; this is the molar Gibbs function of reaction at standard pressure p = 1 bar, the units are kJ/kmol.

Therefore if 5 mol of H_2 gas is reacted with 2.5 mol of oxygen gas the Gibbs free energy change G would be:

-237 x 5 = -1185 kJ.

and the products of the reaction would be 5 mol of H_2O.

4.3 Ideal behaviour of an electrochemical cell

The Gibbs free energy represents the exploitable energy potential, or work potential of the system [68], and in terms of an electrochemical cell, is the maximum amount of chemical energy that can be converted into electrical energy and vice versa [54].

4.3.1 Reaction Enthalpies

From equation 4.10 the Gibbs free energy

$G = U - TS + pV$

And 4.13 gives enthalpy as

$H = U + pV$

Therefore

$G = H - TS$ 4.20

Differentiating 4.16 gives:

$dG = dH - TdS - SdT$ 4.21

Holding the temperature constant (isothermal process) and writing this relationship in terms of molar quantities gives

$\Delta G = \Delta h - T\Delta s$ 4.22

It can be seen from equation 4.20 that ΔG values can be calculated from Δh and Δs values, the isothermal reaction assumes that the reaction takes place at a constant temperature.

4.3.2 Gibbs Free Energy and Electrical Work

From equation 4.19 the change in Gibbs free energy can be expressed as

$dG = dH - TdS - SdT$

The change in enthalpy from 4.15

$dH = dU + pdV + Vdp$

Therefore

$dG = dU + pdV + Vdp - TdS - SdT$ 4.23

From 4.4 the change in internal energy dU

$dU = dQ - dW$

And as the heat transfer

$dQ = TdS$

The change in internal energy can be expressed as

$dU = TdS - dW$ 4.24

If the term dW is expanded to include mechanical and electrical work.

$dW = pdV + dW_{elec}$ 4.25

Therefore equation 4.24 is modified to give

$dU = TdS - (pdV + dW_{elec})$ 4.26

Equation 4.23 becomes

$dG = -SdT + Vdp - dW_{elec}$ 4.27

For a constant temperature-pressure process (dT,dp =0) this reduces to

$dG = -dW_{elec}$ 4.28

Therefore the maximum electrical work output from a system during a constant-temperature, constant-pressure process is equal to the negative of the change in Gibbs free energy for the process.

For a reaction using molar quantities the electrical work output can be expressed as:

$W_{elec} = -\Delta G$ 4.29

Note that the constant-temperature, constant-pressure process is a reasonable assumption for electrochemical cells, as long as the operating conditions have stablised.

From equation 4.22 at constant temperature (isothermal) conditions ΔG can be determined in terms of Δh and Δs.

$\Delta G = \Delta h - T\Delta s$

Therefore ΔG can be calculated at a range of temperatures, taking a lead-acid cell as an example the reaction is:

$Pb(s) + PbO_2(s) + 2H_2SO_4 <=> 2PbSO_4 + 2H_2O(l)$

The Gibbs free energy change ΔG for this reaction is determined using table 4.1 as follows.

	Δh_f (kJ/mol)	S (J/ K mol)
Pb(s)	0	64.81
$PbO_2(s)$	-276.6	68.6
H_2SO4	-909	156.9
$PbSO_4$	-919.84	148.57
$H_2O(l)$	-285.8	69.91

Table 4.1: Table of properties [54]

$\Delta h = [(2x\Delta h_f PbSO_4) + (2x\Delta h_f H_2O(l))] - [\Delta h_f Pb(s) + \Delta h_f PbO_2(s) + 2x\Delta h_f H_2SO4]$

$\Delta h = [(2 \times -919.84) + (2x-285.8)] - [0 + (-276.6) + (2x-909)]$

$\Delta h = -512.08$ kJ/mol

$\Delta s = [(2x\Delta s\ PbSO_4) + (\Delta s\ H_2O(l))] - [\Delta s\ Pb(s) + \Delta s\ PbO_2(s) + 2x\ \Delta s\ H_2SO4]$

$\Delta s = [(2 \times 148.57) + 69.91] - [64.81 + 68.6 + (2x156.9)]$

$\Delta s = -80.16$ J/K mol

$\Delta G = \Delta h - T\Delta s$

$\Delta G = -512.08 - T\ (-0.08016)$ kJ/mol

Therefore the free energy will be negative until the temperature rises above:

$T = (-412.08) / (-0.0816)$

$T = 5112.65$ K (4839.5^oC)

Conversely the electrical work will remain negative until the temperature rises above this temperature, which is unrealistic, as the components of the cell would have vaporised before reaching this temperature.

From equation 4.29

$W_{elec} = -\Delta G = 226.28 + (-0.08016)T$ kJ/mol

Which is the expression for the electrical work from a lead-acid cell.

4.3.3 Gibbs Free Energy and Voltage

The potential of a system to do electrical work is measured by voltage, or electrical potential. The electrical work done by a charge Q, measured in coulombs through an electrical potential difference E is:

$W_{elec} = EQ$ 4.30

If the charge is assumed to be carried by electrons

$Q = nF$ 4.31

Where n is the number of moles of electrons transferred and F is Faradays constant. Combining equations 4.27, 4.28 and 4.29 gives

$\Delta G = -nFE.$ 4.32

Therefore the Gibbs free energy sets the magnitude and direction of the reversible voltage for an electrochemical reaction.

In a galvanic cell, where spontaneous reduction/oxidation (redox) potential drives the cell to produce an electrical potential Gibbs free energy ΔG^o must be negative, in accordance with the following equation:

$\Delta G^O = -nFE^O_{cell}$ 4.33

Where n = the number of moles of electrons

F = Faraday constant = 96485 Coulombs/mol

The following applies for an electrochemical cell:

$$E^{O}_{cell} = E^{O}_{Positive\ \ electrode} + E^{O}_{Negative\ \ electrode}$$

If $E^{O}_{cell} > 0$, then the process is spontaneous (galvanic cell)

If $E^{O}_{cell} < 0$, then the process is non-spontaneous (electrolytic cell)

Rearranging equation 4.33

$$E = \frac{-\Delta g}{nF} \qquad 4.34$$

Taking the example of hydrogen-oxygen fuel cell, the reaction

$$H_2 + \frac{1}{2}O_2 \lhd\rhd H_2O$$

has a Gibbs free energy change of -237 kJ/mol under standard conditions for liquid water products. The reversible voltage generated by a hydrogen-oxygen fuel cell under standard conditions is:

$$E_0 = -\frac{\Delta g}{nF}$$

$$E_0 = \frac{-237{,}00\,J/mol}{(2\,mole/mol\,reactant)(96{,}400\,C/mol)}$$
$$= 1.23\,V$$

Where E_o is the standard state reversible voltage and ΔG is the standard state Gibbs free energy change for the reaction [67].

4.3.4 Equilibrium conditions

Note that in the equations above the symbol E_o is used to represent the reversible cell voltage, reversible implies equilibrium, a process is thermodynamically reversible when an infinitesimal reversal in the driving force causes it to reverse direction; such a system is always at equilibrium.

Equations relating to reversible cell voltages apply only to equilibrium conditions, as soon as current is drawn from a cell; equilibrium is lost and reversible cell conditions no longer apply.

If a cell is connected to an external circuit and current flows, and there will be a voltage or cell potential between the two electrodes of the cell in the external circuit, therefore the system is no longer in equilibrium and equations developed from thermodynamic principles can not be applied to non-equilibrium conditions. Therefore the cell potential must be measured under conditions that permit no current to flow between the electrodes. This can be achieved by including in the external circuit a variable source of potential that can be balanced against the potential of the cell under test.

When no current is being drawn from a reversible cell, the potential difference across the terminals, or open circuit voltage (OCV), is known as the electromotive force or emf.

When measuring cell potential it is important to check that the cell is operating reversibly, a slight imbalance in the potentials should lead to a flow of current in one direction or the other.

A sign that a cell is not operating reversibly is that there is very little current produced in the vicinity of the balance point; therefore it becomes difficult to locate the balance point of the cell. When the cell is operating reversibly the measured potential is the emf and given the symbol E [56].

When the emf of a cell is zero, no net reaction takes place, this can be taken as a true state of equilibrium at which the emf E =0.

To distinguish between reversible and non-reversible cell voltages the symbol E is used to denote a reversible cell voltage, and V denotes a non-reversible cell voltage.

4.3.5 Nernst Equation

The voltage generated in electrochemical cells depends on the concentration of the substance in the cell, to investigate the relationship between voltage and concentration

It is necessary to introduce the concept of chemical potential.

Chemical potential (μ) J/mol measures how the Gibbs free energy of a system changes as the chemistry of the system changes. For n moles of a pure substance:

$G = n\mu$ Joules 4.35

Chemical potential is related to concentration through activity a, at standard conditions this relationship can expressed as.

$$\mu_i = \mu_i^o + RT \ln a_i \qquad 4.36$$

where μ_i^o is the standard chemical potential of substance i at standard conditions and a_i is the activity of substance i.

Chemical activity (a) is a measure of how different molecules in a non-ideal gas or solution interact with each other, and can be considered to be the active mass or effective concentration of active ions in solution, activity is dimensionless. The activity of a substance depends on its nature. Figure 4.5 shows the variation of activity of Sulphuric Acid plotted against acid concentration [69].

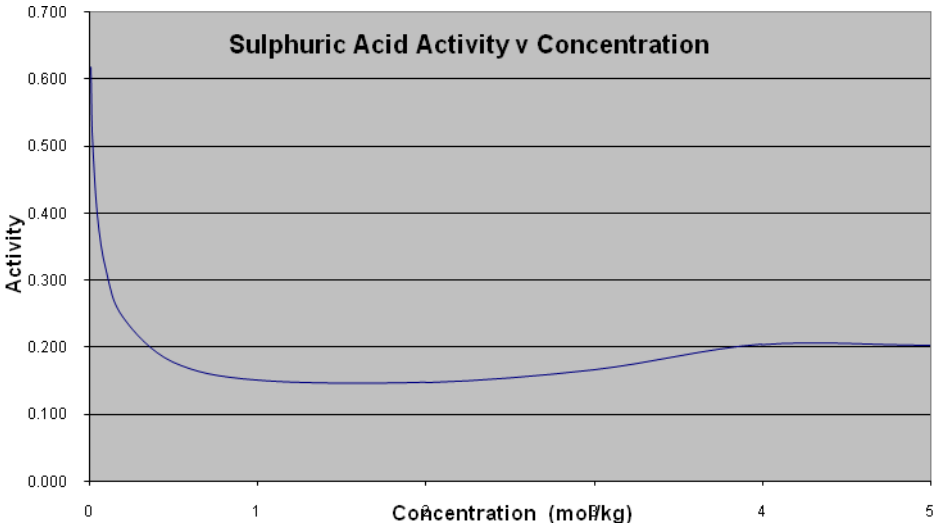

Figure 4.5: Sulphuric Acid Activity v Concentration.

To use equation 4.36 it is necessary to know how the standard conditions (also called standard state) are defined and what is meant by the term activity. These two

concepts are intimately related. The standard state is arbitrary and is chosen such that the activity of the substance can be related to measurable quantities.

For an ideal gas:

$\mu_i = \mu_i^o + RT\ln\left(\frac{p_i}{p^o}\right)$ where p_i is the partial pressure of the gas and p^o is the standard-state pressure (1 atm).

The chemical potential has its standard value when $p_i = p^o = 1\,\text{atm}$

as $\mu_i = \mu_i^o + RT\ln 1 = \mu_i^o + 0 = \mu_i^o$.

$\therefore \mu_i = \mu_i^o$ 4.37

Activity $a_i = \frac{p_i}{p^o}$, for example the activity of oxygen in air at 1 atm is approximately 0.21. The activity of oxygen in air pressurised to 2 atm would be 0.42.

For a non-ideal gas:

$a_i = \gamma_i\left(\frac{p_i}{p^o}\right)$ where γ_i is the activity coefficient describing the departure from ideal conditions. ($0<\gamma_i<1$). The activity coefficient is concentration and temperature dependant, and is determined experimentally. For very dilute solutions i.e. << 1.0 x 10^{-3} M, γ_i may be approximated to unity.

For a dilute (ideal) solution:

$\mu_i = \mu_i^o + RT\ln\left(\frac{c_i}{c^o}\right)$, where c_i is the molar concentration of the substance and c^o is the standard-state concentration (1 M =1 mol/litre). $a_i = \frac{c_i}{c^o}$,

For non-ideal solutions, $a_i = \gamma_i\left(\frac{c_i}{c^o}\right)$. For example, the activity coefficient of 0.1M H_2SO_4 is 0.130

For pure substances, $a_i = 1$. Therefore $\mu_i = \mu_i^o$, that is the chemical potential of a liquid or solid depends only on temperature, the standard state is simply the pure substance at that temperature.

Gibbs energy is also the chemical potential that is minimized when a system reaches equilibrium at constant pressure and temperature. As such, it is a convenient criterion of spontaneity for processes with constant pressure and temperature [68]. Therefore it is an appropriate measure of the energy transfer in electrochemical cells.

The Gibbs free energy for a mixture of substances can be written as a sum of terms, one for each substance in the mixture, for example based on a mol of substance A.

1A + bB <=> mM + nN 4.38

Where A and B are reactants, M and N are products, and 1, b, m, and represent the number of moles of A, B, M, and n respectively. On a molar basis for substance A, ΔG for this reaction may be calculated from the chemical potentials of the various substances involved in the reaction.

$$\Delta g = \left(m\mu_M^o + n\mu_N^o\right) - \left(\mu_A^o + b\mu_B^o\right) + RT\ln\left(\frac{a_M^m a_N^n}{a_A^1 a_B^b}\right) \quad 4.39$$

4.39 can be simplified to the form,

$$\Delta g = \Delta g^o + RT\ln\left(\frac{a_M^m a_N^n}{a_A^1 a_B^b}\right) \quad 4.40$$

$$\Delta g^o = \left(m\mu_M^o + n\mu_N^o\right) - \left(\mu_A^o + b\mu_B^o\right) \quad 4.41$$

Δg^o is standard-state molar free-energy change for this reaction.

from 4.33

ΔG = -nFE

The reversible cell voltage

$$E = -\frac{\Delta g}{nF} \quad 4.42$$

Therefore 4.41 can be written as

$$E = E^o - \frac{RT}{nF}\ln\left(\frac{a_M^m a_N^n}{a_A^1 a_B^b}\right) \qquad 4.43$$

This important result is known as the **Nernst** equation, and it relates the open circuit cell reversible voltage under arbitrary conditions to the standard value E^o.

The group of terms $\left(\frac{a_M^m a_N^n}{a_A^1 a_B^b}\right)$ from the Nernst equation is known as the equilibrium constant symbol K. At standard conditions each of the activities is unity and equation 4.43 becomes.

$$E = E^o - \frac{RT}{nF}\ln\left(\frac{a_M^m a_N^n}{a_A^1 a_B^b}\right)$$

$$E = E^o - \frac{RT}{nF}\ln(\quad)$$

$$E = E^o$$

That is the emf becomes the standard emf; from equation 3.33

$$\Delta G = -nFE$$

$$\Delta G^o = -nFE^o$$

$$\therefore E^o = -\frac{\Delta G^o}{nF} \qquad 4.44$$

Again taking the example of hydrogen-oxygen fuel cell, at standard temperature conditions T = 298.15 K, $\Delta G^o = -237.4\ \text{kJ/mol}$, from equation 4.44 the corresponding value of E^o is

$$\therefore E^o = -\frac{\Delta G^o}{nF}$$

$$E^o = -\frac{-237.4\times10^3}{2\times96485}$$

$$E^o = 1.23\text{V}$$

The reaction for the hydrogen-oxygen fuel cell is:

$$2H^+ + \frac{1}{2}O_2(\quad) + 2e \Leftrightarrow H_2O$$

Given that E^o = 1.23 V for this reaction, and using the form of the Nernst equation from 4.43

$$E = E^{o} - \frac{RT}{2F}\ln\left(\frac{a_{H_2O}}{\left(\right)_{O_2}^{\frac{1}{2}}\left(\right)_{H^+}^{2}}\right) \qquad 4.45$$

Taking $a_{H_2O} = 1$, and assuming that the pressure of the oxygen is 1 atmosphere

(that is $a_{O_2} = \frac{p_{O_2}}{p^0} = 1$), 3.46 becomes:

$$E = E^{O} + \frac{RT}{2F}\ln\left(\right)_{H^+}^{2} = E^{O} + \frac{RT}{F}\ln a_{H^+} \qquad 4.46$$

Substituting constants (at 298.15K):

$$E = E^{O} + \frac{8.314 \times 298.15}{96485}\ln a_{H^+}$$

$$E = 1.23 + 0.0257\ln a_{H^+} \qquad 4.47$$

Therefore the reversible voltage under arbitrary conditions of an H_2-O_2 fuel cell is dependant on the hydrogen ion activity, which in turn is dependant on the partial pressure of the hydrogen since the activity of a perfect gas (a).

$$a_i = \frac{p_i}{p^o}$$

Thermodynamic calculations are always based on a complete cell, and the derived voltage refers the potential difference between two electrodes. The potential difference between the electrode and the electrolyte, the "absolute potential", cannot be determined. The name electrode potential always refers to a potential measured with the aid of a reference electrode, which is the standard hydrogen electrode (SHE).

4.4 Chemistry of the Lead-Acid Cell

A lead-acid cell comprises a negative electrode of metallic lead and a positive electrode of lead oxide, together with an electrolyte of dilute sulphuric acid. Sulphuric acid can exist in three states, at very high concentrations (>10^6 molar) the acid comprises entirely of H_2SO_4 molecules, as the concentration decreases the

sulphuric acid dissociates into H^+ and $SO4^-$ ions, this takes place in two dissociation phases.

4.4.1 Dissociation

Dissociation is the process whereby the molecules of a compound split into smaller molecules or ions in a reversible manner. In general for a compound AB:

$$AB \Leftrightarrow A + B \quad 4.48$$

A dissociation constant K, quantifies the degree to which the dissociation takes place using a ration of the dissociated to un-dissociated compound.

$$K = \frac{[A][B]}{[AB]} \quad 4.49$$

In general the dissociation of an acid is represented by the acid dissociated constant.

$$K_a = \frac{[H^+][A^-]}{HA} \quad 4.50$$

For the generic acid dissociation:

$$HA \Leftrightarrow H^+ + A^- \quad 4.51$$

The acid dissociation constant is a particular example of equilibrium constant.

Taking the particular example of sulphuric acid, which is a polyprotic acid, as it can lose either one or both protons (H^+) therefore there are two dissociations to consider. At concentrations below 3 molar a second dissociation takes place where the $HSO4^-$ ions dissociate into $H^+$and SO_4^{2-} ions. This process can be expressed as follows:

The first dissociation:

$$H_2SO_4 \Leftrightarrow H^+ + HSO_4^-$$

$$K_{a1} = \frac{[H^+][HSO_4^-]}{[H_2SO_4]} \quad 4.52$$

The value of K_a for the first dissociation is $K_{a1} = 1000$

4.4.2 The second dissociation:

$$HSO_4^- \Leftrightarrow H^+ + SO_4^{2-}$$

$$K_{a2} = \frac{[H^+][SO_4^{2-}]}{[HSO_4^-]} \quad 4.53$$

The value of K_a for the second dissociation is $K_{a2} = 0.012$

In the concentration used in lead acid batteries, the diluted sulphuric acid (H_2SO_4) is dissociated mainly into hydrogen ions (H^+) and hydrogen bisulphite (HSO_4^-) ions. Only about 1% of the H_2SO_4 molecules dissociate into H^+ and sulphate SO_4^{2-} ions.

Figure 4.6 shows the relative proportion (α) of the H_2SO_4, HSO_4^- and SO_4^{2-}. plotted against pH in the range –10 to 10.

At pH values below –6 the sulphuric acid is composed entirely of H_2SO_4 molecules, as the pH decreases the H_2SO_4 molecules dissociate into HSO_4^- and H^+ ions, the H^+ ions in fact exist as H_3O^+ ions, known as hydronium.

4.4.3 Fractional composition of Sulphuric Acid

The fractional composition α of sulphuric acid is used to indicate the composition of the acid in terms of all possible components; in the case of sulphuric acid the three components are H_2SO_4, HSO_4^- and SO_4^{2-}.

The fractional composition α is determined by the following expressions.

For H_2SO_4

$$\alpha_0 = \frac{[H_3O^+]^2}{[H_3O^+]^2 + K_{a1}H_3O^+ + K_{a1}K_{a2}} \quad 4.54$$

For HSO_4^-

$$\alpha_1 = \frac{K_{a1}H_3O^+}{[H_3O^+]^2 + K_{a1}H_3O^+ + K_{a1}K_{a2}} \quad 4.55$$

For SO_4^{2-}

$$\alpha_2 = \frac{K_{a1}K_{a2}}{[H_3O^+]^2 + K_{a1}H_3O^+ + K_{a1}K_{a2}} \quad 4.56$$

The fractional composition of H_2SO_4 is plotted over the range -10>pH>10 and is shown in figure 4.6

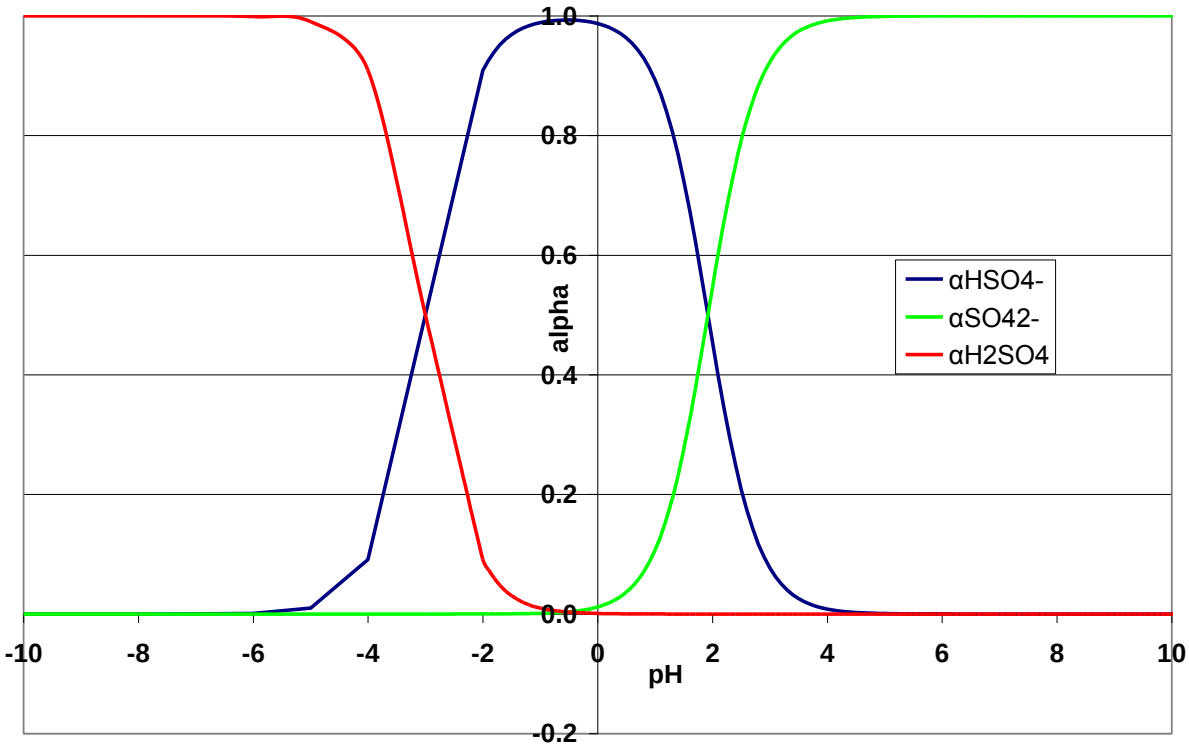

Figure 4.6: Fractional composition of Sulphuric Acid

The range of pH of interest in terms of the operation of a lead-acid battery is -1.0>pH>1.0, the corresponding ratios of the constituents is shown in table 4.2

pH	-1.0	1.0
H_2SO_4	<1%	0
HSO_4^-	99%	89%
SO_4^{2-}.	<1%	11%

Table 4.2: Dissociation of H_2SO_4

Therefore it can be seen from the above that the HSO_4^- ion is predominant across the range of pH associated with the operation of the lead-acid battery.

4.5 The Nernst Equation and the Lead Acid battery

The reaction in the lead acid battery following the first dissociation can be written as:

$$Pb(s) + PbO_2(s) + 2H^+(aq) + 2HSO_4^-(aq) <=> 2PbSO_4(s) + 2H_2O(l)$$

Using 3.33

$$E = E^o - \frac{RT}{nF}\ln\left(\frac{a_M^m a_N^n}{a_A^1 a_B^b}\right)$$

$$E = E^o - \frac{RT}{nF}\ln\left(\frac{(a_{PbSO_4})(a_{H_2O})}{(a_{Pb})^{\frac{1}{2}}(a_{PbO_2})^{\frac{1}{2}}(a_{H^+})(a_{HSO_4^-})}\right) \qquad 4.57$$

Following the second dissociation:

$$Pb(s) + PbO_2(s) + 2H^+(aq) + 2SO_4^{2-}(aq) <=> 2PbSO_4(s) + 2H_2O(l)$$

Using 4.44

$$E = E^o - \frac{RT}{nF}\ln\left(\frac{a_M^m a_N^n}{a_A^1 a_B^b}\right)$$

$$E = E^o - \frac{RT}{nF}\ln\left(\frac{(a_{PbSO_4})(a_{H_2O})}{(a_{Pb})^{\frac{1}{2}}(a_{PbO_2})^{\frac{1}{2}}(a_{H^+})^2(a_{SO_4^{2-}})}\right) \qquad 4.58$$

The expression can be simplified as the activities of solids, the this case the Lead (Pb), Lead Oxide (PbO_2) and Lead Sulphate ($PbSO_4$) can be taken as unity as can the activity of the solvent (H_2O), 4.58 becomes:

$$E = E^o - \frac{RT}{nF}\ln\left(\frac{1}{(a_{H^+})(a_{HSO_4^-})}\right) = E^o - \frac{RT}{nF}\ln(a_{H^+})^{-1}(a_{HSO_4^-})^{-1} \quad 4.59$$

The ideal reversible cell voltage E_o is determined using equation 4.43

$$E = -\frac{\Delta g}{nF}$$

The free enthalpy of this reaction is ΔG = -372.6 kJ [19].

$$E = -\frac{\Delta g}{nF} = -\frac{-372.6}{2\times 96485} = 1.931\,\text{Volts}$$

$$E = 1.931 - \frac{RT}{nF}\ln\left(\frac{1}{(a_{H^+})(a_{HSO_4^-})}\right) = 1.931 - \frac{RT}{nF}\ln(a_{H^+})^{-1}(a_{HSO_4^-})^{-1}$$

This can be rearranged into the form:

$$E = 1.931 + \frac{RT}{nF}\ln(a_{H^+})(a_{HSO_4^-}) \quad 4.60$$

For the second dissociation, and again using 4.44

$$E = E^o - \frac{RT}{nF}\ln\left(\frac{a_M^m a_N^n}{a_A^1 a_B^b}\right)$$

$$E = E^o - \frac{RT}{nF}\ln\left(\frac{(a_{PbSO_4})(a_{H_2O})}{(a_{Pb})^{\frac{1}{2}}(a_{PbO_2})^{\frac{1}{2}}(a_{H^+})^2(a_{SO_4^{2-}})}\right) \quad 4.61$$

Again as above, the expression can be simplified as the activities of solids, the this case the Lead (Pb), Lead Oxide (PbO_2) and Lead Sulphate ($PbSO_4$) can be taken as unity as can the activity of the solvent (H_2O), 4.61 becomes:

$$E = E^{o} - \frac{RT}{nF}\ln\left(\frac{1}{(a_{H^+})^2(a_{SO_4^{2-}})}\right) = E^{o} - \frac{RT}{nF}\ln(a_{H^+})^{-2}(a_{SO_4^{2-}})^{-1}$$

The ideal reversible cell voltage E_o is determined using equation 4.43

$$E = -\frac{\Delta g}{nF}$$

The free enthalpy of this reaction is ΔG = -395.6 kJ [74].

$$E = -\frac{\Delta g}{nF} = -\frac{-395.6}{2\times 96485} = 2.05 \text{ Volts}$$

$$E = 2.05 - \frac{RT}{nF}\ln\left(\frac{1}{(a_{H^+})^2(a_{SO_4^{2-}})}\right) = 2.05 - \frac{RT}{nF}\ln(a_{H^+})^{-2}(a_{SO_4^{2-}})^{-1}$$

$$E = 2.05 + \frac{RT}{nF}\ln(a_{H^+})^2(a_{SO_4^{2-}}) \qquad 4.62$$

Therefore the reversible voltage under arbitrary conditions of a lead-acid cell is dependant on the sulphuric acid activity a, that is the active mass within the sulphuric acid:

$a = \gamma C$ 4.63

γ = ionic activity coefficient

C = molar concentration.

Using equation 4.63 and substituting in 4.60

$$E = 2.05 + \frac{RT}{nF}\ln(a_{H^+})(a_{HSO_4^-})$$

$$E = 2.05 + \frac{RT}{nF}\ln(C_{H^+})(C_{HSO_4^-})$$

$$E = 2.05 + \frac{RT}{nF}\ln(2)(C_{H^+})(C_{HSO_4^-}) \qquad 4.64$$

Using equation 4.63 and substituting in 4.64

$$E = 2.05 + \frac{RT}{nF} \ln\left(\gamma_{H^+}^{2}\right)\left(\gamma_{SO_4^{2-}}\right)$$

$$E = 2.05 + \frac{RT}{nF} \ln\left(C_{H^+}^{2}\right)\left(C_{SO_4^{2-}}\right)$$

$$E = 2.05 + \frac{RT}{nF} \ln\left(4^{3}\right)\left(C_{H^+}^{2}\right)\left(C_{SO_4^{2-}}\right) \quad 4.65$$

Therefore it has been shown that the Nernst equation relates the reversible voltage (emf) of electrochemical cells, to properties of its active components, in particular the ionic activity coefficient γ and the molar concentration C. However, it this only applies under equilibrium conditions. Behaviour of electrochemical cells under non-equilibrium conditions has to be considered as non-equilibrium, or non-ideal conditions are the actual conditions under which the cell operates in reality.

In practice, passage of any finite amount of electricity results in a certain degree of irreversibility as some of the electrical energy is dissipated as heat either in the internal resistance of the cell, or at the electrodes where application of a potential difference is required to drive the current at the desired rate. Galvanic cells can only supply electric work equal to the free energy change of the cell reaction. The cell voltage under an external load is always smaller than the open circuit voltage, so that only part of the thermodynamically available work can be utilised [4].

4.6 Non-Ideal behaviour

The foregoing work has been based in ideal behaviour in electrochemical cells. The restriction of electrode reaction quoted at standard concentrations is overcome by the Nernst equation, however the Nernst equation still relates to ideal conditions.

In practice, passage of any finite amount of electricity results in a certain degree of irreversibility as some of the electrical energy is dissipated as heat either in the internal resistance of the cell, or at the electrodes where application of a potential difference is required to drive the current at the desired rate. Galvanic cells can only supply electric work equal to the free energy change of the cell reaction. The cell

voltage under an external load is always smaller than the open circuit voltage, so that only part of the thermodynamically available work can be utilised [75].

4.6.1 Polarisation

The battery voltage as described by the Nernst equation assumes that the battery is in equilibrium. As a battery under load is not in equilibrium, the measured voltage and battery capacity may differ significantly from the equilibrium values, and the further from equilibrium, the larger the deviation between the actual and equilibrium voltage.
The difference between the equilibrium voltage and the actual voltage when under load is called polarisation.

When current flows, the cell reaction must happen at a corresponding rate, for every delivered ampere-second, a corresponding number of electron exchanges must have occurred. To achieve this current flow, additional energy is required, which intensifies the electron and ion flow in the desired direction. This effect is expressed in terms of over-voltages, i.e. deviations from the equilibrium voltage. Furthermore, current flow through conducting elements causes ohmic voltage drops. As a result, the voltage under current flow E is reduced below the equilibrium voltage E^0. The difference E^0-E, when measured as cell voltage deviation, comprises the overvoltage of the electrochemical reactions and ohmic voltage drops, caused by the electronic as well as ionic currents in the conducting parts of the cell.
The sum of all of the voltage drops caused by the current flow is called Polarisation.

Polarisation = Overvoltage + Ohmic Voltage Drops

The quantity determined in practice is always polarisation. Overvoltage can only be determined by special electrochemical methods [67].

Polarisation has a significant impact on battery performance, both beneficial and detrimental. For example polarisation depresses cell voltage and suppresses but does completely eliminate the secondary reaction of electrolysis due to the presence of water in the electrolyte, during battery discharging. Polarisation adversely affects battery performance by reducing battery capacity and efficiency.

The thermodynamic treatment of electrochemical processes describes the equilibrium condition of a system but does not present information on non-equilibrium conditions such as current flowing from electrode polarisation (overvoltage) imposed to effect electrochemical reactions. Experimental determination of the current-voltage characteristics of many electrochemical systems has shown that there is an exponential relationship between current and applied voltage. The generalised equation is called the Tafel equation.

$$\eta = a \pm b \log i \qquad 4.66$$

where:

η = overvoltage or polarisation

i = current

a, b = characteristic constants of the electrode system

Typically, the constant b is referred to as the Tafel slope [70]. A plot of electrode potential versus the logarithm of current density (amperes per cm^2) is called the "Tafel plot" and the resulting straight line the "Tafel line".

"b" is the "Tafel slope" that provides information about the mechanism of the reaction, and "a" provides information about the reaction rate constant (and exchange current density) of the reaction. The Tafel equation is a limiting case of the Butler-Volmer equation for high for high overpotential (larger than 50 to 100 mV, depending on the system) [71].

Figure 4.7 is a plot of η versus log of anodic current with $\alpha = 0.5$ (where α is the cathodic electron transfer coefficient). The linear plot is of the Tafel equation. The slope b is given by equation 4.67.

$$b = \frac{2.303RT}{\alpha nF} \quad 4.67$$

The intercept at η = 0 gives the exchange current density i_o. This is known as a Tafel plot, permitting calculation of the intercept a, and the exchange current density i_o [72].

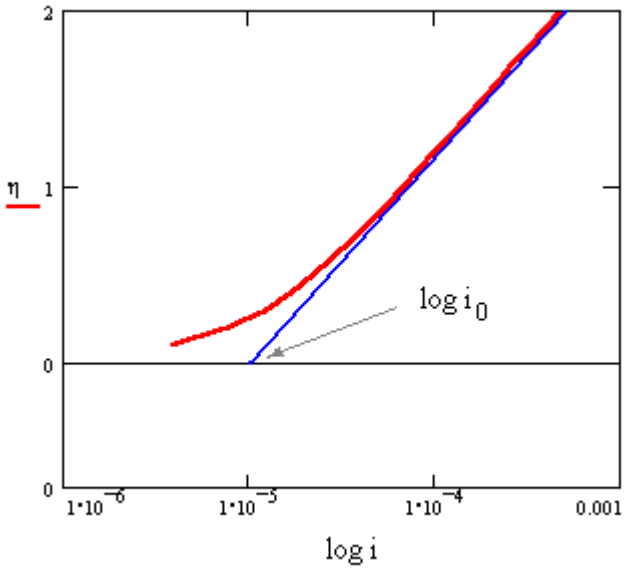

Figure 4.7: Tafel plot.

Where an electrochemical reaction occurs in two half reaction on separate electrodes, as in a lead-acid battery, the Tafel equation is applied to each electrode separately. The Tafel equation is applicable where the values of polarisation are high. At low values of polarisation, the dependence of current on polarisation is usually linear and not logarithmic, in this region the Tafel equation has the form shown in equation 4.67. This linear region is called "polarisation resistance" due to its formal similarity to Ohm's law.

$$i = i_0 \frac{nF}{RT} \Delta E \quad 4.67$$

where: i = current density

i_o = exchange current density

Note: Current density is simply current divided by area, and is used as a measure of the rate of charge transfer.

As mentioned the Tafel equation is in fact a limiting case of the Butler-Volmer equation. The Butler-Volmer equation has a sound theoretical basis and can be developed by considering how a change in potential difference affects the activation energy for the charge transfer processes (both oxidation and reduction) at a single electrode [56].

The Butler-Volmer equation is one of the most fundamental relationships in electrochemistry. It describes how the electrical current at an electrode depends on the electrode potential, considering that both a cathodic and anodic reaction occur on the same electrode.

$$I = Ai_o\left\{\exp\left[\frac{1-\alpha)nF}{RT}\right.\right.E - E_o\left.\right\] - \exp\left[-\frac{\alpha nF}{RT}(E - E_o)\right] \quad 4.68$$

where:

I: electrode current, A

i_o: exchange current density, A/m^2

E: electrode potential, V

Eo: equilibrium potential, V

A: electrode active surface area, m^2

T: absolute temperature, K

n: number of electrons involved in the electrode reaction

F: Faraday constant

R: universal gas constant

α: so-called symmetry factor, dimensionless

Equation 4.68 is named after chemists John Alfred Valentine Butler and Max Volmer, values of i_o and α can be determined from Tafel plots.

The equation is valid when the electrode reaction is controlled by electrical charge transfer at the electrode (and not by the mass transfer to or from the electrode surface from or to the bulk electrolyte). Nevertheless, the utility of the Butler-Volmer equation in electrochemistry is wide, and it is often considered to be "central in the phenomenological electrode kinetics" [73].

There are two limiting cases of the Butler-Volmer equation:

The low overpotential region (called "polarisation resistance"), where the Butler-Volmer equation simplifies to

$$i = i_o \frac{nF}{RT}\left(E - E_{eq}\right)$$

The high overpotential region, where the Butler-Volmer equation simplifies to the Tafel equation.

$E - E_o = a - b \log (i)$ for a cathodic reaction, or

$E - E_o = a + b \log (i)$ for an anodic reaction,

Where a and b are constants (for a given reaction and temperature) and are called the Tafel equation constants.

Therefore by focusing on the events at an electrode solution interface it is possible to model non-ideal behaviour of electrode processes. This can be summarised as follows.

- For electrode processes, the observed dependence of reaction rate on the potential difference, E across the electrode-solution interface can be recorded as plot of the net current density against overpotential.
- The net process at a single electrode is dictated by the sign of the overpotential.
- At equilibrium, both the overpotential and the net current density are zero.

Therefore important information on electrode can be represented be these relationships, and can help in the understanding of electrochemical processes. However, relationship between overall cell potential and current flowing through the

cell are necessary in order to develop a model of the cell discharge and charge process.

4.6.2 Cell Discharge and Charge

The voltage of a battery measured on load will be lower than under open circuit. This is a result of the internal impedance of the battery, which is made up of:

- Polarisation losses at the electrodes;
- Ohmic (resistive) losses [i.e. current (I) x resistance (R) =IR] in the grid, electrolyte and active mass.

When current flows through a battery, there is departure from equilibrium conditions and the useful work performed by the battery is always less than the maximum value. The shift in potential of an electrode away from the reversible (equilibrium) value is termed the electrode overpotential (ή). Overpotential can be partitioned into many different subcategories that are not always well defined. A likely reason for the lack of strict definitions is that it is difficult to determine how much of a measured overpotential is derived from a specific source. There is precedence for lumping overpotentials into three categories.

1. Activation overpotential caused by kinetic limitations to the charge-transfer process at the electrode; this is an intrinsic property of the electrode material immersed in the electrolyte, i.e. an interface phenomenon.
2. A concentration overpotential, which results in depletion of reactants in the vicinity of the electrode due to slow diffusion from the bulk of the electrolyte solution. This is an extensive property, which depends on the thickness and porosity of the electrode and ease of diffusion through it, as well as the mass transport process in the electrolyte.
3. Reaction overpotential is caused by chemical kinetics in the boundary layer or at the electrode surface.

Together, these overpotentials result in a voltage drop at the electrode, which is termed the polarisation loss, and the electrode is said to be polarised. Similarly, the

voltage drop due to the internal resistance of the battery (i.e. resistance losses) is commonly referred to as the resistance (or ohmic) polarisation (or overpotential).

Polarisation losses consume energy, which means that not all of the theoretical energy available in the battery is fully converted into useful electrical energy.
In principle polarisation can be determined by calculation if some electro-chemical parameters and the mass-transfer condition are available. However, in practice it is difficult to determine the values for both because of the complicated physical structure of the electrodes [70].

The current, which can be drawn from, a cell, will gradually reduce with time due to polarisation. Furthermore, polarisation occurs due to hydrogen bubbles produce by electrolysis at the metal cathode adhering to this electrode. This has to two effects:

1. Hydrogen, being an excellent insulator, introduces a layer of high electrical resistance.
2. Due to the electric field present, a double layer of positive and negative ions form on the surface of the hydrogen layer and results in a reverse or back e.m.f.

Placing inert separators between the positive and negative electrodes reduces hydrogen production at the electrodes; and also prevents short circuits between the adjacent plates.

Polarisation losses occur at each electrode and are responsible for a reduced cell voltage during discharge (V_d) and an increased cell voltage during charging (V_{ch}).

$$V_d = V - \eta_+ - \eta_- - IR \qquad 4.69$$

$$V_{ch} = V + \eta_+ + \eta_- + IR \qquad 4.70$$

Where η_+ and η_- are the overpotentials at the positive and negative electrodes respectively. At low overpotentials, the relationships between ή and I takes the same form as Ohms law and, under these conditions, equations 4.69 and 4.70 reduce to

$$V_d = V - IR' \qquad 4.71$$

$$V_{ch} = V + IR' \qquad 4.72$$

Where R' is the sum of the internal resistances of the cell and the equivalent resistances corresponding to the activation and concentration overpotentials at both electrodes. The relationships between the practical cell voltage on both discharge and charge as shown in figure 4.7

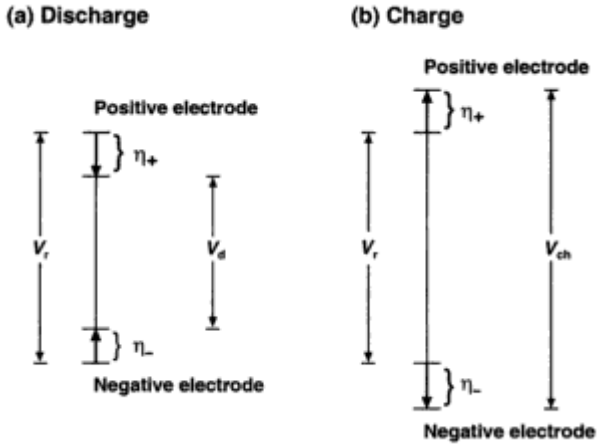

Figure 4.7 Relationship between practical cell voltages and the reversible cell voltage [73].

To illustrate the effects of non-ideal behaviour in practice Figure 4.8 compares the reversible and actual cell voltage of a lead-acid cell. It is apparent that the actual discharge voltage lies below reversible cell voltage of 2.05 volts; the deviation from the reversible voltage is a measure of the combined influence of the internal resistance of the cell and the polarisation losses.

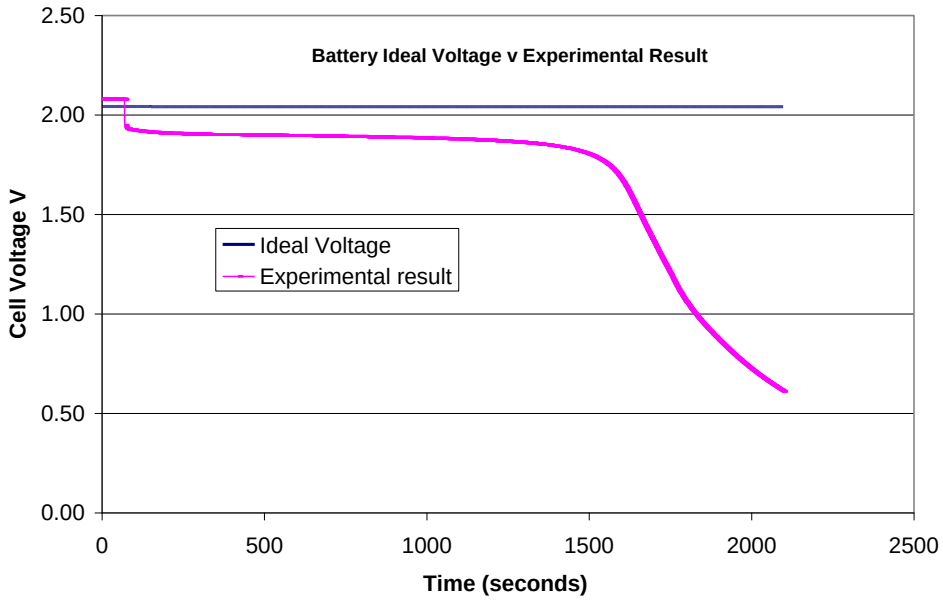

Figure 4.8 Comparison of reversible and actual cell discharge voltage characteristic.

The difference between the ideal and actual cell voltage can be explained with the aid of figure 4.9 a plot of terminal voltage against current representing the cumulative effect of the losses; this characteristic is given the term *polarisation curve.*

The actual cell potential is decreased from its equilibrium potential because of irreversible losses. Multiple phenomena contribute to irreversible losses in an actual fuel cell. The losses, which are called polarisation, over-potential, or over-voltage, originate primarily from three sources.

This curve can be separated into three regions corresponding to these losses:

1. Region of activation resistance losses, or activation polarisation.
2. Region of ohmic resistances, or ohmic polarisation.
3. Region of concentration (concentration polarisation) or mass transport losses.

These losses result in an open circuit cell voltage (V) that is less than its ideal potential, that is:

$$E = V + \text{Losses.} \qquad 4.73$$

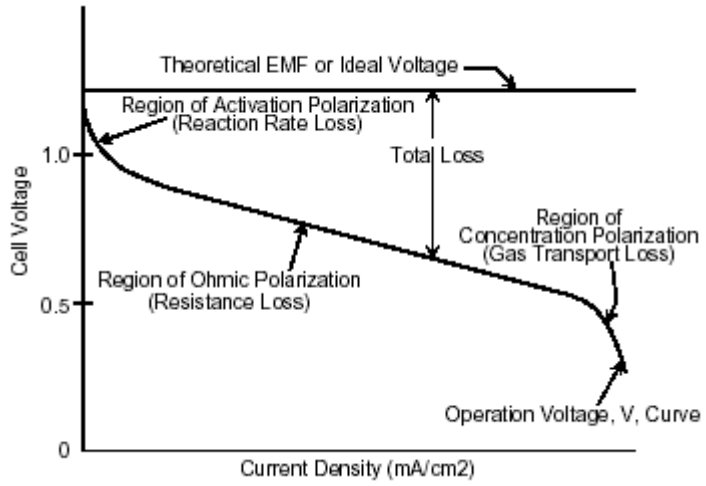

Figure 4.9: Ideal and Actual Fuel Cell Voltage/Current Characteristics [74].

4.6.3 Activation Polarisation

Activation polarisation is present when the rate of an electrochemical reaction at an electrode surface is controlled by sluggish electrode kinetics. In other words, activation polarisation is directly related to the rates of electrochemical reactions.

The activation polarisation loss is dominant at low current density. At this point, electronic barriers must be overcome prior to current and ion flow. Activation losses increase as current increases.

The sharp drop in voltage of the first region associated with the activation resistance is attributed to the type of catalyst and the active catalyst surface area that is in contact with the electrolyte and the electrical network in the electrode that is accessible to the reacting gases. Lowering this resistance will raise the whole polarisation curve. Using catalysts with lower activation resistance and increasing the catalyst surface area available for reaction per unit volume of electrode can reduce this voltage loss.

4.6.4 Ohmic Polarsation

Ohmic losses occur because of resistance to the flow of ions in the electrolyte and resistance to flow of electrons through the electrode. Decreasing the electrode separation and, enhancing the ionic conductivity of the electrolyte reduce the dominant ohmic losses through the electrolyte. Because both the electrolyte and fuel cell electrodes obey Ohm's law, the ohmic losses can be expressed by the equation

$E_{ohm} = iR$ 4.74

Where i is the current flowing through the cell, and R is the total cell resistance, which includes electronic, ionic, and contact resistance.

Ohmic polarisation (loss) varies directly with current, increasing over the entire range of current because cell resistance remains essentially constant.

The gradual drop in voltage of the second region known as the ohmic voltage loss is attributed to the ohmic resistance of the components within the electrical network of the cell, such as the electrical and contact resistances.

When a current flows through a cell, the various components conform to Ohms law, and the cell voltage falls due to their resistance. This applies to both electrodes and to the electrolyte. The resulting potential loss is termed *Ohmic* polarisation

Lowering the ohmic resistance will reduce the slope of the V-I curve and consequently higher power densities at higher energy efficiencies.

4.6.5 Concentration Polarisation

The sharp voltage drop in the third region is the voltage loss associated with the mass transport resistance and is attributed to concentration polarisation, which occurs as a result of depletion of the reactant at the reactant interface as its transport to the reaction sites fails to keep pace with the reaction rates.

As a reactant is consumed at the electrode by electrochemical reaction, there is a loss of potential due to the inability of the surrounding material to maintain the initial concentration of the bulk fluid [75].

As current is drawn from the cell polarisation losses increase to the point of maximum limiting current density; beyond which point the cell voltage falls rapidly.

The desirable case is a cell with a flat polarisation curve and a high limiting current density, and correspondingly high efficiency. This requires electrodes with a large surface area, and therefore a relatively big and heavy cell. Smaller and lighter cells will therefore suffer from reduced efficiency [76].

In order to eliminate the effect of the electrode size, the current is expressed as current per unit area of electrode or current density (mA/cm^2).

When no load is drawn, the cell voltage is the open circuit voltage, at some point below the ideal voltage.

4.7 Chapter Conclusions.

This chapter has discussed thermodynamic theory with respect to electrochemical theory, and in particular the development of the Nernst equation. This equation has particular relevance in terms of modelling the ideal or reversible behaviour of electrochemical cells. There are significant differences in the ideal and non-ideal or actual voltage characteristics due to irreversible processes taking place during discharge of a cell. This creates difficulties when attempting to model the actual discharge process. This aspect of cell behaviour is discussed further in Chapter 6.

CHAPTER 5 FUEL CELLS

Fuel cell monitoring systems have to monitor and control fuel cell operation under widely varying conditions, and accurately capture information relating to performance and operational characteristics. A fuel cell was used as part of the hybrid power system installed in the electric vehicle, where the fuel cell acts as an on-board battery charger or "range extender", improving the working range or duration of the hybrid vehicle when compared to a solely battery powered electric vehicle. A key element of a fuel cell monitoring system is individual cell voltage measurement. As discussed in Chapter 2 the failure of a single cell within a fuel cell stack may lead to catastrophic failure of the entire stack, hence a cell voltage monitor can be employed to measure individual cell voltages and identify 'weak' cells which are approaching reversal. If a cell does reverse polarity it will be charged by the other 'healthy' cell in the stack resulting in gas evolution which if allowed to continue will cause irreversible damage to the cell and has the potential to damage the entire stack. The author set out to design a low cost cell voltage monitoring system for the vehicle fuel cell stack, as the cost of purchasing such a system was prohibitive.

5.1 The Fuel Cell System

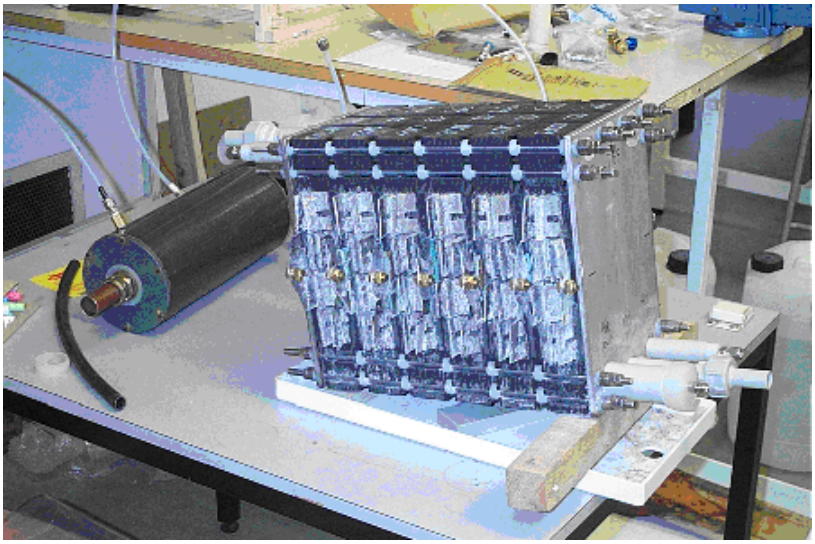

Figure 5.1 Zetek Fuel Cell Stack

The Alkaline Fuel Cell (AFC) was developed in the 1930s by F.T. Bacon and is one of the oldest fuel cell technologies. In 1954 Bacon demonstrated a six cell fuel cell that produced 150W

Then in 1956 his team built a 40 cell unit based on the same design. The larger unit produced 6kW and was used to power a fork-lift truck, welding equipment and a circular saw. In 1961, Bacon formed Energy Conversion (Ltd) and the company began the development of fuel cells which could be produced commercially [77].

The fuel cell system used in the hybrid electric vehicle for this thesis was designed around a Zetek Power alkaline fuel cell stack, of 1.2 kW nominal electrical power output as shown in figure 5.1. Zetek Power went into receivership and its technology was acquired by Cenergie in 2002.

This fuel cell stack is of a modular construction each module containing 6 cells connected in a series parallel array (4p x 6s) to give a nominal working voltage per module of 4.0 volts. Modules are connected in series up to a recommended maximum of 8 modules [78].

There a number of parameters, which require to be monitored, and/or controlled, including liquid and gas pressures, temperatures, levels and flow rates, as well as cell voltage and current. Therefore, an integrated control and monitoring system has been developed to permit the fuel cell system to function efficiently and safely.

The initial stages of the development of the control system were focused on the various sub systems required for the operation of the fuel cell system, see figure 5.2.

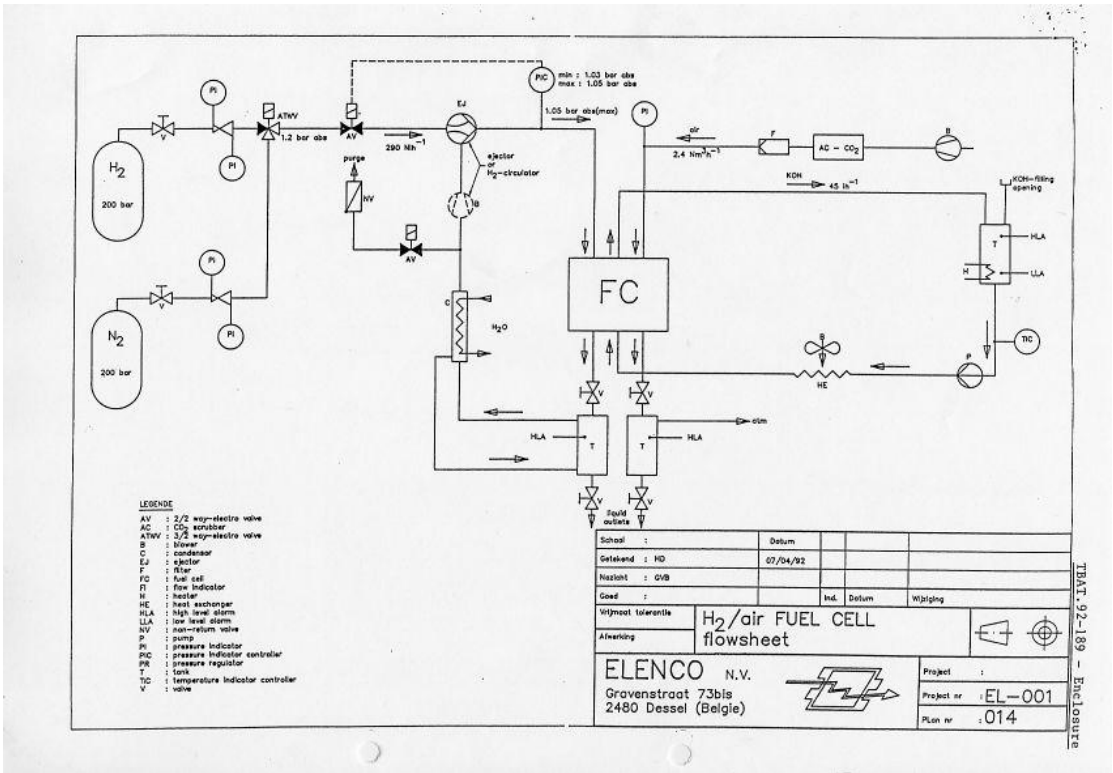

Figure 5.2: Schematic of Zetek Fuel Cell system [79].

The fuel cell system illustrated in figure 5.2 has four process loops:

1. Electrolyte
2. Hydrogen/Nitrogen
3. Air
4. Water

5.1.1 Electrolyte

The electrolyte used in this fuel cell stack is a 30% Potassium Hydroxide (KOH) solution; this requires to be circulated within a closed circuit at a flow rate of 100 litres per hour per kW of stack electrical power output. The electrolyte will typically be at a temperature of 70^{o}C, at a pressure marginally above atmospheric pressure. During the start-up phase, the KOH is pre-heated by the water circuit, which brings the stack up to operating temperature; this water circuit also acts as a heat sink while the stack is at operating temperature. Good control of the electrolyte flow and temperature, and, therefore water temperature is important, as the power output from

the fuel cell stack is temperature dependent as shown in figure 5.3 Electrolyte temperature determines the power output from the stack, and, it is recommended that the stack should only be operated when the electrolyte temperature is at least 15^{o}C. Figure 5.3 shows the relationship between electrolyte temperature and percentage of maximum electrical power output.

Reasonable performance is exhibited by alkaline fuel cells operated at low temperatures (room temperature up to 70^{o}C), however, alkaline fuel cells designed to operate at 70^{o}C will reduce to approximately 30% of maximum power when the electrolyte temperature is at room temperature [80].

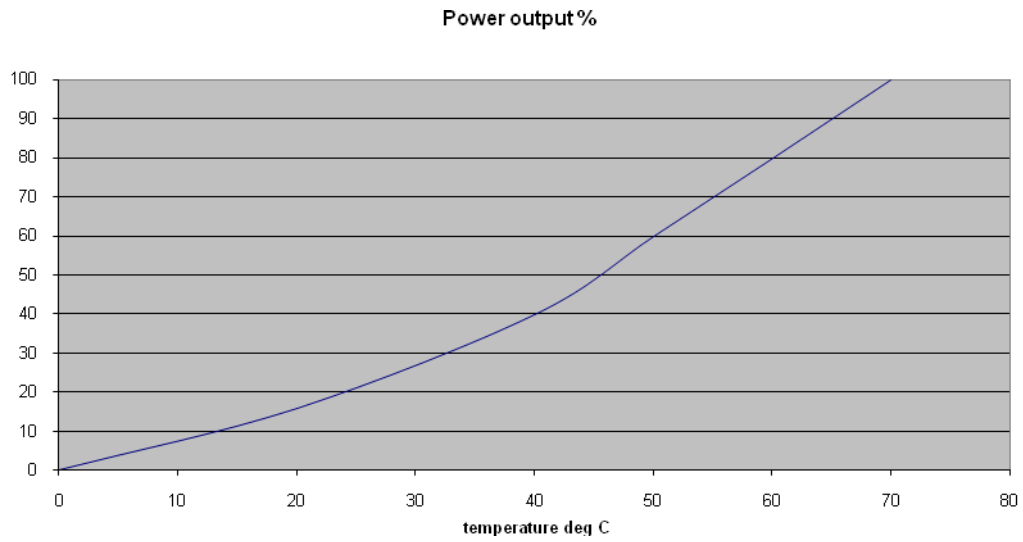

Figure 5.3: Relationship between electrolyte temperature and percentage of maximum power output [84].

During operation of the fuel cell stack, the temperature, pressure and tank level of the KOH fluid are constantly monitored. Pressure differentials have to be maintained between the process fluids to prevent damage to the membrane structure of the fuel cell stack.

5.1.2 Hydrogen/Nitrogen System

It is recommended that Nitrogen gas is purged through both the anode and cathode of the fuel cell stack during the start-up phase, prior to introduction of the reactants namely, oxygen derived from air, and hydrogen. Pressure switches set at pre-defined high and low-pressure limits ensure that the gas pressures are maintained within the specified operating range that is the hydrogen inlet pressure is within 10 mbar of the inlet air pressure, while the dynamic pressure of the electrolyte at the stack outlet must be about 40 mbar above the average gas pressure. Additionally the hydrogen circuit includes a condenser to reduce the hydrogen stream humidity. The hydrogen fuel and nitrogen purge gases are stored in pressurised gas bottles, and electrically operated solenoid valves control delivery of the gases into the fuel cell stack. These solenoid valves are arranged to control the sequence and flow of gases to the fuel cell stack, during the start-up and shut down phases.

5.1.3 Air

Oxygen for the electrochemical reaction is derived from atmospheric air; the air at room temperature is compressed, and then passed through a Carbon Dioxide scrubber, before entering the fuel cell stack. It is essential that carbon dioxide is removed from the air prior to entry into the fuel cell stack. This is to prevent contamination of the electrolyte and catalyst materials. The CO_2 scrubber unit removes CO_2 from the air supplied to the fuel cell stack to levels below 10ppm, compared with the 400ppm associated with atmospheric air.

5.1.4 Water

A water system is used for heating and cooling the electrolyte and is maintained within a closed circuit, incorporating an electric heater for start-up, and, a fan cooled radiator to reject heat while the system is under load. A compact heat exchanger is used to transfer heat from the water circuit to the electrolyte during the start up phase, when the electrolyte is below its operating temperature. Once the fuel cell stack is under load, the direction of the heat transfer process is reversed; the water circuit then acts as a heat sink, rejecting heat through an air-cooled radiator.

Two thermocouples are installed to monitor the water temperature, and provide the control signals to operate the radiator cooling fan and water heater, with a further two thermocouples in the electrolyte circuit. A pump is used to provide circulation in the water circuit, and a flow meter monitors the water flow rate to ensure that an adequate circulation of water is maintained at all times.

Temperature measurement is an important feature of a fuel cell monitoring system. Pressure measurement is also a feature required of a monitoring system; in particular the differential pressures between the fluid streams in the fuel cell stack have to be maintained in order to protect the membranes separating the fluid streams.

The measured parameters on the fuel cell stack used in this research included, flow rates, pressure and liquid levels. In addition to measurement, outputs to control fans, pumps, solenoid valves and stack electrical load switching were required.

5.2 Monitoring and control system for the fuel cell system

The monitoring and control system for the fuel cell system used in this research consisted of a desktop computer, Data Acquisition card, control software and hard-wired interface. The monitoring and control software has been developed using National Instruments LabVIEW software. Input signals from the cell voltages, stack current, pressure switches, thermocouples and level switches are monitored and logged; output signals control the pumps, cooling fan, and gas valve solenoids.

There are two operating modes, manual and automatic, which are operator selectable, the mode selected dependent on the nature of the test being undertaken. The LabVIEW© programming environment is used to construct a 'Virtual Instrument', or VI. The VI panel for the fuel cell system is shown in Figure 5.4. This arrangement is suitable for monitoring and control of the fuel cell system whilst in the laboratory environment, although a robust industrial system could be readily implemented based on this design.

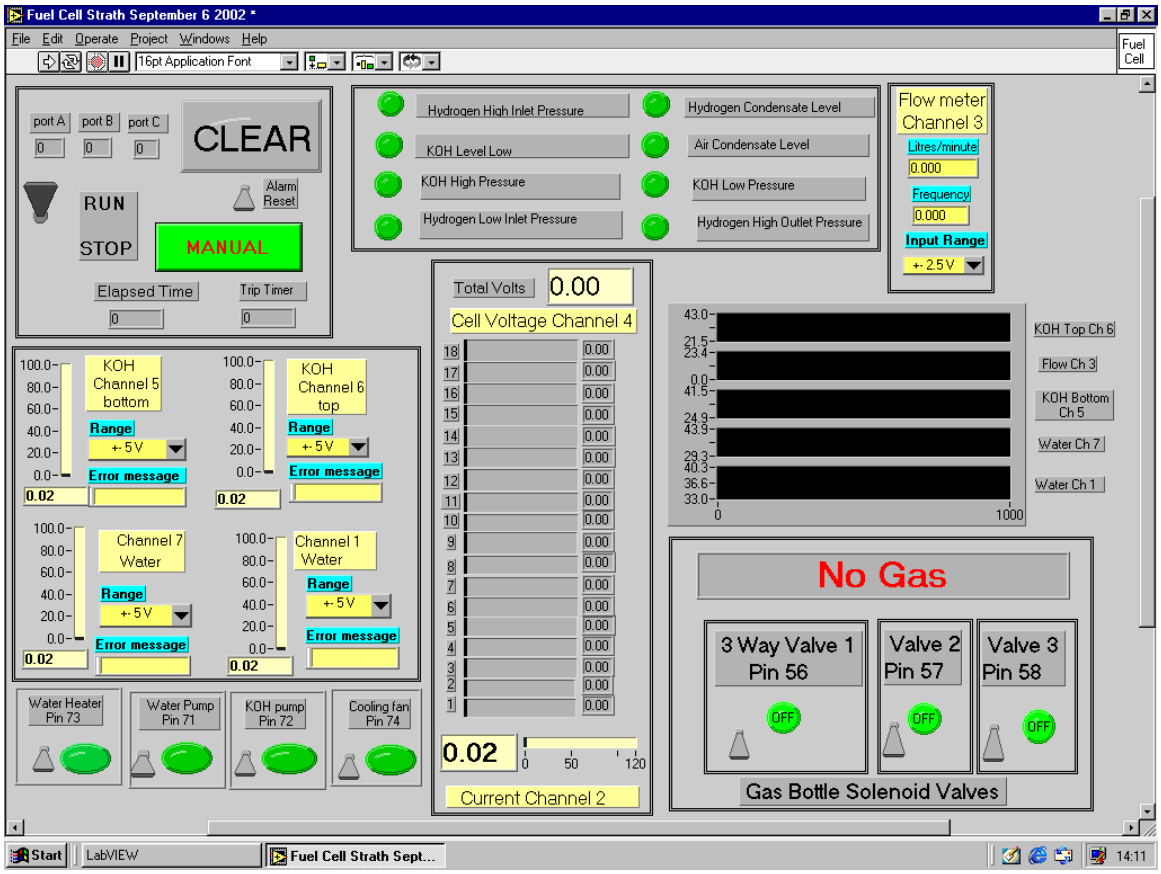

Figure 5.4: Authors LabVIEW© Front Panel

Figure 5.4 shows the user interface, or front panel of the VI, which is used to monitor and control the fuel cell system. The panel displays information necessary for the safe operation of the fuel cell system, whilst simultaneously logging all data inputs and outputs to a spreadsheet file for the duration of the test.

The VI front panel also displays the electrolyte and water circuit inlet and outlet temperatures as well as the electrolyte flow rate. Historical data for each of these inputs is displayed on charts seen on the mid-right of the front panel so any irregular trends can be detected and appropriate action taken.

As well as the monitoring and data logging function, the VI incorporated status indication of eight critical measurements with green indication for values within acceptable limits changing to red to indicate potentially critical conditions, these indicators latch in the ‘on’ condition and can only be reset once the fault has been

rectified. The VI also had digital output capability for switching loads via the interface circuit shown in figures 5.6 and 5.7.

Fault finding during development of this system was aided by including channel/pin numbers in the instrument tags. Individual cell voltages are displayed as well as total fuel cell stack voltage and current. Provision for up to 18 cells has been made on this particular VI however the cell voltage monitor has capacity for monitoring up to 24 cells.

Following initialisation routines, the main programme of the VI loops approximately once per second, this cycle time being predominantly governed by the acquisition rate of the cell voltage monitor. There are two modes of operation, manual mode permits the operator to control start-up, and shut down of the fuel cell stack, whereas automatic mode will provide sequenced control of these phases, with automatic shut down in the event of a fault condition occurring.

5.3 Development of the monitoring and control system

A desktop PC is a suitable platform for the monitoring and control of the fuel cell system, particularly in the laboratory environment, and with a suitable data acquisition card and compatible software a viable control system can be readily developed.

The data acquisition card used was a PCI-DAS1200 type manufactured by Measurement Computing Corp, USA.

National Instruments LabVIEW© software was used from the start of this project, LabVIEW© uses Virtual Instruments or VIs to provide an interface between the user and the system. Experience was gained initially by developing VIs for control applications; a fuel cell simulator was specifically constructed for this purpose.

The simulator shown in figure 5.5 consisted of a mimic panel, which used a Zetek process diagram with embedded LEDs to represent key items of the process. Potentiometers located on the front of the simulator provided feed back signals, to represent the system variables, the simulator communicated with the PC data acquisition board via a ribbon cable just visible in figure 5.5, power for the simulator came from a PC power supply recovered from an unserviceable PC base unit. A LabVIEW© VI was written for use with the simulator, which provided a useful ‘first

step’ in the design of the control and monitoring VI while the actual fuel cell system was under construction.

Figure 5.5 Fuel cell system simulator.

LED

Power supply unit

Input signal potentiometers

Ribbon cable to Data Acquisition card.

A fuel cell VI was developed for the fuel cell system with the facility to integrate with computer software packages such as Microsoft Excel, making the storage, manipulation and presentation of test data a relatively straightforward task. As the fuel cell system developed the VI was modified to incorporate any changes relevant to the monitoring and control philosophy.

The hardware interface is shown in figures 5.6 and 5.7; figure 5.6 shows the interface circuits for controlling output devices such as the pumps, solenoid-operated valves and cooling fan which were switched by the LabVIEW© VI via the data acquisition board digital outputs. Opto-isolation is incorporated into the output circuit to protect the hardware and the PC from external fault conditions.

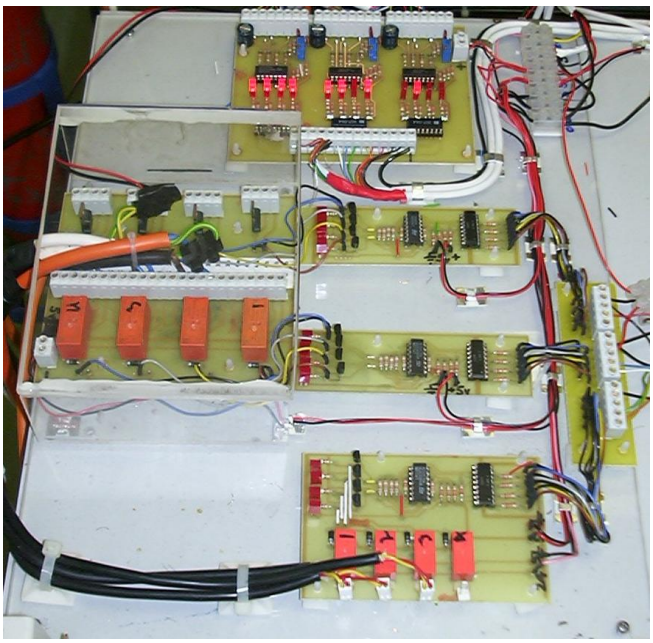

Figure 5.6: output interface circuit.

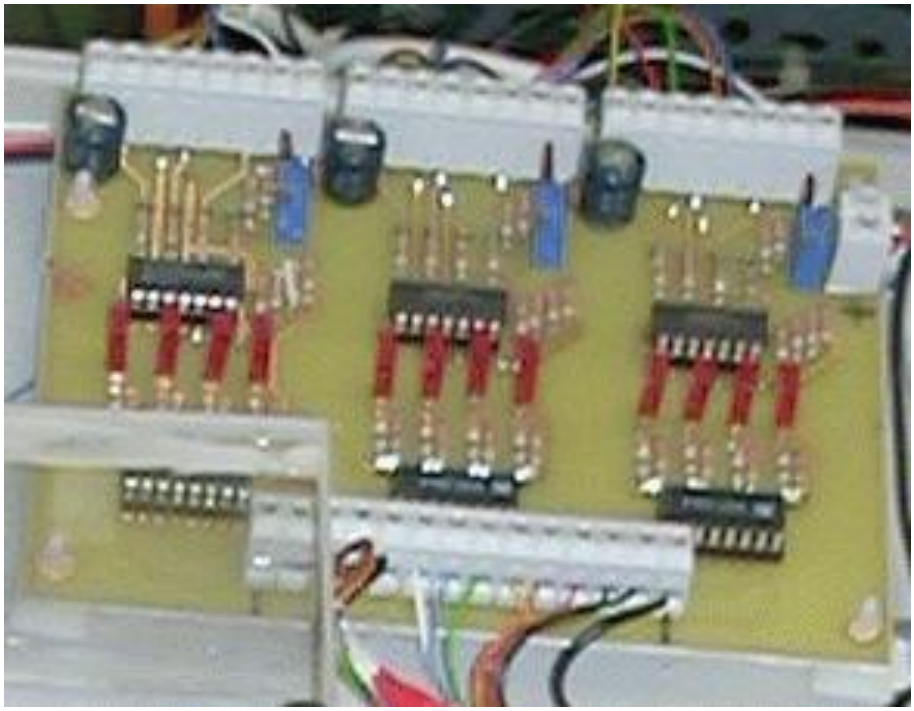

Figure 5.7: input interface

Figure 5.7 shows the input interface for the digital input signals, which simply comprises pull-up resistors to provide clearly defined logic levels on the input terminals of the data acquisition card, the logic levels being read as digital inputs by the LabVIEW© VI.

The first major test of the fuel cell control system came during the so called 'leeching' process; this process takes place the first time that a fuel cell stack is filled with electrolyte, the electrolyte having to be circulated continuously for a period of several days. During this process the main parameters which require to be monitored and/or controlled are, electrolyte pressure, temperature and flow rate, and the temperature and flow rate of the cooling/heating water circuit. Controls for the pumps, fans and heater used in these circuits can be seen bottom left in the VI shown in figure 5.4.

Following the completion of the leeching process, the control and monitoring system was developed to the next stage; this involved monitoring the gas pressures in the

Hydrogen/Nitrogen and Air gas paths. The gas pressures in these paths have to be regulated within a few millibars of atmospheric pressure, necessitating the use of pressure switches of an appropriate sensitivity to operate as high and low pressure alarms to prevent excessive pressure build up within the fuel cell stack. The Labview VI was modified accordingly to provide visual indication of either high or low pressure in the gas paths, during normal operation of the fuel cell stack. The gas supplies were isolated from the stack by electrically operated solenoid valves.

Temperature indicators can be seen centre left on the VI shown in Figure 5.4, with corresponding temperature charts showing temperature variation during the test period. The switches for the gas solenoid valves are directly below the thermocouple displays, with a Boolean indicator showing that Hydrogen gas is currently being supplied to the fuel cell stack. Alarm status indication is located centre top on this VI.

From the outset of this project it was clear that measurement of the cell voltages would be a critical function within the overall control and monitoring system, with the voltage across each cell group requiring to be monitored in isolation.

5.4 Fault Conditions

The value for the hydrogen–oxygen couple is 1.23 volts at standard conditions. However, under practical conditions the open circuit potential (voltage at zero current) will settle at a value below this [81]. Ideally all cells in the stack should have the same voltage, however, if an individual cell fails to attain 80% of the expected open circuit voltage it is likely that the cell has exceeded its service life [82]. The expected open circuit cell voltage on this particular fuel cell stack is 0.915 to 1.17 volts and the nominal operating voltage is 0.67 volts.

There are a range of fault conditions associated with fuel cell operation, which if left unchecked can result in severe, and, sometimes, irreversible damage to the fuel cell stack.

In order to sustain the chemical reaction the cells must be supplied with reactant gases at stoichiometric or, preferably higher values, as the completely uniform

distribution of the reactant gases to the many gas channels cannot be guaranteed. An even fluid distribution to all channels is difficult to achieve, since slight deviation in the flow resistance leads to variation in the flow. At high utilisation rates these flow discrepancies translate into variations in cell voltage across the stack. These discrepancies are assumed to result from liquid water droplets forming in the flow channels and thereby interfering with the gas flow. An undersupply to these cells of reactant gases will lead to a breakdown of the chemical reaction and a rapid loss in voltage. The voltage might even drop to negative values and decomposition of the electrochemical components and local heat generation ("hot spots") would damage the cells permanently. Therefore, an undersupply of reactant gases must be avoided under any circumstances. Special care must be taken particularly under dynamic load changes, when the current changes very quickly compared to the response of the reactant supply system [88].

With this in mind it is particularly important to monitor both the overall stack voltage and individual cell voltages. Reactant gas supplies are fed to cells, either in series or parallel flow configuration. As described in the previous paragraph the flow rate through each cell should be approximately the same, or some cells may be starved of gas. It is relatively easy for a droplet of liquid, such as condensed water, to become lodged in the inlet or exit port of a cell. Preferential flow will cause this cell to be by-passed, and the other cells will receive a higher flow rate. The blocked cell will still be having current drawn from it, as it is electrically connected in series with the remainder of the stack, but, as it cannot obtain reactants, its reverses its polarity and electrolyses the electrolyte [82].

Insufficient air supply, particularly when the stack is under load, can also result in cell voltage reversal and subsequent destruction of the cell cathodes. Furthermore polarity reversal can lead to membrane rupture or "burn-through" that is a loss of separation between the hydrogen and the air in the stack [1]. Individual cell voltage drop is often the first indication of insufficient gas flow within a particular cell, hence the importance of continuous cell voltage monitoring.

In addition there are fault conditions, which can occur when the fuel cell stack is under load. Reverse power protection should be provided to isolate the fuel cell stack from its load in the event that it is back fed from the load, to prevent the fuel cell voltage exceeding safe limits. If the fuel cell voltage rises above the hydrogen-oxygen couple of 1.23 volts, the cell begins to function as an electrolyser, with the attendant production of hydrogen, resulting in disruption to the gas flows within the fuel cell stack.

Fuel cell electrodes and catalysts degrade on activated standby without load more than under load. The high voltage on open circuit causes carbon oxidation processes and catalyst changes [83]. Unfortunately, the AFC with KOH electrolyte combines all the known disadvantages namely the electrolyte had to remain in the cells, residual carbonate (from any incomplete air clean-up) accumulated, separators (matrices) deteriorated, gas cross-over began during drying out or crystallisation periods during storage times without careful maintenance. Therefore, life expectancy definitely increases by emptying the electrolyte from the cells between operating periods. Isolation of the H_2 electrodes from air eventually establishes a nitrogen atmosphere. This shut down also eliminates all parasitic currents. The ability to replace the KOH electrolyte offers the possibility to operate on air with less than complete removal of the CO_2 [84].

5.5 Cell Voltage Monitoring

An important function of the fuel cell monitoring and control system is monitoring of the stack voltage and current. In terms of voltage monitoring there are two issues to be addressed:

1. Overall stack voltage.
2. Individual cell voltages.

The overall stack voltage is monitored in order to determine the operating condition of the stack in terms of the voltage versus current characteristic, thereby ensuring that the stack remains within its acceptable limits of safe operation.

Individual cell voltages are monitored to ensure that in the event of a single cell, or perhaps group of cells developing a fault the stack can be safely shutdown in order to limit damage to the stack.

The design of the modules, which make up the Zetek stack, precludes measurement of individual cell voltages due to the series/parallel arrangement of the modules. Therefore measurement of groups of 4 cells in parallel, in each module is employed, which means that there are 6 measurements per module.

5.5.1Cell Voltage Monitor 1

It was decided early in this project that there would be a requirement to measure individual cell voltages within the fuel cell stack. In order achieve this two different designs were employed. The first design known as Cell voltage monitor 1 (CVM1) was based on a simple design employing relays to connect each cell in turn to an analogue measurement channel on the PC data acquisition board.

The CVM1 circuit shown in figure 5.8, records each cell voltage during the operation of the fuel cell system.

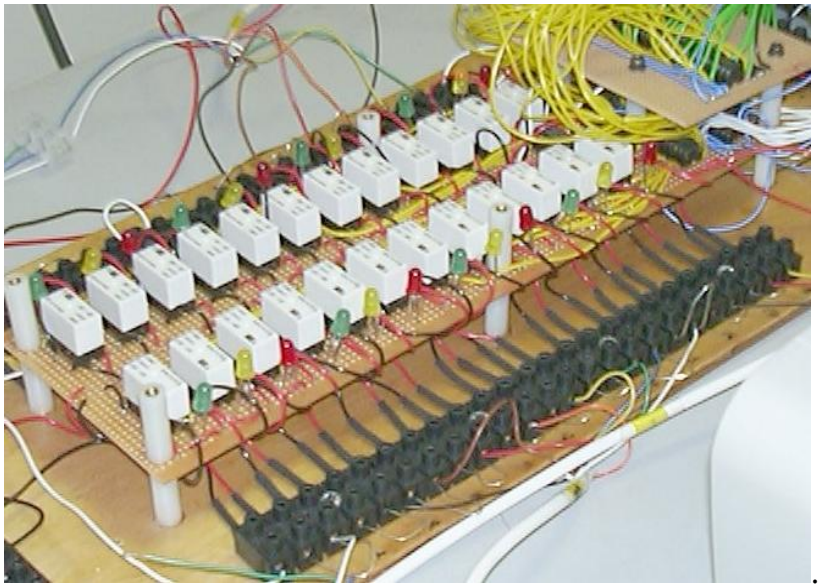

Figure 5.8 CVM1

Figure 5.8 shows the layout of the CVM1, the 24 relays, one per cell, can be clearly seen as the white rectangular blocks, the black terminal strip in the foreground connects the measurement points on the fuel cell stack to the relays. The multiplexer section is on the top right of the figure.

This CVM1 circuit has been designed around the Texas Instruments 74LS154 multiplexer device, the control signals from the PC being switched through to 24 double pole relays (figure 5.9), only one of which can be energised at any one time, with a dedicated LED indicating which relay is energised at any instant in time.

Figure 5.9: Double pole changeover relay

The measured cell voltage is then switched by its dedicated relay, to the PC via an analogue channel on the data acquisition card. A single channel of the CVM1 circuit is shown in figure 5.10.

To sequence the CVM1, five digital output lines of the data acquisition card are used in a binary fashion, providing for up to thirty-two individual voltage measurements, of which, only eighteen were required for this particular fuel cell stack configuration. A buffer /driver circuit is used between the multiplexer and the relays to provide the required switching current for the relays, and to invert the output of the multiplexer in order to obtain the required switching sequence.

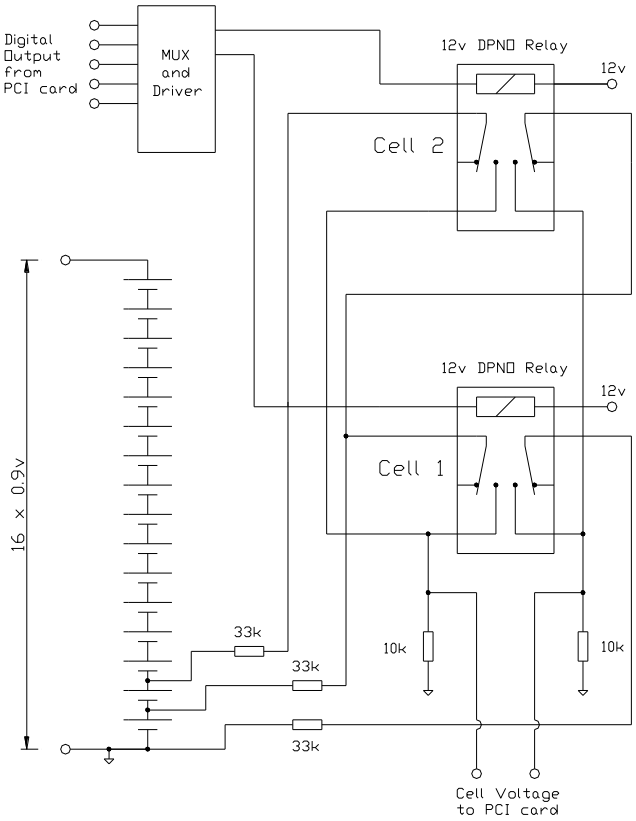

Figure 5.10: Details of one channel.

The sequencing of the CVM1 requires that only one cell voltage is read at a time. This is achieved within the programming of the LabVIEW© VI, by using a sequential structure ensuring that only one relay can be energised. Figure 5.11 illustrates the relay configuration.

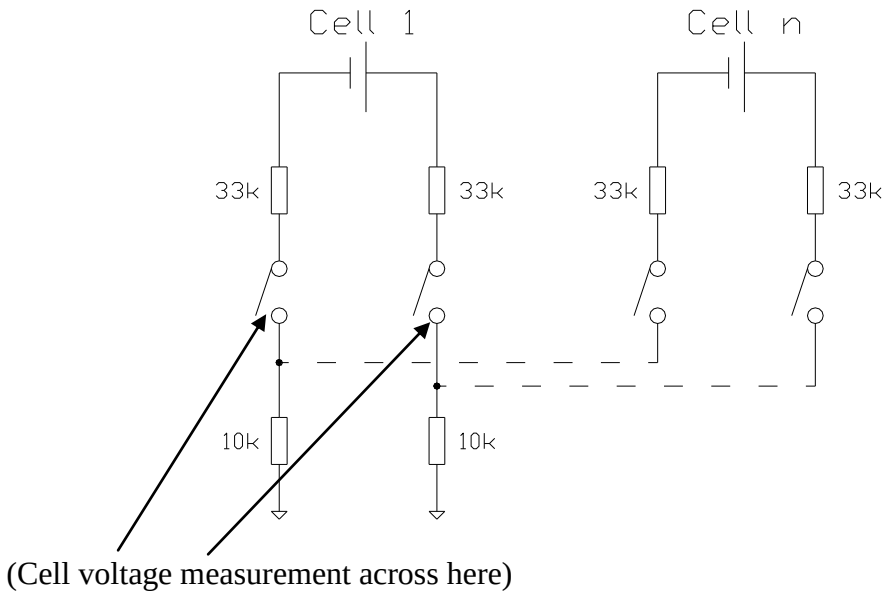

Figure 5.11: Relay configuration.

The CVM1 measures individual cell voltages, which range from 0.915 volts at no load, to around 0.67 volts at full load [87]. Care has to be taken when measuring an individual cell voltage, as the maximum voltage with respect to ground is 16 volts at no load with this particular stack. Therefore, on the output of the cell voltage monitor circuit a voltage divider arrangement is used to ensure that the measured voltage remains within the specified limits of the data acquisition card which is ± 5 volts.

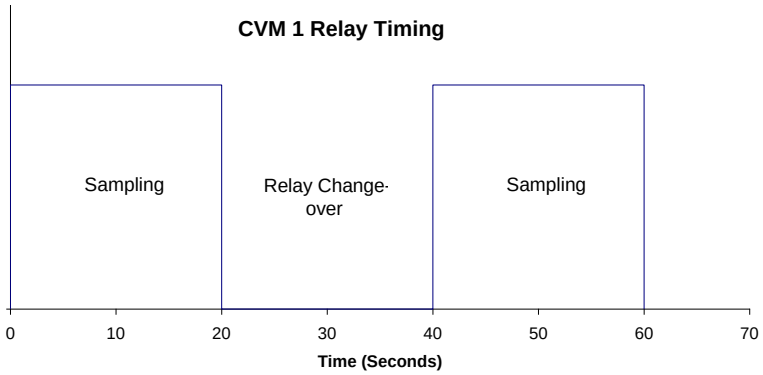

Figure 5.12: Relay change-over timing.

The double pole relays used in the circuit have operating and release times of 10 ms, illustrated by figure 5.12, and a further 20 ms is allowed for actual sampling time, making a total of 40 ms per cell, that is a maximum sampling rate of 25 Hz. There being 3 modules in this stack, each module having 6 series connected blocks, each block having 4 parallel-connected cells in this particular Zetek fuel cell stack arrangement, giving a total of 72 cells, giving a no-load stack voltage of approximately 16 volts, falling to approximately 12 volts under load. This arrangement of the cell voltage monitor means there are 18 voltage measurements to be made, giving a cycle time of 720 ms. This cycle time could be reduced by cutting back the sampling time, however, the present sampling rate seems adequate at the moment.

Future requirement for analysis of fuel cell transients would require lower cycle times, and therefore the cell voltage monitor in its current form could not cope with the substantially higher sampling rates required for transient measurement. It was therefore decided that a micro-controller based solution should be considered for use in subsequent systems, which should result in reduced cycle times.

5.5.2 Cell Voltage Monitor 2

With the experience gained from CVM1 it was decided to design a new cell voltage monitor based around a Programmable Interface Controller (PIC), which is an 8 bit micro-controller. A product of Arizona Microchip, these devices come in a wide range of configurations. The device chosen for this project was the PIC 16C77 from the PIC 16CXX family of devices, the layout of the PIC 16C77 is shown in figure 5.13. There are three digital input/output (I/O), namely ports B, C and D, and, 5 analogue inputs on port A. A circuit diagram of CVMII and flow chart for the PIC16C77 programming code is given in appendix 1.

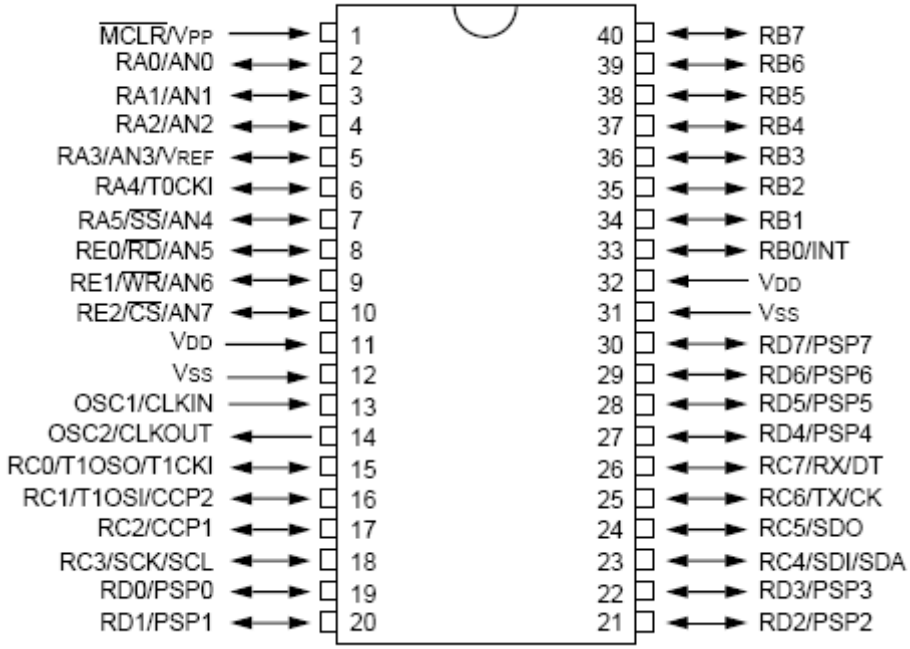

Figure 5.13: PIC 16C77 device pin-out diagram.

The cell voltage monitor 2 (CVM2) was designed to measure the 18 cell voltages to match the existing configuration of the Zetek fuel cell stack. However, the design of CVM2 is such that stack operating at a higher voltage, such as the 28 volt 2.5 kW Zetek stack could be monitored.

Like its predecessor, the CVM2 scans the fuel cell continuously and transmits the cell voltage data to the fuel cell system controller, the cell voltage is sent as an analogue value, while the number of the cell, being measured is sent as a binary number. The CVM2 has the facility to permit selection of any cell in the stack, so that a particular cell could be monitored continuously.

Figure 5.14, shows the CVM2 unit, the PIC device can be seen along side the peripheral devices mounted on the printed circuit board (PCB) used in the CVM2 unit. The peripheral devices used in the CVM2 unit are:

- ADG507 analogue multiplexer (2 off).
- AD7524 digital to analogue converter.

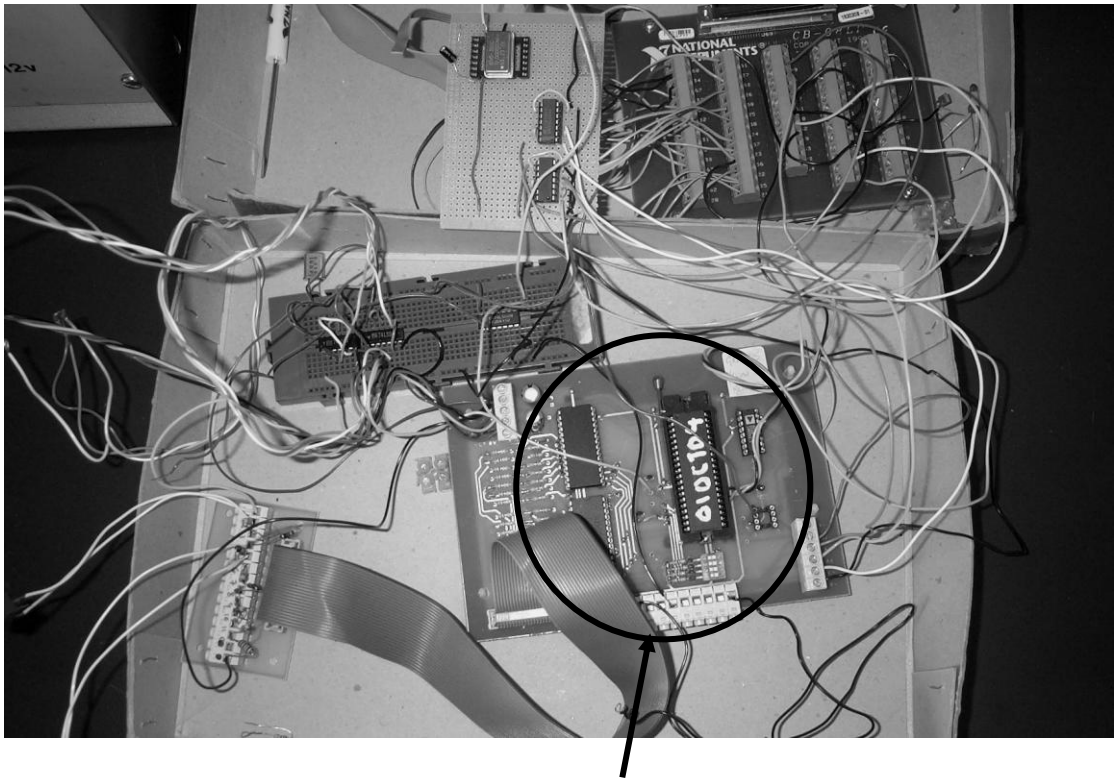

Figure 5.14: CVM2

The programme code for PIC micro-controller was developed using Microsoft's Notepad text editor, and was assembled and debugged using an ICEPIC II in circuit emulator. The fuel cell stack was simulated using a bank of resistors in series.

Development of the code for the CVM2 required an interface to represent the fuel cell system controller. This was achieved using the same combination of desktop PC and National Instruments Labview software used to control the Zetek laboratory fuel cell stack. A virtual instrument (VI) as shown in figure 5.15 was developed to receive the data being transmitted from the CVM2 to the fuel cell system controller. This VI displayed all of the cell voltages in the form of a bar chart along with an indicator to display individual cell voltage. This VI permitted the data being transmitted from the CVM2 to be checked for accuracy and repeatability.

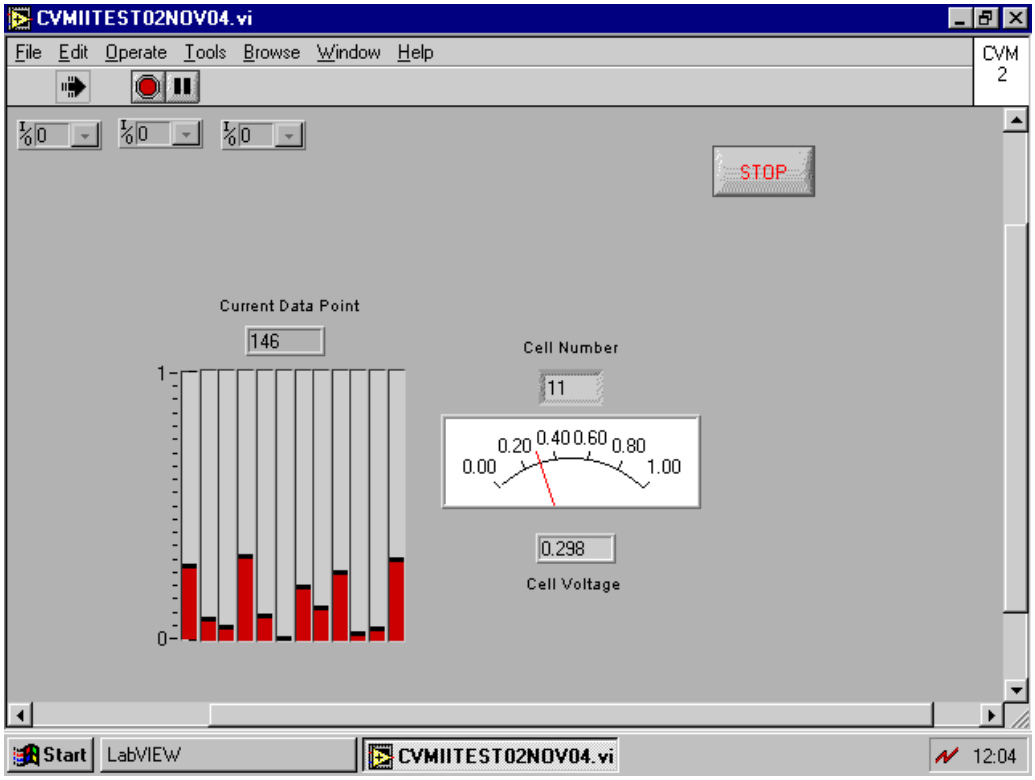

Figure 5.15: Authors LabVIEW© Front Panel CVM2

The sampling rate of the CVM2 is much higher than CVM1 and testing showed that the sampling rate is in excess of 300 cell voltage readings per second, however, when connected to a controller, the sampling rate is governed by the capability of the controller, in this case the PC system.

The sampling rate of the CVM2 was thus set to 60 cell voltage readings per second, when connected to the PC/ LabVIEW© system by simplifying the LabVIEW© programme and reducing the cycle time the sampling rate was increased to 90 cell voltage readings per second.

Once the code had been developed and proven using the ICEPIC, the code was converted to hex format and downloaded to a one-time programmable (OTP) 16C77 device. Figure 5.16 shows a similar device, the 16C77JW, the JW suffix indicates this is an UV erasable device.

Figure 5.16: PIC16C77JW device

5.6 Test results for CVM1

Testing of the fuel cell system has shown the monitoring and control system to be functional, reliable and providing good quality test data. Figure 5.17 shows the results from initial testing of the fuel cell stack of Figure 5.1, this shows each of the 18 cell voltages measured by the cell voltage monitor and the LabVIEW© VI of Figure 5.4. The VI then stores the data in a spreadsheet file which is then loaded into Microsoft Excel and plotted to a base of time (seconds) as shown in Figures 5.17 and 5.18.

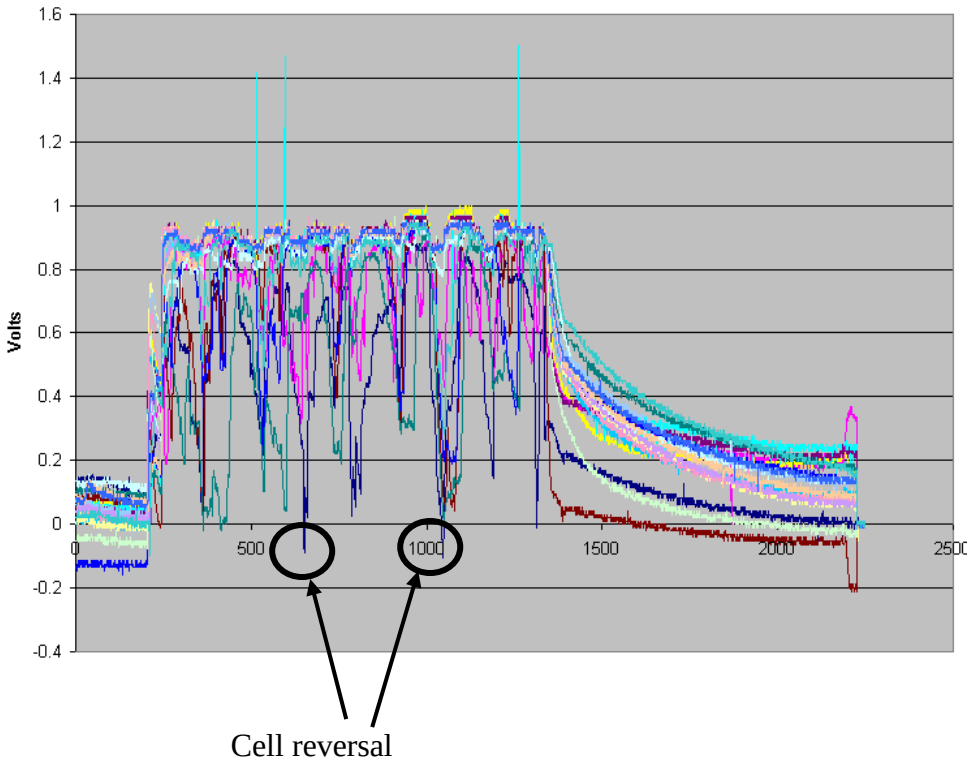

Figure 5.17: Test results showing cell reversal.

Studying the test results from figure 5.17, this clearly shows some of the 18 cells going into reversal, and many of the cells having voltages approaching reversal, a situation which could have resulted in the failure of one and possibly all cells in the stack. The fuel cell stack was taken off load, shut down and physically removed from the test rig so that the cause of the low cell voltages could be determined.

Note that the spikes of approximately 1.4 volts seen on figure 5.17 were eventually traced to a loose connection on one of the relay bases.

Subsequent inspection identified that some seals between the modules of the fuel cell stack were faulty. These modules were removed from the stack, and inspection revealed the faulty seals. The seals were replaced the fuel cell stack was re-instated in the test rig and testing was resumed. Test results for the repaired stack (figure 5.18) clearly shows that all the cell voltages had been restored to acceptable levels, with cell voltages in the range 0.5 to 0.7 volts at the point of highest loading at about 1600 to 2000 seconds.

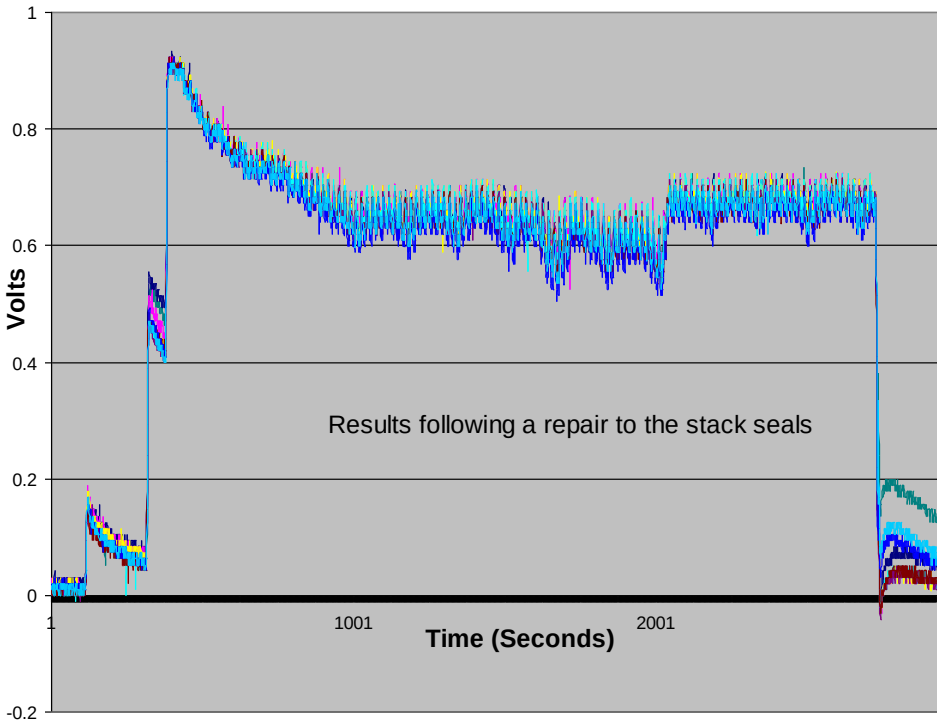

Figure 5.18: Test results following seal replacement.

5.7 Chapter Conclusions.

This chapter describes the development of a PC based monitoring system for an alkaline fuel cell system, and in particular the development of individual cell voltage monitoring systems referred to as CVM1 and CVM2 respectively.

The author claims to have produced a low cost solution for monitoring individual cell voltage on a fuel cell stack. The cost of a commercial fuel cell voltage monitoring system from a supplier such as Cellcense is $950 for up to 48 cells. Webb and Møeller-Holst [1], produced an 80 cell monitor with a material cost of $400-$500

In comparison the CVM1 system samples up to 24 cells, with a material cost of $80. Therefore a low-cost but effective monitoring and control system has been designed and developed, using readily available components, computer hardware, and software. This is a particularly useful solution for experimental and research applications where budgets may be restrictive and a low cost solution is desirable.

Preliminary testing has shown the system to be capable of supervising the operation of the laboratory fuel cell system, and identifying faulty cells and faulty operation of the fuel cell stack.

CHAPTER 6 LEAD-ACID BATTERIES

6.1 Batteries

The key components, which determine many of the basic properties of the battery, are the materials used for both the electrode and electrolyte for both the reduction and oxidation (redox) reactions. The electrode is the physical location where the core of the redox reaction, that is the transfer of electrons, takes place. In many battery systems, including lead acid and alkaline batteries, the electrode is not only where the electron transfer takes place, but is also a component in the chemical reaction that either uses or produces electrons. However, in other systems, notably fuel cells the electrode material itself is inert and is only the site for electron transfer from one reactant to another. For a discharging battery, the electrode at which the oxidation reaction takes place is called the anode and by definition has a negative voltage, and the electrode at which the reduction reaction occurs is the cathode and it has a positive voltage.

The electrode alone is not sufficient for a redox reaction to take place, since a redox reaction involves the interaction of more than a single component. The other chemical components of the reaction are contained in the electrolyte, which for many practical battery systems, is an aqueous solution. One reason for having an aqueous solution is the oxidised or reduced form of the electrode exists in an aqueous solution. Furthermore, it is important that the chemical species in the electrolyte are mobile in order that they can move to the site on the electrode where the chemical reaction takes place, and also such that ion species can travel from one electrode to another.

The current in the battery arises from the transfer of electrons between the electrodes. During discharging, the oxidation reaction at the negative terminal releases electrons and the reduction reactions absorb these electrons. Therefore during discharge, electrons flow from the negative to the positive electrode, in the external circuit, which connects the external load to the battery; this corresponds to electrons flowing from the negative to the positive electrode.

However, unlike a conventional electrical circuit electrons are not the only charge carriers in the circuit. Within the battery cell, electrons travel from the negative electrode, but do not return from the positive electrode to the negative electrode. Instead, electrical balance or neutrality is maintained by the movement of ions in the electrolyte, the direction of the ion movement acts to prevent a charge build-up at either the positive or negative electrodes.

In most practical battery systems, the same electrolyte is used for both the positive and negative electrodes and ion transport can take place via the electrolyte itself.

A separator is inserted between the positive and negative electrodes, the separator prevents the positive and negative electrodes from physically touching each other as they are usually in close proximity to one another, and if they were to touch it would short-circuit the battery cell as the electrons could transfer directly without flowing through the external load.

6.2 Lead-acid Batteries

The lead-acid accumulator was the first practical accumulator or rechargeable battery, also referred to as a secondary cell, (as opposed to a primary cell, which is non-rechargeable). The positive electrode consists of lead dioxide, while the negative electrode is made from lead. The electrolyte is a mixture of sulphuric acid and water. The first lead-acid batteries used an open glass container; however, modern batteries used a either sealed or vented plastic container. Each cell has a nominal voltage of 2 volts.

Lead-Acid cells or accumulators have been in use since the nineteenth century; in 1860 Gaston Plantè first demonstrated a Lead-acid cell to the French Academy of Sciences. Plantè therefore invented the world's first rechargeable battery.

In the 1870's magnetoelectric generators and dynamos began to be installed in central electricity plants, and lead-acid batteries found an early market to provide load levelling and to average out peak demands. They were charged at night, similar to the procedure now planned for modern load-levelling energy-storage systems.

Plantè realised that immersing a pure lead plate and a lead dioxide plate into 33.5% sulphuric acid and water would result in the lead plate attracting a negative charge from the solution, and the lead dioxide plate becomes positively charged.

The greater the surface area of the plates, the greater the power output of the battery as the redox reactions are area driven. Initially Plantè had difficulty in getting a useable power output from his battery and his solution was to replace the flat lead plates with lead grids; the holes in the grid were packed with "Faure Paste". Faure was a French chemical engineer who in 1881 significantly improved the capacity of the Plantè lead-acid battery and resulted in the manufacture of lead-acid batteries on an industrial scale.

Faure paste consists of red lead, carbon black, barium sulphate and lignosulphonates, and is pressed into the spaces in the lead grid allowing the sulphuric acid to react with the lead inside the plate, significantly increasing the area of the active material. The paste components are:

- Red lead (which is lead tetraoxide, Pb_3O_4, also used in the manufacture of lead glass and rust-proof primer paint) forms the active material, which reacts with the sulphuric acid.
- Carbon black is a material produced by the incomplete combustion of heavy end petroleum products such as bitumen and tar. Carbon black is a form of amorphous carbon that has a high surface area to volume ratio, and as such is one of the first of the so-called nano-materials to find common use. It is similar to soot but with a much higher surface area to volume ratio. Carbon black is used as a pigment and reinforcement in rubber and plastic products. [85].
- Barium Sulphate ($BaSO_4$) is a white crystalline, which is soluble in sulphuric acid; the barium sulphate acts as a seed crystal for the formation of the lead sulphate during the discharge process.
- Lignosulfonates are water-soluble polymers; the function of the lignosulfonate in the plate structure is more complex. It is chemically adsorbed on the lead active material resulting in a significant increase in its surface area. Without lignosulfonate, the surface area is of the order of approximately 0.2 square meters per gram while, with 0.50% of lignosulfonate this is increased to approximately 2 square meters per gram. This high surface area increases the efficiency of the electrochemical process,

which improves the performance of the negative plate. The lignosulfonate also stabilizes the physical structure of the negative active material, which retards degradation during operation of the battery. This property increases the life of the battery in service [86].

The thin lead grids used as electrodes by Plantè were very fragile; he subsequently changed from a pure lead plate to an alloy of lead and antimony. This modification strengthened the grid and also improved the electrical properties of the electrodes. This pasted grid structure of lead and antimony was used with little modification until the 1970's.

Lead-antimony grid plates filled with Faure paste made the lead acid battery useable, but it also brought a number of disadvantages. Antimony induces a chemical reaction, which results in self-discharge of the battery and causes excessive "gassing", that is evolution of hydrogen and oxygen gas when the battery is being recharged. The gassing during the recharging of the battery resulted in a loss of water from the electrolyte which required periodic addition of distilled water to restore the level of electrolyte in the battery.

The first major improvement in lead acid battery design was the positive electrode being made from a lead-calcium alloy in place of lead-antimony. Lead-calcium plates reduce gassing during the recharging of the battery; Lead-Calcium batteries have lead-calcium for both positive and negative plates and further reduce gassing compared to the lead-calcium battery.

A further development in lead-acid batteries was the so-called "maintenance free" batteries, which use recombination technology to return the hydrogen and oxygen evolved during recharging to the electrolyte. This development eliminated the requirement to maintain the correct level of electrolyte in the battery. Another name for "maintenance free" is Valve Regulated Lead Acid (VRLA), meaning there is a valve assembly fitted to the battery that is designed to vent off excessive gassing that the recombination technology cannot cope with, which would only occur if the battery were being excessively overcharged.

The latest development in lead-acid battery technology is the addition of silver to the lead-calcium alloy plates, which reduces plate corrosion and is claimed to increase service life of the battery by approximately 20% [87].

The lead-calcium and lead-calcium-silver alloys are usually reserved for batteries at the higher end of the battery product range, with the majority of SLI batteries sold being of the lead-antimony type.

A niche area of development in lead-acid battery design is the use of an immobilised electrolyte, which are preferable for applications were it is more likely that the batteries could be tilted or perhaps punctured. For example motor-sports involving vehicles and in particular motor-cycles where there could be a considerable degree of inclination from the vertical, and also in the event of an accident where the battery casing may be punctured, the use of conventional lead-acid batteries could result in spillage or leakage of acid from the battery casing with the attendant safety implications.

6.2.1 Immobilised Electrolyte Batteries.

There are two main types of battery designs which employ immobilised electrolyte, that is:

1. Gel Batteries.

Gel batteries replace the wet electrolyte solution with an acidic gel, which enhances safety and reduces internal corrosion; however there is a reduction in power output when compared with the flooded or wet equivalent battery. Although the capacity may be similar, there is a reduction in the effective duration of heavy discharge loads, for example when cranking (starting) vehicle engines. This is due to the higher viscosity of the gel compared to the liquid electrolyte in a flooded or wet cell, which slows the movement of the charge carriers in the electrolyte, therefore the charge in the electrolyte adjacent to the plates (electrode) is depleted at a higher rate than it is being replenished from the bulk electrolyte within the cell of the battery. This in turn slows the internal rate of reaction and restricts the available output from the battery. In a flooded or wet cell the acid solution is more mobile and is more able to support large discharge loads.

2 Absorbent Glass Matting (AGM)

Absorbent Glass Mat (AGM) batteries are a variation on the original Planté design, AGM batteries use pure lead grids but with a spiral cell design. Instead of the conventional rectangular plates the AGM design uses long narrow plates made from a thin lead grid with a narrow layer of fibreglass matting laid onto the lead grid, and the sandwich of lead grid and fibreglass matting is then rolled either into a cylindrical casing or laid out vertically in a rectangular casing which supports the grid/matting structure and the electrolyte solution soaks into the absorbent fibreglass material. The advantage of this design over the original Plantè design is that the lead grid does not have to support itself; the fibreglass matting material supports it.

The much larger plate surface area means that the AGM cells can receive charge more rapidly than the conventional rectangular plate designs, and therefore the output of AGM batteries is significantly higher than conventional types of battery.

The fibreglass matting soaks up the electrolyte and tends to acts like a separator preventing internal short circuits. The use of pure lead reduces the rate of self-discharge and gassing to almost zero, which means that AGM batteries can be left in a state of low charge without causing long-term damage, unlike conventional batteries, which are more prone to self-discharge.

The cost of immobilised electrolyte batteries tends to be much higher than conventional lead-acid batteries, costing more than twice as much; also they tend to come in a limited range of sizes, which means that there are not suitable for some applications.

The practical value of the lead-acid cell arises largely from the facts that not only are the active materials (lead and lead dioxide, PbO_2) insoluble in the dilute acid, but also the lead sulphate formed during the discharge process is also insoluble. Consequently the lead and PbO2 are returned to their original state during the charging process. Therefore there is no material change in the distribution of the masses of the active material; also the active materials are in a porous, spongy condition making them accessible to the sulphuric acid.

6.3 Battery Duty

Depending on the specific composition of the electrodes, lead-acid batteries may be optimised for shallow or for deep discharge operation. Shallow discharge batteries are used in the automotive Starting, Lighting and Ignition (SLI) application, whereas deep discharge batteries are used in stationary applications and for electric vehicles.

The shallow discharge batteries have calcium combined with the lead to strengthen the lead plates (electrodes), allowing the plates to be made thinner with a greater surface area to produce the high starting currents required for SLI applications, although typically shallow discharge units should not be discharged to less than 75% of their capacity. In SLI applications this is a compatible design for the automotive operating conditions, as the battery is primarily required for engine starting using the starter motor. Once the engine has been started the alternator charges the battery, and a voltage regulator ensures the battery and electrical system voltage does not rise above a preset voltage, usually 13.8 volts. This voltage ensures that the battery is maintained fully charged, but below the point at which gassing can occur. Shallow discharge batteries require less lead than deep discharge batteries, and are therefore less expensive.

Deep discharge batteries use antimony to strengthen the lead plates (electrodes), and can be routinely discharged or cycled down to around 20% of their fully charged capacity. The plates are thicker than shallow discharge battery plates, with less area than shallow discharge batteries and are designed for sustained low current discharges.

Deep discharge batteries are designed for use in a range of applications, which include:

- Golf carts
- Marine applications
- Electrically powered fork lift trucks
- Solar (Photovoltaic) systems
- Standby power and Uninterruptible Power Systems (UPS)
- Electric vehicles
- Hybrid vehicles

Although deep discharge batteries are designed for deep discharge applications, their service life depends on the depth of discharge during normal operations. Figure 6.1 shows how the depth of discharge affects the number of operating cycles of a deep discharge battery. Therefore the battery system designer must carefully consider the trade-off between using more batteries operating at shallower discharge rates to extend the overall life of the battery, compared to using fewer batteries with deeper discharge rates, with a shorter service life but at a correspondingly lower initial cost.

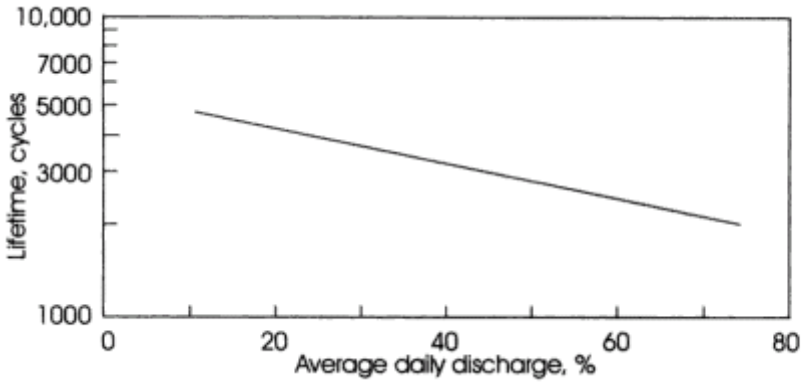

Figure 6.1: Lead-acid battery lifetime in cycles v depth of discharge [65].

Lead-acid batteries are available in open (vented) or sealed casings, and there are considerations to be made with regard to the battery casing. In lead-calcium batteries, minimal hydrogen and oxygen is lost during charging, which means that minimal water is lost during charging, making these batteries essentially maintenance free. This requires these batteries to be discharged to only 75% of their capacity, making them suited to SLI applications.

Deep discharge batteries using lead-antimony plates may be discharged down to 20% of their fully charged capacity.

For example a typical 100 Ah SLI lead-calcium battery has only 25 Ah available for use, compared to a typical 100 Ah lead-antimony battery which has 80 Ah available for use that is more than 3 times the available energy of the lead-calcium battery [88]. However, the lead-antimony battery produces significantly more hydrogen and oxygen gas from the dissociation of the water in the electrolyte, and therefore water must be added to the battery relatively frequently in order to maintain the correct level of electrolyte in the battery [89].

Water loss can be reduced by using a catalyst to produce recombination of the hydrogen and oxygen back into water, and this technique is used on SLI batteries, however, deep discharge batteries are generally of the open (vented) or non-sealed type. An advantage of open battery design is that the filling caps can be removed in order to measure the specific gravity of the electrolyte in the battery cells. Specific gravity is a used as a measure of the state of charge of the battery, the state of charge being the fraction of the full capacity that is still available for further discharge.

For applications where performing maintenance of the batteries is difficult, maintenance free, sealed deep cycle batteries exist, but are generally at least twice the price of equivalent non-sealed lead-acid units. These batteries use a gas recombination process to minimise water loss, and additionally these batteries have an immobilised electrolyte to overcome problems associated with leakage of electrolyte. While non-sealed units are designed for occasional over-charging; sealed units should never be overcharged.

6.4 Battery Environment

A battery should be housed in a suitable enclosure, and safe-working practices should be adhered to when working with battery installations. Lead-acid batteries operated at temperatures above 25^{o}C will have a reduced service life, for example at a temperature of 35^{o}C the battery lifetime will be reduced to approximately 50% of its lifetime at 25^{o}C. Therefore it is important to provide adequate ventilation for batteries, not only for venting of hydrogen or other gases, but also to maintain the battery operating temperature as close as possible to 25^{o}C [90].

Low temperatures will also affect battery performance. It is important to be aware of the freezing temperature of the electrolyte, which will vary as the water content varies depending on the state of charge of the battery. Figure 6.2 shows the effect of temperature on the energy available in the battery. The C-curves represent differing rates of discharge current, for the highest rate of discharge curve, C, at 0^{o}C there is only 40% of rated battery capacity available. A good example of the effect of temperature is the increased occurrence of vehicle starting failures in the colder

winter months, when batteries, which are nearing the end of their service life, do not have enough capacity or available energy to turn the starter motor and start the engine.

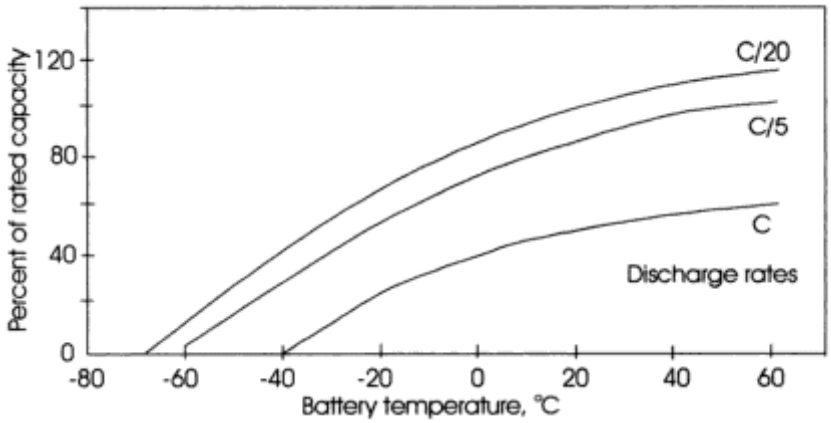

Figure 6.2: The effect of temperature and discharge on the available energy from a lead-acid battery [65].

6.5 Lead-Acid Battery Construction.

The lead-acid cell can be represented as having a negative electrode of porous lead, Pb (lead sponge) and a positive electrode of lead dioxide, PbO_2, both immersed in an aqueous solution of sulphuric acid.

6.5.1 Sulphuric Acid

Sulphuric acid is very strongly acidic and in aqueous solutions it ionises (dissociates) completely to form hydronium ions (H_3O^+) and hydrogen sulphate ions, (HSO_4^-). In dilute solutions the hydrogen sulphate ions undergo a second dissociation, forming more hydronium ions and sulphate ions (SO_4^{2-}).

Hydronium is the cation that forms from water in the presence of hydrogen ions.

$$H_2O + H^+ \rightarrow H_3O^+ \quad 6.1$$

These ions do not exist in a free state: they are extremely reactive. An acid is generally the source of these ions however, since water can behave as an acid and a base, hydronium exists even in pure water. This special case of water reacting with water to produce hydronium (and hydroxide) ions is commonly known as the self-ionisation of water

Hydronium is very acidic, at 25°C, it is the most acidic species that can exist in water (assuming sufficient water for dissolution) as any strong acid will ionize and protonate a water molecule to form hydronium. The acidity of hydronium is the standard used to judge the strength of an acid in water, and strong acids must be better proton donors than hydronium; otherwise a significant portion of acid will exist in a non-ionized state. Unlike the hydronium that results from water's auto-dissociation, these hydronium ions are long-lasting and concentrated, in proportion to the strength of the dissolved acid.

6.5.2 Properties of Sulphuric Acid

The electrolyte used in lead-acid batteries is a solution of pure sulphuric acid (H_2SO_4) in pure (distilled) water. The specification for the purity of the sulphuric acid used is given in British Standard B.S. 3031.

The theoretical amount of sulphuric acid required to produce 1 Ah (amp-hour) of capacity is 3.66 grammes, this reacts with the required theoretical amount of active material in the electrodes in the proportion 4.46 g lead dioxide/3.87 g lead/3.66 g H_2SO_4.

In practice, the actual amounts above required to produce 1 Ah exceeds the theoretical amount, see table 6.1. In practice all of the acid in the cell is not utilised in the reactions, and this is particularly true of the acid below the plates, and to a lesser degree above the tops of the plates.

In most stationary-type cells, where the plates are more widely spaced, there is an ample volume of electrolyte for the capacity required. In such cells the density of specific gravity of the electrolyte can be lower that that used in the more compact portable types of cell, where the plates are packed together with little acid space between adjacent plates [91].

6.5.3 Specific Gravity

The specific gravity of the sulphuric acid electrolyte for the lead-acid cell at 15.6 ^{o}C are shown in table 6.1

Sulphuric Acid Properties			
Content	Specific gravity	Electrochemical Equivalent	Cell Voltage
%wt	(20 deg C)	Ah/Litre	Volts
6	1.036	16.9	1.876
8	1.05	22.9	1.89
10	1.064	29.1	1.904
12	1.089	35.4	1.929
14	1.092	41.9	1.932
16	1.108	48.4	1.948
18	1.122	55.1	1.962
20	1.136	62	1.976
22	1.152	69.3	1.992
24	1.168	76.5	2.008
26	1.183	84	2.023
28	1.199	91.5	2.039
30	1.215	99.5	2.055
32	1.231	106.9	2.071
34	1.248	116.8	2.088
36	1.264	124	2.104
38	1.281	133	2.121
40	1.299	141.9	2.139

Table 6.1: Sulphuric acid properties [92].

The specific gravity of pure water is 1.000 and sulphuric acid has a specific gravity of 1.830, thus sulphuric acid is 1.84 times heavier than water. The specific gravity of a mixture of sulphuric acid and water varies with the strength of the solution from 1.000 to 1.840 [93].

Specific gravity (SG) of an acid and water solution may be calculated using equation 6.2:

$$SG = \frac{(C \times \nu) + (1000 - C \times \nu)}{1000} \qquad 6.2$$

Where:

SG = Specific gravity

ρ = Density of the acid (kg/mol)

C= Concentration of acid (mol)

ν = Specific volume of the acid (ml/mol)

The specific gravity falls during discharge and increases during charging. The specific gravity therefore provides an indication of the state of charge (SOC) of a lead-acid battery, as the fall in specific gravity is directly proportional to the number of amp-hours supplied by the battery.

Table 6.1 also lists the electrochemical equivalent of each of the different concentrations of sulphuric acid. Electrochemical equivalent is the theoretical capacity of the electrolyte per gramme (Ah/gm), or in this case per litre of material (Ah/litre).

However, a battery cannot be discharged at its theoretical voltage due to polarisation phenomena and ohmic losses and furthermore the theoretical capacity cannot be exploited as the battery is not discharged to zero volts in practice. With these premises, the actual energy delivered by the battery is 20 to 40% of the theoretical value. A comparison of theoretical and actual parameters for a lead acid battery is given in table 6.2 [94].

Theoretical				Actual		
Voltage	Electrochemical equivalents		Specific energy	Nominal Voltage	Specific energy	Energy density
V	g/Ah	Ah/kg	Wh/kg	V	Wh/kg	Wh/Litre
2.1	8.32	120	252	2	35	70`

Table 6.2. A comparison of theoretical parameters for a lead acid battery.

The cell voltages given in table 6.1 are calculated using an approximation which relates cell voltage to acid densities given in equation 6.3.

Equilibrium voltage = acid density (in g/cm3 or kg/dm3) + 0.84 6.3

This relationship is shown graphically in figure 6.3.

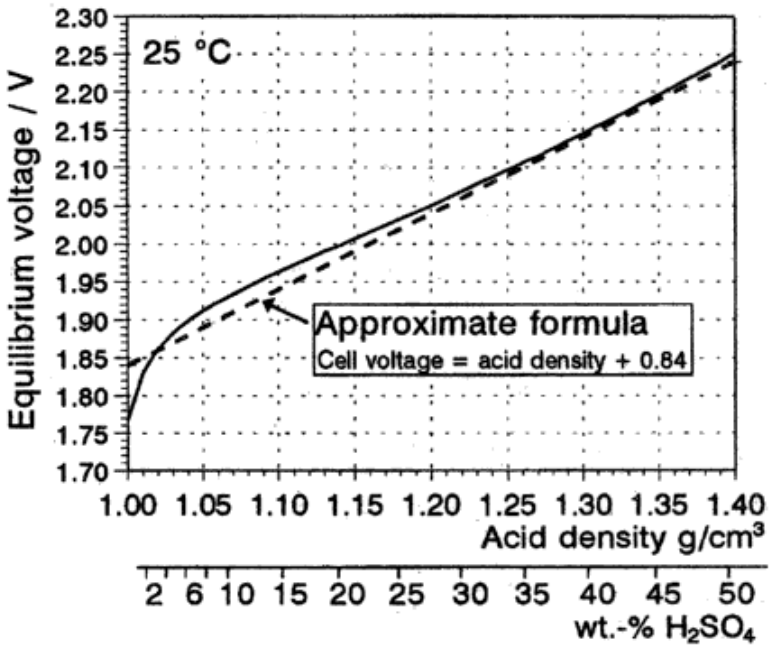

Figure 6.3: Equilibrium cell voltage of a lead-acid battery referred to acid density and acid concentration in weight% H_2SO_4 [54].

As the cell is discharged, the sulphuric acid is consumed and water is formed as expressed in equation 6.4.

$$Pb(s) + PbO_2(s) + 2H_2SO_4(aq) \rightarrow 2PbSO_4 + 2H_2O(l) \qquad 6.4$$

Consequently, the electrolyte composition and density vary from about 40% by weight of H_2SO_4 (1.30 kg/m^3), with an associated open circuit voltage of 2.14 V at 25^{o}C at full charge, reducing to about 16% by weight of H_2SO_4 (1.10 kg/m^3), at an open circuit voltage of 1.95 V at 25^{o}C, when fully discharged.
The actual open circuit voltage depends on the sulphuric acid (and water) activity that is the effective concentration, and also temperature.

The change in electrolyte specific gravity provides a convenient method of determining the state of charge (SOC) of a cell. The state of charge SOC is the capacity of the battery at any point in time. It is measured by referring the existing state of charge to some reference, usually taken to be a fully charged state.

As the sulphuric acid concentration changes so does the electrical resistance of the electrolyte, which in turn changes the internal resistance of the entire cell.

Lead-acid batteries rely on a high standard of purity of materials to be used in their manufacture for successful performance and long life. It is very important that the sulphuric acid used for the first filling of the battery, and the water used for diluting the acid is of an acceptable purity and has a neutral pH. The standard of acid used in lead-acid batteries is detailed in standard number BS 3031.

Pure sulphuric acid has a specific gravity of 1.840; however, the casings used for modern batteries are only suitable for dilute acid up to a maximum specific gravity of 1.400.

The approximate quantities of water required to dilute concentrated acid are given in table 6.3.

Initial Specific Gravity	Final Specific Gravity	Approximate proportions by volume of		
		Acid	Water	Acid/Water (%)
1.840	1.400	1	2	33/66
	1.250	1	3.5	22/77
	1.230	1	4	20/80
	1.200	1	4.5	18/82
	1.170	1	5.5	15/85
1.400	1.280	2	1	66/33
	1.250	3	2	60/40
	1.230	1	1	50/50
	1.200	3	3.5	46/54
	1.170	1	2	33/66

Table 6.3: Approximate proportions by volume of Acid/Water

6.6 Lead Acid Battery Operation

The dependence of the cell equilibrium voltage on the concentration of the dissolved components in the electrolyte is given by the Nernst equation as discussed in Chapter 3. The equilibrium voltage is independent of the amount of lead, lead dioxide, or lead sulphate as long as these are available in the active mass of the electrodes.

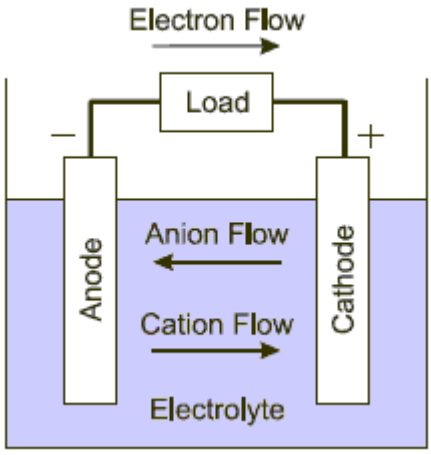

Figure 6.4: Diagrammatic representation of cell discharging.

The operation of the cell during discharge is shown in figure 6.4. When the cell is connected to an external load electrons flow from the anode, which is oxidised, through the external load to the cathode, where the electrons are accepted and the cathode material is reduced. The electric circuit is completed by the electrolyte by the flow of anions (negative ions) and cations (positive ions) to the anode and cathode respectively [75].

For the lead-acid battery the negative electrode is the lead (Pb) electrode, and the positive electrode is the lead (PbO_2) electrode. An oxidation process, that is loss of electrons, takes place at the lead (Pb) electrode and a reduction process that is gain of electrons takes place at the lead dioxide (PbO_2) electrode. The combination of a reduction and oxidation process is referred to as a redox reaction; in general electrode reactions are oxidation-reduction processes of the type shown in equation 6.5:

$$\text{Oxidant} + ne \Leftrightarrow \text{Reductant} \qquad 6.5$$

Note: The term *ne* representing a transfer of *n* electrons:

Electron-exchange reactions at electrodes are concerned essentially with the layer of electrolyte solution very close to the electrode surface. It must be borne in mind, however that an oxidant or reductant in solution has to have some means of reaching the electrode. There are a number of variables which affect the rate of an electrode reaction, which are summarised in figure 6.5 [95].

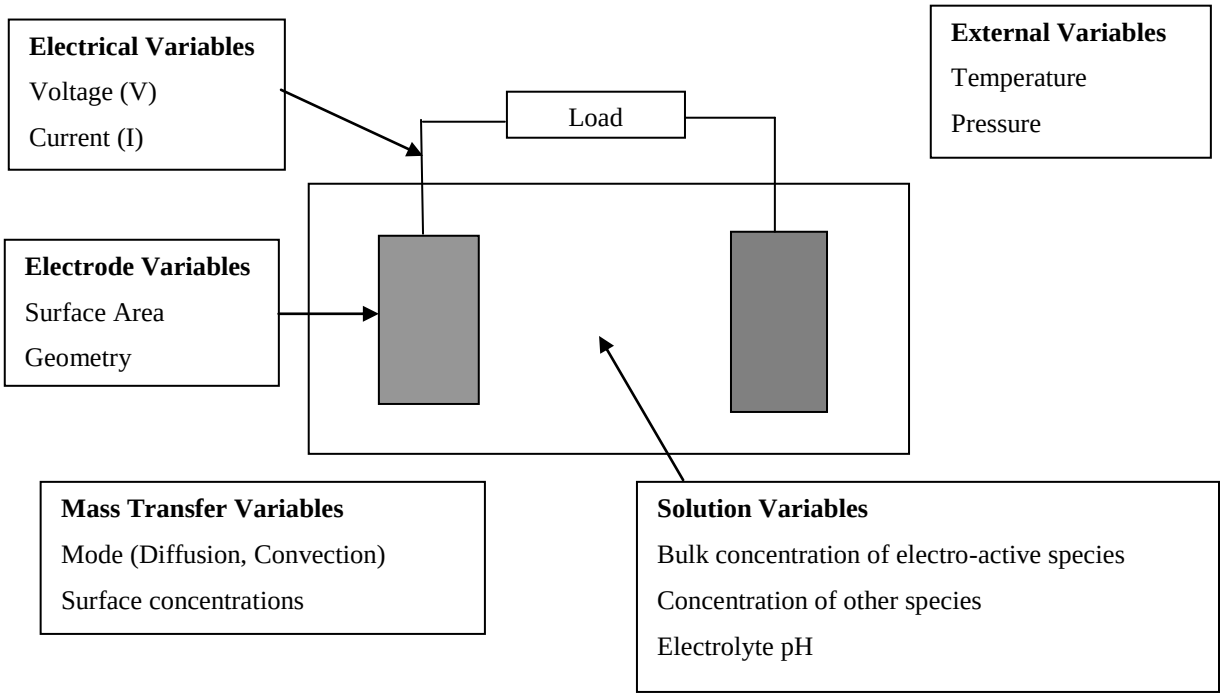

Figure 6.5: Variable affecting the rate of an electrode reaction [96].

6.6.1 Cell Discharge

During the cell discharge electrons are consumed at the positive lead dioxide (PbO_2) electrode, the supply of which comes from the negative lead (Pb) electrode. The electron flow is, therefore out of the negative electrode into the load, with the battery acting as the source.

When two electrochemical redox systems are connected together, where one electrode provides electrons and the other taking up electrons, as in the case of the lead-acid battery, the net effect is as shown in figure 6.6.

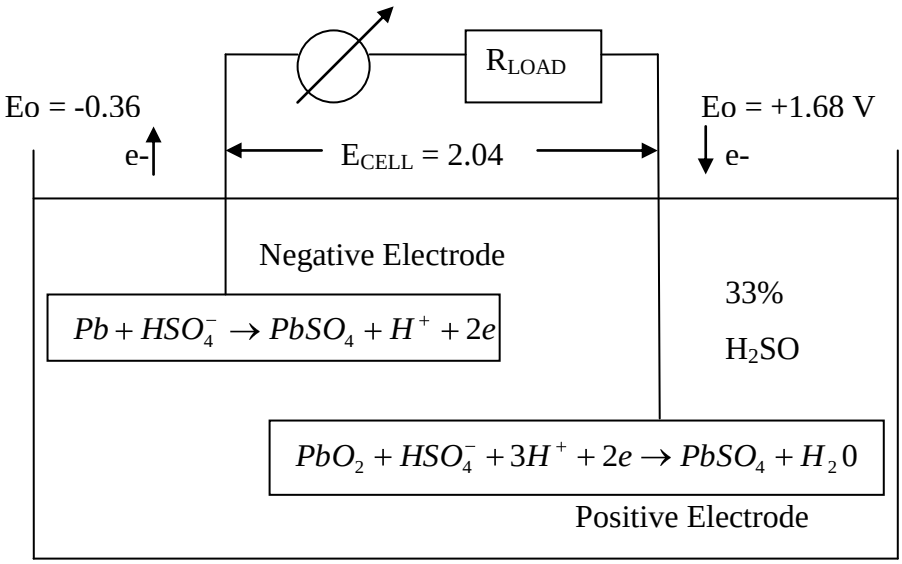

Figure 6.6: Lead-acid cell reactions.

The electrolyte solution is sulphuric acid and water, which dissociates into hydrogen ions H^+ and HSO_4^- bisulphate ions.

When the circuit is complete and the cell is discharging two electrons are detached from the lead in the negative lead electrode, an oxidation process, and the electrons flow through the external circuit to the positive lead dioxide electrode, thereby providing power to the external load.

$$Pb \rightarrow Pb^{2+} + 2e^- \qquad 6.6$$

The lead ion (Pb^{2+}) reacts with bisulphate ion leaving a free hydrogen ion (H^+). The lead sulphate ($PbSO_4$) precipitates onto the electrode surface.

$$Pb^{2+} + HSO_4^- \rightarrow PbSO_4 + H^+ \qquad 6.7$$

The total negative electrode (oxidation) equation during cell discharge is therefore, combining equations 6.6 and 6.7,

$$Pb(s) + HSO_4^-(aq) \rightarrow PbSO4(s) + H^+ + 2e^- \qquad 6.8$$

Note that equation 6.8 has a standard potential of -0.36 volts.

After passing through the load the electrons approach the lead dioxide (positive) electrode. The electrons weaken the lead oxide bond:

$$PbO_2 + 2e^- \rightarrow Pb^{2+} + 2O^{2-} \qquad 6.9$$

The lead ion (Pb^{2+}) reacts with bisulphate ion leaving a free hydrogen ion (H^+). The lead sulphate ($PbSO_4$) precipitates onto the electrode surface.

$$Pb^{2+} + HSO_4^- \rightarrow PbSO_4 + H^+ \qquad 6.10$$

The two oxygen ions (O^{2-}) react with the hydrogen ions in the electrolyte solution.

$$2H^+ + O^{2-} \rightarrow H_2O \qquad 6.11$$

The positive electrode equation is given

by:

$$PbO_2(s) + HSO_4^-(aq) + 3H^+(aq) + 2e^- \rightarrow PbSO4(s) + 2H_2O(l) \qquad 6.12$$

Note that equation 6.12 has a standard potential of +1.68 volts.

The overall cell discharge chemical equation is:

$$Pb(s) + PbO_2(s) + 2HSO_4^-(aq) + 3H^+ + 2e^- \rightarrow 2PbSO_4 + H^+(aq) + 2e^- + H_2O(aq) \qquad 6.13$$

This can be written as:

$$Pb(s) + PbO_2(s) + 2H_2SO_4(aq) + 2H^+ \rightarrow 2PbSO_4 + 2H_2O(aq) \qquad 6.14$$

Note that equation 6.14 has a standard potential of +2.04 volts.

The discharge process results in the formation of insoluble lead sulphate $PbSO_4(s)$ on both electrodes. The discharge reaction is limited by the formation of $PbSO_4$, which reduces cell capacity significantly when compared to the theoretical capacity.

The lead sulphate is a very poor electrical conductor and its deposition in a dense, fine-grained form can shield and render passive both electrodes severely restricting the capacity of a cell [4].

In an actual discharge not all of the lead dioxide in the positive electrode, and lead in the negative electrode, are converted to lead sulphate. The following equations based on the work of Garche et al [97] represent actual discharge processes and in particular over-discharge which is of interest in Chapters 9 and 10 of this thesis.

Positive electrode

During discharge the main reaction is:

$$2PbO_2 + 4H^+ + SO_4^{2-} \rightarrow PbSO_4\,[PbO_2] + 2H_2O \qquad 6.15$$

At the end of the discharge, $PbSO_4$ will block further discharge of PbO_2, and the remaining PbO_2 ([PbO_2]) will be electrochemically inactive, i.e. $PbSO_4$ [PbO_2], hence the electrode potential will fall.

Note square brackets [ ] indicate material which has remains unchanged during the reaction for example $PbSO_4[PbO_2]$ means that some of the lead dioxide (PbO_2) has reacted with the electrolyte (sulphate ions) and converted to lead, but some of the lead dioxide (PbO_2) remains unchanged.

During the reverse reaction the polarity of the positive half-cell changes to the $Pb/PbSO_4$ potential and the lead sulphate is converted to lead in the reverse reaction 6.16.

$$PbSO_4\,[PbO_2] + 2e^- \rightarrow Pb + SO_4^{2-} + [PbO_2]^- \qquad 6.16$$

Negative electrode

During discharge the main reaction is:

$$2Pb + SO_4^{2-} \rightarrow PbSO_4\,[Pb] + 2e^- \qquad 6.17$$

At the end of the discharge, lead sulphate will block further discharge of Pb and any remaining lead ([Pb]) will be electrochemically inactive, i.e. $PbSO_4$ [Pb] is formed.

During the reverse reaction the polarity of the negative electrode will change and the lead sulphate will be oxidised to lead dioxide in the reverse reaction 6.18.

$$PbSO_4\,[Pb] + 2H_2O \rightarrow PbO_2 + SO_4^{2-} + 4H^+ + 2e^- + [Pb]^- \qquad 6.18$$

6.6.2 Cell Charging

In the case of secondary (rechargeable) batteries, having been discharged the cell can be restored by reversing the flow of current through the cell in order to "recharge" the cell with electrical energy. Cells, which can be recharged by the action of reverse current, are called accumulators because they "accumulate" chemical energy. Accumulators are more commonly known as storage batteries, where the term battery is used to denote that there are a number of single cells connected together. The term secondary battery is also used, this term dates from the early days of electrolysis, and the term primary battery is used for disposable batteries that cannot be chemically recharged.

One of the most common examples of recharging is the automotive SLI battery.

Shown in figure 6.7, the lead-acid battery is recharged by current from the vehicles alternator.

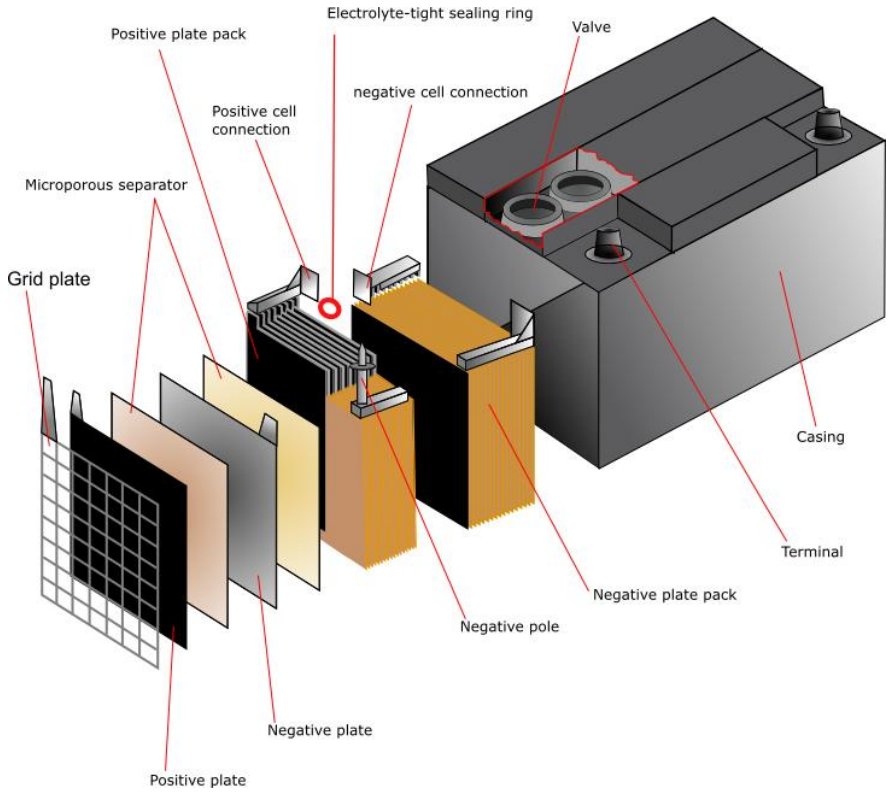

Figure 6.7: SLI Battery [98].

Cell charging is the reverse of the cell discharge operation. During cell charging lead sulphate ($PbSO_4$) is converted back to lead and lead oxide. The electrons are

consumed from the charging unit, and the positive electrode releases electrons. The current flow is into the positive electrode from the charging unit delivering electrical energy into the cell where it is converted to chemical energy. The chemical reaction at the positive electrode during charging is:

$$PbSO_4(s) + 2H_2O \rightarrow PbO_2(s) + 3H^+(aq) + HSO_4^-(aq) + 2e \qquad 6.19$$

The chemical reaction at the negative electrode during cell charging is:

$$PbSO_4(s) + H^+ + 2e \rightarrow Pb(s) + HSO_4^-(aq) \qquad 6.20$$

The overall chemical reaction during charging is, by combining 6.19 and 6.20.

$$2PbSO_4(s) + 2H_2O(l) \rightarrow Pb(s) + PbO_2(s) + 2H_2SO_4(aq) \qquad 6.21$$

During recharging $PbSO_4$ is reconverted to lead at the negative electrode and to PbO_2 at the positive electrode.

During charging deposited lead tends to form long crystals (dendrites), which, if they were to reach the opposite electrode, would cause short-circuiting of the cell. To prevent this, and also to prevent buckling of the soft lead plates, separators made of plastic are placed between the plates [98].

A lead-acid battery should not be run to complete discharge. As the sulphuric acid concentration decreases due to the loss of electrolyte and the resistance of the cell increases, due to the conversion of the plates to lead suphate, which is a poor conductor, this leads to a drop in the voltage of the cell. Also lead suphate is a bulky material and if the consequent expansion of the plates progresses too far can cause buckling and eventual disintegration [98].

6.6.3 Battery Efficiency

Ideally, the charging and discharging processes of the lead-acid system should be completely reversible, however, they are not. The temperature of operation, rate of charge and discharge all affect the performance of the battery. The electrical path of the battery presents ohmic resistance and therefore some of the electrical energy intended for charging, i.e. storage, is converted to heat. If hydrogen is vented during the charging process, this also represents an energy loss. Typically the charging process is about 95% efficient. The discharge process also results in some losses due

to the internal resistance of the battery, so only about 95% of the stored energy can be recovered. The overall efficiency of charging and discharging a lead-acid battery is thus about 90% [99].

Since battery losses due to internal resistance are proportional to the square of the current, this means that high current charging or high current discharging will tend to result in higher internal losses and lower overall efficiency. This effect is offset somewhat by the increase in temperature of the battery during charging or discharging as the battery efficiency increases with temperature. However, higher temperatures over a prolonged period reduce the service life of a battery [100].

6.6.4 Battery Capacity

The amount of free charge generated by the active material at the negative electrode and consumed by the positive electrode of the cells within a battery is called the battery capacity. The battery capacity is a measure of the charge or energy stored in the battery. The fundamental units of battery capacity are coulombs (C), although in most situations the capacity is measured in ampere-hours (Ah). Where 1 Ah = 3600 C, or coulomb, and 1 C is the amount of charge transferred in 1 second by a current of 1 A. The battery capacity in Ah can be ideally calculated from the weight/volume or number of moles of materials of the electrodes and electrolyte in the battery.

6.6.5 Ideal Battery Capacity

The ideal battery capacity under equilibrium conditions (which differs substantially from the actual battery capacity under load) is calculated from the number of moles of available reactants, from which the moles of electrons can be determined.

Using Faradays constant, which gives the number of Coulombs for a mole of electrons (F = 96,484.56 C/mol) and *n* as the number of moles of reactants, the total available coulombs (charge) can be determined for a battery. As the battery capacity expressed in Ah is a measure of the total stored charge then the battery capacity can be determined from equation 6.22.

$$Capacity\,(Ah) = n \times F \times \frac{1\,hour}{3600\,\mathrm{sec}} \qquad 6.22$$

As the primary function of a battery is to store electrical energy rather than electrical charge, the energy storage of a battery is also an essential parameter. A simple way to determine the energy storage capacity of a battery is to multiply the Ah capacity by the nominal battery voltage.

Energy Capacity (Wh) = Capacity (Ah) x Battery Voltage (Volts). 6.23

While ampere-hours are technically not units of energy, but rather units of charge, the amount of charge in a battery is approximately proportional to the energy stored in the battery. If the battery voltage remains constant, then the energy stored is simply the product of the charge measured in ampere-hours and the battery voltage measured in volts.

The theoretical capacity of a battery is the quantity of electric charge involved in the electro-chemical reaction. It is denoted by C_T and is given by:

$C_T = xnF$ 6.24

Where x = number of moles of reaction, n = number of electrons transferred per mole of reaction and F= Faraday's constant.

The capacity is usually given in terms of mass, not the number of moles:

$C_T = nF/M_m$ 6.25

Where M_m = Molecular Mass (g). This gives the capacity in units of Ampere-hours per gram (Ah/g).

In practice, the theoretical battery capacity can never be realised due to parasitic reactions sometimes called self-discharge that take place within a secondary battery cell, particularly when the battery is in storage. Self-discharge is a function of various factors such as temperature and storage period.

In practice capacity testing is undertaken to determine capacity relative to a standard procedure, such as BS EN 61982-1:2006,' Secondary batteries for the propulsion of electric road vehicles Part 1'.

Section 5 of this standard, details a capacity testing procedure based on specific start and finish voltages, where the capacity is denoted by C_N where C is the capacity in Ampere-hours, and N is the number of hours of discharge [101].
The discharge rate is the current drain at which the battery is being discharged. The rate is expressed as C_N/h rate, where C_N is the rated battery capacity as declared by the battery manufacturer, and h is the discharge time in hours. The discharge rate is expressed as a current based on battery capacity and discharge time.

For example a battery with a capacity of 100 Ah discharged over 5 hours, gives the discharge rate as:
100 Ah/5 = 20 A
This is referred to as the C_5 discharge rate.
Figure 6.8 shows the effect of discharge rate on the energy or charge which can be removed from a lead-acid battery. The higher the discharge rate the greater the rate of charge depletion.

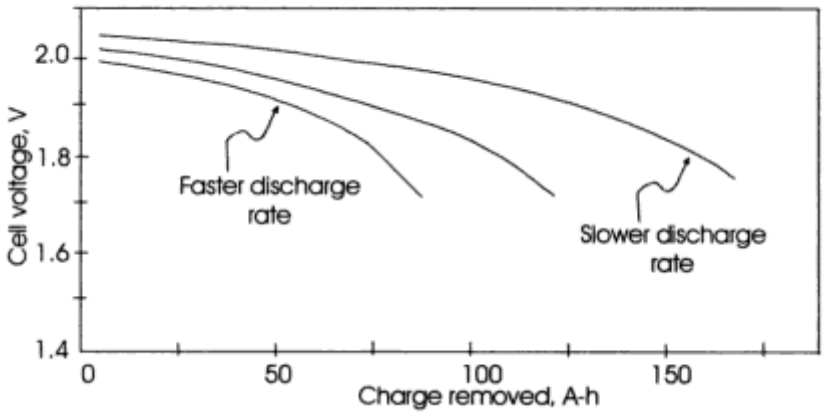

Figure 6.8: The effect of discharge rate on the available energy in a lead-acid battery [65].

6.6.6 Depth of Discharge

The depth of discharge (DoD) is the percentage of rated battery capacity to which a battery is discharged. The consumption of at least 80% of the rated battery capacity is referred to as a deep discharge.

6.6.7 Cold Cranking Amps (CCA)

The maximum amount of current a battery can provide for a short period of time is called the cranking current. This parameter is often specified for SLI batteries, where the battery must provide sufficient current to start the vehicle engine.

Cut – Off Voltage

In most battery types, including lead acid batteries, if the battery is discharged below a certain voltage permanent damage may be done to the battery. This voltage is called the "cut-off" voltage and depends upon the battery temperature and rate of discharge.

6.6.8 Cell Reversal

Cell reversal can occur when a number of cells are connected in series. As cells cannot be perfectly matched during manufacture, a negative voltage potential, also known as cell reversal, will occur across a weak cell if the discharge is allowed to continue uncontrolled. The more cells that are connected in series, the greater the variance in cell condition and the likelihood of cell reversal occurring.

When discharged in a series configuration the capacity of the weakest cell in the chain will be depleted before the others. If the discharge is continued (to discharge the remaining good cells), the voltage on the low capacity cell will reach zero then reverse due to the IR voltage drop across the cell.

The reversed cell will be charged by the other cells in the series string with subsequent heat and pressure build up within the cell due to "cell reversal". The initial tolerance spread which caused these interactions may be very low but it can build up over time as the damage increases with every charge-discharge cycle until the weak cells eventually fail [102]. Detection of cell reversal would be a significant improvement in terms of battery safety, as it can in some cases result in catastrophic failure.

6.6.9 Sulphation

One of the main problems in lead-acid cells is sulphation, this occurs when the sulphate ions become chemically attached to the lead on the cell plates. As the cell is

discharged, the lead oxide (positive plate) and lead (negative plate) react with the sulphuric acid electrolyte to produce lead sulphate and water. The sulphate ions combine chemically with both electrodes forming lead sulphate deposits, lowering the concentration of the electrolyte, and consequently the battery voltage falls. As power is drawn from the cell sulphate continues to build up on the electrodes, and the concentration of the electrolyte decreases until the cell is discharged to an extent where it is unable to power its load.

To reverse the chemical reaction, a charging system is used to sense the drop in voltage; a charging voltage is applied to the cell to separate the sulphate from the electrodes and back into the electrolyte solution. The concentration of the electrolyte increases, and the battery voltage increases.

Even when no current is being drawn from the cell, "spontaneous discharge" i.e. self-discharge occurs and an irreversible reaction takes place. This constitutes attack of the lead supporting the effective electrode material. The sulphate deposit from both this spontaneous discharge and from the normal discharge coagulates with time and retards further electrode processes, an effect known as sulphation.

The sulphate ions in the electrolyte solution can bond with the battery electrodes at three different levels [103]:

- Level one is the bond associated with normal charging and discharging of the cell; regular charging can reduce the effects of sulphation.
- Level two bonds occur after the battery has been in service, the time being dependent on the duty cycle of the battery; level two bonds can be broken by controlled overcharging of the battery, this transforms the level two bonds to level one bonds which can be broken by the normal charging process, allowing the sulphate ions to re-enter the electrolyte.
- Level three bonds are irreversible and cannot be broken, irrespective of the amount of charging applied. The longer sulphate ions remain attached to the lead plate, the more likely the bonding will progress to the next level.

If some the sulphate ions become attached irreversibly (level three bonds) the amount of free sulphate ions and free electrode area decreases, and therefore the

concentration of the electrolyte is effectively reduced. However, this process of sulphation does not affect the concentration of the hydrogen ions.

6.7 Battery Modelling

In order to better understand the nature of the changes taking place as a lead acid battery is discharged it was decided to model a battery undergoing discharge due to an external load.

This analysis is based on a Plantè cell which has a normal operating range of 2.04 to 1.70 volts. The greater range of operating voltage and the low cut off voltage differs from that of an SLI, due to the duty cycle of the Plantè cell which is designed for greater depth of discharge than the SLI battery.

The first consideration in the modelling process was the battery capacity. The theoretical value of lead acid battery capacity is 120 Ah/litre based on the value of electrochemical equivalence for a lead acid battery given in table 6.2. The manufacturers stated capacity for this particular Plants cell is 15 Ah, for a one litre cell.

This gives a ratio of:

$$\frac{15}{120} = 0.125$$

Which is less than the previously stated range of 0.2 to 0.4 [104], this low value of may be accounted for by the fact that the Plantè cell capacity is based on a cut off or low voltage limit of 1.70 volts, whereas the theoretical capacity is based on a discharge to zero volts, furthermore the activity of the sulphuric acid, discussed in Chapter four is not accounted for in the theoretical value. The influence of activity can be seen in Figure 6.9 which shows the variation of theoretical cell voltage with the Ionic Activity Coefficient (IAC) [105].

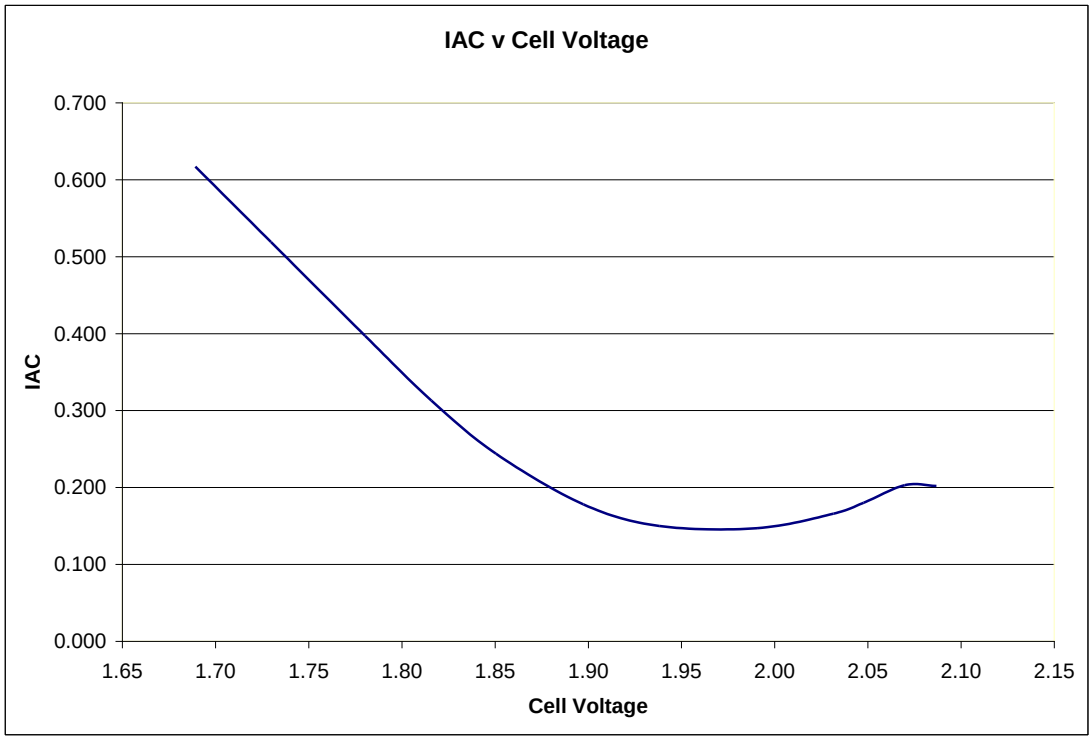

Figure 6.9 Ionic Activity Coefficient (IAC) v Cell voltage [99].

Therefore the activity of sulphuric acid has an effect on the capacity of the Plantè cell.

During the tests on the Plantè cell the open circuit voltage (OCV) ranged from approximately 2.04 volts at the beginning to 1.90 volts at the end of the discharge test. From figure 6.9 the average IAC over this range of OCV values is 0.158. Given that the activity expresses the availability of the molecules during the reaction the available capacity becomes:

Q = 0.158x120 = 18.96 Ah.

This is close to the manufacturers rated capacity of 15 Ah for this particular Plantè cell. The above therefore provides a reasonable means of relating theoretical and actual battery capacity.

Before proceeding with the battery model, the dissociation (discussed in Chapter 3) of sulphuric acid and the fractional composition α should be considered in terms of its possible effect on the model.

The fractional composition (α) of sulphuric acid is used to indicate the composition of the acid in terms of all possible components; in the case of sulphuric acid the three components are H_2SO_4, HSO_4^- and SO_4^{2-}. The effect of fractional composition should be considered before modelling the discharge of the cell. Figure 6.10 shows the fractional composition (α) of sulphuric acid in terms of these three components over the pH range –10 to 10.

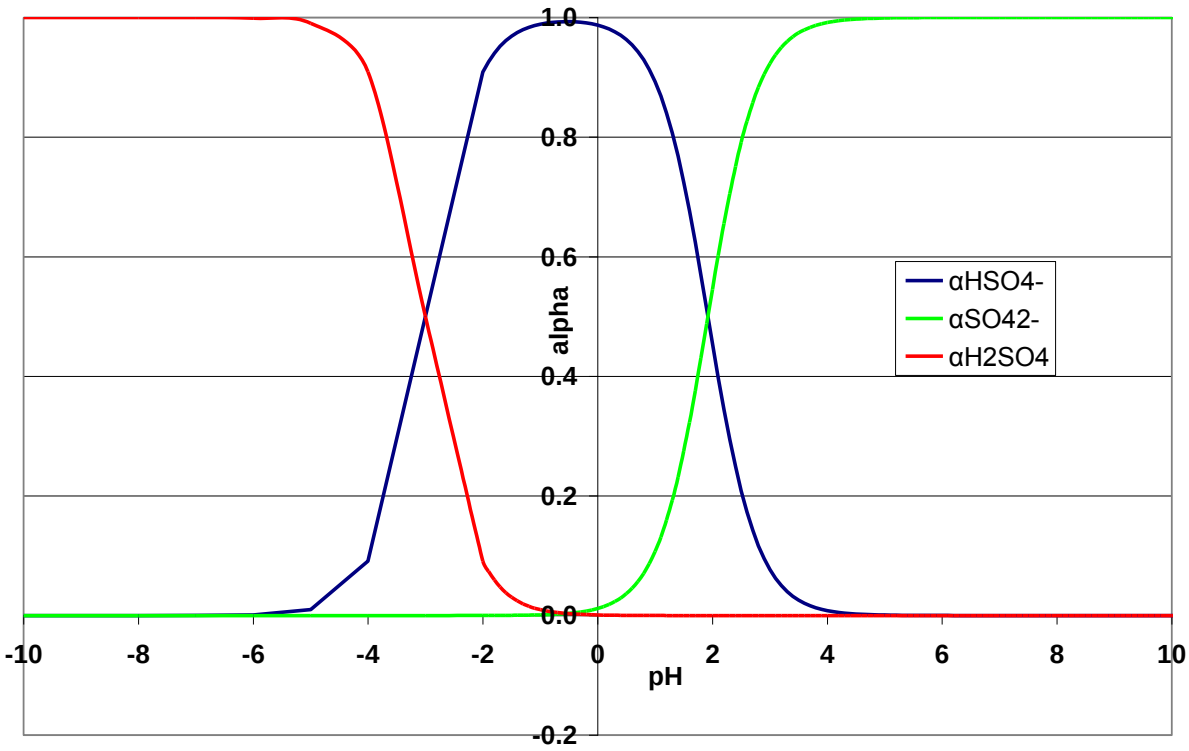

Figure 6.10: The fractional composition (α) of sulphuric acid.

The range of pH relevant to the discharge of a lead acid battery is –1.0 < pH < 1.0, the fractional composition of sulphuric acid over this range of pH is shown in more detail in figure 6.11 below:

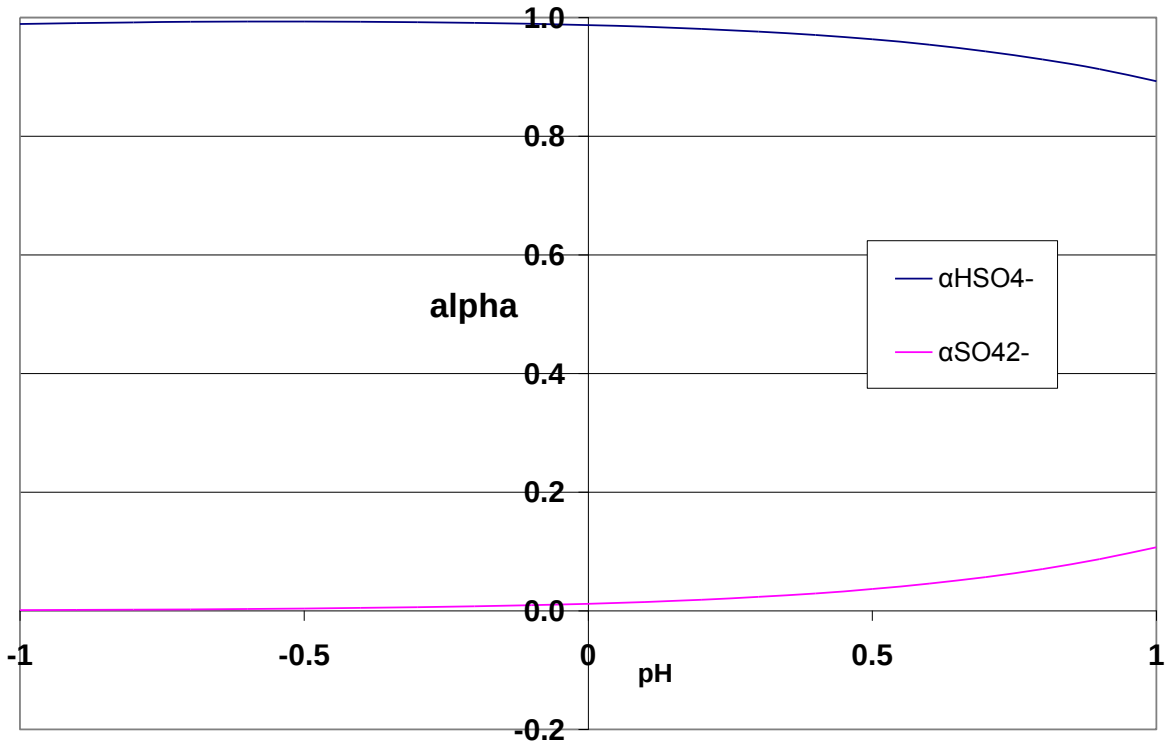

Figure 6.11: The fractional composition α of sulphuric acid between –1.0 < pH < 1.0.

It can be seen that in the range 0 < pH < 1.0 that the second dissociation as shown in equation 4.53 becomes noticeable and therefore the battery model should include the effects of dissociation.

The following section attempts to model variation in the OCV during the discharge of a lead acid cell, allowing a comparison to be made between the results generated by the battery model and the results obtained from discharge tests out carried during the experimental part of this thesis.

The theoretical electrical potential that can be developed by a single lead-acid cell is given in equation 6.26

E^{θ} = +2.05 V @ 298.15K 6.26

The chemical reactions relating to a lead acid cell are:

$$Pb(s) + PbO_2(s) + 4H^+(aq) + 2SO_4^{2-}(aq) \leftrightarrow 2PbSO_4(s) + 2H_2O \quad 6.27$$

Discharging $\longrightarrow$

Charging $\longleftarrow$

The half-cell reactions during discharge are:

At the positive electrode:

$$PbO_2(s) + 3H^+ + HSO_4^- + 2e^- \leftrightarrow PbSO_4(s) + 2H_2O\,(aq) \quad 6.28$$

At the negative electrode

$$Pb(s) + HSO_4^- \rightarrow PbSO_4(s) + H^+ + 2e \quad 6.29$$

From equations 6.28 and 6.29 it can be seen that each reaction results in the transfer of 2 electrons

The battery model is based on the Nernst equation which can be represented by the equation 6.30

$$E = E^{\theta} + \frac{RT}{nF}\ln\left(a_{H^+}\right)\left(a_{HSO_4^-}\right) \quad 6.30$$

The cell emf can be expressed as

$$E = 2.05 + \frac{RT}{nF}\ln\left(C_{H^+}\right)\left(C_{HSO_4^-}\right) \quad 6.31$$

$$E = 2.05 + \frac{RT}{nF}\ln\left(2\right)\left(C_{H^+}\right)\left(C_{HSO_4^-}\right) \quad 6.32$$

As the molar concentration of the H^+ $\left(C_{H^+}\right)$ HSO_4^- $\left(C_{HSO_4^-}\right)$ ions is the same, the cell theoretical OCV can be written as:

$$E = 2.05 + \frac{RT}{nF}\ln\left(2\right)\left(C^2\right) \text{ Volts} \quad 6.33$$

According to the manufactures' instructions when the Plantè cell is fully charged the specific gravity should be between 1.205 and 1.215 [106].

Taking the mean value as 1.210 and interpolating the results of table 6.1, sulphuric acid electrolyte with a specific gravity of 1.210 corresponds to a percentage weight of 28.93% H_2SO_4. The density of sulphuric acid is 1.84 g/litre, therefore 1 litre of pure H_2SO_4. has a weight of 1840 grammes. The molar weight of H_2SO_4 is 98 grammes per mole, therefore pure H_2SO_4 has a concentration of:

$$\frac{1840}{98} = 18.78 \text{ Moles.}$$

Therefore 28.93% weight equates to 5.43 moles of H_2SO_4

The mean IAC over the range of operation of the cell is 0.158 from figure 6.9, from equation 6.33 the theoretical OCV is:

$$E = 2.05 + \frac{RT}{nF} \ln\left(0.158^2 \times 5.43^2\right) \qquad 6.34$$

$$E = 2.05 + 0.026 \text{ x } \ln(0.736) \qquad 6.35$$

$$E = 2.05 - 0.008$$

$$E = 2.042 \text{ volts}$$

Taking this value of OCV as a starting value the model now has to simulate the battery undergoing discharge due to an external load.

For a discharge current of I = 1 amp

$$\mathrm{I} = \frac{\mathrm{Q}}{\mathrm{T}} = 1 \text{ Coulomb/Second} \qquad 6.36$$

Therefore a discharge current of 1 amp is equivalent to:

$$1 \text{ A} = \frac{1}{1.6022 \times 10^{-19}} = 6.241 \times 10^{18} \text{ electrons per second} \qquad 6.37$$

From equations 6.28 and 6.29 it is evident that each reaction taking place during the discharge process generates 2 electrons. From above a fully charged cell with sulphuric acid with a concentration of 5.43 moles contains:

$5.43 \text{x} 2 \text{x} 6.023 \text{ x} 10^{23} = 65.41 \text{ x} 10^{23}$e (electrons).

Therefore a discharge current of 1 Amp will deplete this concentration at a rate of:

$$\Delta C = \frac{6.241 \times 10^{18}}{2 \times 6.023 \times 10^{23}} = 5.18 \times 10^{-6} \text{ Moles per second} \qquad 6.38$$

Therefore as the battery discharges due to a load of 1 Amp the acid concentration reduces at a rate of 5.18 $x10^{-6}$ moles per second.

The battery model was designed to simulate a lead acid battery discharge including the effects of dissociation and using the rate of acid concentration depletion calculated in equation 6.38. After a second has elapsed the acid concentration is reduced by 5.18 $x10^{-6}$ moles, from the staring value of 5.43 moles, equation 6.35 is then used to calculate the new value of OCV.

Using the model for a one-hour discharge at a discharge current of 6 Amps starting with a concentration of 5.43 moles reduces the theoretical OCV of the cell from 2.042 volts to 2.041 volts as shown in figure 6.12. This represents a decrease in OCV of 0.001 volts.

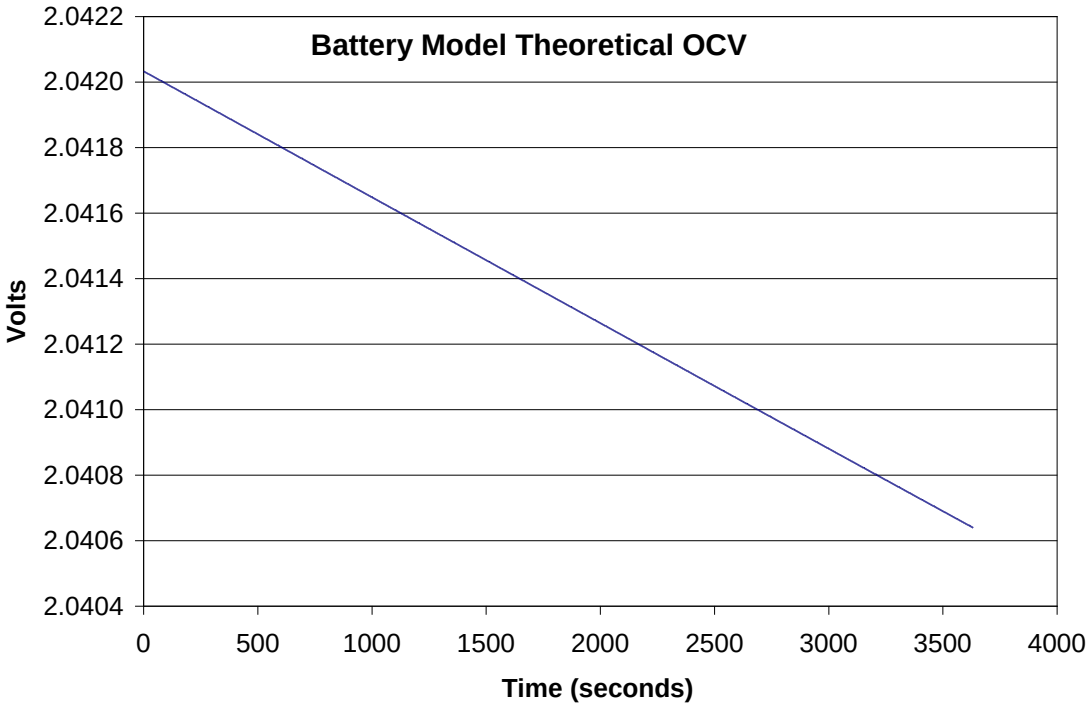

Figure 6.12: Cell OCV over one hour discharge at 6 amps

The theoretical discharge shown above differs considerably from an actual discharge characteristic shown in figure 6.13.

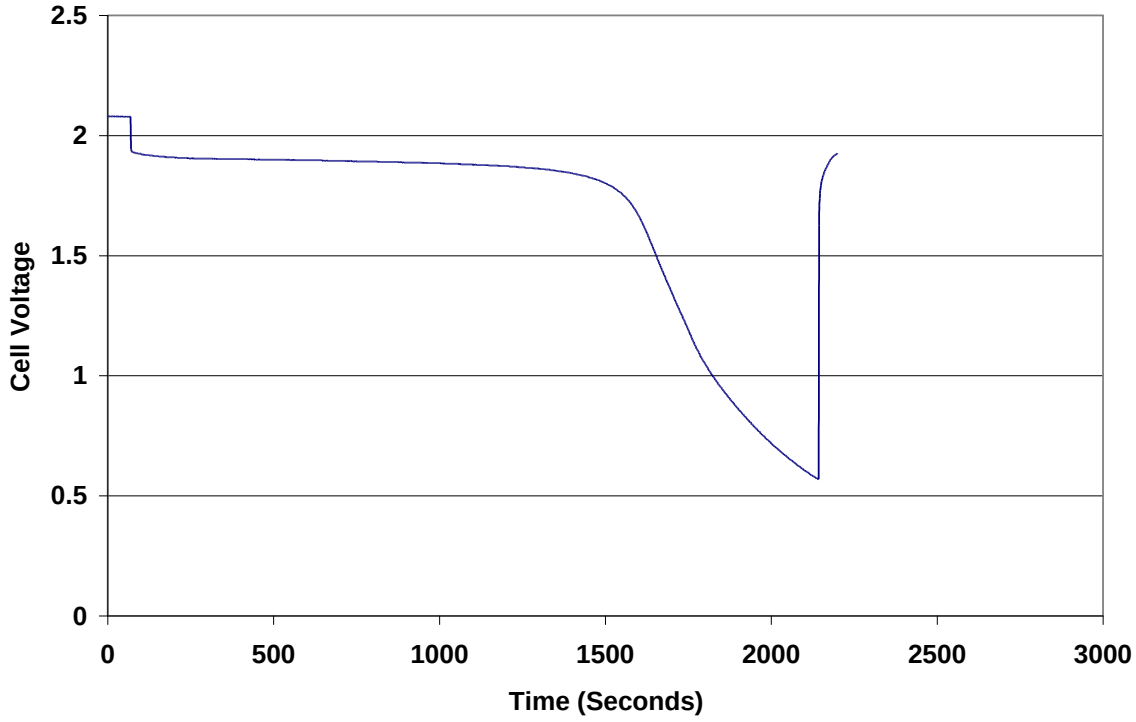

Figure 6.13: Actual cell voltage discharged at 6 amps

The OCV at the beginning of the discharge is 2.08 volts at the end of the test the OCV is 1.921 volts, a decrease of 0.159 volts, compared with a decrease of 0.001 volts predicted by the battery model. Therefore there is a significant discrepancy between the values predicted by the model and the test results.

The author then looked to ways of improving the model to be more representative of an actual discharge process. Most of the voltage-current/SOC relations for lead-acid batteries are modifications of the relation for constant-current discharge proposed by C.M.Shepherd (1965) [107].

The Shepherd model equation is often used to model batteries for Hybrid Electric Vehicle (HEV) analysis, where HEVs tend to use deep discharge batteries which have similar characteristics to the Plantè cell tested in this thesis. The Shepherd model describes the electrochemical behaviour of the battery directly in terms of voltage and current. It is often used conjunction with the Peukert equation to obtain battery voltage and state of charge [108].

The Shepherd Model for the battery voltage is given in equation 6.39:

$$E_t = E_o - \left(R_i \times I\right) - \frac{K_i}{\left(-f\right)} \qquad 6.39$$

Where: E_t = battery terminal voltage (Volts)

E_o = open circuit voltage of a fully charged battery (Volts)

R_i = internal (ohmic) resistance of the battery (ohms)

K_i = polarisation resistance (ohms) typically 0.1 ohms [109].

I = instantaneous current (amps)

f = accumulated ampere-hours divided by full battery capacity

The Shepherd model includes the effect of the battery internal resistance, therefore before proceeding further with the battery modelling it is necessary to discuss internal resistance.

6.7.1 Internal Resistance

The battery in its simplest form can be represented by the equivalent circuit as shown in figure 6.14

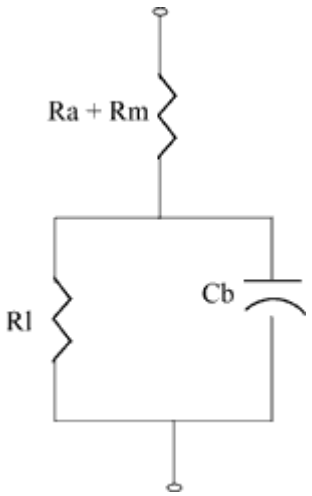

Figure 6.14 Battery (Randal) equivalent circuit [110].

Where:

R_m is the resistance of the metallic path through the cell including the terminals (ohms).

R_a is the resistance of the electrochemical path through the electrolyte, and the separators (ohms).

C_b is the capacitance of the parallel plates, which form the electrodes of the cell (farads).

R_1 is the non-linear contact resistance between the plate or electrode and the electrolyte (ohms).

The overall resistance of the cell is determined primarily by R_1 that is the electrochemical resistances of the two electrode-electrolyte interfaces, which are in series with the electrolyte resistance.

During discharge of the battery while connected to an external load the actual voltage available at the battery terminals is less than the ideal voltage; the relationship between the actual terminal voltage and the ideal voltage can be expressed as shown in equation 6.40:

$$E = E_o - IR_i \qquad 6.40$$

Where

E is the terminal voltage (volts)

E_o is the Ideal (Nernst) voltage (volts)

I is the discharge current (amps)

Ri is the measured battery internal resistance (ohms)

The ideal voltage E_o is replaced by the measured cell voltage V for the purpose of analysis of the cell; this gives a revised equation 6.41:

$$V = V_{OCV} - IR_i \qquad 6.41$$

Equation 6.41 was used to estimate the internal resistance of the Plantè cell used in the experimental work of this thesis.

The internal resistance of a battery is often quoted as a characteristic parameter. A battery that is suitable for high rate discharge must have a low internal resistance otherwise the voltage drop caused by the current would limit the discharge.

The meaning of the term ‘internal resistance’ has to be considered with some caution, because it is not simply electrochemical resistance. The following have to be taken into account:

1. The current/ voltage characteristics are not symmetrical for charging and discharging, values quoted for internal resistance in general concern the discharge of the battery.
2. The internal resistance of the battery depends on the state of charge of the battery.
3. The internal resistance is increased at reduced temperature owing to reduced conductivity and retarded kinetic parameters.

For these reasons, the values quoted for internal resistance of a battery can only be approximations that depend on the measurement method.

Equation 6.41 was used to calculate the internal resistance for some of the discharge tests carried out during the experimental work. Typically a three-hour discharge of a Plantè cell at a discharge current of 6 Amps increased the internal resistance of the cell from 0.014 ohms to 0.647 ohms as shown in figure 6.15.

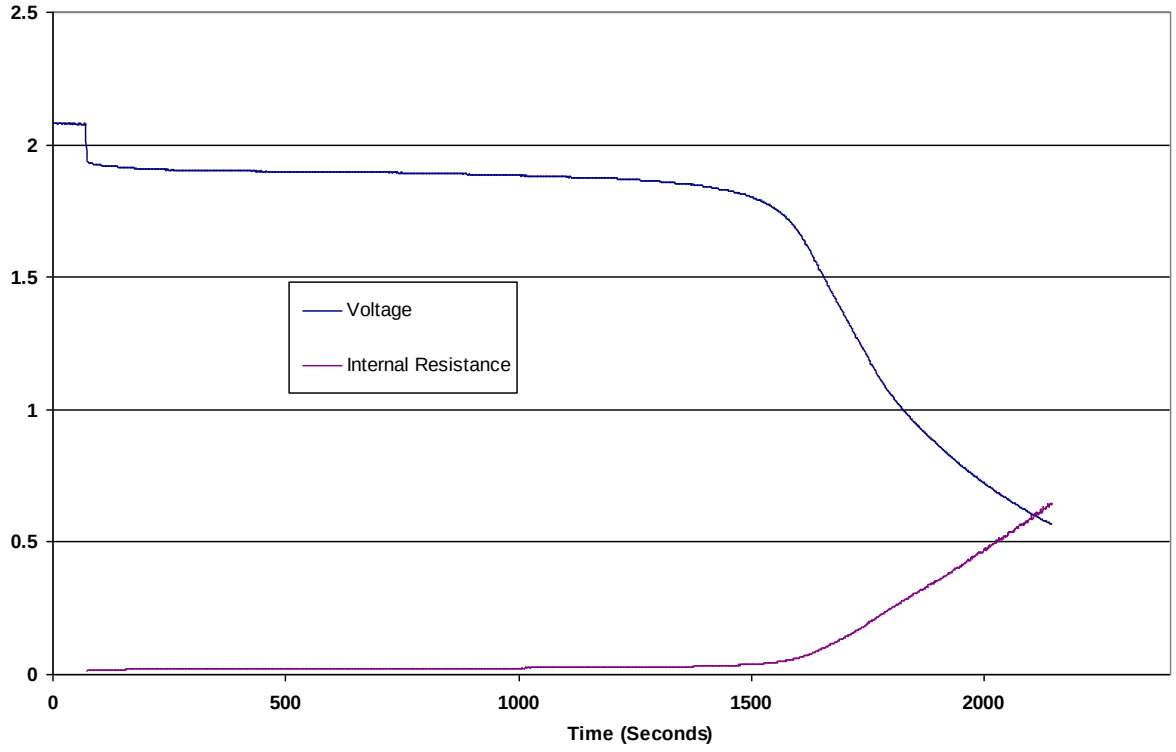

Figure 6.15: Internal resistance (ohms) versus cell voltage (volts) of a Plantè cell under nominal discharge current of 6 Amps.

Having identified a way of measuring the internal resistance of a battery the battery model was modified to include the Shepherd model

Figure 6.16 shows a comparison between actual discharge and Shepherd model for a discharge current of 6 amps.

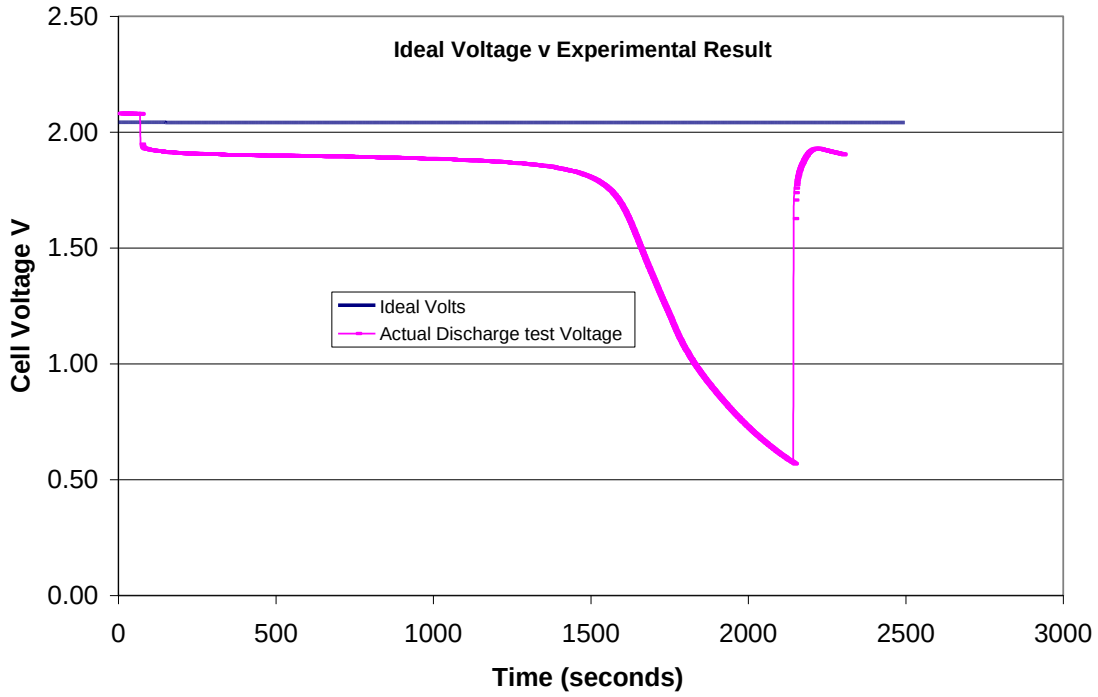

Figure 6.16: Comparison of actual discharge with Shepherd model.

It can be seen from figure 6.19 that the actual (measured) cell voltage returned to a value close to the Shepherd voltage once the load is removed if the initial effect known as the 'Coup de Fouet' discussed in Chapter 9, is ignored.

When the load is applied to the battery the measured voltage is 1.943 volts, and the corresponding Shepherd voltage is 1.948 volts. At the end of the test the open circuit measured voltage from the discharge test is 1.904 volts and the Shepherd voltage is 1.909 volts.

This would suggest that the battery model is now a reasonable approximation for the beginning and end of the discharge test.

However, during the discharge test the Shepherd model fails to simulate the collapsing cell voltage. This was investigated by the author, and the discharge time was increased beyond the time taken for the actual discharge test. Figure 6.17 shows the resulting discharge curve based on the Shepherd model.

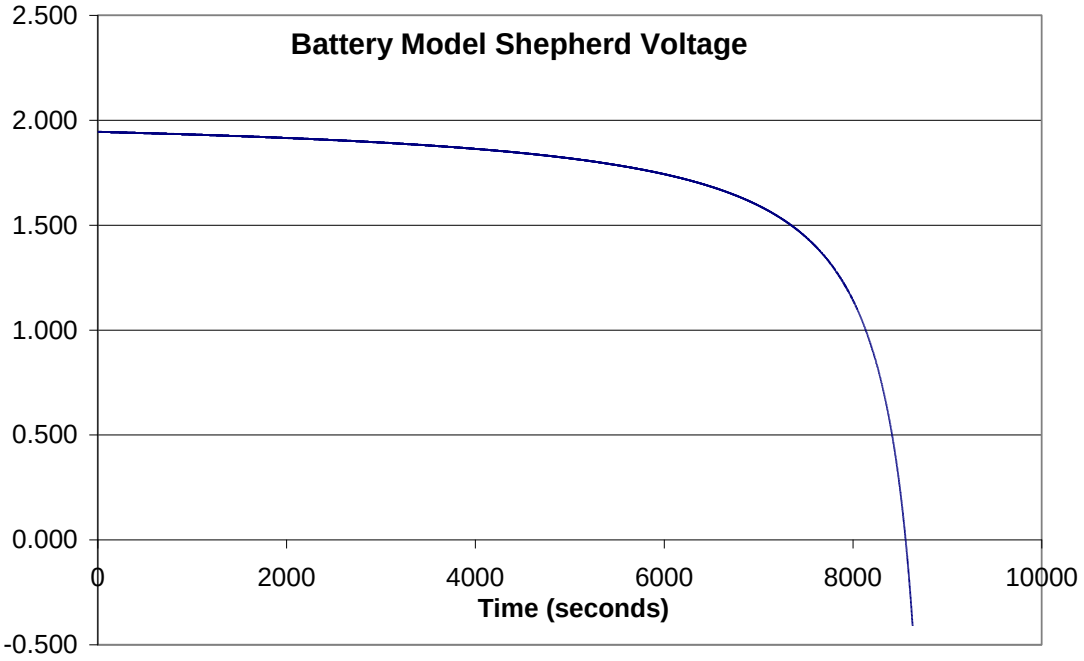

Figure 6.17: Battery model discharge curve using shepherd model, cell voltage (Volts) versus time (Seconds).

Figure 6.17 shows that the discharge curve based on the Shepherd model show a similar decline in voltage to the experimental results but over a longer timescale.

Inspection of the Shepherd equation 6.38 shows that given product $R_i \times I$ will increase as the internal resistance increases during cell discharge, as will the term $\frac{K_i}{(-f)}$ as the term f (accumulated ampere-hours divided by full battery capacity), approaches the value 1.

$$E_t = E_o - R_i \times I - \frac{K_i}{(-f)}$$

To evaluate which of the two terms has the greater effect figure 6.18 shows the battery model with of figure 6.17 with each of these terms removed.

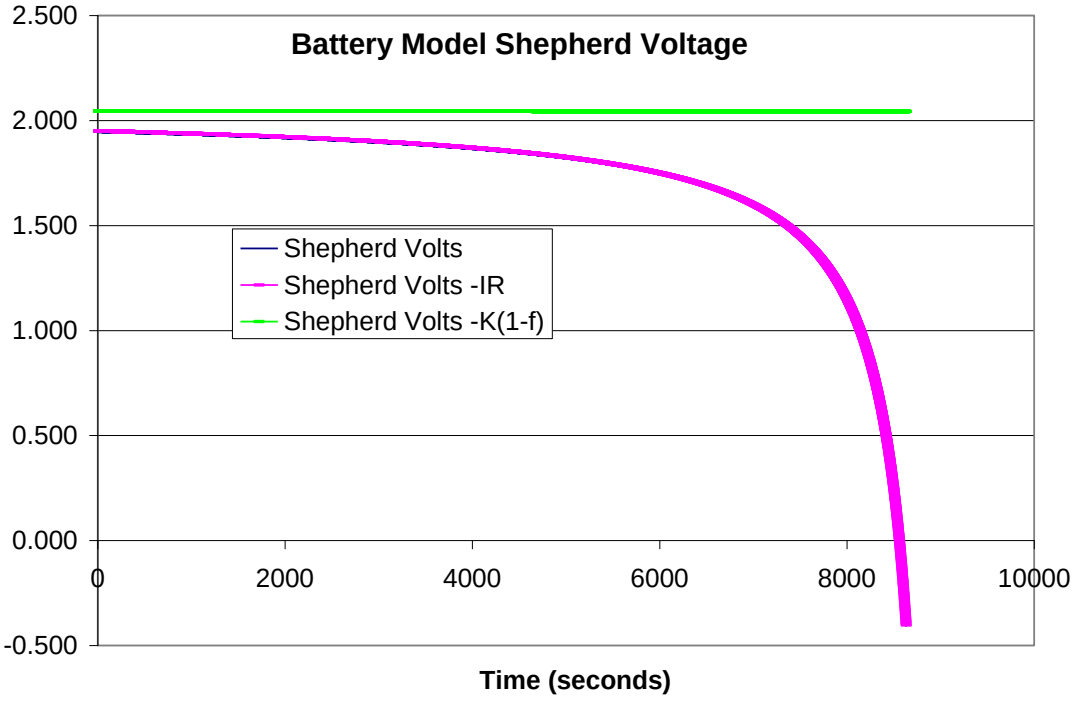

Figure 6:18 Battery Model showing shepherd voltage (Volts) versus time (Seconds) with elements removed.

It can be seen that when the capacity term $-\frac{K_i}{(1-f)}$ is removed (green discharge curve) the discharge curve reverts back to a discharge characteristic similar to the Ideal voltage characteristic of figure 6.16, this indicates that it is the term $-\frac{K_i}{(1-f)}$ which accounts for decreasing battery capacity which has the greater effect of the two terms.

The model was based on a new Plantè cell, which according to the manufacturers data has a capacity of 15 Ah, however the experimental results used for comparison were based on a cell which had been repeatedly over-discharged during the experimental work and had on several occasions been deliberately driven into reverse polarity, with resulting deterioration in the condition of the cell. The actual capacity

had in fact not been 15 Ah and in some tests the actual capacity discharge has been found to be as low as 3Ah for a 6 amp discharge test. With this in mind the term f (accumulated ampere-hours divided by full battery capacity) from equation 6.39 was adjusted to 3Ah in order to represent the actual battery capacity of an aged cell such as the one used in this test, rather than the manufacturers capacity for a new cell, this resulted in a much shorter discharge period for the model discharge and was more representative of the actual cell discharge characteristic as shown in figure 6.19.

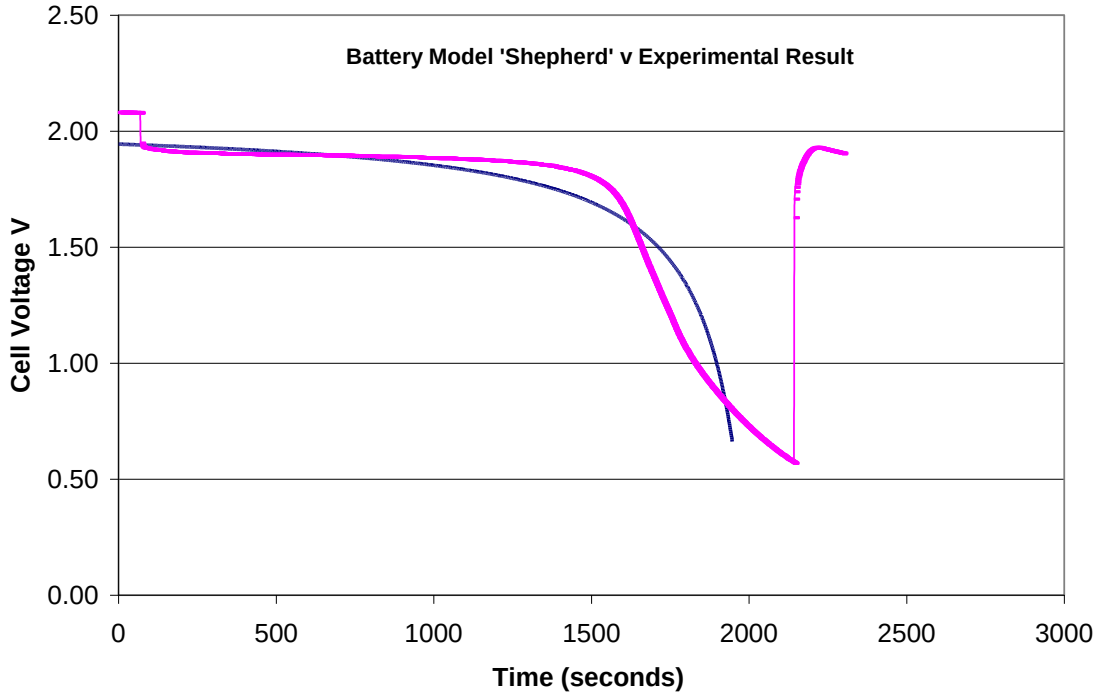

Figure 6.19 Battery model with reduced capacity term.

However, the Model discharge still does not replicate the actual discharge completely and an explanation for this is discussed in Chapters 9 and 10.

Voltage alone is not a reliable indication of the state of charge of a battery, except when the voltage is close to the low voltage limit (1.70 volts for the Plantè cell) on discharge [99]. Therefore the battery model was further developed to include pH, specific gravity acid concentration in addition to cell voltage. The output of the model for a discharge at a discharge current of 6 Amps is shown in figure 6.20.

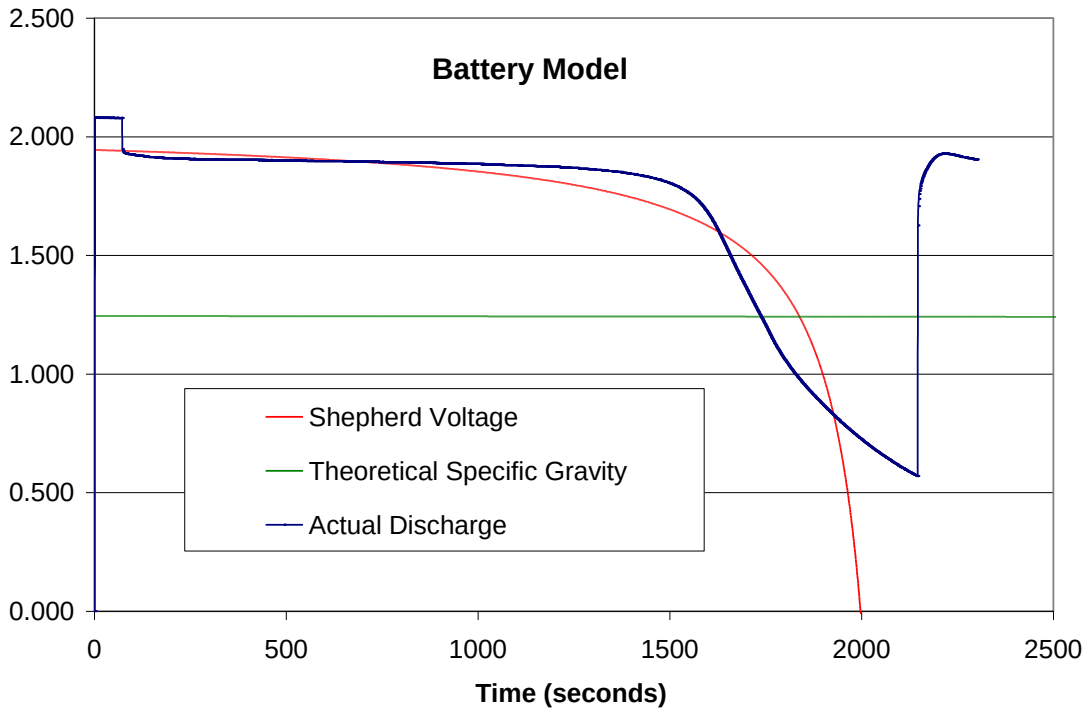

Figure 6.20: Model of a Plantè cell voltage (Volts) being discharged at 6 amps, versus time (Seconds).

The pH of the electrolyte is of particular importance in terms of this thesis.
As the battery discharges the concentration of H^+ ions decreases as shown previously in equation 6.27.

$$Pb(s) + PbO_2(s) + 4H^+(aq) + 2SO_4^{2-}(aq) \leftrightarrow 2PbSO_4(s) + 2H_2O$$

Using the model the change in electrolyte pH can be determined as follows.
The pH of the electrolyte can be determined by using equation:

$$pH = -\log_{10}(a_{H^+}) \text{ [111].} \qquad 6.42$$

Given that the activity a, is the product of the acid concentration (C) and the ionic activity constant (γ).

$$a = \gamma C \qquad 6.43$$

The pH can be expressed as:

$$pH = -\log_{10}\left(C_{H^+}\right) \qquad 6.44$$

As pH is a function of the H^+ ion concentration as shown in equation 6.44, as the battery discharges the electrolyte pH decreases.

Using equation 6.44 in the battery model and starting from an electrolyte concentration of 5.43 moles a one-hour discharge at a discharge current of 6 Amps increases the pH as shown in figure 6.21.

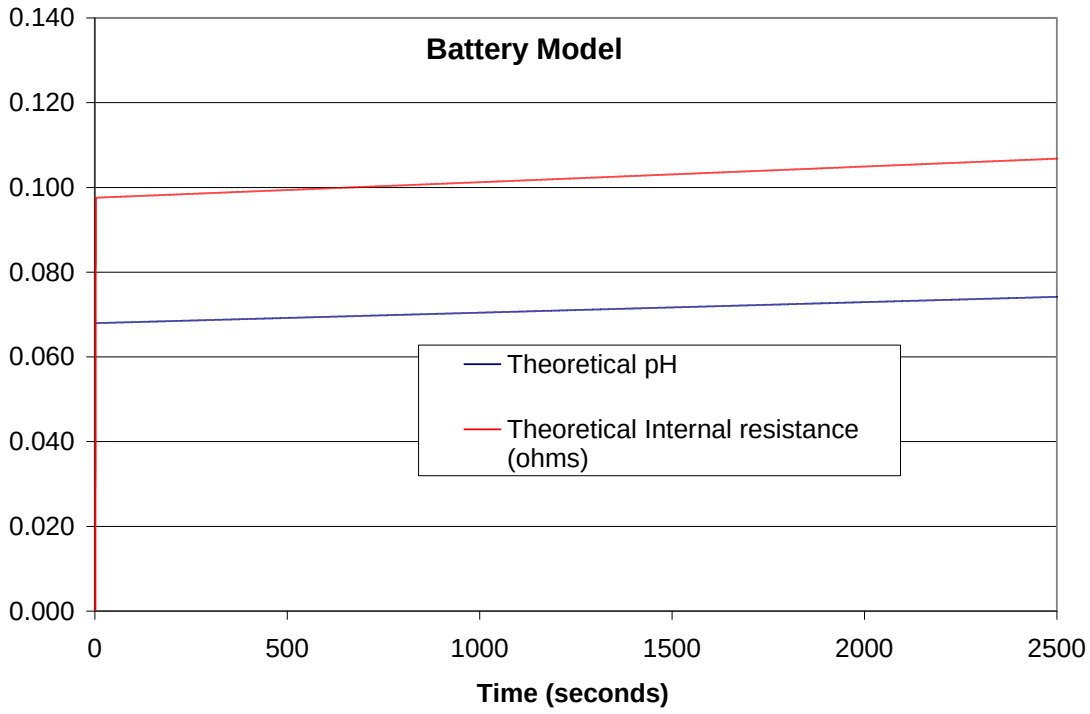

Figure 6.21: Theoretical electrolyte specific gravity and theoretical internal resistance (ohms) over one hour discharge at a current of 6 amps.

Figure 6.22 shows the results of a discharge on a Plantè cell in terms of the cell voltage and pH, it can be seen that the pH decreases until about 2600 seconds, thereafter however, there is a disturbance in the pH with the pH increasing until about 4000 seconds, then increasing finally returning closer to pre-disturbance values

at about 4500 seconds. This pH disturbance is not replicated by the battery model and is discussed further in Chapter 10.

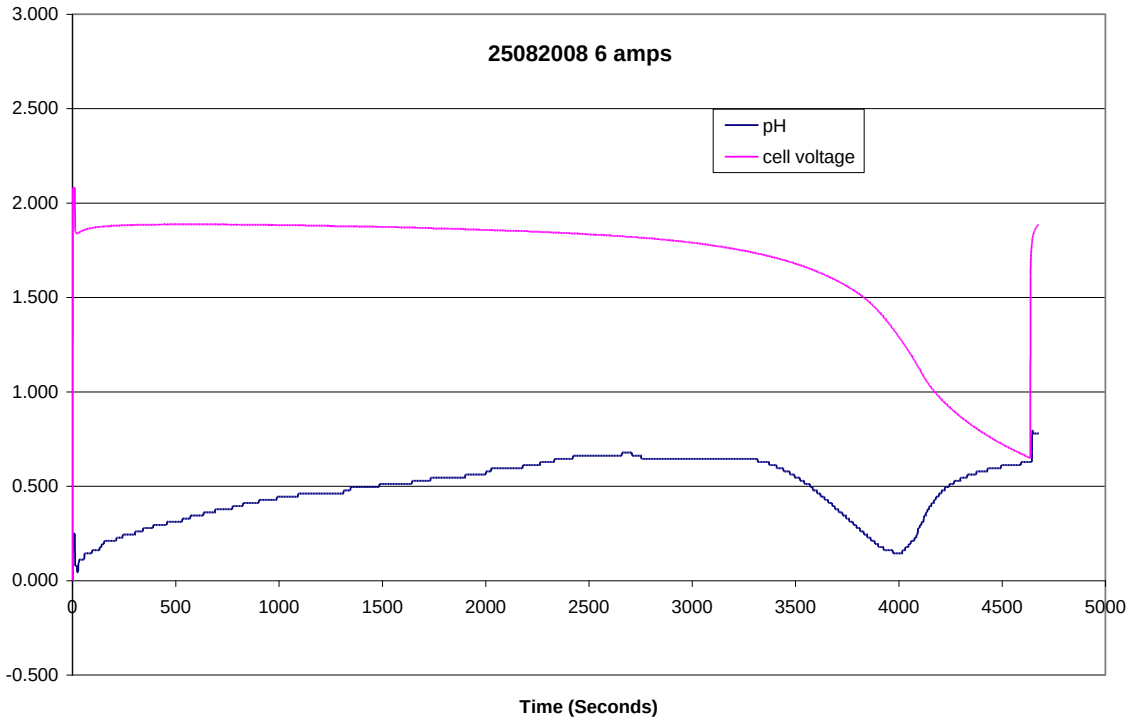

Figure 6.22 Discharge test on Plantè cell showing cell voltage (Volts) and pH, versus time (Seconds) under a nominal discharge current of 6 Amps.

6.8 Chapter Conclusions

This chapter began with a brief review of the development of lead acid batteries, the different types of lead acid battery and their applications. The sulphuric acid electrolyte was discussed in terms of its chemical reactions and its properties, in particular specific gravity as the specific gravity is used as an indication of battery state of charge.

The electrochemical processes which take place during battery charging and discharging were then discussed as were a series of terms and conditions relevant to lead acid battery operation.

The last section in this chapter looked at battery modelling, and looked at the stages in the development of a theoretical model of the lead acid battery. This model only simulated the discharging process and it was initially developed to model the cell voltage during discharge.

Limitations of the model became apparent when the model discharge voltage characteristic was effectively constant, with only marginal reduction in cell voltage at the end of the discharge.

The voltage model was then modified and based on the ‘’Shepherd Model’, an established model which takes into account the battery internal resistance and reduction in battery capacity.

This revised model showed some improvement insofar as the initial and final open circuit voltages of the model were close in value to the experimental values, however, the model did not seem to replicate the period of accelerated voltage decline which occurs just after the cut-off voltage. Further inspection of the model revealed that the model did in fact replicate this decline, but that is occurred after a much longer discharge time than in the experimental case. Further analysis of the model revealed that the term which represented the change in battery capacity was based on a new cell, when the age of the cell was factored into the model the output was more representative of the corresponding experimental discharge, however, models such as the Shepherd model do not fully represent the discharge process..

Other parameters included in the model were internal resistance, specific gravity and pH. Of these pH is the most accessible ‘on-load” measurement, and although there are significant differences in the theoretical and measured values of pH during a battery discharge the variation of pH during battery discharge form the focus of the rest of this thesis.

CHAPTER 7 MEASUREMENT AND TESTING

This chapter discusses ways of determining, by measurement, the condition of electrochemical cells. Most of the discussion in this chapter relates to batteries rather than fuel cells as estimating the available energy available within the battery is of particular interest.

Assessing the exact condition of batteries is not possible however, two estimation methods are often used.

1. State of Charge (SoC)
2. State of Health (SoH)

Knowing the amount of energy left in a battery compared with the initial energy it had gives the user an indication of how much longer a battery will continue to perform before it needs recharging. Using the analogy of a fuel tank in a car, State of Charge (SOC) estimation is often called the "Fuel Gauge" function.

7.1 State of charge

The SOC is defined as expressing the remaining available capacity. The preferred SOC reference should be the rated capacity of a new cell rather than the current capacity of the cell, because the cell capacity gradually reduces as the cell ages. For example, towards the end of the cell's life its actual capacity will be approaching only 80% of its rated capacity and in this case, even if the cell were fully charged, its SOC would only be 80% of its rated capacity. Temperature and discharge rate effects reduce the effective capacity even further. This difference in reference point is important if the user is depending on the SOC estimation as they would in a real fuel gauge application e.g. in a car.

Unfortunately the SOC measurement reference is often defined as the current capacity of the cell instead of the rated capacity. In this case a fully charged cell, nearing the end of its life, could have an SOC of 100% but it would only have an effective capacity of 80% of its rated capacity and adjustment factors would have to

be applied to the estimated capacity to compare it to its rated new capacity. Using the current capacity rather than the rated capacity is usually a design shortcut or compromise to avoid the complexity of determining and allowing for the age related capacity adjustments which are conveniently ignored.

Basing the SOC estimate on the current capacity of the battery rather than its rated capacity when new is equivalent to progressively reducing the capacity of the fuel tank over the lifetime of the vehicle without informing the driver. If an accurate estimate of the charge remaining in the battery is required the ageing and environmental factors must be taken into account [112].

The actual state-of-charge technologies that the main companies use in practice is shown in table 7.1.

Technique	Application field	Advantages	Drawbacks
Discharge test	All battery systems Used for capacity determination at the beginning of life.	Easy and accurate: Independent of state-of-health	Offline, time intensive, modifies the battery state, loss of energy
Ah balance	All battery systems, most applications (consumer, PV, EV)	Online, easy accurate if enough re-calibration points are available and with good current measurement	Needs a model for the losses Sensitive to parasite reactions Cost intensive for accurate current measurement Needs regular re-calibration points
Physical properties of electrolyte (density, concentration, colour)	Lead possibly Zn/Br and Va	Online Gives information about state-of-health	Error if acid stratification, Low dynamic, problem of stability of sensors in electrolyte. Sensitive to temperature and impurities.
OCV	Lead, lithium, Zn/Br	Online, cheap	Low dynamic, error if acid stratification and needs long rest time (current=0) for lead systems. Problem of parasite reaction (e.g. Sb poisoning by lead)
Linear model	Lead PV, possibility for other battery systems? (not tried yet)	Online, easy	Needs reference data for fitting parameters
Artificial neural networks	All battery systems	Onjline	Needs training data of a similar battery
Impedance spectroscopy	All systems	Gives information about state-of-health and quality. Possibility of online measurement.	Temperature sensitive, cost intensive.
DC internal resistance	Lead, Ni/Cd	Gives information about state-of-health, cheap. Possibility of online measurement. Easy	Good accuracy, but only for low state-of-charge.
Kalman filters	All battery systems, PV dynamic applications (e.g. HEV)	Online, Dynamic	Needs large computing capacity. Needs a suitable battery model. Problem of determining initial parameters.

Table 7.1: Overview of methods for state-of-charge determination [113].

7.2 State of Health

The State of Health is a "measurement" that reflects the general condition of a battery and its ability to deliver the specified performance compared with a new battery. It takes into account such factors as charge acceptance, internal resistance, voltage and self-discharge.

During the lifetime of a battery, its performance or "health" tends to deteriorate gradually due to irreversible physical and chemical changes which take place with usage and with age until eventually the battery is no longer usable, or ‘dead’. The State of Health is an indication of the point which has been reached in the life cycle of the battery and a measure of its condition relative to a fresh battery.

Unlike the state of charge which can be determined by measuring the actual charge in the battery there is no absolute definition of the State of Health. It is a subjective measure in that different people derive it from a variety of different measurable battery performance parameters which they interpret according to their own set of rules. State of Health is estimation rather than a measurement, which is fine so long as the estimate is based on a consistent set of rules but it makes comparisons between estimates made using different test equipment and methods unreliable.

Battery manufacturers do not specify the State of Health because they only supply new batteries. The SOH only applies to batteries after they have started their ageing process either on the shelf or once they have entered service. The State of Health definitions are therefore specified by test equipment manufacturers or by the user. Its purpose is to provide an indication of the performance which can be expected from the battery in its current condition or to provide an indication of the how much of the useful lifetime of the battery has been consumed and how much remains before it must be replaced. In critical applications such as standby and emergency power plant the SOH gives an indication of whether a battery will be able to support the load when called upon to do so. Knowledge of the SOH will also help the plant engineer to anticipate problems to make fault diagnosis or to plan replacement. This is essentially a monitoring function tracking the long term changes in the battery.

For EV applications, the ability to achieve the range when called upon to do so is most important, hence the SOH is based on a comparison of current capacity with capacity when new.

7.2.1 Determining State of Health

Any parameter which changes significantly with age, such as cell impedance or conductance, can be used as a basis for providing an indication of the SOH of the cell. Changes to these parameters will normally signify that other changes have occurred which may be of more importance to the user. These could be changes to the external battery performance such as the loss of rated capacity or increased temperature rise during operation or internal changes such as corrosion. In practice the SOH is estimated from a single measurement of either the cell impedance or the cell conductance.

As the SOH indication is relative to the condition of a new battery, the measurement system must hold a record of the initial conditions or at least a set of standard conditions. Thus if cell impedance is the parameter being monitored, the system must keep in its memory as a reference, a record of the initial impedance of a fresh cell. If counting the charge / discharge cycles of the battery is used as a measure of the battery usage, the expected battery cycle life of a new cell would be used as the reference.

An alternative method of specifying the SOH is to base the estimation on the usage history of the battery rather than on some measured parameter. The number of charge - discharge cycles completed by the battery is an obvious measure, but this does not necessarily take into account any extreme operating conditions experienced by the battery which may have affected its functionality. It is however possible to record the duration of any periods during which the battery has been subject to abuse from out of tolerance voltages, currents or temperatures as well as the magnitude of the deviations. From this data a figure of merit representing the SOH can be determined by using a weighted average of the measured parameters.

Battery usage data can be stored in memory in a Battery Management System in a "History Chip" and downloaded when required. This alternative method does not use any external test equipment but it adds complexity and cost to the battery [114].

7.2.2 Peukert Equation

This is an empirical formula which approximates how the available capacity of a battery changes according to the rate of discharge. $C = I^n T$ where "C" is the theoretical capacity of the battery expressed in amp hours, "I" is the current, "T" is time, and "n" is the Peukert Number, a constant for a given battery. The equation shows that at higher currents, there is less available energy in the battery. The Peukert Number is directly related to the internal resistance of the battery. Higher currents mean more losses and less available capacity.

The value of the Peukert number indicates how well a battery performs under continuous heavy currents. A value close to 1 indicates that the battery performs well; the higher the number, the more capacity is lost when the battery is discharged at high currents. For Lead acid batteries the number is typically between 1.3 and 1.4 [115].

Both state of charge and state of health are indications of battery condition, however, as no standard definitions' exist for either term their usefulness in terms of indicating battery condition is debatable, and they can only be treated estimates of cell condition.

7.3 Measurement of Cell Condition

Measurement of cell condition requires measurement of variables relating to the electrochemical cell. These can be classified under two headings.

1. Direct Measurement.
2. Book keeping systems.

7.3.1 Direct Measurements

There are no simple direct measurements, such as placing a voltmeter across the terminals, to determine the condition of a battery. The voltmeter reading gives an indication the state of charge, but it cannot indicate how well the battery will deliver current when under load.

There are a number of parameters, which can be measured in order to determine cell condition.

1. pH
2. Specific Gravity
3. Impedance Spectroscopy
4. Conductance
5. Internal resistance

7.3.2 pH

The pH of a solution is a measure of its hydrogen ion concentration, the letters pH meaning "power of hydrogen". Since free protons react with water to form hydronium, the acidity of an aqueous solution is determined by its hydronium concentration.

pH can be measured using either pH indicators, such as phenolphtaleine in the form of solution or strips, or a potentiometric method can be used. Potentiometric methods measure the potential difference between known a reference electrode and the measuring pH electrode. The potential difference between these electrodes is dependent on the activity of the ions in the solution being measured; once the potential is measured the activity can be determined.

7.3.3 pH Meter

A pH meter is a device used for potentiometric pH measurements; however, it is nothing more than a precise voltmeter, scaled in such a way as to measure pH.

pH is defined as the negative log of the hydrogen ion activity. The standard method for pH measurement uses an H+ ion specific electrode that generates an electrical potential across a glass membrane. The pH meter is simply a voltmeter that measures this potential.

The pH probe measures the activity of the H^+ ions, therefore accurate measurement of pH of strong acids and alkalis is problematic. pH measurement is temperature sensitive and compensation has to be made accordingly. Figure 7.1 shows correction factors for temperatures of 0, 25, and 100^{o}C.

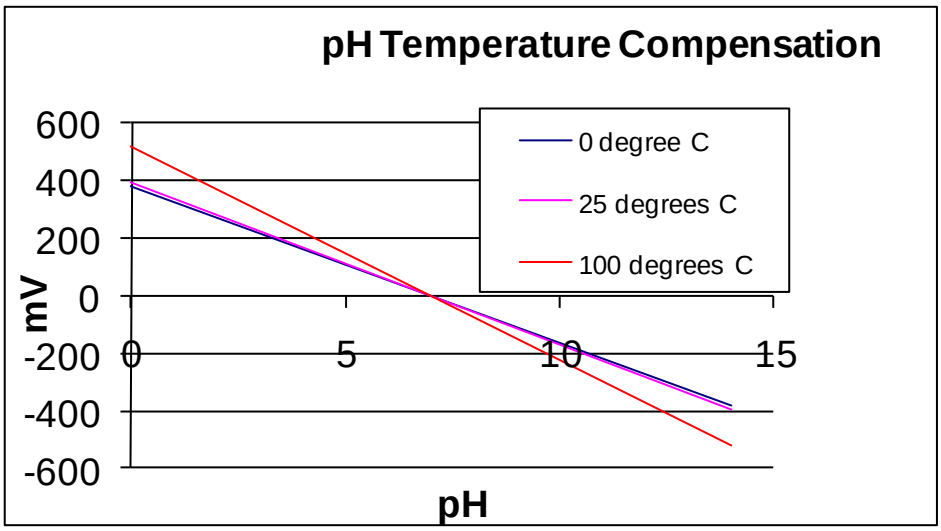

Figure 7.1: Temperature compensation for pH measurements.

Patent number GB1372214 held by Varta AG, November 1971, refers to the swelling of an ion exchange membrane to move a pointer in accordance with the pH of an electrolyte in which it is immersed as an indication of the state of charge of a lead-acid battery.

Field effect transistors (FETs) are being developed as chemical sensors pH probes using FET technology are now available for measurement of pH [116]. FETs have an advantage over glass electrodes in terms of faster response time and are smaller and less fragile.

7.3.4 Theory of pH measurements

pH is a unit of measurement that determines the degree of acidity or alkalinity of a solution, on a scale of -3.5 to 14. Note that the lowest recorded value of pH is -3.6 [117].

If the pH is less than 7 the solution is acidic, if it is greater than 7 then it is alkaline or basic.

The 'p' in the term pH is defined as the mathematical representation of "negative logarithm". The 'H' is the chemical symbol for hydrogen. Therefore pH stands for negative logarithm of the hydrogen activity and is given by the equation 6.44.

There are several ways to measure pH, from simple methods using pH sensitive papers, colour indicators to different kinds of pH electrodes where glass electrodes are the most common. Glass electrodes can be used to relative high temperatures and modern pH meters have temperature compensation to correct for the temperature variation in the electrode response. It is, however, necessary to calibrate the electrode at the measuring temperature to obtain accurate data. Measuring pH at high pressure is far more difficult because the glass membrane in traditional pH electrodes can not withstand pressure. Different types of electrodes have therefore been developed for higher pressures. The two main types are solid state electrodes which can be used at very high pressures, and glass electrodes with pressure equilibration between the inner and the outer part of the electrode.

pH, or *pondus hydrogeni*, the power of hydrogen, was defined by Sørensen and Lindstrøm-Lang [118] as the negative logarithm of the hydrogen ion activity:

$$pH = -\log a_{H^+} = -\log m_{H^+}\gamma_{H^+} \qquad 7.1$$

Where:

a_{H^+} is the activity, (dimensionless).

m_{H^+} is molality (moles)

γ_{H^+} is the activity coefficient of the H^+ ion, (dimensionless).

This definition is more troublesome than it may look because single ion activities, or activity coefficients, are immeasurable quantities. pH can therefore only be measured *relative* to other solutions where pH has been defined in some way. Such standard solutions, covering a large range of pH and temperatures have been defined and are commercially available. They are normally made of acid/base systems with high buffer capacities, where buffer capacity can be defined as quantity of strong acid or base that must be added to change the pH of one liter of solution by one pH. While there are plenty of low ionic strength buffers on the market, buffers with a high ionic strength are not available. This makes pH measurements in systems with high ionic strength very difficult because it is necessary to correct for changes in the liquid

junction potential of the reference electrode. A change of 1 pH will record a shift of approximately 59 mV on a voltmeter [119].

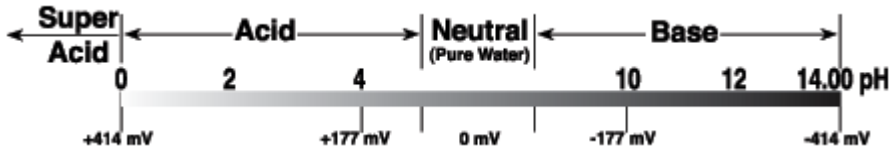

Figure 7.2: pH scale of measurement [119].

Figure 7.2 shows the full range of the pH scale and the corresponding voltages measured by a pH probe.

The 'p' prefix is used in other scales of chemical measurement where a logarithmic scale is used: pCO_2 (carbon dioxide) and pO_2 (oxygen), being two examples.

7.3.5 pH Measurement

There are two main methods of measuring the pH of a solution:

1. Colormetric or Indicator method.
2. Electrometric or pH meter method.

1. Colourmetric or Indicator method.

The most common method is pH paper, which gives only approximate results, but has the advantages of speed and low cost.

2. Electrometric or pH meter method.

pH is measured using a pH probe and an instrument amplifier, the pH probe has two parts; that is the measuring (sampling) and reference electrodes [120].

pH sensors

The most common pH sensor is the combination type, which has 3 components:

1 The reference electrode

2 The measuring (sampling) electrode

3 An amplifier

The measuring and reference electrodes are usually encased within a single unit made of glass.

The glass electrode is the most widely used electrode for pH measurement, and it operates on the principle that the potential difference between the surface of a glass membrane and a solution is a linear function of pH [121].

The mode of action of the glass electrode is very complex and, of all the theories put forward, no single one can account for all of the observed properties. It is very likely, however, that an important stage involves the absorption of hydrogen ions into the lattice of the glass membrane. The potential of the glass electrode can be expressed as

$$E = K + \left(\frac{RT}{F}\right)\ln \alpha_{H^+} \qquad 7.2$$

Measuring pH involves comparing the potential of solutions with unknown [H+] to a known reference potential. pH meters convert the voltage ratio between a reference half-cell and a sensing half-cell to pH values. Today, most electrodes are combination electrodes with both the reference and sensing half-cells in the same body.

Reference Half-Cells contain a conductor (usually silver with a silver chloride coating) immersed in a solution with known [H^+]. The potential between this internal conductor and the known solution is constant, providing a stable reference potential.

Sensing Half-Cells (measuring half-cells) are made of a nonconducting glass (or epoxy) tube sealed to a conductive glass membrane. Like the reference half-cell, the sensing half-cell also contains a conductor immersed in a buffered electrolyte solution, ensuring constant voltages on the inner surface of the glass membrane and the sensing conductor.

When the pH electrode is immersed in the solution to be measured, a potential is established on the surface of the sensing glass membrane. If the unknown solution is neutral, the sum of fixed voltages on the inner surface of the glass membrane and on the sensing conductor approximately balances the voltage on the outer surface of the glass membrane and the reference half-cell. This results in a total potential difference of 0 mV and a pH value of 7.

In acidic or alkaline solutions, the voltage on the outer membrane surface changes proportionally to changes in [H^+]. The pH meter detects the change in potential and determines [H^+] of the unknown by the Nernst equation as shown in equation 7.3.

$$E = E^o + \frac{2.3RT}{nF} \log\left(\frac{unknown\,[H^+]}{internal\,[H^+]}\right) \qquad 7.3$$

where:

E = total potential difference (mV)

E° = reference potential (mV)

R = gas constant (kJ/kg K)

T = temperature in Kelvin (K)

n = number of electrons

F = Faraday's constant (C/mol)

$[H^+]$ = hydrogen ion concentration [122].

A glass electrode must always be standardised at regular intervals with buffers solutions of known pH. At least two such solutions should be used covering the range of pH values to ensure constancy over this selected range [110].

The measuring (sampling) electrode is sensitive to the hydrogen ion and develops a voltage related the concentration of the hydrogen ions in the electrolyte solution in which it is immersed [120].

The reference voltage, sometimes referred to as the "rest potential", is compared with the sampling electrode measurement voltage, the measurement electrode has a very high internal resistance, making the voltage change with pH difficult to measure. Therefore the pH probe is connected to a high input impedance amplifier, which enables the voltage changes of the probe to be displayed on a meter [120].

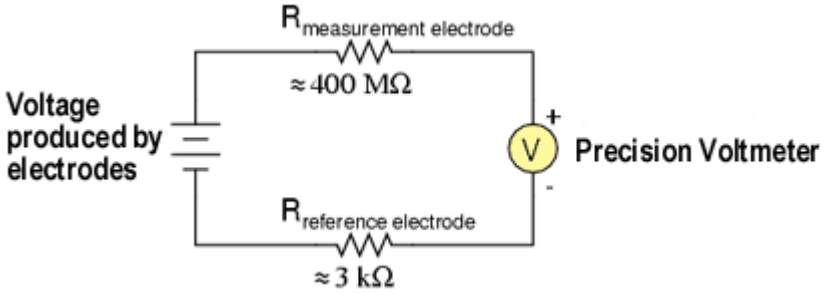

Figure 7.3: Model of pH probe [119].

7.3.6 Specific Gravity

Specific gravity is the density of a fluid when compared with the density of water, for example the specific gravity of sea water is 1.020, which means that as water has a density 1 kg per litre, the density of sea water is therefore 1.02 kg per litre.

Measurement of specific gravity is a convenient indicator of the concentration of the acid, which relates directly to the state of charge of an electrolytic cell.

Specific gravity can be measured by a hydrometer, which is an inexpensive float device used to measure the specific gravity and therefore concentration of the acid in a cell. The hydrometer takes a sample of the electrolyte into its glass chamber; the specific gravity is read at the point where the surface of the electrolyte crosses the scale of the hydrometer float.

Electronic hydrometers are available which are easier to use than the traditional float type. The example shown in figure 7.4 has the capability to download measurement data to a data logger.

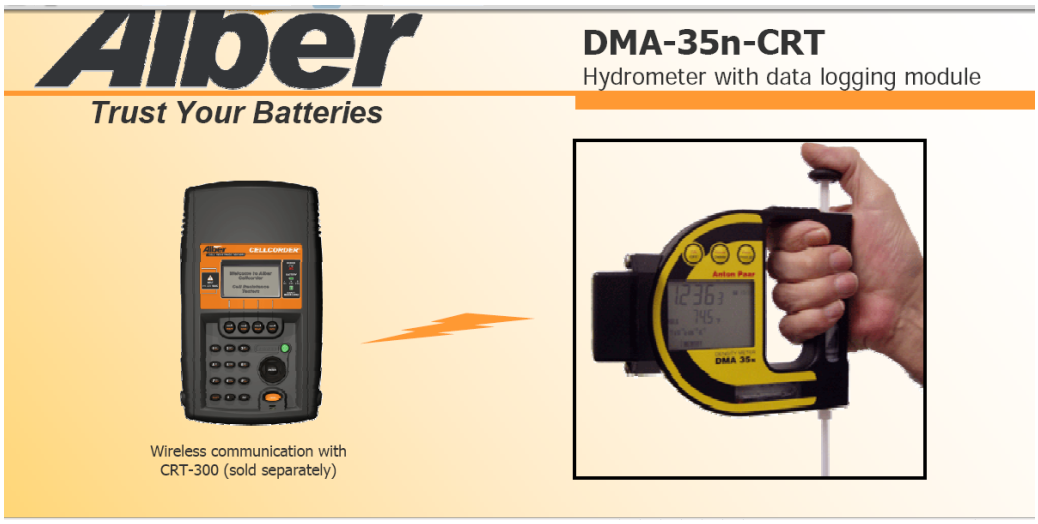

Figure 7.4: Electronic hydrometer with data logging

While the hydrometer is an inexpensive and convenient means of assessing the state of charge of a cell, it requires physical access to the electrolyte and as this access

may not always be available, other means of determining specific gravity have been implemented.

One of the better-known devices is the built in hydrometer or “magic eye” fitted to one of the cells of an automotive battery, if the indicator shows green the state of charge is in satisfactory condition, however, if the indication is not green, the specific gravity is low and the heavier green ‘eye’ will not float, and this indicates that the battery requires recharging or possibly replacement, see figure 7.5.

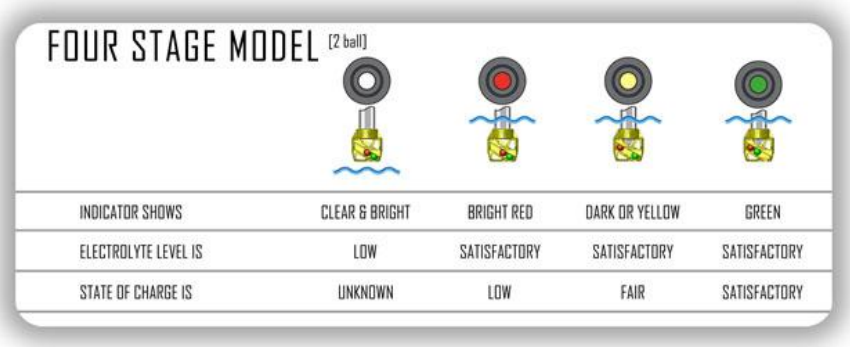

Figure 7.5 Battery magic eye indicators [123].

Development of a reliable and inexpensive specific gravity sensor has proved to be more problematic, a number of solutions have been developed using various techniques to achieve a working specific gravity measurement system, such as the patent (JP61294770) for specific gravity measurement which used a fibre optic method

7.3.7 Internal Resistance

Comparing the actual internal resistance with the resistance of a new battery will provide an indication of any deterioration in battery performance.

Note that DC measurements, unlike measurement of impedance, do not recognise capacitance changes. A DC measurement circuit cannot handle slow capacitance changes without the use of a very high input impedance amplifier. DC measurement will also admit other unwanted disturbances such as cable noise, thermocouple

voltages, power frequency cross-talk, semiconductor 1/f noise and slow variation of component parameters [124].
Therefore measurements of the internal resistance of the cell do not correlate well with the SOH of the cell.

Using a conventional ohmmeter for measuring the resistance of the cables, contacts and inter-cell links is not satisfactory because the resistance is very low and the resistance of the instrument leads and the contacts causes significant errors. More accuracy can be achieved by using a Kelvin Bridge which separates the voltage measuring leads from the current source leads and thus avoids the error caused by the volt drop along the current source leads.

It is necessary to know the internal resistance of the cell in order to calculate the Joule heat generation or I^2R power loss in the cell; however a simple measurement with an ohmmeter is not possible because the current generated by the cell itself interferes with the measurement. To determine the internal resistance, first it is necessary to measure the open circuit voltage of the cell. Then a load should be connected across the cell causing a current to flow. This will reduce the cell voltage due to the IR voltage drop across the cell which corresponds to the cell's internal resistance. The cell voltage should then be measured again when the current is flowing. The resistance is calculated by ohms law from the voltage difference between the two measurements and the current which is flowing through the cell. Figure 7.6 illustrates this approach.

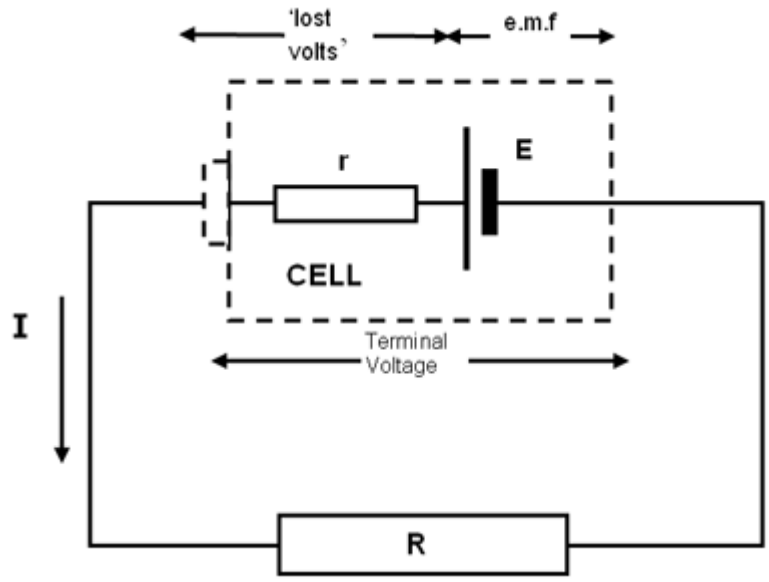

Figure 7.6 Measurement of cell resistance [125].

Commercial internal resistance test meters such as the example shown in figure 7.7 are widely available.

Figure 7.7: Internal resistance tester © Storage Battery Systems.

7.3.8 Open Circuit Voltage (OCV)

Voltage has traditionally been the means of determining battery health, given that a decline in cell voltage indicates that a battery is nearing the end of its service life.

However, degradation of the cell can take place that can be masked from a voltage only test. The test still commonly employed is a periodic discharge test. However, a battery can become faulty a matter of days following a routine discharge test. This is caused by chemical changes taking place in the cell brought about by the charge and discharge cycles. In addition, corrosion can occur in all of the connecting hardware of the battery string, internal to the cell or external.

Measuring a battery's open circuit voltage is not a reliable measure of its ability to deliver current. Battery voltage is a highly inaccurate indication of a batteries capacity, because it changes with temperature, discharge rates and aging [126]. As a battery ages, its internal resistance increases. This will reduce the battery's ability to accept and to hold charge, but the open circuit voltage will still appear normal despite the reduced capacity of the battery.

In 1963, Curtis Instruments pioneered gauges to monitor the state of charge of vehicle traction batteries. One of the methods used by Curtis involves predicting the remaining capacity of a battery by measuring the elapsed time period since the unloaded voltage dropped below a certain value [127].

7.3.9 Impedance and Conductance Testing

Measurement of battery impedance as a means of determining battery health is a fairly recent innovation. The source resistance or impedance of the cell is a good indicator of cell condition, indicating both chemical degradation as well as physical damage. Impedance testing can be used as a means of determining the condition of fuel cells.

A new method to measure the impedance of fuel cells connected to a constant load has been developed. This method is used to measure the impedance of a polymer electrolyte membrane fuel cell. It has been shown that membrane resistance measurements can be made by this new method [128].

Impedance testing involves excitation of the cell by an ac voltage of small amplitude, and evaluating the resistive and reactive components of the cell.

The test method involves applying a small AC voltage "E" of known frequency and amplitude across the cell and measuring the in phase AC current "I" that flows in response to it.

The Impedance "Z " is calculated by Ohm's Law to be Z=E/I

The Conductance "C" is similarly calculated as C=I/E (the reciprocal of the impedance)

The impedance increases as the battery deteriorates while the conductance decreases. Thus C correlates directly with the battery's ability to produce current whereas Z gives an inverse correlation. The conductance of the cell therefore provides an indirect approximation to the State of Health of the cell. This measurement can be refined by taking other factors into account. In addition to impedance and conductance these tests will obviously detect cell defects such as shorts, and open circuits.

These test methods can be used with different cell chemistries however different calibration factors must be built into the test equipment to take into account differences in the aging profiles of the different chemistries.

Impedance and conductance testing does not affect the battery performance. They can be carried out while the battery is in use or they can be used to continuously monitor the battery performance, avoiding the need for load testing or discharge testing. An example of impedance testing equipment is shown in figure 7.8

Figure 7.8: Battery Impedance test equipment. © Megger.

Conductance measurement has been applied to battery state of charge and state of health monitoring, an example being the Automotive "Smart" Battery tester with State of Health Conductance Testing and Monitoring Technology [129] shown in figure 7.9. This device measures voltage, temperature and conductance to determine the battery state-of-health. The manufacturer claims that this device could be integrated into a vehicle to provide battery state-of-health indication.

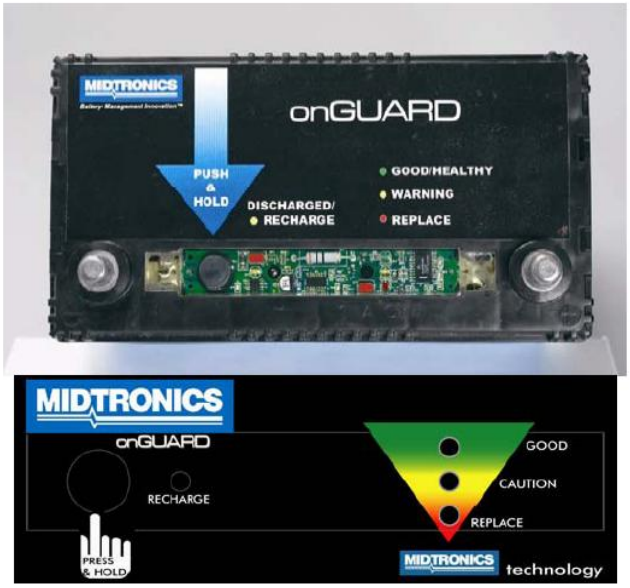

Figure 7.9: "Smart" battery state-of-health tester.

7.3.10 Book keeping systems

Book-keeping is a method of state of charge indication based on current measurement and integration, sometimes referred to as coulomb counting, which literally means counting the charge flowing into and out of the battery, or more likely to measured as a change of capacity in ampere-seconds or ampere-hours. The main problem with book-keeping systems is to define reliable calibration opportunities that occur enough during battery use.

7.3.11 Battery Analysers

Battery analysers are designed to provide a quick indication of the State of Health of the battery. Some analysers also have the dual function of reconditioning the battery. There are no industry standards for this equipment, mainly because there is no standard definition of State of Health. Each equipment manufacturer has their own way of defining and measuring it, from a simple conductance measurement to a weighted average of several measured parameters and the test equipment is designed to provide the corresponding answer. This should not be a problem if the same equipment is used consistently, however it does cause problems if equipment from different manufacturers is used to carry out the tests. The battery analyser shown in figure in7.10 can test batteries of up to 50 volts (1 kW) and has a price of $5450.

Figure 7.10: Battery analyser © MTI Corporation

7.4 Chapter Conclusions

This chapter has reviewed some of the methods used to determine electrochemical cell condition, and in particular battery condition. There is no single measurement which alone can be said to give reliable indication of cell condition, and even

proprietary systems measuring a number of parameters and using sometimes complex algorithms cannot give guaranteed accurate measurement of cell condition. However, with reference to table 7.1 there are no measurement methods which could be described as ideal.

Measurement of electrolyte pH is not currently used as an indication of battery condition, The author has used electrolyte pH measurement during discharge tests on lead acid batteries and has observed a pH disturbance which may be useful in indentifying cells which are about to reverse polarity. With reference to table 7.1 pH measurement is relatively cheap, can be online offering a possible solution for detection of cell reversal.

CHAPTER 8 BATTERY TESTING

After reviewing the various methods of assessing battery condition it was decided to investigate measurement of the electrolyte pH as means of determining battery condition for the following reasons:

1. Electrolyte pH is a function of concentration, and is therefore similar to specific gravity insofar as the state of charge could be indicated by measuring the pH of the electrolyte.
2. Continuous measurement of specific gravity is difficult to achieve in practice whereas pH can be monitored on a continuous basis offering the possibility of 'on line' monitoring of state of charge.

A programme of tests was undertaken on lead-acid batteries in order to investigate the variation of the pH of the electrolyte during the discharge of the battery under load. Initially the tests were undertaken using 6-cell, nominal 12 volt SLI batteries. The test programme then moved on to testing deep discharge Plantè-type cells. The theoretical variation of electrolyte pH with cell voltage generated by the author's battery model developed in Chapter 6 is shown in figure 8.1. The theory used to generate figure 8.1 is based on equations 4.47, 4.65, 6.32 and 6.44, which identifies relationships between ideal voltage, activity and pH.

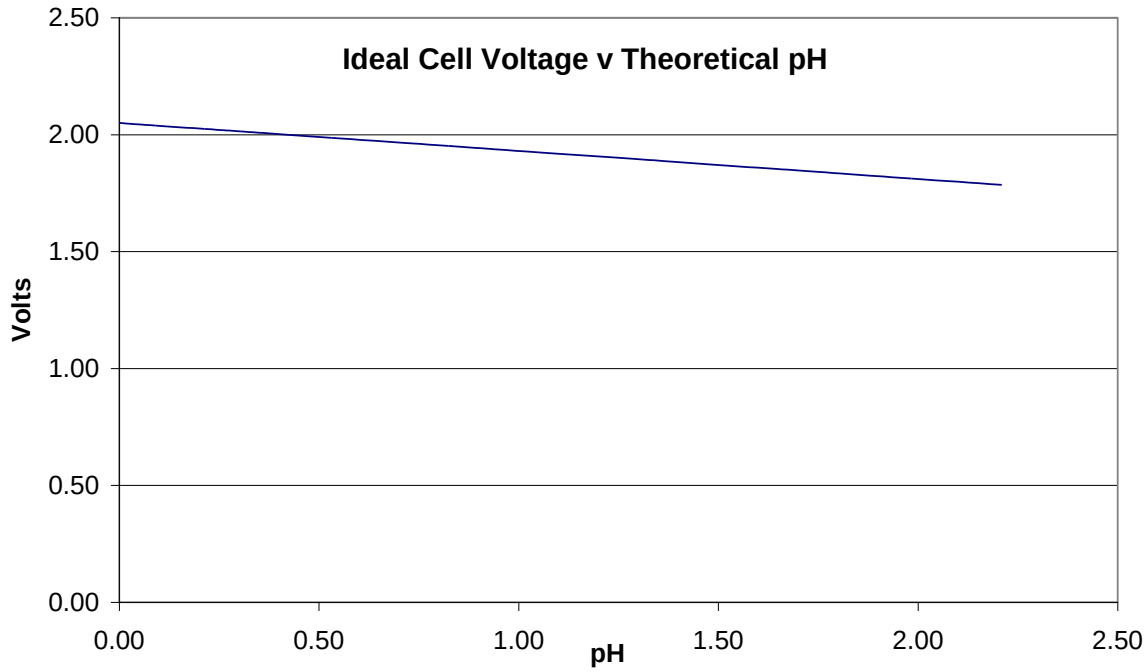

Figure 8.1: Variation of sulphuric acid electrolyte with ideal cell voltage.

The pH is determined using the Nernst equation as a basis, and is therefore determined under conditions of equilibrium when the net current flow is assumed to be zero. Under real conditions the relationship between pH and cell voltage cannot be determined theoretically, as the cell is not in a state of equilibrium when it is undergoing charging or discharging as the net current flow is not zero.

A series of discharge tests were undertaken to monitor the variation of electrolyte pH when a battery is under load. During the tests pH, cell voltage and current were all monitored.

Tests were carried out on single cells, in this case Plantè cells as shown in figure 8.2, and multiple cells, that is 6 cell automotive batteries.

8.1 Plantè Cells

Plantè cells are deep discharge cells designed for use in emergency and standby systems, from table 8.1 it can be seen that Plantè cells are designed to discharge to 1.70 volts under normal operation. In a 6 cell automotive battery this would

correspond to 10.2 volts, which is well below the nominal voltage of an automotive battery of 12.6 volts. The duty cycle of automotive batteries is of a different nature with long periods under float charge at approximately 13.8 volts from the charging circuit interspersed, with short durations of high discharge current during starting.

Figure 8.2: Plantè cell

Figure 8.2 shows the type of Plantè cell used in the tests. It is an Enersys YAP 5 cell rated at 15 Amp-hour capacity. Tables 8.1 and 8.2 show the manufacturer's data for discharge current and power versus time data for the YAP 5 cell.

YAP5
CONSTANT CURRENT DISCHARGE
(Amperes) at 20°C to 1.70 volts per cell

STANDBY TIME (Minutes)	Discharge Current (Amperes)
5	34.5
10	26.8
15	22.8
30	15.5
60	10
120	6.2
180	4.6
240	3.6
300	3
360	2.5
420	2.3
480	2
540	1.8
600	1.7

Table 8.1: Plantè cell current data.

YAP5
CONSTANT POWER DISCHARGE
(Watts per cell) at 20°C to 1.70 volts per cell

STANDBY TIME (Minutes)	Power (Watts)
5	61
10	47.4
15	40.2
30	28
60	18.2
120	11.4
180	8.6
240	6.7
300	5.6
360	4.8
420	4.3
480	3.8
540	3.5
600	3.2

Table 8.2: Plantè cell power data.

The discharge characteristic for the YAP5 cell based on the manufacturer's data from tables 8.1 and 8.2 is shown in figure 8.3, showing the time to discharge from a fully

charged condition to the minimum operating voltage of 1.7 volts at specified values of current.

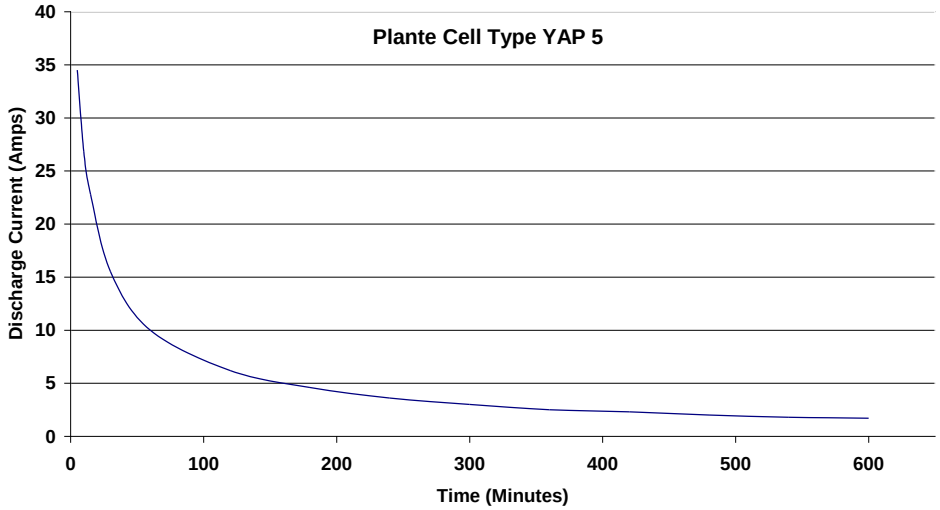

Figure 8.3: YAP5 Plantè cell discharge curve.

8.2 Test procedure

In order to determine the change in condition of a battery under test the author created a data-logging programme using National Instruments LabVIEW © software. This software can be used to develop "Virtual Instrumentation" or VIs, reducing the amount of hardware required in data acquisition, monitoring and control applications.

A battery under test had its voltage and current monitored and recorded continuously by the LabVIEW programme. The LabVIEW programming environment is controlled via a front panel shown in figure 8.4. The software displays and records the battery voltage, current and electrolyte pH.

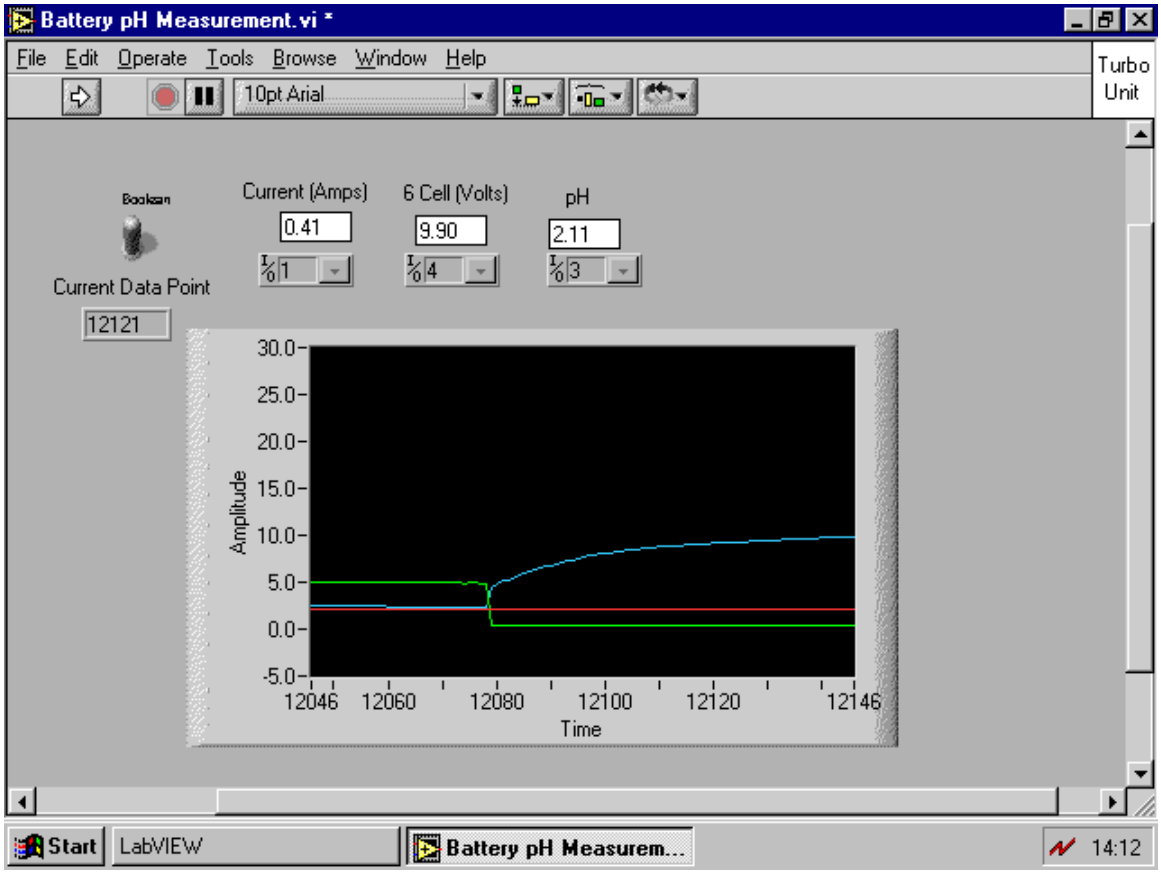

Figure 8.4: Author's LabVIEW© Front panel for pH testing.

The front panel has indicators for each of the measurements, that is voltage and current, and the variation of each of the measurements can be plotted on a chart, while the test is in progress.

The block diagram, which is only used in the development of the application VI, is shown in Figure 8.5

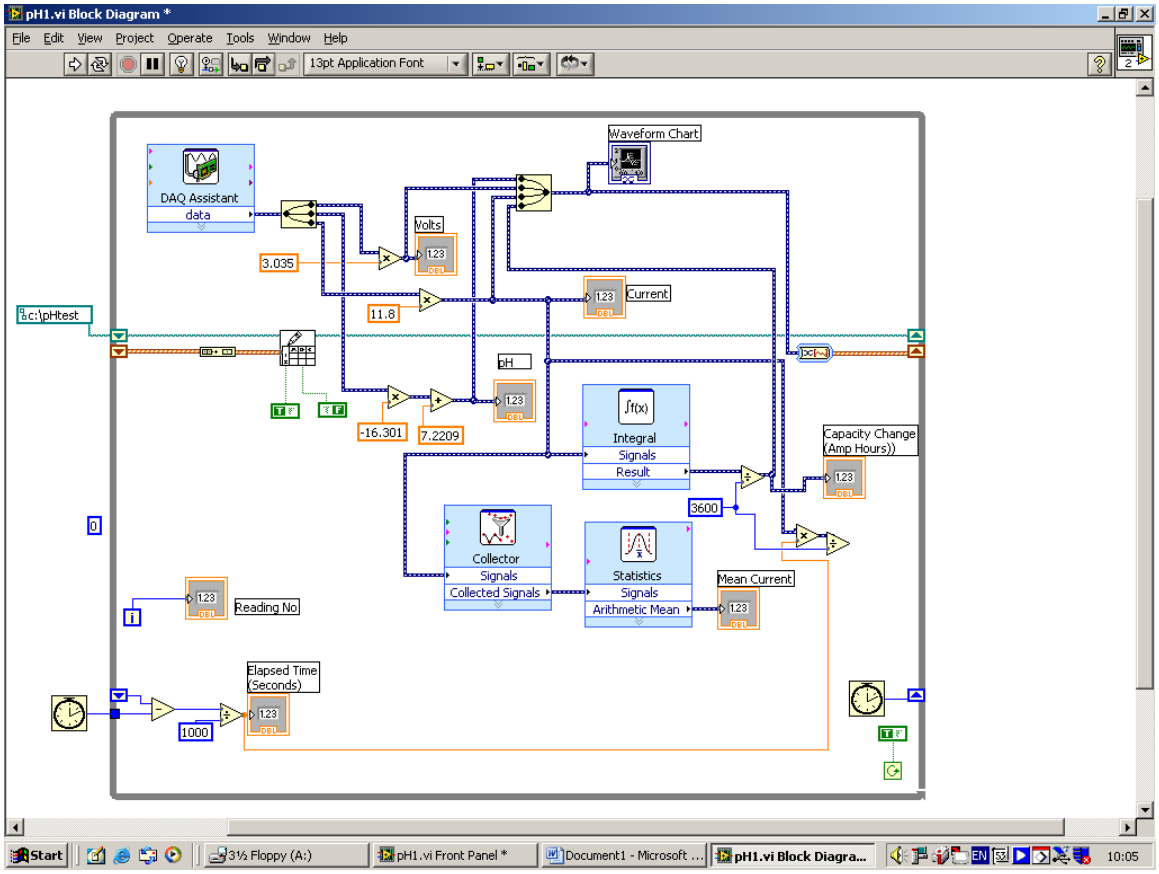

Figure 8.5: Author's LabVIEW© Block diagram.

The block diagram in figure 8.5 shows the interconnection of the various blocks, which form the elements of the LabVIEW© programme structure, which is based on conventional programming methods, the outer frame of the programme representing a "while loop", whilst the various measurement blocks (or subroutines) are nested inside the loop, in the same way as conventional programming structures.

This LabVIEW© programme acts as a data logger, with the data being stored in a text file format which can be downloaded into a spreadsheet, for subsequent analysis of the test data. Figure 8.6 shows data from a typical discharge test on a Plantè cell.

The test period is dependent on the rate of discharge, higher rates of discharge reduce the test period, while lower currents, will extend the test period. Test data such as

that obtained from the test shown in figure 7.5 can be analysed to determine other parameters such as the change in battery capacity during the discharge test.

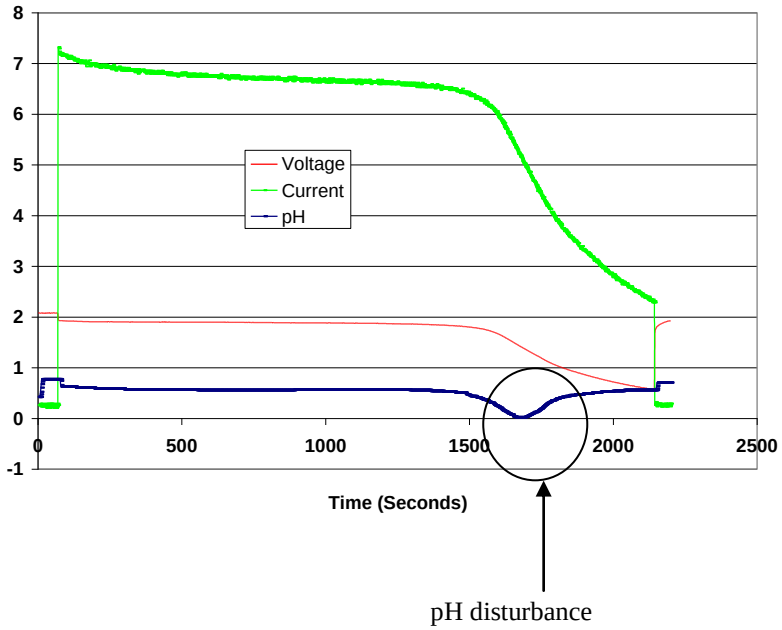

Figure 8.6: Plantè cell discharge test showing pH disturbance, showing cell voltage (Volts), discharges current (Amps) and electrolyte pH.

Figure 8.6 shows the results of a discharge test on a Plantè cell. In this test the voltage, current and electrolyte pH have been recorded during discharge, and a 'disturbance' in the pH can be clearly seen around 1700 seconds. This disturbance is further discussed in Chapter 9. The current trace shows an offset from zero this due to an inherent offset in the current transducer of 0.3 amps, as there was no facility for calibrating the transducer, although suppression of the zero could be easily achieved by manipulation of the LabVIEW © programme if required.

The pH measurements were recorded using a pH meter connected to a pH probe. The reading could be displayed either directly as a pH measurement or as a milli-volt signal equivalent as shown in figure 8.7.

Figure 8.7: one of the pH meters used in experimental work.

Figure 8.7 shows one of the pH meters used in the test work, a second pH meter can be seen in the left hand side of figure 8.8 which shows the battery test facility. A 6-cell automotive SLI battery can be seen next to a wooden crate which contains a Plantè cell undergoing a discharge test. The two 12 volt vehicle light units were used as loads to discharge the SLI batteries, whereas wire-wound resistors were used to discharge the Plantè cells.

Frequent checks were made on the test instrumentation, in particular different pH meters were used to ensure that the values of pH being measured were correct, and frequent calibration checks were made using buffers solution to ensure the accuracy of the pH meters.

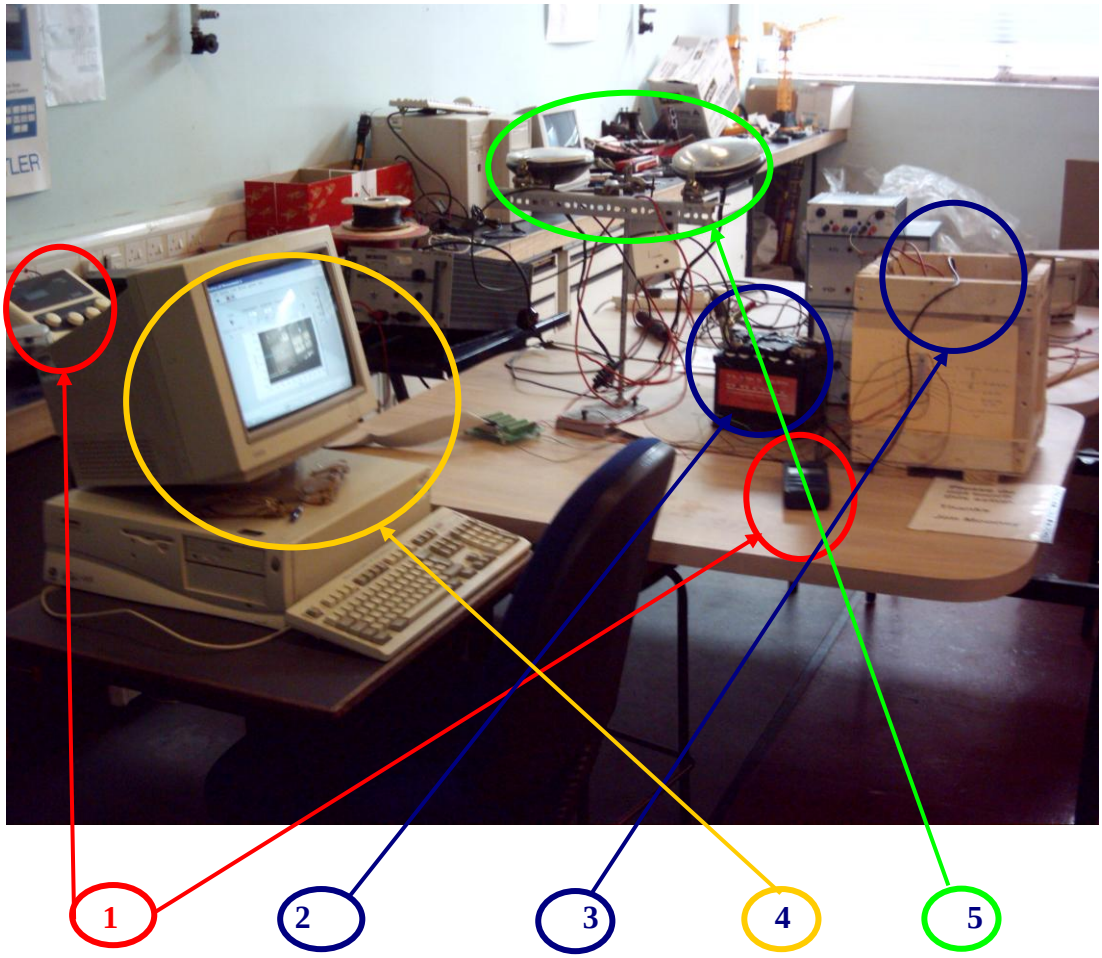

1. pH meters.
2. SLI battery.
3. Plantè cell inside protective wooden crate.
4. PC with LabVIEW© software for monitoring tests and recording data.
5. Lights used as load on SLI battery.

Figure 8.8: Elements of battery testing facility.

The specific gravity of the electrolyte solution was checked at the beginning and end of each discharge tests. This was a fairly cumbersome procedure to try to obtain an accurate measurement of the sulphuric acid specific gravity change over each test. Hydrometers covering the range 1.100 to 1.300 were used to measure the specific gravity, one hydrometer covering the range 1.100 to 1.200, the other 1.200 to 1.300.

It was necessary to siphon the electrolyte from the cell and drain sufficient electrolyte into a measuring cylinder in order for the hydrometer to float. The siphoning procedure is shown in figure 8.9.

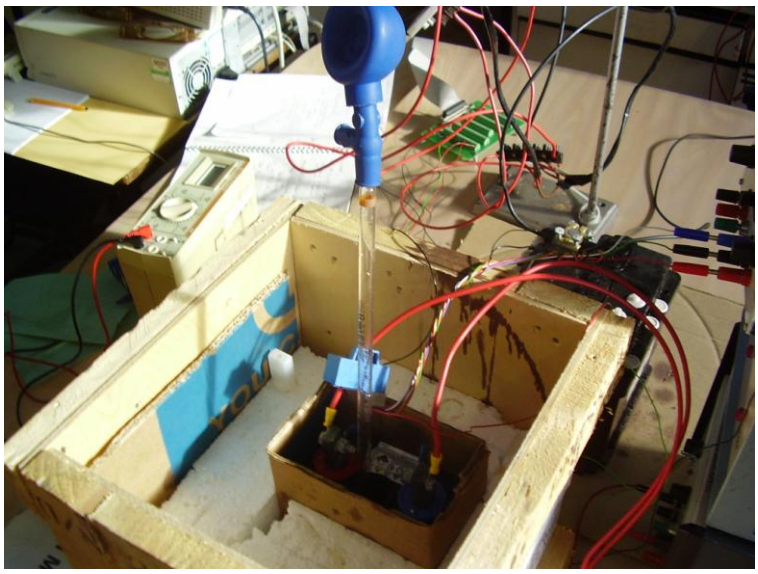

Figure 8.9: Siphoning sulphuric acid electrolyte from a Plantè cell.

One side effect of this procedure was to disturb the electrolyte which should reduce any effects of stratification in the cell; following each test the cells were tilted as far as possible to try to mix the electrolyte and prevent stratification occurring. Figure 8.10 shows the measuring cylinder with the hydrometer floating in the electrolyte which has been siphoned from the battery enabling a specific gravity reading to be taken.

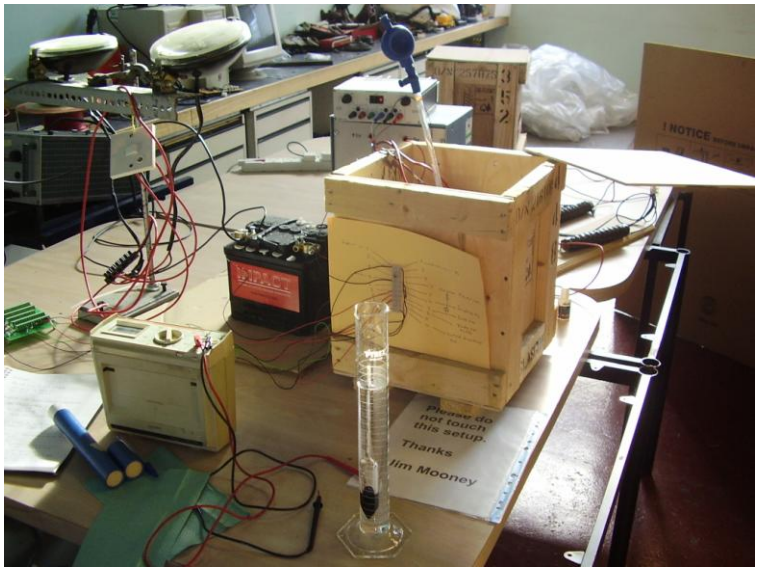

Figure 8.10: Measuring sulphuric acid electrolyte specific gravity.

Figure 8.11: Hydrometer floating in sulphuric acid electrolyte.

Figure 8.11 clearly shows the hydrometer floating in the sulphuric acid electrolyte.

The results of the battery test are discussed in Chapter 9. One of the problems encountered during this testing was the length of time taken to recharge the batteries following the discharge tests, as the batteries were subjected to very deep discharges extending well beyond the normal cut-off voltages. This deep discharge was required to investigate the disturbance in the electrolyte pH which occurred at cell voltages below 1.4 volts.

As a result prolonged periods of charging were required to bring the batteries back to a fully charged state, and consequently limited charging data is presented in this thesis.

The battery testing environment was stable in terms of ambient temperature during the testing period, with the ambient temperature being between 19 and 21^{o}C and the relative humidity in the range 50 to 60%.

8.3 Chapter Conclusions

This chapter has discussed the experimental work undertaken on lead-acid batteries as part of this thesis. Monitoring of the battery tests was achieved using same the LabVIEW © software described in chapter 5, with a different VI being written for monitoring and logging the battery test data. Tests were carried out on single cell Plantè cells as well as six cell SLI batteries at different loads.

CHAPTER 9 DISCUSSION OF BATTERY TEST RESULTS

A series of discharge tests were carried out on two main types of battery.

1. SLI automotive 6 cell batteries
2. Plantè cell used for stationary applications.

The initial series of discharge tests were carried out on aged SLI batteries with a typical test result as shown in figure 9.1. The remaining figures, that is figures 9.2 to 9.11 relate to a Plantè cell.

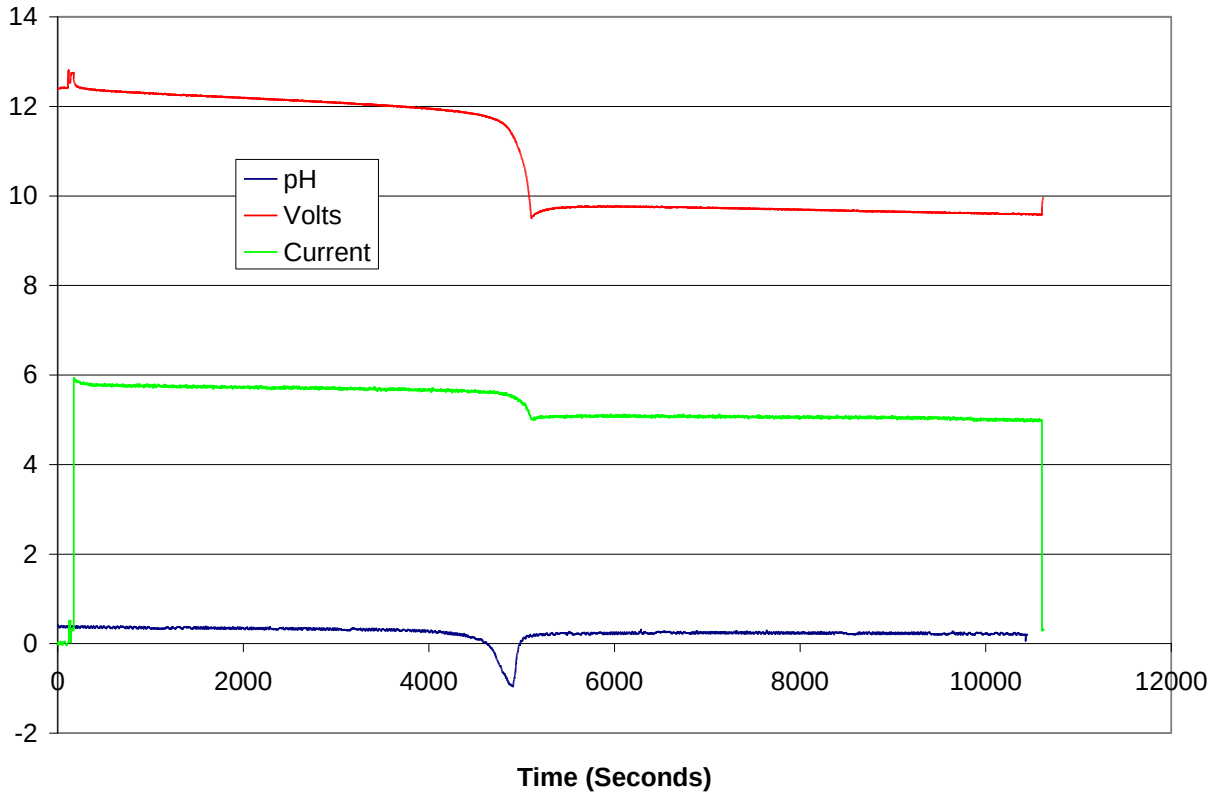

Figure 9.1: Discharge test on SLI battery, showing battery voltage (Volts), discharge current (Amps), and electrolyte pH.

The 3 parameters measured in the discharge test of figure 9.1 were:

1. Battery voltage (Volts).
2. Discharge current (Amps)
3. pH

It had been decided to investigate the possibility of using pH as an indication of battery state of charge, a review of literature revealed that some work had previously been done in this area. The concept of using pH as means of state of charge (SOC) measurement has been reported by Bayoumy et al [130] in a photovoltaic hybrid power system. It was then decided to investigate if this could be applied to batteries in a hybrid electric vehicle.

A pH probe was inserted into one of the 6 cells in the SLI battery and the pH was measured as the battery was being discharged by an external load using the test equipment shown in figure 8.8.

Tests were carried out on both aged and new SLI batteries, and further tests were also carried out on Plantè cells. The pH data returned from these tests had a notable feature in that there was a clearly discernable disturbance in the pH reading during the discharge test.

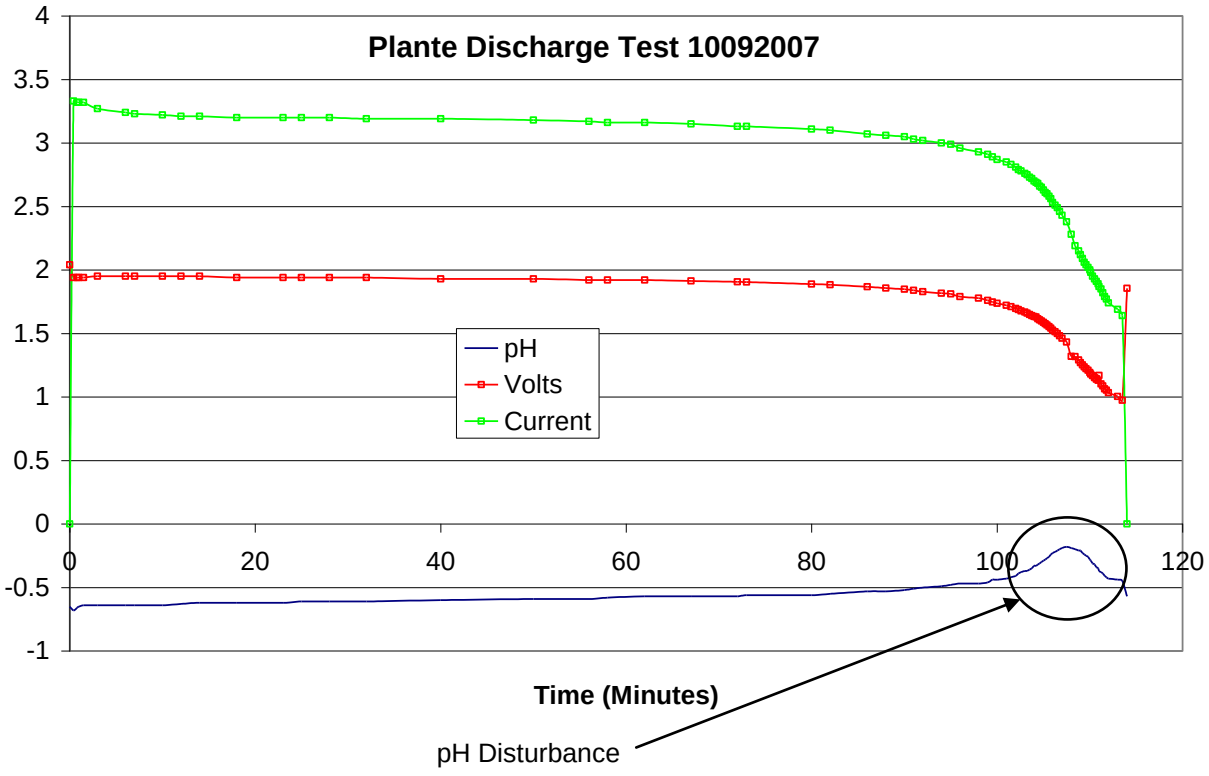

Figure 9.2: Discharge test of a Plantè cell in a 'new' condition, showing cell voltage (Volts) discharge current (Amps) and electrolyte pH with pH disturbance.

Figure 9.2 shows the results of a discharge test on a Plantè cell in a 'new' condition, the pH of the electrolyte is decreasing as the cell discharges until at about 100 minutes into the discharge the pH disturbance takes place, with 13.98 Amp-hours capacity having been discharged out of rated capacity of 15 Amp-hours at point at which the pH is at a maximum value of -0.18 pH.

It was observed that in the case of a cell in a 'new condition' the pH disturbance is characterised by an accelerated decrease in pH, followed by a decrease in pH. However, as the battery became aged as a result of repeated charge/discharge cycles it was observed that the nature of the pH disturbance changed, and in fact became the inverse of the case for a new battery. This is shown in figure 9.3 at about 1500 seconds (25 minutes) into the discharge test, notice that the capacity of the cell is reduced as indicated by the time duration of the test which is about one third of the test of figure 9.2 the 'new' condition and with 3.42 Amp-hours capacity having been discharged out of rated capacity of 15 Amp-hours at point at which the pH is at a minimum value of 0.23 pH.

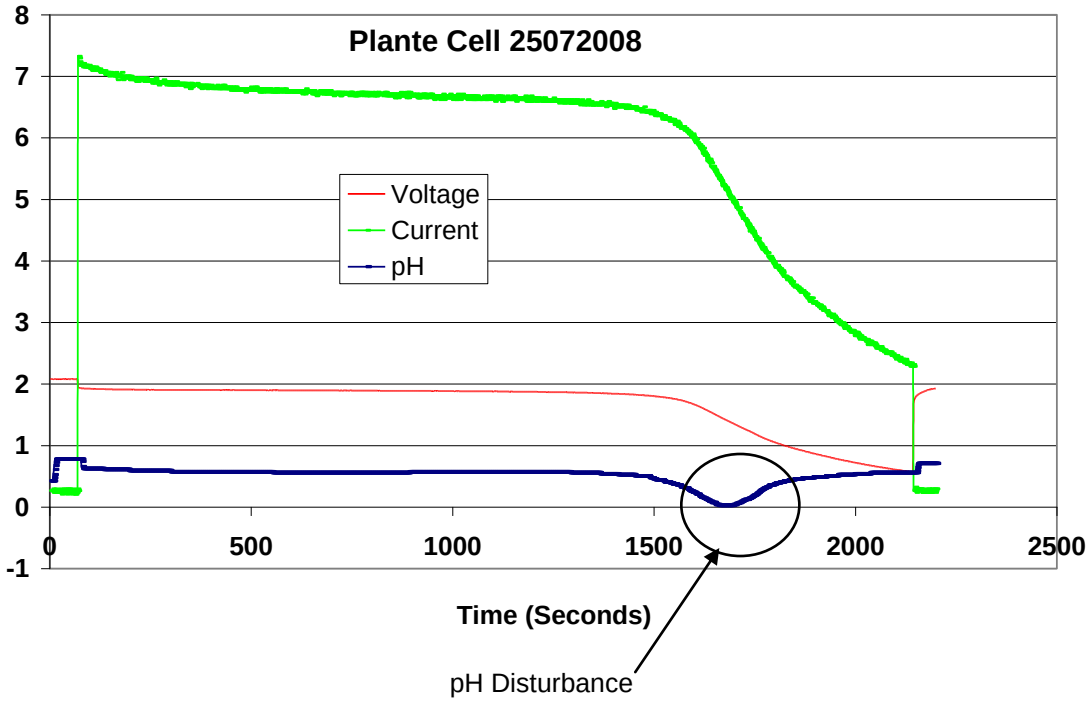

Figure 9.3: Discharge test of a Plantè cell in a 'aged' condition, showing cell voltage (Volts) discharge current (Amps) and electrolyte pH with pH disturbance.

At this point this cell had undergone repeated over-discharge testing that is discharging below the recommended cut-off or lower limit voltage of 1.70 volts, and had also been driven into polarity reversal as discussed later in this chapter therefore the cell had been aged significantly with a resulting decrease in cell capacity.

A further aspect of the pH disturbance noted during analysis of the results of the discharge test was that the magnitude of the pH disturbance increased as the discharge current increased as evidenced by figures 9.4, 9.5 and 9.6.

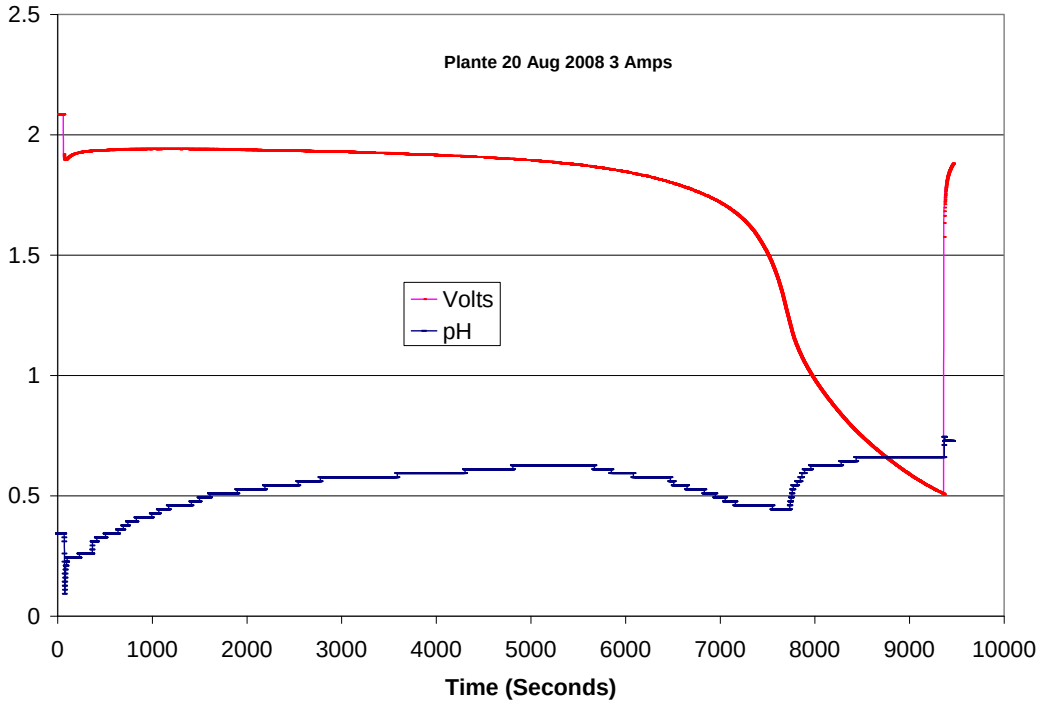

Figure 9.4: Plantè cell discharged at nominal current of 3 amps, showing cell voltage (Volts) and electrolyte pH.

The results of the tests carried out on lead acid batteries during the experimental work of this thesis are identified the following points:

1. The occurrence of a disturbance in the measured value of the pH of the sulphuric acid electrolyte.

2. The magnitude of the pH disturbance increased as the discharge current increased.
3. The direction of the pH disturbance changed as the cell aged.
4. The mean value of the pH increased as the cell aged.

The following figures illustrate the points made in 1 to 4 above.

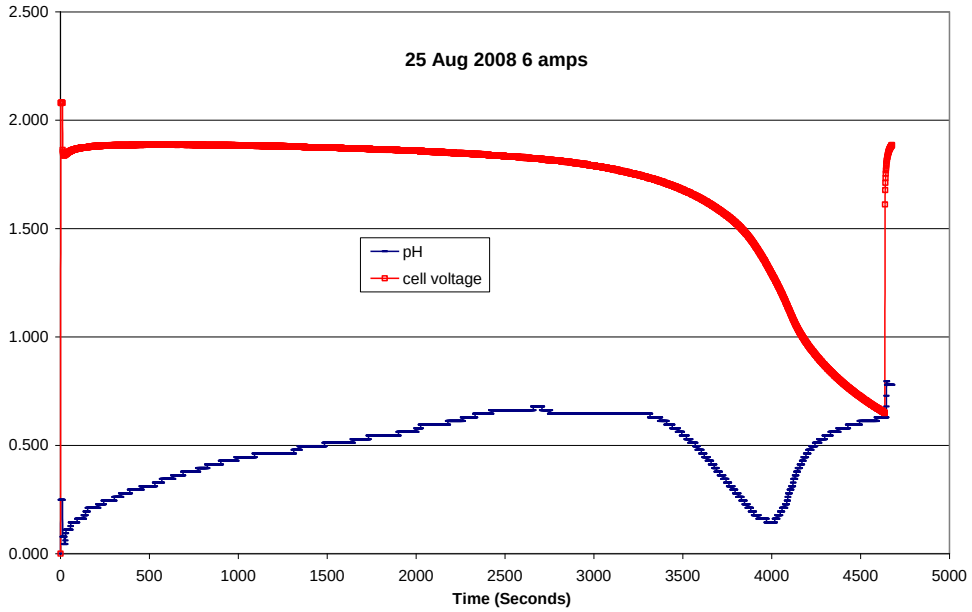

Figure 9.5: Plantè cell discharged at nominal current of 6 amps, showing cell voltage (Volts) and electrolyte pH.

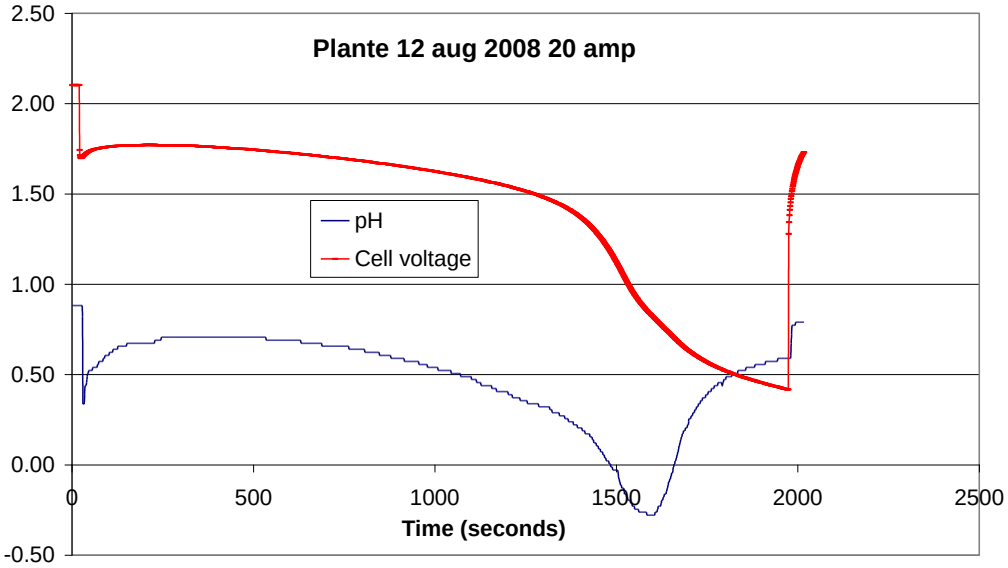

Figure 9.6: Plantè cell discharged at nominal current of 20 amps, showing cell voltage (Volts) and electrolyte pH.

The effect of cell aging can be seen in figure 9.7, where the mean value of pH increases with the age of the cell.

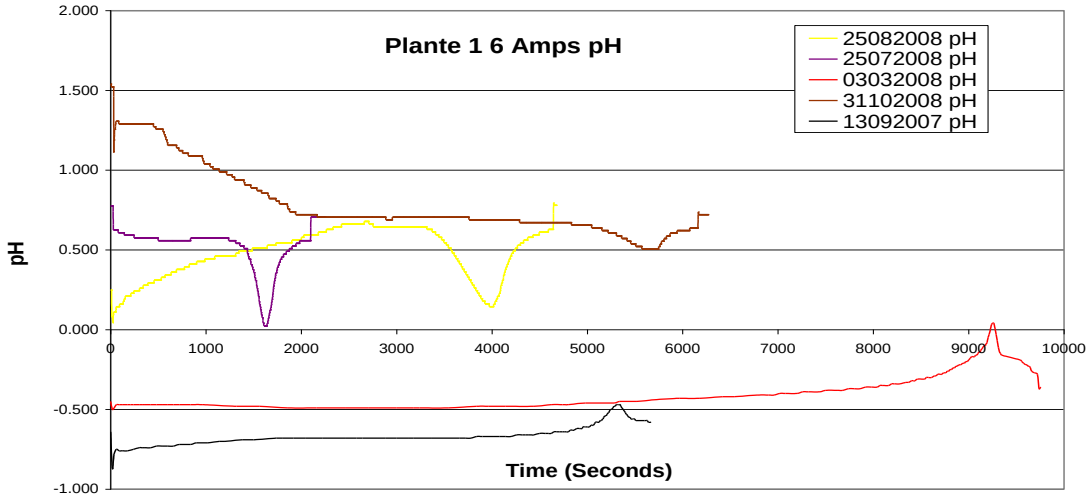

Figure 9.7: Variation of pH with cell age, showing the change in the nature of the pH disturbance.

Figure 9.7 show two points of interest.

1. The pH disturbance changing from a disturbance where the pH temporarily decreases (new cell), to a temporarily decreasing pH (aged cell).
2. The mean value of ph increases as the cell ages.

Figure 9.8 shows the relationship between discharge current and magnitude of the pH disturbance.

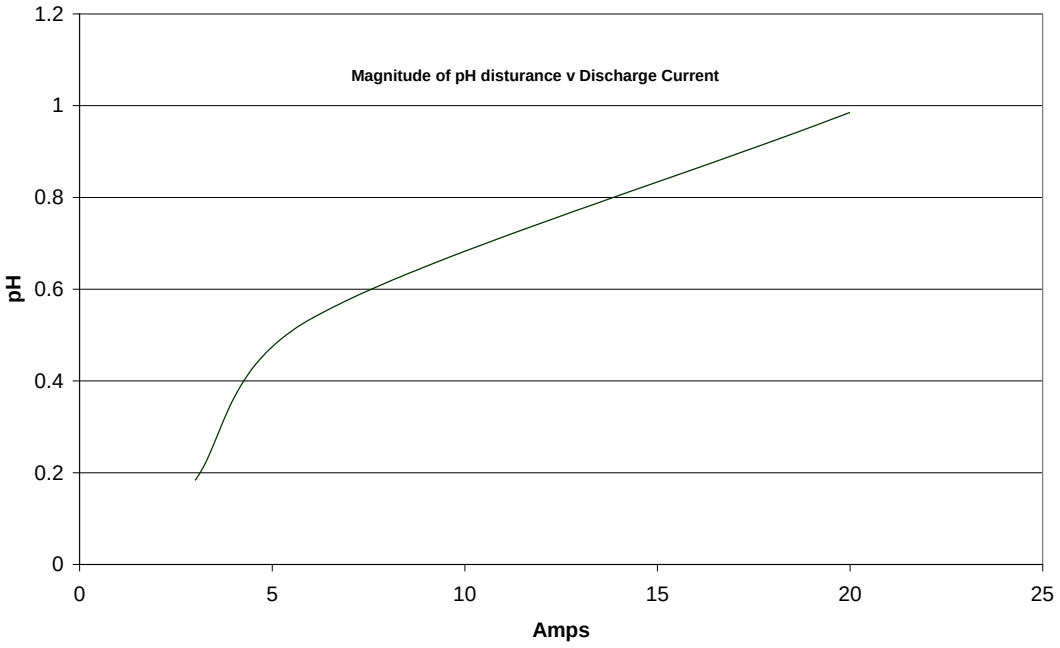

Figure 9.8: Discharge current (Amps) plotted against magnitude of the pH disturbance.

As mentioned above, in addition to over-discharge testing, the Plantè cells were driven into reverse polarity. This was achieved by connecting a Plantè cell electrically in series with a SLI battery, effectively resulting in a 7 cell battery. The Plantè cell was connected to the SLI battery to give it the highest potential with respect to zero volts. It was arranged such that the SLI battery was fully charged, however, the Plantè cell was deliberately not fully charged in order to ensure that it would the 'weakest' cell of the 7 cell in series.

The combined Plantè-SLI battery was then discharged and the discharge was continued until the Plantè cell was driven into reversal. The results of one of these tests are shown in figure 9.9.

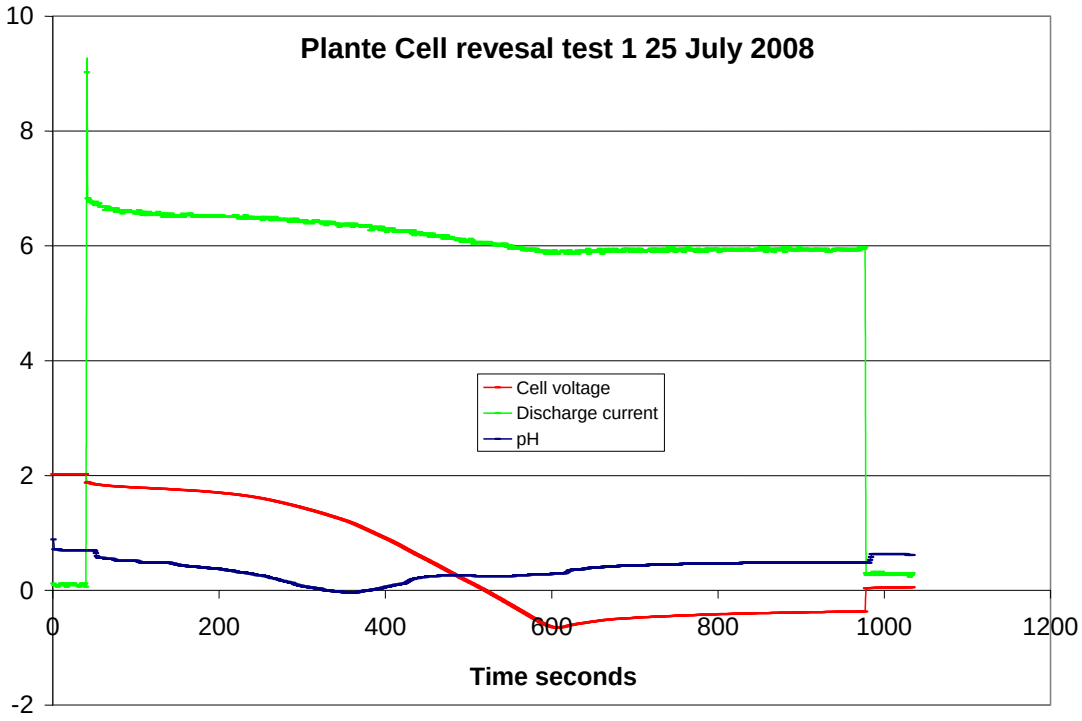

Figure 9.9: Plantè cell reversal test, showing cell voltage (Volts), discharge current (Amps) and electrolyte pH.

Figure 9.9 shows the pH disturbance at about 300 seconds into the discharge test, with the cell going into reverse polarity at about 500 seconds. It can be seen therefore that the Plantè cell is in fact considerably 'weaker' with the pH disturbance occurring at approximately 300 seconds into the discharge test, compared to figure 9.5, where the pH disturbance occurs at 4000 seconds.
It therefore seems that the pH disturbance could possibly be used as an indication of impending reversal of a cell within a battery pack.

The above discussion relates only to discharging. Some investigation of the pH of a battery undergoing charging was carried out, and theory predicts that the pH should decrease as the cell is charged. This was in fact found to be the case as a number of charging tests were undertaken. No pH disturbance was noted during the charging tests, and results of some of the charging tests are shown in figures 9.10 and 9.11.

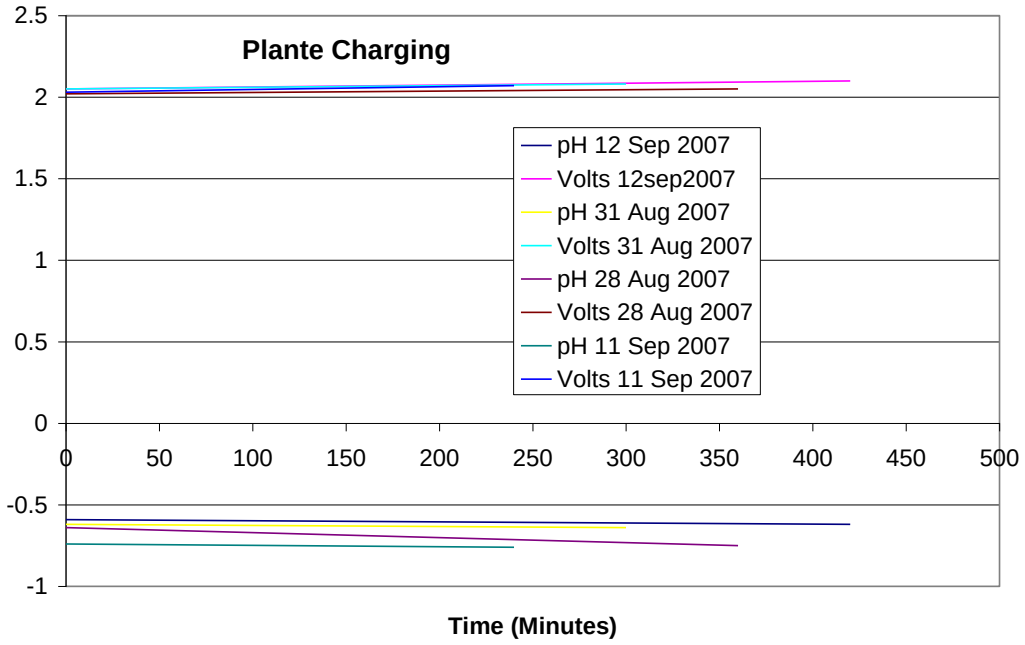

Figure 9.10: Plantè cell charging tests, showing cell voltage (Volts) and electrolyte pH.

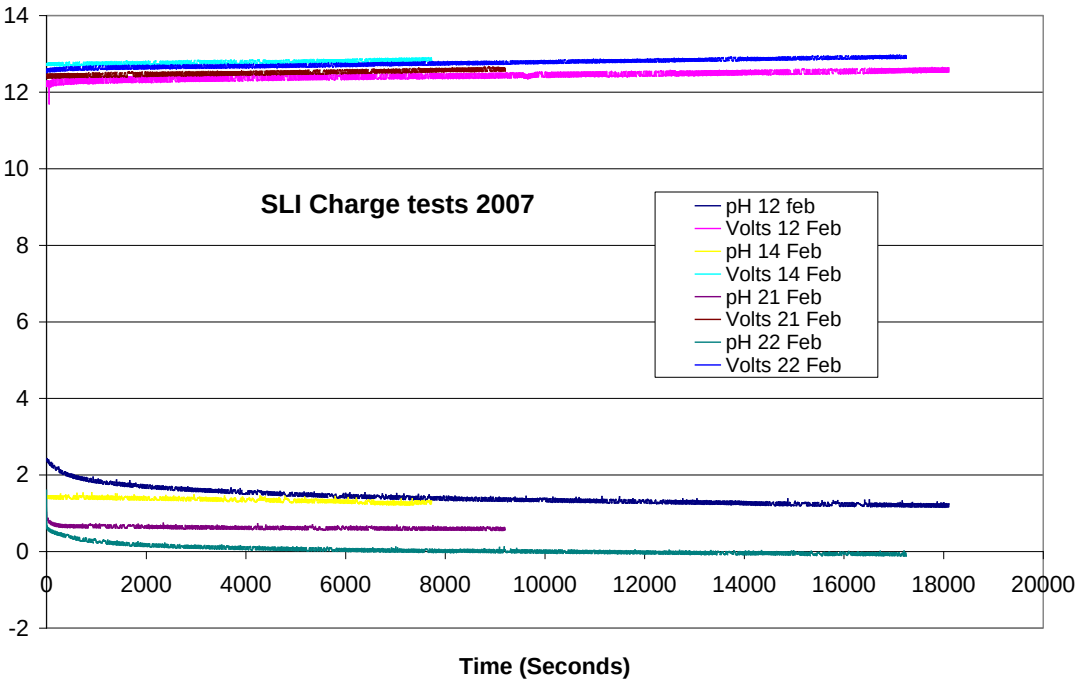

Figure 9.11: SLI battery charging tests, showing cell voltage (Volts) and electrolyte pH.

9.1 Chapter Conclusions

This chapter has discussed the results obtained from discharge tests carried out on single cell Plantè and six cell SLI batteries.

As results of the tests carried out on lead acid batteries during the experimental work of this thesis a phenomenon was discovered and is characterised the following:

1. The occurrence of a disturbance in the measured value of the pH of the sulphuric acid electrolyte.
2. The magnitude of the pH disturbance increased as the discharge current increased.
3. The direction of the pH disturbance changed as the cell aged.
4. The mean value of the pH increased as the cell aged.

Therefore during the process of undertaking these discharge tests the author has identified a new pH disturbance previously unreported and the author claims the discovery of this effect.

In particular the nature of the pH disturbance changes due to:

1. The age or state-of-health of the battery
2. The discharge current.

The effect was apparent in the discharge tests but not during subsequent charging of the batteries. An explanation of this pH disturbance is given in Chapter 10.

CHAPTER 10 EXPLANATION OF THE PH DISTURBANCE.

During testing of the batteries the author observed that as the battery discharged there was a noticeable disturbance in the measured value of pH of the electrolyte toward the end of the discharge test. This "pH disturbance" is highlighted in figure 10.1. Also visible in figure 10.1 is an effect known as the Coup de fouet.

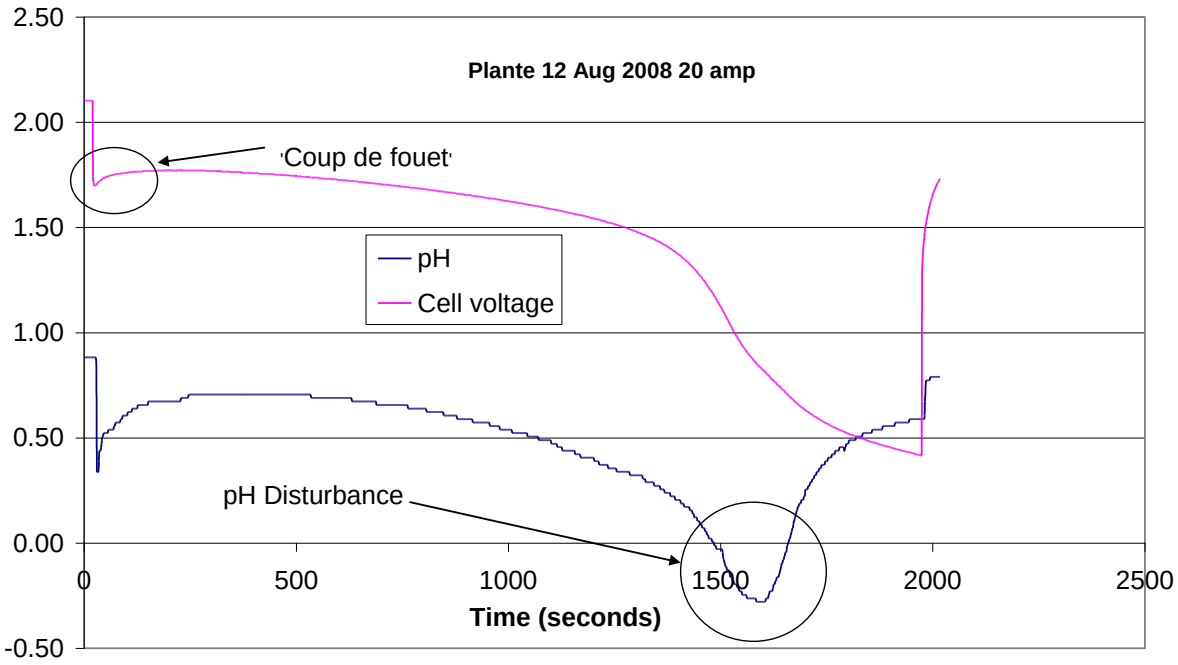

Figure 10.1: Discharge test of a Plantè Cell, showing cell voltage (Volts) and electrolyte pH with pH disturbance.

On examining the results of the discharge tests it was found that certain patterns emerged from the test results:

1. A pH disturbance occurs at a point below the normal operating voltage range (below the cut-off voltage of 1.70 volts).
2. The pH disturbance occurs when approximately 90% of the cell capacity has been discharged.
3. The pH disturbance coincides with an increase in internal resistance and a decrease in the rate of charge output.

4. The nature of the pH disturbance changed as the cell aged.

The pH disturbance occurs beyond what would be considered to be the normal operating range of the battery cell that is below the cut-off voltage. It occurs at a point where the cell voltage and current are declining at a higher rate than during the normal operating range of the battery, which for an automotive battery is 12.7 to 11.8 volts and for a Plantè cell is 2.05 to 1.70 volts. This pH disturbance occurred in all of batteries tested.

The science of lead-acid cells, even 150 years after Gaston Plantè demonstrated the first lead-acid cell, is still not completely understood. Many facets of the operational characteristics of the lead-acid cell have not been explained, an example being the so-called 'Coup de fouet' [131], a phenomenon which occurs at the beginning of a discharge as shown in figure 10.1. A number of explanations have been offered for this phenomenon, but as yet cannot be fully verified.

The pH disturbance discussed in this chapter is similar to the 'Coup de fouet' insofar as it has been demonstrated with repeatability. The remainder of this chapter offers an explanation of the pH disturbance based on the observations of the author during the experimental work and subsequent analysis of the results, and more importantly appears to support a theoretical explanation found in the published work of other researchers in the field of lead-acid cells.

10.1 Explanations for the occurrence of the pH Disturbance.

As the cell discharges the reaction between the electrolyte and the electrodes is generally accepted as being represented by the equation:

$$Pb(s) + PbO_2(s) + 2H_2SO_4(aq) \rightarrow 2PbSO_4 + 2\,H_2O(l) \qquad 10.1$$

The active materials in the cell include the positive and negative electrodes and the electrolyte. As the cell is charged and discharged the active materials undergo changes which affect the performance of the cell.

The nominal equilibrium voltage of a lead-acid cell amounts to E_0 = 2.04 V, given the difference between the equilibrium values of the electrode reactions

$E_{0,PbSO_4/PbO_2}$ = + 1.68 V and $E_{0,Pb/PbSO_4}$ = -0.36 V (which to some extent depends on acid concentration).

It is important to mention that the theory relating to the following explanations is based on equilibrium conditions. When a cell is connected to an external load, as is the case in these tests, the test conditions are non-equilibrium. Based on the Nernst equation the lead-acid cell equilibrium voltage E_o, varies from approximately 2.04 volts in a fully charged condition, to 1.7 volts in a fully discharged condition. This is evident from the range of tests carried out during the experimental work of this thesis, where following disconnection of the external load the cell voltage recovered to approximately equilibrium values.

However, if a cell is left unused over a period of weeks or longer, internal discharge, corrosion and other effects will gradually reduce the cell voltage to the point where even prolonged periods of charging will not recover the cell to a useable condition.

Furthermore the values of pH recorded are determined by the activity of the H^+ ions in the electrolyte solution. As the electrochemical cell electrolyte is a solution of approximately 66% water and 34% sulphuric acid, which is in a non-equilibrium state during test, the values of pH obtained during the discharge tests will not equal the values of pH for an equivalent solution of acid solution in isolation from the electrochemical environment of the cell. Therefore it is the trend of the pH measurements which is of interest as opposed to the absolute recorded values of pH.

In terms of the processes taking place in the electrochemical cell apart from the main reactions there are secondary reactions that occur at electrode potentials within the cell voltage, e.g. water decomposition according to:

Oxygen evolution occurs at the positive (Lead dioxide) electrode at an electrode potential above 1.23 V, which is about 0.5 V below the positive electrode potential.

$$2H_2O \Rightarrow O_2 \uparrow + 4H^+ + 4e^- \qquad 10.2$$

Hydrogen evolution occurs at an electrode potential below 0 V which is about 0.3 V above the open circuit voltage of the negative electrode.

$$4H^+ + 4e^- \Rightarrow 2H_2 \uparrow \qquad 10.3$$

Oxygen reduction, as the reversal of oxygen evolution is possible below 1.23 V.

$$O_2 + 4H^+ + 4e^- \Rightarrow 2H_2O \qquad 10.4$$

10.2 Explanation of the pH disturbance in a new cell

It was noted during the experimental work that when the battery was new the pH disturbance was characterised by a reduction in pH followed by an increase as shown in figure 10.2.

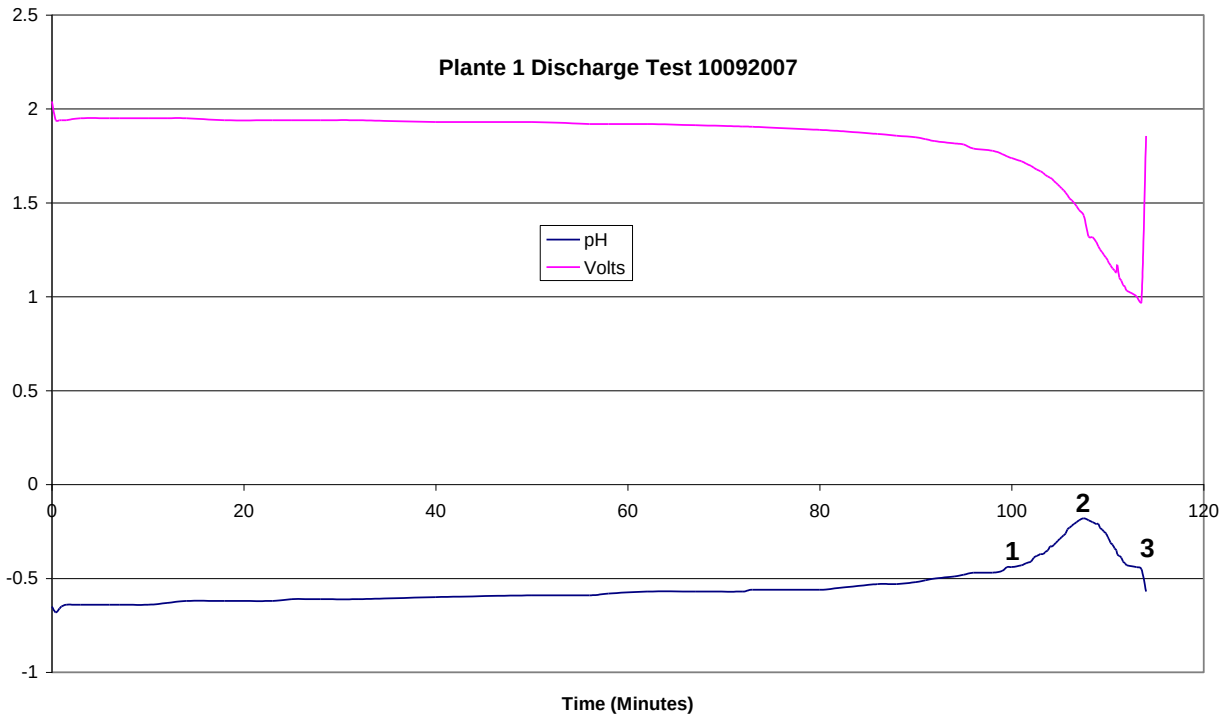

Figure 10.2: Discharge characteristic of a new Plantè cell, showing cell voltage (Volts) and electrolyte pH with pH disturbance.

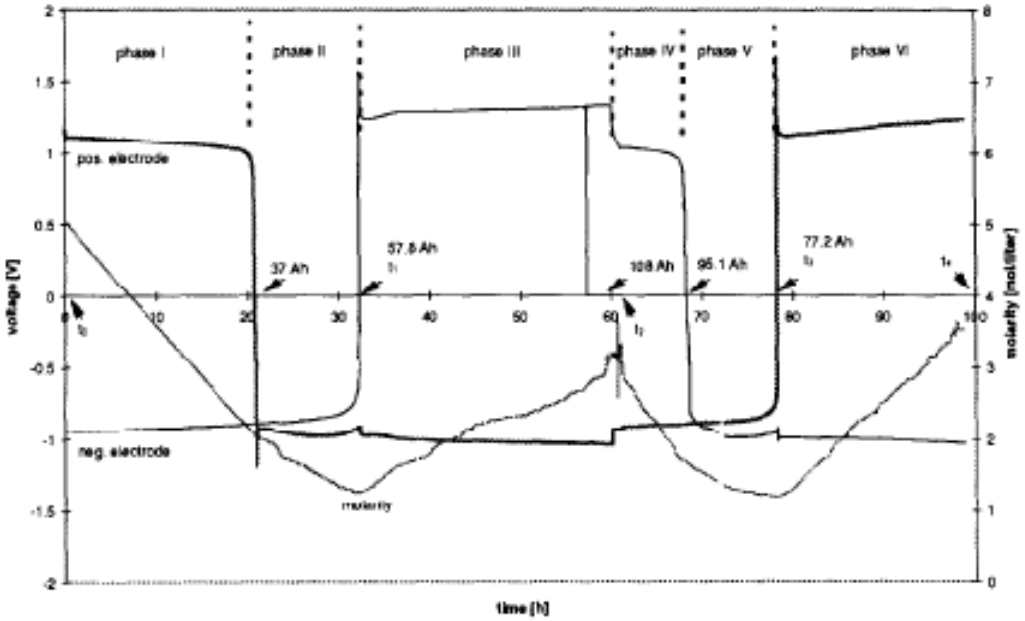

Fig. 11. Sulfuric acid concentration and electrode potentials during the overcharge experiment.

Figure 10.3: Sulphuric acid concentration and electrode potentials during over-discharge experiment battery ‘b’ (new) [103].

As reported by Pavlov [132] the positive electrode is considered to be limiting the battery capacity when the cell is new, that is as shown in figure 10.3, which shows the positive electrode going into reverse polarity at approximately 20 hours, followed by the negative electrode some 10 hours later.

The influence of the electrolyte concentration is important in a new battery, and it has been established experimentally that the electrochemical activity of the $PbO_2/PbSO_4$ electrode depends on the concentration of the HSO_4^- ions in the solution. As the cell discharges the concentration of the electrolyte decreases and the performance of the positive electrode deteriorates as the acid concentration enters the passive low concentration region where the concentration of HSO_4^- ions in the solution decreases at the expense of the formation of SO_4^{2-} ions. Furthermore the activity of the Lead-dioxide decreases due to changes in the morphology of the Lead dioxide electrode as the electrolyte concentration decreases below 0.5 M [164].

The condition of the cell at the **point 1** on figure 10.2 is within the region referred to by Pavlov et al as the "Passive low concentration region", where the bulk electrolyte concentration is below 0.5 M and the morphology of the lead dioxide (PbO_2) is α-PbO_2, which is the less active form of the two forms of PbO_2.

Furthermore the tests on a new battery, referred to as battery "b" by Garche et al [97] (Figure 10.3) indicates that it is the potential of the positive electrode which reduces first, therefore assuming that the negative electrode has not reversed polarity, the positive electrode potential must have been reduced proportionally by a greater amount, in this case to approximately 1.2 volts, that is at the point at which the pH disturbance occurs.

It is worth pointing out that in the tests carried out by Garche [97] the cell shown in figure 10.3 was driven into reverse polarity and the change in polarity of the positive electrode is clearly demonstrated in figure10.3 at about 20 hours into the test, with the negative electrode reversing polarity at approximately 33 hours, further demonstrating that in a new battery the limiting factor in the positive electrode and supporting the findings of Pavlov. Therefore is seems appropriate to focus initially on the positive electrode.

Note that in the case of the discharge test of figure 10.2; unlike the test of 10.3 carried out by Garche [97], the positive electrode does not reverse as the lowest possible cell potential is zero volts.

According to Garche [97] during cell discharge the main reaction at the positive electrode is given in 10.5:

$$2PbO_2 + 4H^+ + SO_4^{2-} + 2e^- \rightarrow PbSO_4 \left[PbO_2\right] + 2H_2O \qquad 10.5$$

At the end of the discharge the lead sulphate will block further discharge of PbO_2, and the remaining PbO_2 $\left[PbO_2\right]$ will be electrochemically inactive i.e. $PbsO_4$ $\left[PbO_2\right]$ lead sulphate and inactive lead dioxide is formed and the potential will fall.

Note: [ ] = inactive for example PbO_2 $\left[PbO_2\right]$ indicates that not all of the lead dioxide is converted to lead sulphate some of the lead sulphate is inactive.

Therefore, as the electrolyte concentration falls below 0.5 M, with a corresponding decrease in pH, the positive electrode becomes effectively passive. Another factor which has to be taken into account at this point is the possible reduction of oxygen at voltages below 1.23 volts as given in equation 10.4 above.

$$O_2 + 4H^+ + 4e^- \Rightarrow 2H_2O$$

The effect of equation 10.4 will further reduce the concentration of hydrogen ions, and therefore further reduce the electrolyte pH; this is **point 2** in figure 10.2. At this point 13.98 Amp-hours capacity had been discharged, the rated capacity of the Plantè cell being 15 Amp-hours.

The negative electrode at this point approaches reversal and lead sulphate on the negative (lead) electrode will be oxidised in the electrode reversal reaction, according to Garche [97], as shown in equation 10.6 where lead sulphate is broken down as the negative electrode reverses polarity.

$$PbSO_4 \; Pb + 2H_2O \rightarrow PbO_2 + SO_4^{2-} + 4H^+ + 2e^- + Pb \quad 10.6$$

Giving an increase in H+ ions, which is detected by the pH meter as an increasing pH of the electrolyte, this effect will increase as the reverse potential of the negative electrode increases, further increasing the pH, at this point in the discharge, **point 3** in figure 10.2, here the cell voltage has declined to less than 1 volt and shortly thereafter the load is disconnected.

The cell voltage rises following the disconnection of the load and approaches the equilibrium voltage.

Note that with respect to figure 10.2 at electrolyte concentration of 0.5 M [164] the theoretical (Nernst) equilibrium voltage is 1.90 volts, and the specific gravity is 1.050. The Nernst voltage being an equilibrium condition relates effectively to open circuit conditions, and inspection of figure 10.2 shows that on disconnection of the load the cell voltage increases and in fact returns to close to the equilibrium condition. This was a typical battery condition following a typical discharge test.

Therefore results of the experimental work undertaken on batteries in a ‘new’ condition would seem to support the theory put forward by Garche et al [97].

10.3 Explanation of the pH disturbance in an aged cell

The identified pH disturbance characteristic of the new cell is reversed as the cell ages, with the pH initially increasing followed by a decrease, as shown in figure 10.4. Both of the tests on the new cell of figure 10.2 and the aged cell of figure 10.4 were carried out at a discharge current of 6 amps.

Comparing the 'new' and 'aged' batteries, it can be seen that the time taken for the cell voltage to fall to 1 volt is approximately 6800 seconds (figure 10.2) when the cell is new, whereas the aged cell takes approximately 4200 seconds (figure 10.4), it can also be seen that the average value of pH is higher in the aged cell, reflecting deterioration in the condition and capacity of the cell.

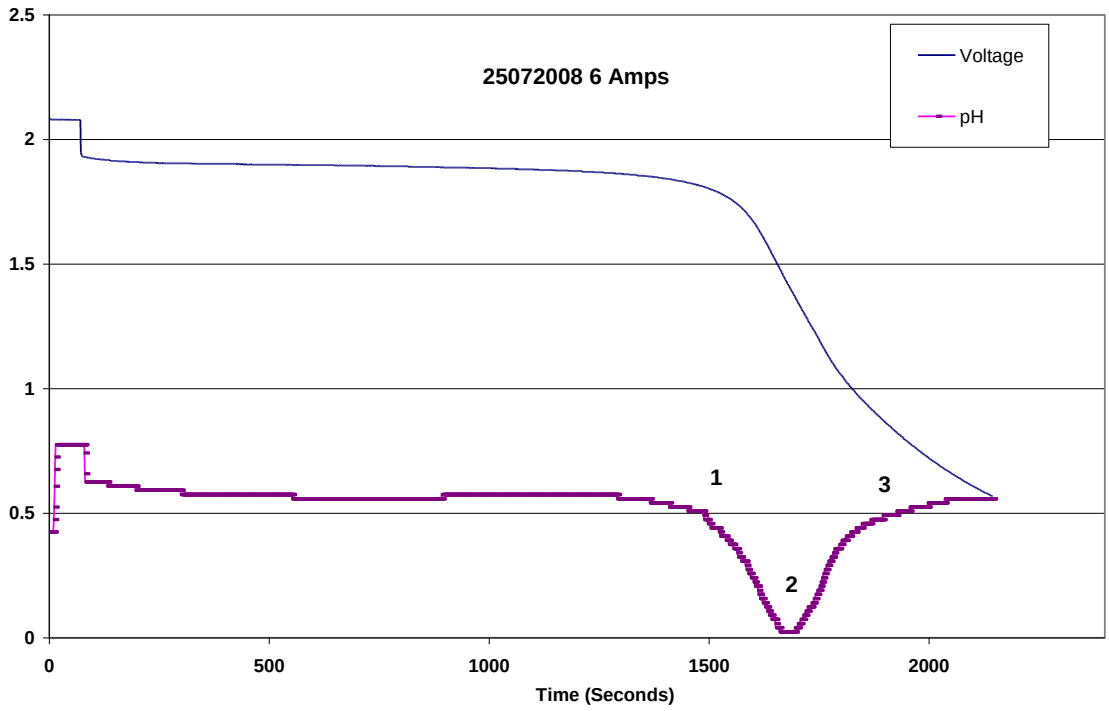

Figure 10.4: Discharge test of an aged Plantè cell, showing cell voltage (Volts) and electrolyte pH with pH disturbance.

The pH disturbance of the aged cell is the inverse of the characteristic of the new cell of figure 10.2, being characterised by a decrease in pH (point 1) followed by a decrease in pH (point 2) and subsequent return to an increasing pH (point 3). The pH disturbance appears to occur at a similar point in the time history of the new cell discharge, as indicated in figure 10.4.

During discharge the main reaction at the negative electrode as theorised by Garche et al [97] is:

$$2Pb + SO_4^{2-} \rightarrow PbSO_4 \left| Pb \right| + 2e^- \qquad 10.7$$

At the end of the discharge the lead sulphate will block further discharge of Pb and any remaining lead [Pb] will be electrochemically inactive, i.e., lead sulphate is formed and residual inactive lead remains, expressed as $PbSO_4 \left| Pb \right|$.

In figure 10.4 the pH increases as the cell discharges, the concentration of the bulk electrolyte decreases with an increasing pH; this corresponds to **point 1** in figure 10.4.

Figure 10.5 shows the over-discharge test carried out by Garche et al [97] on battery "a" which is an aged cell. Due to the loading arrangement employed in this test the shift in potential is significantly higher with the reverse cell voltage approaching negative 2.5 volts. The discharge current being 2.5 amps compared to the 6 amps used in the Plantè cell discharge tests, in the test involving the Plantè cell it is not driven into reversal.

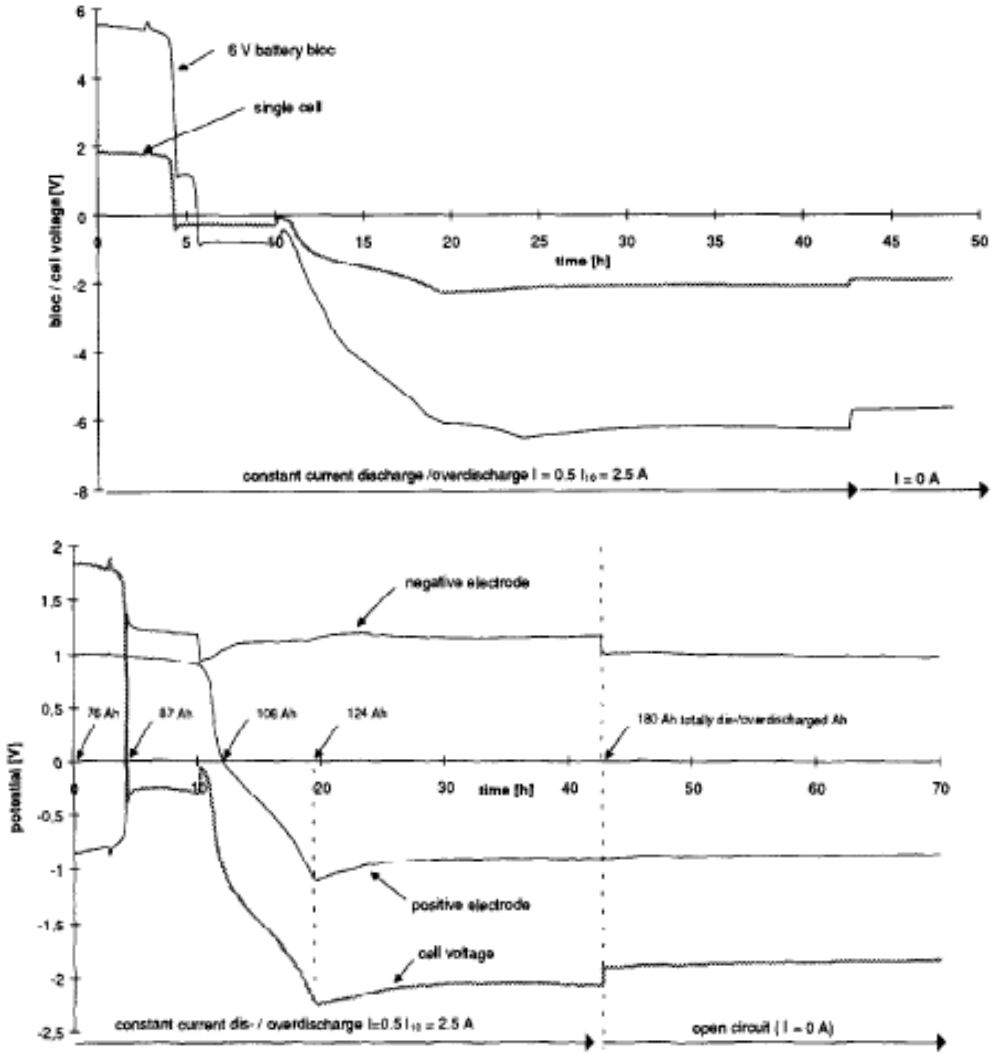

Figure 10.5: battery ‘b’ cell and electrode potentials of a single cell over-discharge [97].

Inspection of figure 10.5 shows that it is the negative electrode which is the first to reverse polarity, as opposed to the new cell, referred to as battery “b” in the tests carried out by Garche [97], where the positive electrode reversed before the negative cell, and the positive electrode was the limiting factor as previously shown in figure 10.3.

Figure 10.6 shows the gas flow and oxygen content measured during the over-discharge test carried out by Garche et al [97], on the aged cell “a”. It can be seen

that there are two significant peaks in gas flow in the first half of the discharge test, these being the points at which the negative and positive electrode reverses polarity.

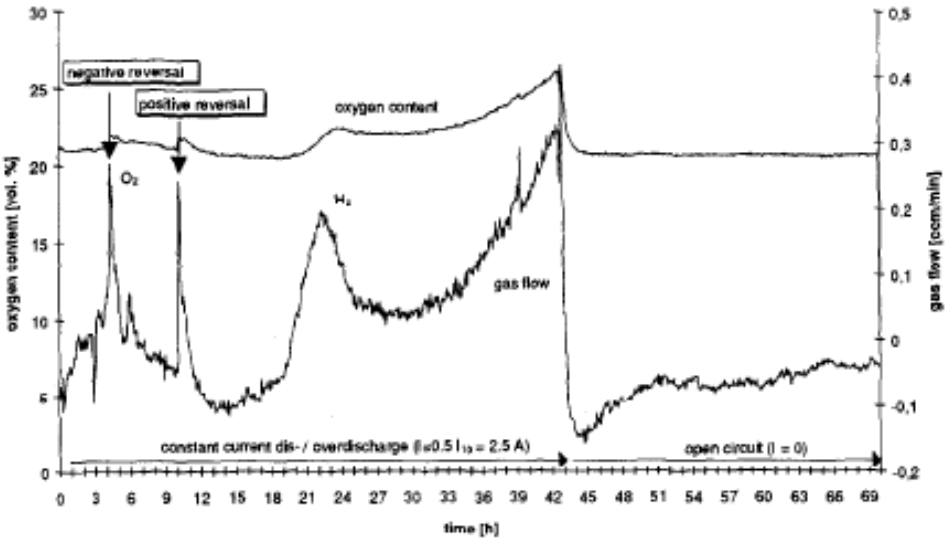

Figure 10.6: gas flow and oxygen content of a single cell during over-discharge experiment [97].

The first peak occurs when the negative electrode goes into reverse polarity at approximately 4 hours into the test, followed at approximately 11 hours by the reversal of the positive electrode. As the tests carried out on the Plantè cell, with the exception of the cell reversal tests, were in isolation, reversal of both electrodes is considered to be unlikely.

As the polarity of the negative electrode reverses the lead sulphate will be oxidised to lead oxide in the reverse reaction as lead sulphate water molecules are broken down resulting in hydrogen ions being formed as given previously in equation 10.6.

$$PbSO_4 \; Pb + 2H_2O \rightarrow PbO_2 + SO_4^{2-} + 4H^+ + 2e^- + Pb \qquad 10.6$$

Further more, oxygen evolution can take also place (equation 10.2), depending on the potential at the beginning of over-discharge (at about 4.5 hours on figures 10.5 and 10.6), or if all of the active material is oxidised to lead dioxide [103].

$$2H_2O \rightarrow O_2 \uparrow + 4H^+ + 4e^- \qquad 10.2$$

The resulting effect is increased release of oxygen gas as can be seen in figure 10.6 and an increase in the concentration of hydrogen ions as the negative cell reverses

this corresponds to **point 2** on figure 10.4. At this point 3.42 Amp-hours capacity had been discharged, the rated capacity of the Plantè cell being 15 Amp-hours.

As the cell continues to discharge and the negative electrode now has a positive potential, inspection of figure 10.6 shows that peak in gas flow decreases, the oxygen content has remained relatively constant following the reversal of the negative electrode, whereas the total gas flow reduces sharply which suggests that the decrease in gas flow is due to reduced hydrogen evolution. Therefore as the peak in gas flow passes following the reversal of the negative electrode at point2 the hydrogen gas evolution decreases, with a corresponding decrease in pH as indicated in equation 10.2.

Considering the positive electrode the process here is similar to that discussed in the case of the 'new' battery in relation to point 2 on figure 10.2.

As discussed the main reaction at the positive electrode is given in equation 10.5:

$$2PbO_2 + 4H^+ + SO_4^{2-} + 2e^- \rightarrow PbSO_4 + PbO_2 + 2H_2O$$

Lead sulphate and inactive lead dioxide is formed and the potential will fall, as the electrolyte concentration falls with a corresponding decrease in pH, the positive electrode again becomes effectively passive, this corresponds to **point 3** on figure 10.4.

The discussion so far has concentrated on the pH disturbance in Plantè cells, however the same pH disturbance was observed during the discharge tests involving SLI batteries, with the pH disturbance for new and aged SLI batteries having the same characteristic as the new and aged Plantè cells.

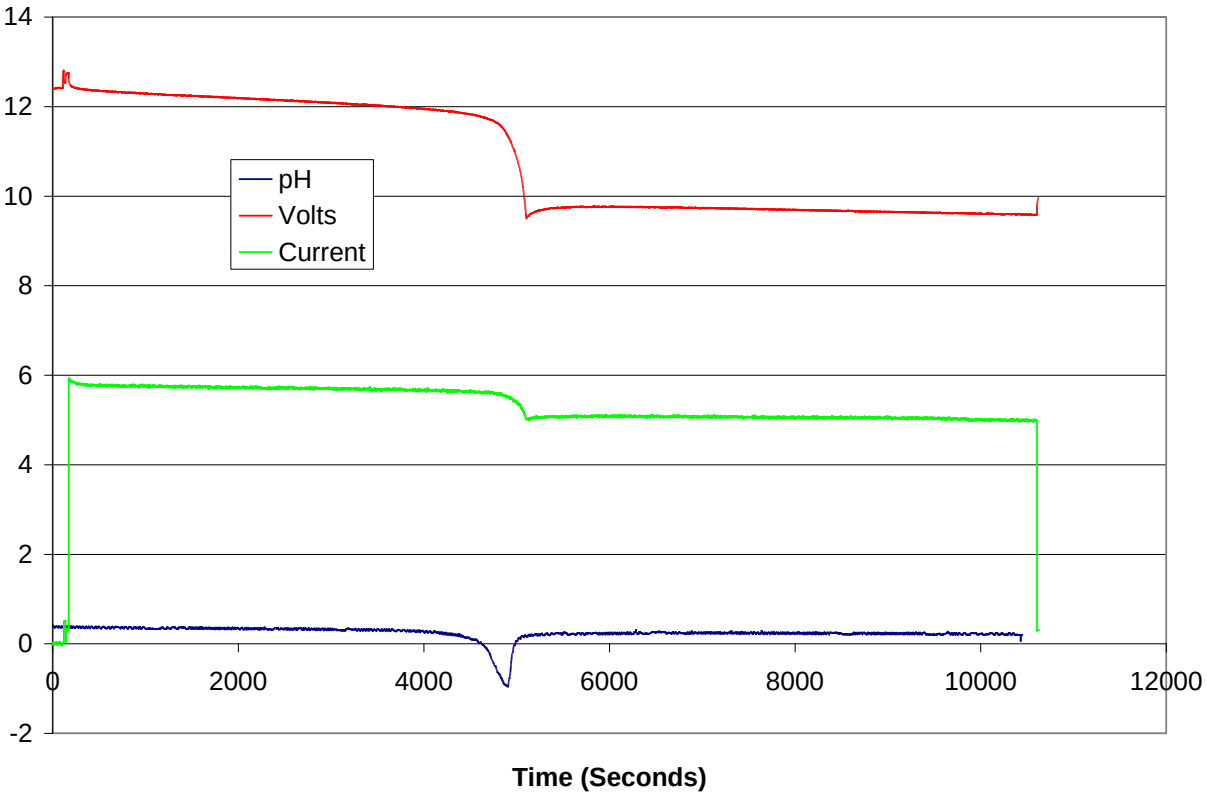

Figure 10.7: 6 cell SLI battery discharge test showing battery voltage, discharge current (Amps) and pH of one cell. Note the pH disturbance where the measured cell has reversed polarity.

Further similarities between the authors work and that of Garche [97] is evidenced by the following.

In the test represented in figure 10.7 the electrolyte pH is being measured in one of the six cells in a 6 cell automotive Starting, Lighting and Ignition (SLI) battery.

It can be seen that a pH disturbance coincides with a potential step in the battery voltage discharge characteristic, the potential exhibited at the first moment of the cell reversal. These recovery overshoots are due to the high resistance of the lead sulphate and the onset of cracking of the sulphate layer [103].

The battery used in this test had been in service and is referred to as aged and corresponds to battery “a” in the tests carried out by Garche et al [97] where one of the tests involved the over-discharge of a three cell battery.

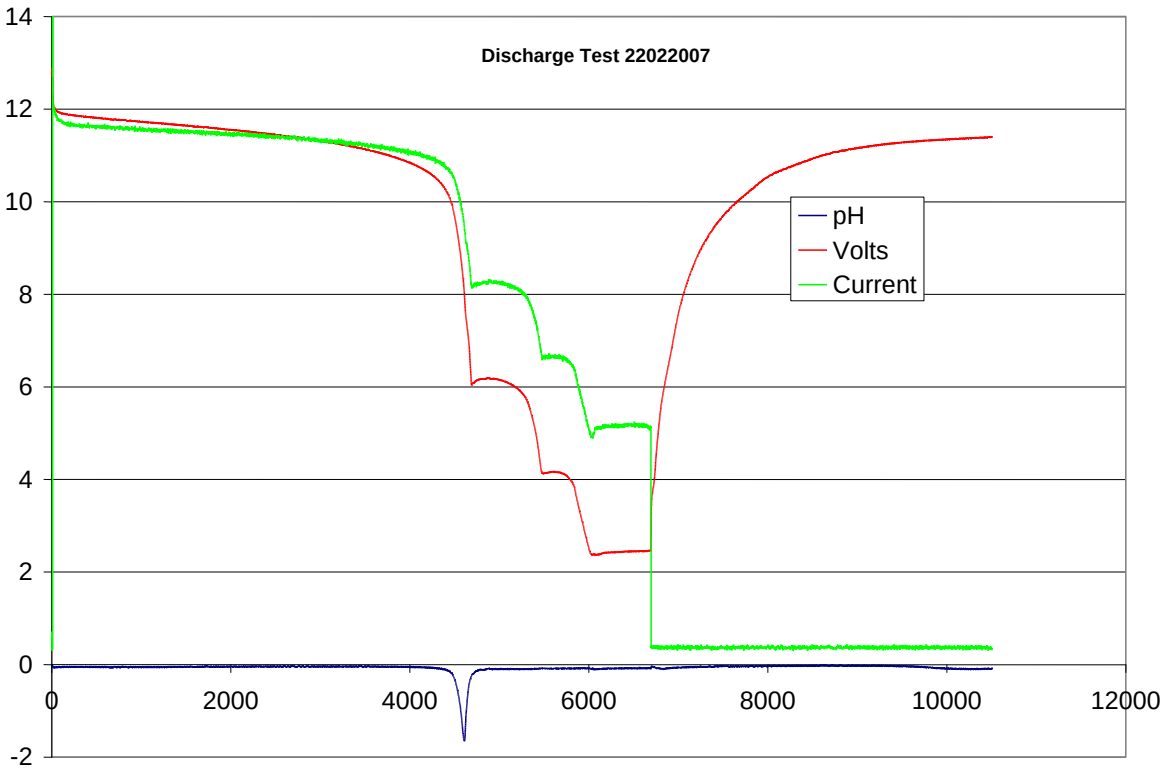

Figure 10.8: SLI battery discharge test, showing batter voltage (Volts), discharge current (Amps). Note the three cell reversals, the first cell reversal also indicated by the cell electrolyte pH.

Figure 10.8 shows a discharge test on a six cell SLI battery where only one cell was being monitored for pH. It can be seen in figure 10.8 that there are in fact three 'potential steps', corresponding to three cell reversals. The cell being monitored with the pH sensor was in fact the first cell to reverse at 4500 seconds, and the reversal of two other cells can be clearly seen at 5500 and 6000 seconds respectively.

A further type of test was carried out during the experimental work for this thesis; a Plantè cell was connected in series with a fully charged 6 cell automotive SLI battery. The Plantè cell was not full charged in order to make it in a lower state of

charge than the SLI battery, the series connected SLI battery and Plantè cell where then subjected to a discharge test, the results of this test are shown in figure 10.9.
Figure 10.5 shows the cell and electrode potentials of an over-discharge as carried out by Garche et al [97], the polarity of both electrodes reverses, resulting in cell reversal that is a similar to the Plantè test the author carried out shown in figure 10.9.

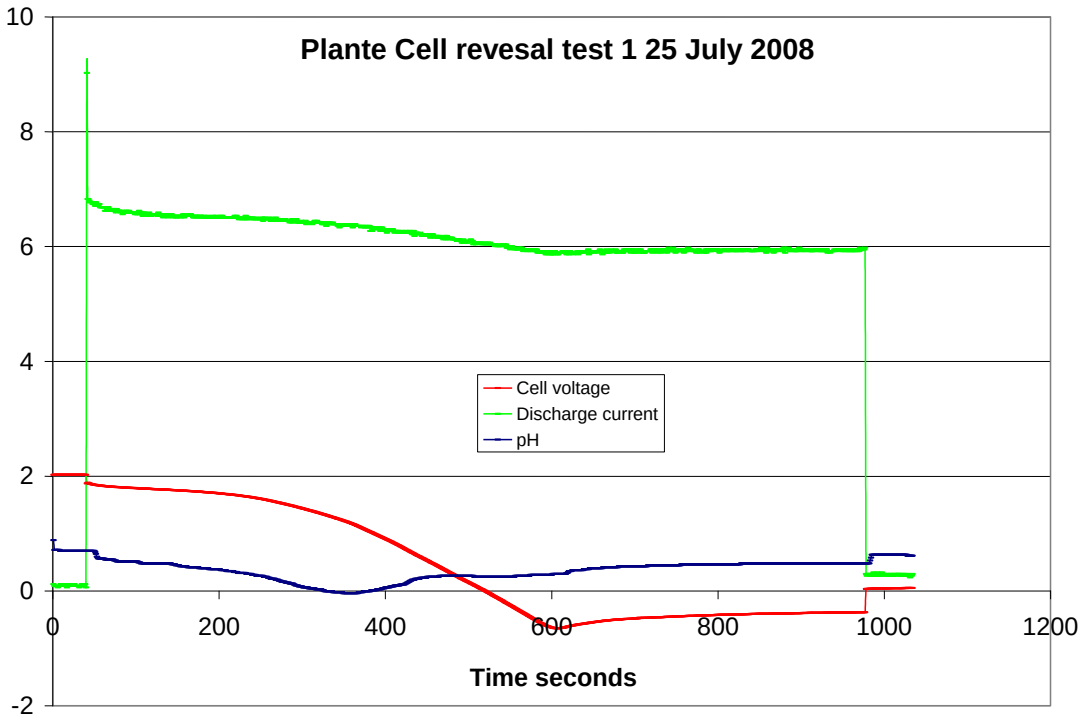

Figure 10.9: Plantè cell discharge test leading to cell reversal, showing cell voltage (Volts), discharge current (Amps) and cell electrolyte pH.

It can be seen in figure 10.9 that the cell voltage declines below zero and then stabilises at approximately negative 0.4 volts, at this point the Plantè cell is being charged by the SLI battery. Therefore, there are similarities in the results of the experimental work of this thesis with the results of Garche et al [97]. The measurement of cell condition used by Garche et al [97] being based on gas flow for the aged cell and electrolyte concentration for the new cell. The work undertaken in this thesis used pH as the main indicator of cell condition.

10.4 Chapter Conclusions

In summary the author has identified the occurrence of a previously unreported pH disturbance while measuring the pH of battery electrolyte during discharge and has offered explanations for the difference in these pH disturbances in new and aged batteries. Furthermore it has been demonstrated that this disturbance supports the published findings and theory proposed by Garche [97]. The identification of this pH disturbance and supporting theory are claimed as novel contributions to the state of the art in lead acid batteries by the author.

An application of this pH disturbance would be the monitoring of individual cells within a large battery pack, typically as found in the multi-cell battery systems of electric vehicles, standby power systems and uninterruptible power supplies (UPS). A faulty or weak cell within a long string of cells under discharge could be driven into reverse polarity during cell reversal in a string of cells resulting in the failed cell being charged by the other healthier cells. The reversed cell could be subject to power dissipation of up to 5% of the entire battery power capacity, which can cause catastrophic failure [24]. If integral monitoring of the electrolyte pH were to be incorporated into individual cells, the pH disturbance would serve as an early and clear warning of impending cell reversal.

Therefore the monitoring of pH should be viewed as a possible additional means of individual cell voltage monitoring of a string of series connected cells or batteries.

The author therefore proposes this effect as a contribution to the field of monitoring cell condition, as an indication of impending cell polarity reversal in individual lead-acid cells

CHAPTER 11 THESIS CONCLUSIONS

This thesis has focused on techniques for predicting impending failure of electrochemical cells based on measurement of certain parameters.

Electrochemical cells are widely used in the form of batteries for a wide range of applications. However, the market for batteries, and fuel cells, may be about to increase significantly if the current development activities of battery and fuel cell electric vehicles translates into full scale production.

This research has been based on a battery/fuel cell hybrid power system for an electrically powered vehicle, and both the battery and fuel cell have been studied in this thesis. There have been two significant outcomes from the work undertaken during this thesis.

1. A low cost and scalable cell voltage monitor which provides isolated cell voltage measurement (CVM).
2. The novel use of pH measurement of the sulphuric acid in a Lead-Acid battery as a means of predicting cell failure.

11.1 Fuel Cell Health monitoring

The fuel cell monitoring system developed by the author is used in the measurement of individual cell voltages as means of identifying weak or failing cells within the fuel cell stack, thereby providing as means of avoiding cell and possibly failure of the entire fuel cell stack due to reversal of one or more cells within a multiple fuel cell stack.

Early warning of cell reversal is therefore crucial in order to prevent the possible catastrophic failure of a fuel cell stack.

A Cell Voltage Monitor (CVM) has been developed by the author and tested on a laboratory based fuel cell system under load conditions. The CVM has been proven to be capable of detecting faulty cells within an operational fuel cell stack as evidenced by the results of chapter 5, in particular figures 5.17 and 5.18 which show the cell voltages recorded before and after repairs to the laboratory fuel cell stack. The CVM developed by the author offers a scalable and low cost solution to the

problem of individual cell voltage monitoring of fuel cell stacks which is of particular interest to researchers and developers working on fuel cell systems. The cost of the cell voltage monitor developed is considerably below that of the commercial systems currently available, and offers a cost effective system for monitoring cell voltages in small to medium size fuel cell stacks.

11.2 Battery Health Monitoring

Measurement of state of health and predicting battery failure has historically been problematic; there are a number of measurements which can be made in order to determine state of health as discussed in chapter 7.

In particular cell reversal in long series strings of lead-acid batteries, such as those found in electric vehicles, is a potentially serious occurrence. The pH disturbance discovered by the author during over-discharge during this research appears to validate published work by Garche et al [97], furthermore the pH disturbance offers a means of identifying weak or failing cells within a long string of series cells and gives an 'early warning' before cell reversal occurs. This can be used to prevent possible catastrophic failure of a cell, which in turn would disable the entire battery string.

During the course of the experimental work undertaken during the thesis it has been found that the magnitude and direction of the pH disturbance is affected by the discharge current and age of the cell respectively. Further more the mean value of pH increases as the cell ages indicating a progressive reduction in the concentration of the electrolyte.

11.3 Future Work

As a result of the work carried out in this thesis systems have been developed which provide early warning of impending cell failures in fuel cell stacks and long strings of batteries, resulting from failing or weak cells being driven into reverse polarity.

The cell voltage monitor for the fuel cell system has been tested on an operational fuel cell stack and identified faulty cells within the stack. A microprocessor version of this cell voltage monitor was developed and tested, but no testing was carried out on an operational fuel cell stack, however, this version offered higher sampling rates

than the initial version. Further work could include testing of this improved cell voltage monitor using a fuel cell stack to prove the performance of this CVM.

The battery cell pH monitor has been tested on various lead acid batteries and the pH disturbance has been clearly identified during the discharge tests. However, further work is required to develop a robust sensor system which could be integrated into a battery, typically for use in long strings of series connected batteries such as those found in electric vehicle power systems.

The pH sensing device could be designed to be an integral part of the cell; the pH sensor would have to be immersed in the battery electrolyte. However, the associated measurement system could be packaged in a similar way to the integral battery management system (BMS) shown in figure 11.1.

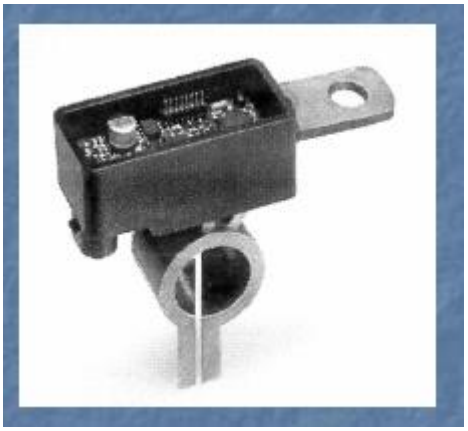

Figure 11.1: Bosch Terminal BMS

Further work could be carried out in order investigate the relationship between the pH disturbance and the discharge current and age of the cell, the magnitude of the pH disturbance increases with increasing discharge current, and the direction of the pH disturbance changes as the cell ages. New cells have a pH disturbance where the pH increases, whereas in aged cells, the pH disturbance exhibits a decreasing value of pH.

This thesis only considered Lead-Acid batteries; however, the pH disturbance may occur in other battery types, flooded Nickel Cadmium (Ni-Cd) and Nickel Metal Hydride (NiMH) batteries both use Potassium Hydroxide (KOH) as the electrolyte,

the concentration of the hydroxyl ion (OH^-) varies as the cell charges and discharges, therefore the variation of the cell electrolyte pH under discharge could be investigated to ascertain if a similar type of disturbance occurs in the measured value of pH as the cell charges and discharges.

The pH disturbance may occur in alkaline fuel cells which also use Potassium Hydroxide (KOH) as the electrolyte. Although the electrodes in a fuel cell do not physically change during the operation of the fuel cell, and only act as a site for the reactants, there may be variations in the electrolyte pH which may warrant further investigation.

Finally the battery model developed in Chapter 6 could be developed by including the pH effects discovered during the work of this thesis in order to develop a more representative model of a battery during discharge.

APPENDICES

Appendix 1

Flowchart for CVM11

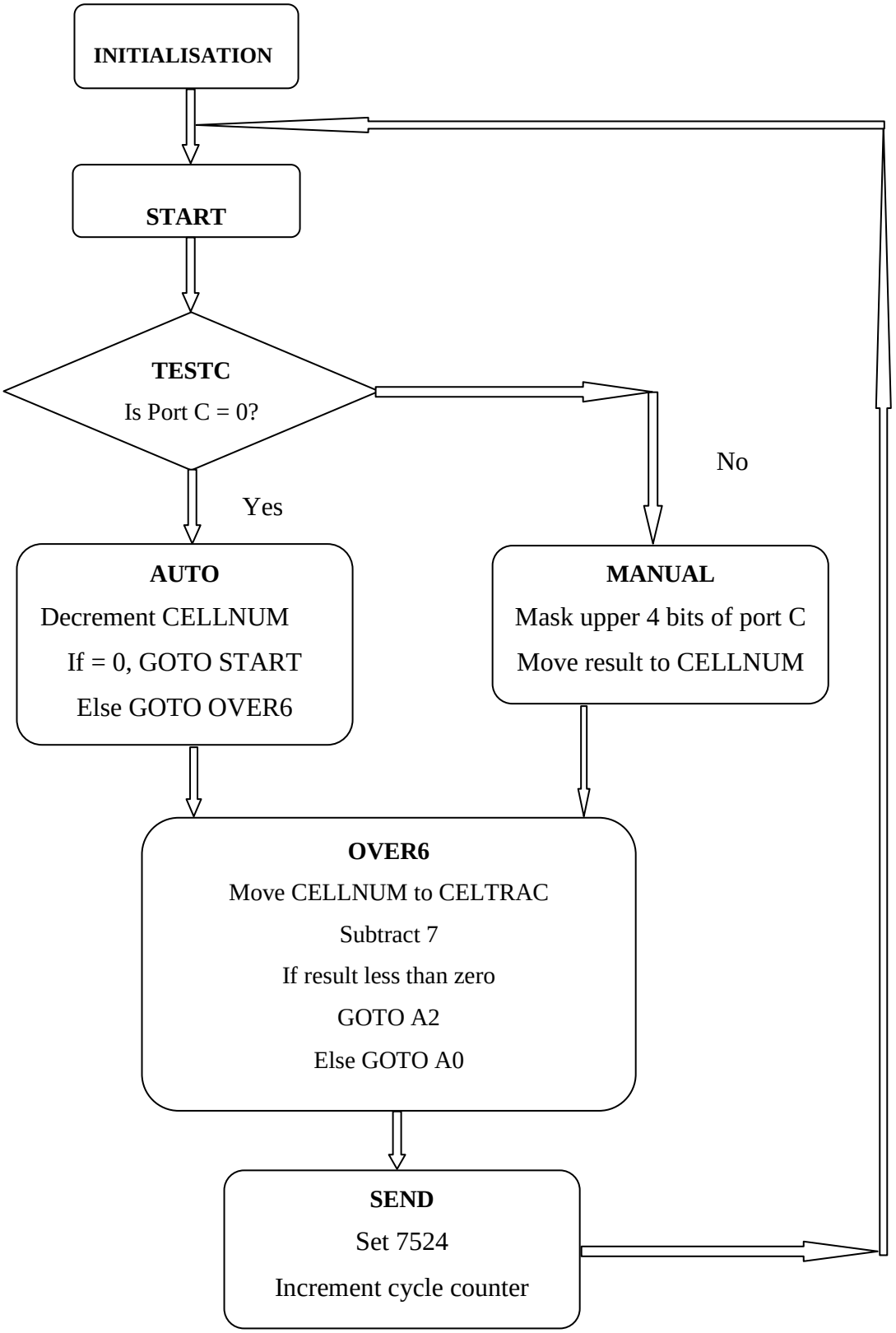

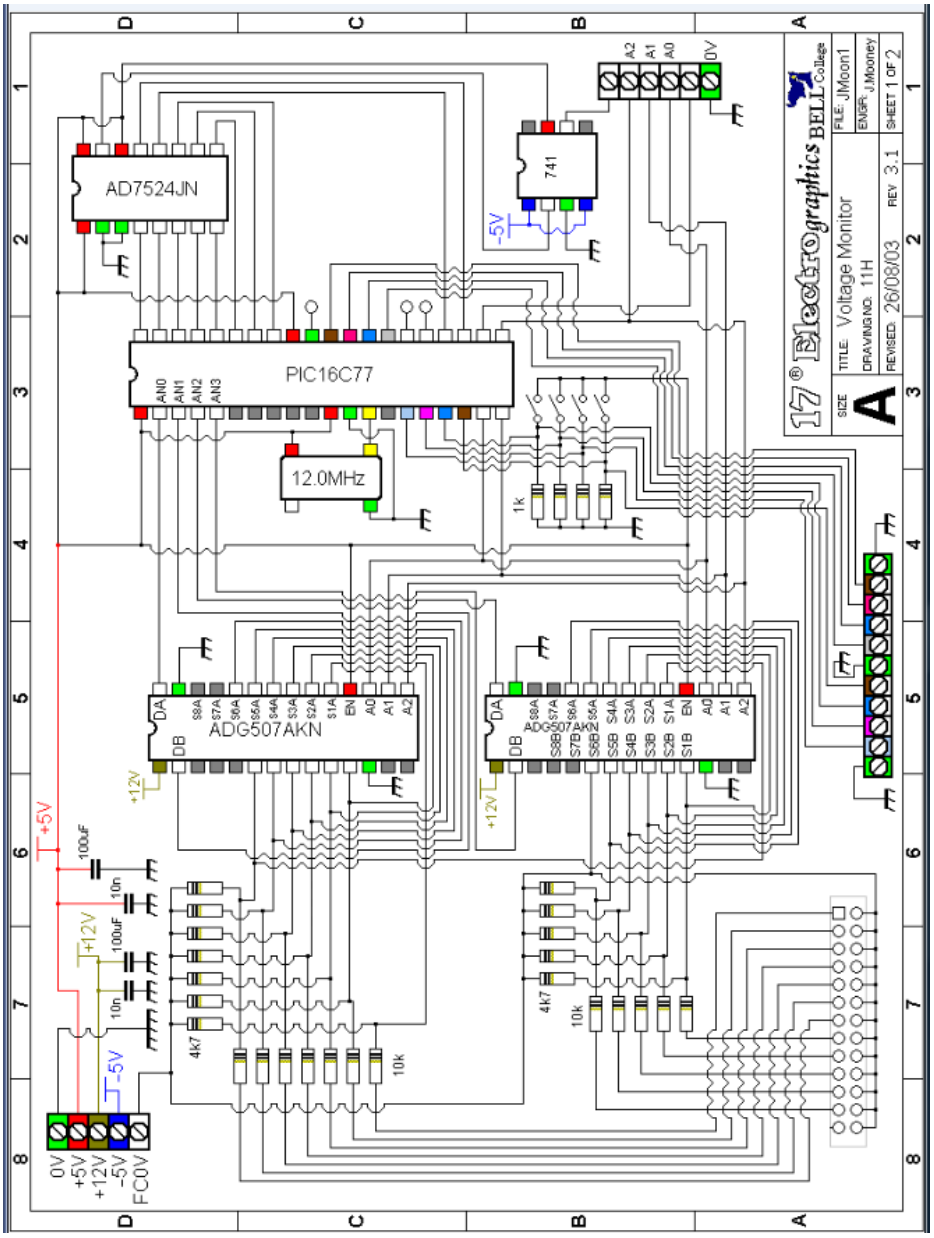

Circuit diagram for CVMII

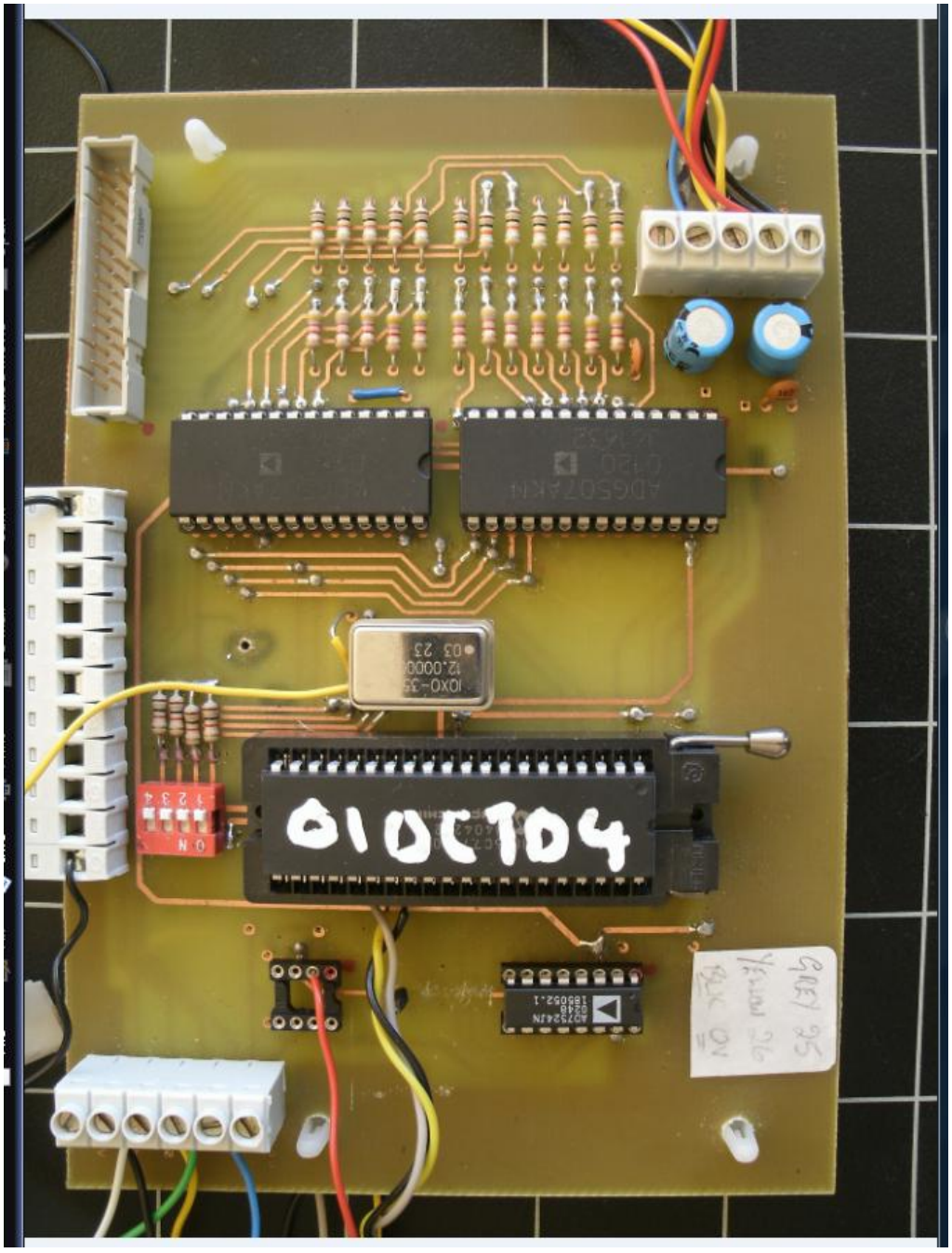

Main circuit board of CVMII

Bibliography

1 Webb, D, et al, Measuring individual cell voltages in fuel cell stacks, *Journal of Power Sources*, Volume 103, 21 May 2001, pp54-60

2 Kiehne, H.A.Battery Technology Handbook, Marcel Dekker Inc 2003, pp493, ISBN 0-8247-4249-4

3 Perone, S.P., Modelling the occurrences of cell reversals in long strings of lead acid cells. Journal of Power Sources, 41 (1993) pp277-290.

4 Vincent,C.A., Scotsati.B., "Modern Batteries. An introduction to Electrochemical Power Sources", Butterworth Heinemann ISBN 0-340-66278-6,1997.

5 Picture of dry cell batteries. Duracell Ltd, [Online] Available from World Wide Web: http://www.duracell.com, [Accessed 19 January 2010]

6 Picture of Lead-acid secondary ,[Online], Available from World Wide Web: <www.exide.com>, [Accessed 19 January 2010]

7 Bergveld H.J, Kruijt,W.S, Notten, P.H.L, Battery Management Systems, Design by Modelling (Phillips Research Book Series) Volume 1, Springer, ISBN 10: 142008230, 2002, pp 5-10

8 Figure Battery cell [Online], Available from World Wide Web: <http://pvcdrom.pveducation.org/>, [Accessed 19 January 2010]

9 "Storage in PV Systems". C.Honsberg Solar Electric Systems. [Online], Available from World Wide Web: <http://pvcdrom.pveducation.org>, [Accessed 19 January 2010]

10 Crompton, T., Battery Reference Book Third Edition Newnes Books 2000, ISBN13: 978-0750646253, pp2/16

11 "Lead Acid batteries". [Online], Available from World Wide Web: <http://www.mpoweruk.com/leadacid.htm>, [Accessed 19 January 2010]

12 "Lead-Acid Battery", [Online], Available from World Wide Web: <http://en.wikipedia.org/wiki/> [Accessed 19 January 2010]

13 Crompton, T., Battery Reference Book, Third Edition Newnes Books, 2000, ISBN13: 978-0750646253, pp32-33

14 Enersys Ltd, “Powersafe Plante Installation Operation and Maintenance Manual”, Publication No EN-PL-IOM-001 May 2004.
15 Tesla electric vehicle, [Online], Available from World Wide Web: <http://www.teslamotors.com/>, [Accessed 19 January 2010]
16 Linden, D, Reddy, T.B., “Handbook of Batteries”. Third edition. McGraw-Hill. ISBN 0-07-135978-8
17 Cullen, B., “Global market for industrial lead acid batteries-past present and future”, Journal of Power Sources. 2003 Volume 116, Issues 1-2, pp 287e7-287-e10
18 “Battery Modelling for HEV Simulation ThermoAnalytics”, Inc, 1999, [Online], Available from World Wide Web: <http://www/thermoanalytics.com/docs/batteries.html>, [Accessed 19 January 2010]
19 Kiehne, H.A., “Battery Technology Handbook”, Taylor and Francis Ltd, 2003 ISBN 0-8247-4249-4
20 Pop, V., et al, “State of the art battery state-of-charge determination”, Measurement Science and Technology 16 (31 October 2005) Volume 16 R93-R110
21 Culpin, et al.,”Failure modes of lead/acid batteries”, Journal of Power Sources, Volume 36, Issue 4,16 December 1991, pp 415-438.
22 McCluer, S, “Battery Technology for Data Centres and Network Rooms. Lead-Acid Battery Options”, White Paper #30, APC Schneider Electric.
23 Bagotskii, V.S., Fundamentals of Electrochemistry, Wiley 2006, ISBN -13-978-0-471-70058-6 p321
24 Crompton, T.,Battery Reference Book., Third Edition, Newnes. ISBN 07506 4625-X p1/62
25 Perone, S.P., “Modelling the occurrences of cell reversals in long strings of lead acid cells”. Journal of Power Sources, 41 (1993) 277-290.
26 Levy, S.C., Bro, P., Battery Hazards and Accident Prevention, Plenum, 1994, ISBN 0-306-44758-4, pp48.
27 Symons, P.,” Pitfalls in using long strings of series-connected lead-acid batteries”.,2004, [Online], Available from World Wide Web:

<http://www.battcon.com/PapersFinal2004/SymonsPaper2004.pdf>, [Accessed 19 January 2010]

28 Duerr, M., Investigation and Analysis of the dynamic behaviour of an Alkaline Fuel Cell, Journal of Power Sources, 2007 171, Issue 2, 27 September 2007, pp1023-1032. "University of Strathclyde,PhD Thesis.

29 Kordesh, K.V., et al , "Advances, aging mechanism and lifetime in AFCs with circulation electrolytes", Journal of Power Sources, Volume 127 (2004) pp234-242.

30 Rajashekara, K., "Propulsion System Strategies for Fuel Cell Vehicles". Fuel Cell technology for Vehicles. *SAE 2000* pp179-187

31 Bekken, M., et al, "An Analysis of the True Efficiency of Alternative Vehicle power plants and Alternative Fuels". Fuel Cell technology for Vehicles. SAE 2000 pp269-281

32 Batra, V.S., et al , "Status of fuel cell technology",
Energy Technology News, Issue 2 and 3, January and April 2001

33 Pindo Mok, P., et al , "Automotive Fuel Cells – Clean Power for Tomorrows Vehicles", Fuel Cell technology for Vehicles. SAE 1999, pp 37

34 Gregory, D.P., "Fuel Cells", Mills and Boon, pp 9, ISBN 0 263.51713.6. 1972.

35 Cole, A., "Is the future upon us? ", Automotive Engineer September 1997.

36 "A new process pathway for the creation of electrolyte membrane layers within solid oxide fuel cells", [Online], Available from World Wide Web: <http://www.people.virginia.edu/~jfg6e/groves/Masters/Chen_2003/Chapter_01.introduction.pdf>, [Accessed 19 January 2010]

37 Alkaline fuel cell image, [Online], Available from World Wide Web: <http://www1.eere.energy.gov/hydrogenandfuelcells/fuelcells/images/fcell_diagram_alkaline.gif>, [Accessed 19 January 2010]

38 Murphy, O.J., et al, Low-cost light weight high power density PEM fuel cell stack , Electrochimica Acta, Volume 43, Issue 24, 21 August 1998, Pages 3829-3840

39 Buchi, R., et al , "Operational aspects of a large PEFC stack under practical conditions".
Journal of Power Sources Volume 128 Issue 2, 5 April 2004

40 “Beyond the static model of fuel cells”. A dynamic approach, [Online], Available from World Wide Web: <http://www.lss.supelec.fr/Internet_php/Fuel_Cell/FC_explanation.html>, [Accessed 19 January 2010]
41 Alkaline fuel cell image, [Online], Available from World Wide Web: <http://corrosion-doctors.org/FuelCell/afc.htm>, [Accessed 19 January 2010]
42 Gouérec, P.,Poletto, et al, The evolution of the performance of alkaline fuel cells with circulating electrolyte, Journal of Power Sources, Volume 129 (2004) pp193-204.
43 M.Cfrain, M., et al, Advances, aging mechanism and lifetime in AFCs with circulation electrolytes, Journal of Power Sources, Volume 127 (2004) 234-242.
44 Lin, B., et al, Performance of alkaline fuel cells: A possible future energy source?, Journal of Power Sources, Volume 161 (2006), pp474-483.
45 Husar, A., et al, Description of a gasket failure in a 7 cell PEMFC stack, Journal of Power Sources, Volume 169 Issue 1 Special Issue Sp Iss SI Pages 85-91 June 10 2007
46 Taniguchi, A., et al, “Analysis of electrocatalyst degradation in PEMFC caused by cell reversal during fuel starvation”, Journal of Power Sources, Volume 130 Issues 1-2, pp 42-49.
47 Huang et al, “Mechanical endurance of polymer electrode membrane and PEM cell durability”, Journal of Polymer Science Part B-Polymer Physics Volume 44 Issue 16, Aug 15 2006, pp 2346-2357.
48 Cfrain, M., et al, “Advances, aging mechanism and lifetime in AFCs with circulation electrolytes”, Journal of Power Sources, Volume 127 (2004) pp234-242.
49 Taniguchi, A., et al, “Analysis of electrocatalyst degradation in PEMFC caused by cell reversal during fuel starvation”, Journal of Power Sources, Volume 130 (2004) pp42-49.
50 Heideck, G., et al, “Multi channel voltage control for fuel cells”, Journal of Power Sources, Volume 145 (2005) 594-597.

51 Mulder, G., et al, “Evaluation of an on-site cell voltage monitor for fuel cell systems”, International Journal of Hydrogen Energy, Volume 33 (2008), pp5728-5737.
52 “On-site cell voltage monitoring”, [Online], Available from World Wide Web: <www.cellsense.eu>, Accessed 19 January 2010]
53 Kiehne, H.A., “Battery Technology Handbook”, Taylor and Francis Ltd, 2003 ISBN 0-8247-4249-4 pp 4.
54 Crompton, T., “Battery Reference Book”, Third Edition Newnes Books 2000, ISBN13: 978-0750646253, pp1-4.
55 “Physical Chemistry” S342 Block, The Open University. ISBN 0 7492 51891
56 Dell, R.M., Rand, D.A., “Understanding Batteries”, Royal Society of Chemistry, 2001, ISBN 0-85404-605-4 p11
57 Crow, D.R., “Principles and Applications of Electrochemistry”, Taylor and Francis Ltd, 1994, ISBN 0-412-30270-5, pp78
58 Lead acid battery image [Online], Available from World Wide Web: <http://www.mpoweruk.com/>, [Accessed 19 January 2010]
59 Hussain, I.,” Electric and Hybrid Vehicles”, CRC Press, 2003, ISBN 0-203-000939-8, pp45
60 Battery and cell technology, [Online], Available from World Wide Web: http://www.mpoweruk.com/chemistries.html, [Accessed 19 January 2010]
61 Image of “The Carnot Cycle on a pressure-volume property diagram”, [Online], Available from World Wide Web: <http://phys.uri.edu>, [Accessed 19 January 2010]
62 Image of “The Carnot Cycle on a temperature-entropy property diagram”, [Online], Available from World Wide Web: <http://phys.uri.edu>, [Accessed 19 January 2010]
63 O’Hayre, R., et al, Fuel Cell Fundamentals, Wiley, 2005, ISBN-13 978-0-471-74148-0 pp 26
64 Luque, A., Hegedus, S., “Handbook of Photovoltaic Science and Engineering”. Wiley. 2003 ISBN 13:978-0-471-49196-5(H/B), pp702

65 Schroeder, D.V., An Introduction to Thermal Physics, Adison Wesley, 1999, pp151
66 Berndt, D., “Maintenance – Free Batteries A Handbook of Battery Technology”, Second edition, Research Studies Press, ISBN 0 86380 198 6
67 “Gibbs Free Energy”, [Online], Available from World Wide Web: <http://en.wikipedia.org/wiki/Gibbs_free_energy>, [Accessed 19 January 2010]
68 O’Hayre, R., et al, Fuel Cell Fundamentals, Wiley, 2005, ISBN-13 978-0-471-74148-0
69 Crompton, T., “Battery Reference Book”, Third Edition Newnes Books 2000, ISBN13: 978-0750646253, pp1/21.
70 Linden, D., Reddy, T B., “Handbook of Batteries”, Third edition, McGraw-Hill. 2002, ISBN 0-07-135978-8
71 Tafel equation, [Online], Available from World Wide Web: <http://electrochem.cwru.edu/ed/dict.htm>, [Accessed 19 January 2010]
72 The Tafel plot, [Online], Available from World Wide Web: <http://people.clarkson.edu/~ekatz/tafel_equation.htm>, [Accessed 19 January 2010]
73 Bockris, O’M.,Reddy, A.K.N, Gamboa-Aldeco, M,. "Modern Electrochemistry 2A. Fundamentals of Electrodics.", Second Edition, 2000, Kluwer Academic/Plenum Publishers, ISBN13 9780306461675, p.1083.
74 Image “Ideal and Actual Fuel Cell Voltage/Current Characteristics”. [Online], Available from World Wide Web: http://corrosion-doctors.org/Batteries/e-icurve.htm
75 Concentration polarisation, PrincetonAppliedResearch, [Online], Available from World Wide Web: <http://www.princetonappliedresearch.com/products/markets/fuel_cell.cfm>, [Accessed 19 January 2010]
76 Gregory.D.P, Fuel Cells, Mills and Boon, 1972, ISBN 0 263.51713.6. pp 16.
77 Energy conversion Ltd, [Online], Available from World Wide Web: <http://www.fuelcelltoday.com/media/pdf/archive/Article_1087_AFC.pdf>
78 Design guidelines for Zetek Power Electrochemical Generators
79 Schematic of Zetek Fuel Cell system, Elenco, N.V.

80 “Fuel Cell Handbook”, Fifth Edition, EG&G Services Parsons Inc, Science Applications International Corporation, .
81 “Design guidelines for Zetek Power Electrochemical Generators”.
82 Rodatz, P., et al, “Operational aspects of a large PEFC stack under practical conditions”, Journal of Power Sources, Volume 128, Issue 2, 5 April 2004, pp208-217.
83 Kordesch, K., et al, “Direct methanol-air fuel cells with membranes plus circulating electrolyte”. Journal of Power Sources, Volume 96 Issue 1,1 June 2001, Pages 200-203.
84 Kordesch, K., et al, “Alkaline Fuel Cell Applications”, Journal of Power Sources, Volume 86 Issue 1-2,1 June 2001, Page 164
85 Carbon black, [Online], Available from World Wide Web: <http://en.wikipedia.org/wiki/Carbob_black>, [Accessed 19 January 2010]
86 Lignosulfonate, [Online], Available from World Wide Web: <http://en.wikipedia.org/wiki/Lignosulfonate>, [Accessed 19 January 2010]
87 Rand, D.A.J., “Valve-Regulated Lead-Acid Batteries”, Elsevier Science 2004, ISBN-13 978 0444507464.
88 Guruswamy, S., “Engineering Properties and Applications of Lead Alloys”, CRC Press 1999, ISBN-13 978-0824782474, pp464.
89 “Department of Energy Handbook, Primer on Lead-Acid Storage Batteries, [Online], Available from World Wide Web: <http://www.osti.gov/bridge/servlets/purl/205011-RduEqy/webviewable/205011.pdf>, [Accessed 19 January 2010]
90 Speirs, D.J., et al, “Predicting the service lifetime of lead/acid batteries in photovoltaic systems”, Journal of Power Sources, Volume 53 Issue 2, 1995, pp245-253.
91 Smith, G., “Storage Batteries”, Second Edition Pitman. ISBN 0 273 36087 6
92 Groves, P.D., “Electro-chemistry”, J Murray, 1974, ISBN 0 7125 2935 2
93 Fogeil, M., “Basic Electricty”, Research and Education Society, 2006, ISBN 0-87891-420-X

94 Pistoia, G., “Batteries for Portable Devices”. Elsevier, 2005, ISBN0-444-51672-7, p 6
95 Bard, A.J, et al, “Electrochemical Methods Fundamentals and Applications”, Wiley, 2002, ISBN 0-471-08753-X
96 Harmann, C.H.,et al, ”Electrochemistry”, Second edition, Wiley-VCH, 1998, ISBN 978-3-527-31069-2
97 Garche, J., et al, “The influence of different operating conditions, especially over-discharge, on the lifetime and performance of lead/acid batteries for photovoltaic systems”, Journal of Power Sources 67 (1997), pp201-212.
98 SLI Battery, [Online], Available from World Wide Web: <http://www.mpoweruk.com/>, [Accessed 19 January 2010]
99 Messenger, R.A., Ventre, J., “Photovoltaic Systems Engineering”, CRC Press Second Edition 2003, ISBN-13 978-0849317934, p59.
100 Luque, A., Hegedus, S.. Handbook of Photovoltaic Science and Engineering. Wiley. 2003 ISBN 13:978-0-471-49196-5(H/B).
101 Secondary batteries for the propulsion of electric road vehicles, BS EN 61982-1:2006
102 Cell reversal, [Online], Available from World Wide Web: <http://www.mpoweruk.com/life.htm>, [Accessed 19 January 2010]
103 Crow, D.R., “Principles and Applications of Electrochemistry”, Taylor and Francis Ltd, 1994, ISBN 0-412-30270-5.
104 Pistoia, G., “Batteries for Portable Devices. Elsevier”, 2005, ISBN 0-444-51672-7, pp 6.
105 Physical Chemistry S342 Block 7, The Open University, ISBN 0 7492 51891, pp 46.
106 PowerSafe Plante, Enersys Power/Full Solutions, Installation Operation and Maintenance Manual, Publication number EN-PL-IOM-001 May 2004 p5
107 Ross, M.D., “A simple but Comprehensive Lead-Acid Battery Model for Hybrid Ststem Simulation”, Proceeding of PV horizon workshop, Renewable Energy Research, 2001

108 Moore, S, et al , “An Empirically Based Electro-source Horizon Lead-Acid Battery Model”, Strategies in Electric and Hybrid Design, SP-1156, 1996, pp135-138.
109 Gonzalez-Longatt, F.M., Circuit Based Battery Models: A Review, 2DO CONGRESO IBEROAMERICANO DE ESTUDIANTES DE INGERERIA ELECTRICA(II CEBELEC 2006)
110 Battery equivalent circuit, [Online], Available from World Wide Web: <http://www.mpoweruk.com/performance.htm>, [Accessed 19 January 2010]
111 The Open University S342 Physical Chemistry, Principles of change, Block 7 Equilibrium Electrochemistry ISBN 0 335 16189, pp46
112 Estimating battery State-of-Charge, [Online], Available from World Wide Web: <http://www.mpoweruk.com/soc.htm>, [Accessed 19 January 2010]
113 Jossen, A., et al, “Methods for state-of-charge determination and their applications”, Journal of Power Sources, Volume 96, 2001, pp113-120.
114 Battery Management System (BMS), [Online], Available from World Wide Web: <http://www.mpoweruk.com/soh.htm>, [Accessed 19 January 2010]
115 Peukert number, [Online], Available from World Wide Web: <http://www.mpoweruk.com/performance.htm#peukert>, [Accessed 19 January 2010]
116 Jackson, R.G., “Novel sensors and sensing”, Taylor and Francis 2004, ISBN-13 9780750309889, pp64.
117 Younger, P.L., “Mine Water Hydrology and Geochemistry”, Geological Society Publishing House 2002, ISBN-13 978-186239110, pp48.
118 S.P. Sørensen and K. Lindstrøm-Lang, Compt. Rend. Trav. Lab. Carlsberg, 15 (1924)
119 pH measurements with high ionic strength, [Online], Available from World Wide Web: <http://www.sensorland.com/>, [Accessed 19 January 2010]
120 pH meter method, [Online], Available from World Wide Web: <http://www.allaboutcircuits.com/vol_1/chpt_9/6.html>, [Accessed 19 January 2010]

121 Dyer, S.A., “Survey of Instrumentation and Measurement”, Wiley Blackwell 2001, ISBN-13 978-04711394846, pp904.
122 Nernst Equation, [Online], Available from World Wide Web: <http://www.coleparmer.com/techinfo/techinfo.asp?htmlfile=pHMeasurement.htm&ID=553>, [Accessed 19 January 2010]
123 Image of Battery magic eye indicators, [Online], Available from World Wide Web: <http://www.itwdelpro.com/battery.html>, [Accessed 19 January 2010]
124 Baxter, L.K., “Capacitive Sensors. Design and Application”, IEEE Wiley-Press, 1996, ISBN 0-7803-5351-X
125 Image of Measurement of cell resistance, [Online], Available from World Wide: <http://www.iop.org/activity/education/Teaching_Resources/Teaching%20Advanced%20Physics/Electricity/Images%20100/img_mid_4092.gif>, [Accessed 19 January 2010]
126 Pop, V., et al, State-of-the-art battery state-of-charge determination, Institite of Physics. Measurement and Science Technology. 16 (2005) R93-R110.
127 Pop, V., et al, “Battery Management Systems”, Springer, ISBN 978-1-4020-6945-1, p17.
128 Diard, J.-P., et al, “Impedance measurements of polymer electrolyte membrane fuel cells running on constant load”, Journal of Power Sources, Volume 74, Issue, August 1998, pp244-245.
129 Cox, M.,et al, Automotive “Smart” Battery with State of Health Conductance Testing and Monitoring Technology (onGUARD) SAE International Document Number 2003-01-0099
130 BAYOUMY, M., et al, “New techniques for battery charger and SOC estimation in photovoltaic hybrid power systems”. Solar Energy Materials and Solar Cells, ISSN 0927-0248
131 Delaille, A., et al, “Study of the “coup de fouet” of lead-acid cells as a function of their state-of-charge and state-of-health”, Journal of Power Sources Volume 156 2006, pp1019-1028.

132 Pavlov, D., et al, B.Monahov, "Influence of H_2SO_4 concentration on the mechanism of the processes and the electrochemical activity of the Pb/PbO2/PbSO4 electrode", Journal of Power Sources, Volume 137 (2004), pp 288-308.